Optimized Solar Water Heater for Scottish Weather Conditions

Haroon A. Junaidi
(2007)

Declaration

I hereby declare that the contents of this thesis are original and have been submitted solely to Napier University in partial fulfilment of the requirements for the degree of Doctor of Philosophy (PhD).

Haroon A. Junaidi

Signed

Dated

Acknowledgements

Firstly, I would like to thank God Almighty for life and everything in it.

This thesis in every context would have been simply "inappropriate" without the assistance of Dr. Douglas Henderson, whose meticulous attention gave me the guidance when I needed it. His enormous patience with me is something I believe I will not witness again from anyone else. The trust he had in me, instilled the confidence to progress. I take this opportunity to thank him for his tremendous support throughout this work and it is in his legacy that this thesis is devoid of the word "specially"

Professor Tariq Muneer, ever present with his untrammelled vision was a real driving force throughout the course of work. My admiration for his tireless passion for work and persevering efforts grows each passing day. I am indebted to life for what I have learnt from him.

Dr. Thomas Grassie's sharp ideas were always there to provide the edge, not to mention his larger than life persona, that for me was inspiring. Mr. John Currie's sporadic contributions were valuable and an important asset in the progress. I owe him a lot particularly my "predator vision" thermacam portraits.

I also take this opportunity to thank Ian Campbell and Kevin McCann for their help throughout the experiments. It still fascinates me, how Ian managed to pull out the plastic rod that got bent inside the collector, a Herculean task indeed in terms of skill. I am grateful to all technicians who helped in the fabrication of the prototypes namely Pete Bruce, Alan Barber, Derek Cogle and Dave Baxter, your input is much appreciated.

"Houston! We have a problem" is all what I had to say to Mr. Bill Campbell, in case of computer breakdown. It was his magic that saved my life several times and I am indeed grateful to him.

A bundle of thanks goes to Celine Garnier for helping me many ways particularly sorting out my data. Peter Clarke -who provided the giggles in the research office- and all my colleagues in present and past, will surely be missed.

The beautiful city of Edinburgh, that has been home to me for the last three years, and perhaps provides the most perfect backdrop for research, deserves a mention.

I salute Charlotte "Charlie Charlie" Fairweather. She was instrumental in boosting my drive and keeping a close eye on my English. In her I have found a true friend who has the decorated my memory of Scotland. I wish her luck for all her future endeavours.

I cannot go any further without mentioning my parents, whose prayers have carried me all the way and I hope the same for times to come. I am grateful to all my family and friends, their well wishes were with me all the time and are herein acknowledged.

Optimized Solar Water Heater for Scottish Weather Conditions

Abstract

The ICSSWH (Integrated Collector Storage Solar Water Heater), apart from being the oldest is also the most economical means of solar water heating. The effect of modifications in the collector geometry has frequently appeared in the literature, and over the time, has resulted in different designs. These designs differ mainly on the site of installation as well as the target application. A novel design created by Professor T Muneer at Napier University, utilizes fins inside the storage tank to improve the heat transfer. The reported field tests of the fin type ICSSWH have indicated a 10 % improvement in the solar fraction compared to unfinned.

As ICSSWH is the lowest cost, it presented a possible solution for the Scottish market where Energy Saving Trust estimates that 50% of hot water demand of a household can be met through solar water heating.

In the present research program, two prototype collectors (one with- and one without fins) were fabricated at Napier University by the author. The collectors were then tested in the laboratory on identical experimental schemes to determine their respective performance. Simulations based on analytical modelling were then undertaken, using numerous experimental data for validation that were obtained during the course of the present work. A high degree of conformance was noted between the two. Furthermore, for a deeper insight, Computational Fluid Dynamics (CFD) analysis was performed.

This research focuses on the qualitative and quantitative assessment of the heat transfer due to the fins. The difference in the performance with respect to the change in tilt angle was also studied. This study can therefore be utilised for developing solar water heating systems for any given location. Note that there is an intrinsic link between the latitude and inclination angle of the collector plate.

The nocturnal loss from the collector is the principal factor that has inhibited the wide spread use of the ICSSWH. The remedies to abate this problem have therefore been attempted. In addition to that, the collectors have to be integrated with the domestic hot water supply system and plumbing considerations have to be incorporated within the overall design. The supply circuits were worked out and the measures for freeze and boil protection were devised.

The optimization of any system is an intrinsic task particularly when several variables are involved. On the basis of the obtained results from simulations and experiments, the influential design variables were identified. The values for these variables which lead to the optimal design in terms of thermal performance were assessed while keeping the overall manufacturing cost of the collector as low as possible. Recommendations for future work have also been presented.

Glossary of Symbols & Abbreviations

2D = Two dimensional (referring to dimensions of problem domain)

3D = Three dimensional (referring to dimensions of problem domain)

α = Absorptance

α_s = Solar Altitude Angle

β = The angle of the plane of the surface in question and the horizontal

γ = Surface Azimuth Angle

γ_s = Solar Azimuth Angle

ρ = Reflectance

ε = Emittance

ε_c = Cover Emittance

ε_p = Plate Emittance

σ = Stefan- Boltzmann constant (5.67×10^{-8} W/m^2T^4)

ϕ = Angle of inclination of the collector or tilt

ϕ_C = Critical angle of inclination of cavity

θ = Angle of inclination of the cavity

θ_c = Critical angle of inclination of the cavity

ϑ = Viscosity

τ = Transmittance/ Transmissivity

A = Vertical aspect ratio of the cavity(A = H/L)

A_c = Frontal Area of the cover plate

A_H = Horizontal aspect ratio (A_H = W/L)

$A_{Surface}$ = Surface Area (m^2)

°C = Temperature in Centigrade/Celsius

C_{pw} = Specific heat of water

C_{psteel} = Specific heat of steel

D^1 = Diameter of the Storage tank

D = Diameter of the cylindrical vessel (m)

F_R = Heat Removal Factor (Dimensionless)

G_{in} = Incident/ Imposed irradiance (W/m^2)

h = Convective heat transfer coefficient (W/ m^2K)

h_{ca}^{c} = Convective heat transfer coefficient for convection from cover to ambient (W/m^2K)

h_{ca}^{r} = Radiative heat transfer coefficient for convection from cover to ambient (W/m^2K)

h_{pc}^{c} = Convective heat transfer coefficient for plate to cover (W/m^2K)

h_{ca}^{r} = Radiative heat transfer coefficient for radiation from plate to cover (W/m^2K)

h_{ca}^{c} = Heat transfer Coefficient of cover to ambient

H = Length of the cavity (m)

K = Temperature in Kelvin

l = Characteristic length for dimensionless numbers (m)

I_{ave} = Average Insolation on collector aperture

L^1 = Height of the Storage tank

lt = Litres of water (dm^3)

I_{ave} = Average insolation over the collector aperture

L = Height of the cavity (m)

m_w = Mass of water (kg)

m_s = Mass of steel (kg)

Q_{useful} = Useful energy gained by the collector

Q_{loss} = Energy lost by the collector

Q_{input} = Imposed heat flux/ incident radiation

$Q_{Toploss}$ = Energy losses from collector top

t = time step (sec)

T = Temperature (˚C,K)

T_f = Film temperature

ΔT = Temperature Difference (˚C)

ΔT° = Difference between the average vessel water temperature of the heating period minus the average ambient temperature over the same period

ΔT^1 = Difference between the inlet and outlet

T_p = Plate temperature (˚C)

T_c = Cover temperature (˚C)

T_a = Ambient Temperature (˚C)

T_{sky} = Sky temperature (˚C)

U_{α} = Free stream velocity

V = Control volume

V_0 = Wind velocity (m/s)

x_o = Distance from the leading edge

y_p = First cell distance (m)

Abbreviations

ATA = Abbreviated Thermal Analysis

Bi = Biot Number

CFD = Computational Fluid Dynamics

HTC = Heat Transfer Coefficient

ICS = Integrated Collector Storage

lpm = Litre per minute

LTP = Linear Temperature Profile

MIG = Metal Inert Gas

MBD = Mean Bias Difference

Nu = Nusselt Nuber

Pa = Prandtl Number

Pe = Peclet Number;

QUICK = Quadratic Upstream Interpolation for Convective Kinetics

RMSD = Root Mean Square Difference

Ra = Rayleigh Number

Ra_c = Critical Rayliegh number

ST = Stratification Factor

SWH = Solar Water Heater/ Solar Water Heating

TIG = Tungsten Inert Gas

TC = Thermocouple

TIM = Transparent Insulation Material

ZHF = Zero Heat Flux

Table of Contents

List of Figures and Tables

Figures

Chapter 1

Chapter 2

CHAPTER 1

Introduction

"Every moment, the sunlight is totally empty and totally full." - **Rumi**

For every research assignment, it is imperative on the outset to substantiate the very basic question "why"? A judicious answer to this not only renders the feasibility of the work, but also categorizes it into a pure academic exercise or an outcome that could have a direct influence on the society. The two questions of why "solar water heating" and why "Scottish conditions" have been addressed in this chapter. The supporting text leading to the conclusive answers is presented with due reasons.

CHAPTER MAP

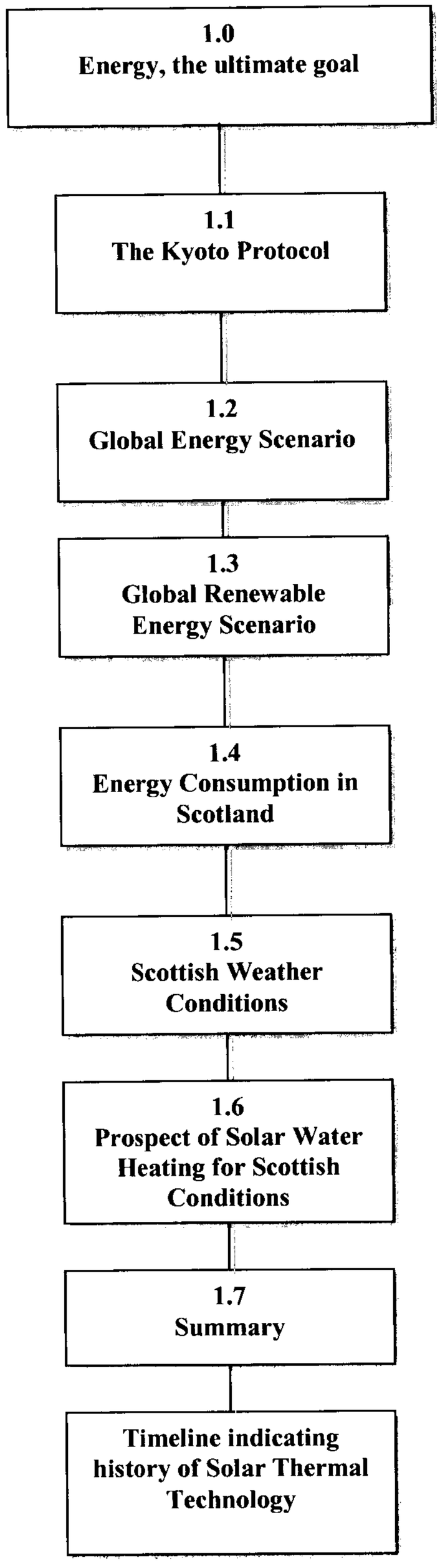
1.0
Energy, the ultimate goal
1.1
The Kyoto Protocol
1.2
Global Energy Scenario
1.3
Global Renewable Energy Scenario
1.4
Energy Consumption in Scotland
1.5
Scottish Weather Conditions
1.6
Prospect of Solar Water Heating for Scottish Conditions
1.7
Summary
Timeline indicating history of Solar Thermal Technology

1.0 Energy, The Ultimate Goal

The annual consumption of iron, Per Capita Income, GDP (Gross Domestic Product), and gold reserves are few of the indices that measure the economic health and prosperity of a society. All these factors more or less relate directly or indirectly to the consumption of energy. Therefore "energy consumption" is the root factor that can visibly differentiate between developed and less developed societies. A cursory look at the energy consumptions by various countries reveals that the per capita energy consumption in developed states is significantly higher than in less developed or developing states [2]. Figure 1.1 explicitly illustrates this difference.

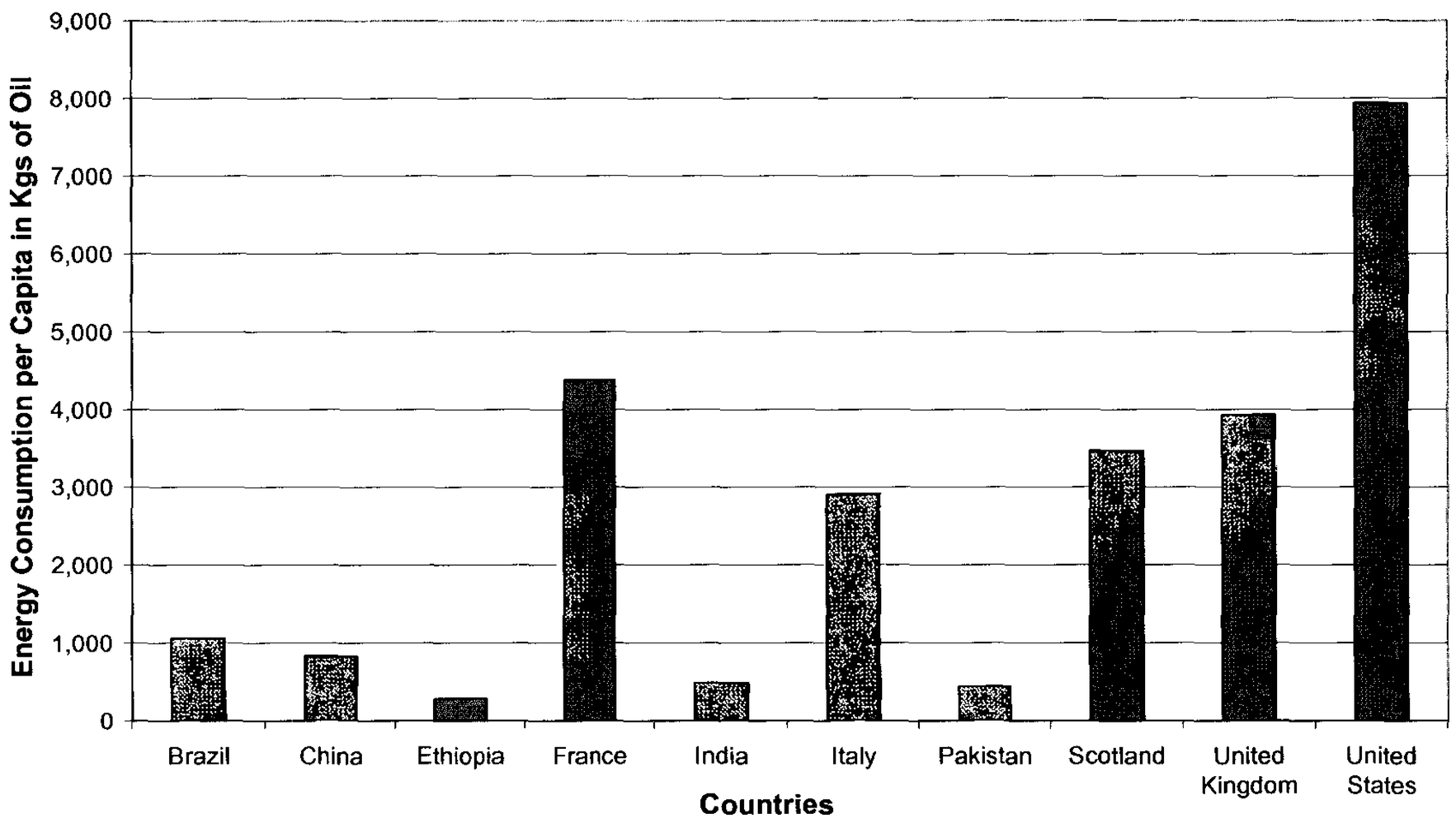

Figure 1.1: Per capita energy consumption for various countries

A world without energy is unconceivable; in more philosophical terms "existence" of all forms, matter, life and even intangible entities would cease if energy perishes. With the exponential growth in global population and the continual endeavor for a better economy, energy consumption has increased dramatically, particularly in the last two centuries. With each passing moment the energy gap (deficit between the energy demand and the

supply) is widening faster than ever and has to be bridged by effectively using the resources at hand. Consciously or subconsciously mankind has chased energy in one way or another and it is the need for this fundamental element that has driven the current study. However in the present era, it is not only the quantity of energy that matters but more importantly the way by which it is accumulated. The following section sheds light on why the manner of energy extraction is crucial.

1.1 Kyoto Protocol (Directives)

On February 16, 2005 Kyoto protocol legislations were implemented, a treaty which enforces the cutting down of CO_2 emissions and has fostered the need for effectively tapping renewable energy. The protocol has stirred global scale efforts to curtail emissions through binding targets. Global warming has been dubbed the biggest challenge to mankind so far. An unprecedented arduous task of abating the threat of climate change looms ahead. Many developed nations have agreed to pursue the plausibly uphill, yet manageable targets of cutting down greenhouse gas emissions. For some, the economic constraints hinder sincere efforts. The protocol however has succeeded in globally embedding a conscience among the general public and creating wide spread awareness that the problem exists and cannot be overlooked.

Under the international Kyoto protocol and European-Union agreements, by 2008-2012 the UK must reduce its baseline emissions of six greenhouse gases by 12.5%. In addition, the UK Government has set its own domestic target to reduce carbon dioxide emissions to 20% beneath the 1990 baseline by 2010. The target set for Scotland is more stringent compared to the overall target of UK. Scotland aspires to meet 40% of its energy through renewables by 2020. A closer objective on the timeline is the Scottish Renewable Obligation (SRO) which enforces attaining 10% of the supplied electricity through renewable resources by 2010[3]. This target has been revised and increased to 20% by the Scottish Executive[4]. Therefore workable, feasible and realistic plans to proceed effectively should be chalked out by the Scottish government if any level of target attainment is desired.

Having noted the energy needs and the legislative drivers it would be important at this point to glance at the current energy situation for a clearer picture of resources at hand.

1.2 Global Energy Scenario

Speaking globally, the present day energy scenario, does not present an encouraging image. Fossil fuel depletion can be very much sighted with a possibility of total exhaustion in a generation's time. Alarm bells for a huge energy crisis are foreseeable to go off, until, or unless radical steps are taken to change the present course of the energy attainment. The coupling of fossil fuel consumption with global warming would have compounded the problem substantially if renewable energy resources were absent. With the increase in the population, the demand for energy is getting higher each passing day. This in effect will result in swifter depletion of high-grade energy resources whereas low grade resources will carry on relatively longer. The detrimental environmental effects caused by fossil fuels are an additional constraint. A snapshot of the world's available energy resources is shown in fig1.2 [5].

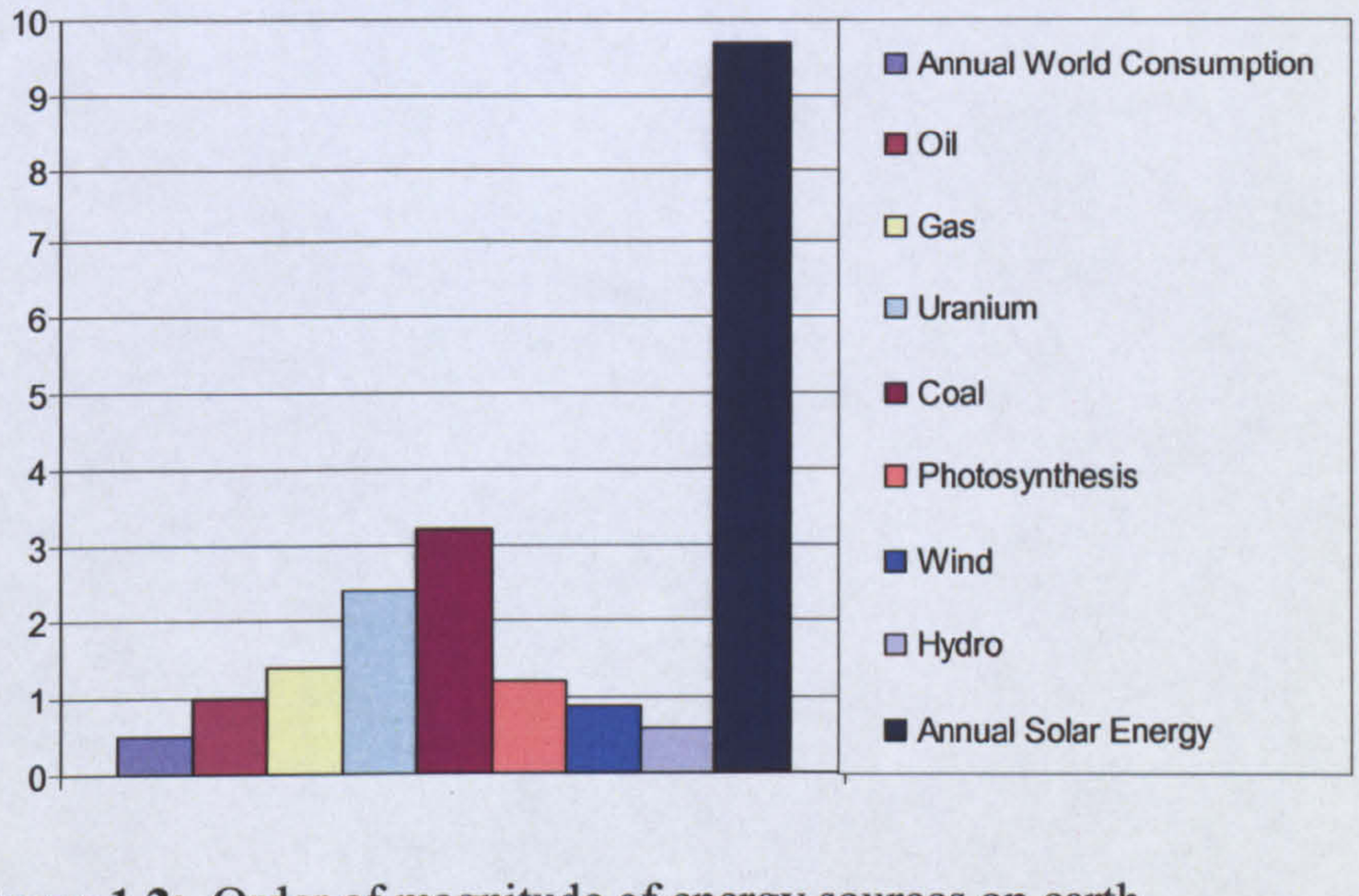

Figure 1.2: Order of magnitude of energy sources on earth

As indicated in fig 1.2, oil reserves cannot be pumped for long while gas and coal will only delay the crisis till they eventually run out. For a more detailed picture, the past and future discovery of oil has been shown in fig 1.3, clearly indicating total exhaustion by 2050 [1]. Nuclear energy is another possible route that can abridge the gap between demand and supply, however the environmental threat it poses would not be worth risking especially if a source of green energy concurrently exists. Nuclear energy currently provides 16-17% of the world's energy demand. However, this figure is expected to decrease as old power plants are being decommissioned and few new ones are being built. Moreover it cannot be relied on, as it is also an exhaustible resource. The only infallible way forward is an energy source that is renewable and sustainable. What catches the eye in fig 1.2 is the exceedingly abundant solar energy that stands out well above all the other types as an extremely lucrative option. Although it is predictable that other more instant forms of energy will be momentarily grasped when transiting from the fossil fuels, however it seems imperative that pool of solar energy would prove to be the eventual reservoir.

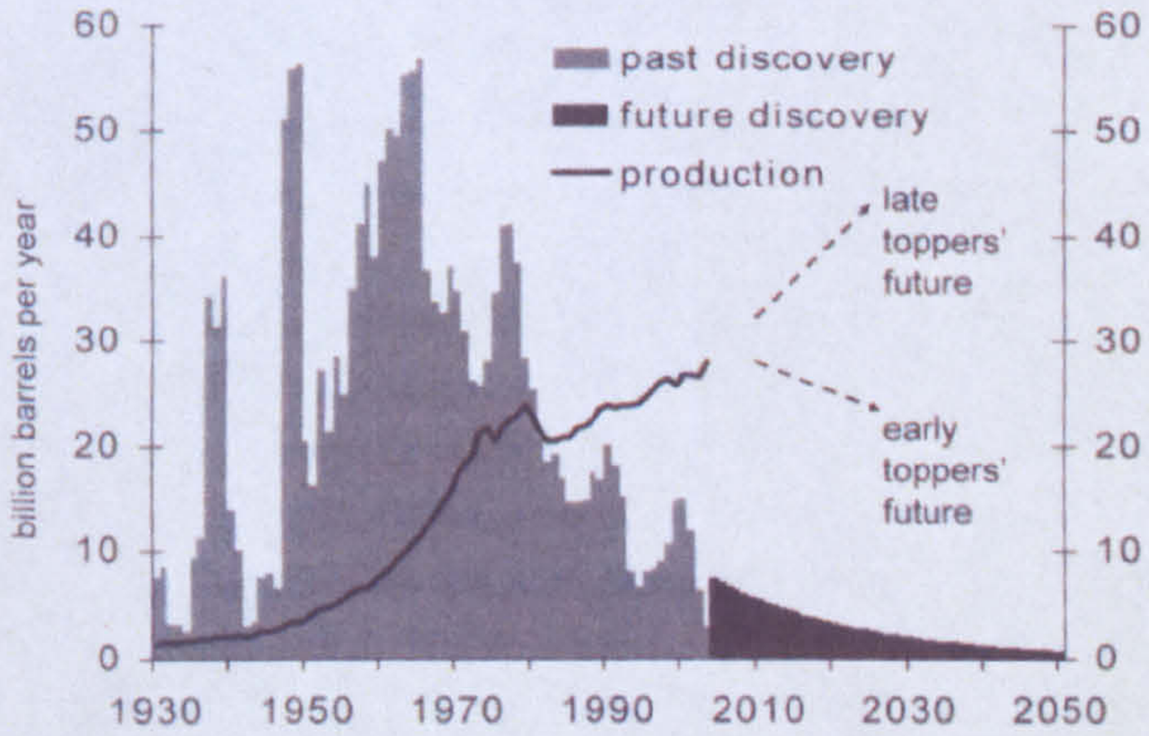

Figure 1.3: Past and future global oil discovery and production [1]

The exploitation of solar energy is hence seeing a renewed interest. Although the abundance of solar energy is unquestionable, nonetheless it is important to consider other renewable sources so as to compare the feasibility.

1.3 Global Renewable Energy Scenario

Renewable energy can be split into two groups; namely hydro and non-hydro energy. Hydropower is the largest and most important renewable resource and generates about 17% of the world's electricity. It is estimated that only 33% of the technically and economically feasible global potential of hydropower has been developed to date, although there are significant regional variations. In Europe and North America, the majority of sites have been developed, while considerable potential for new development remains in Africa, Asia and South America. Large hydropower schemes, however, often face challenges due to their environmental impacts and long-term returns on investment. The non-hydro category of renewable energy is estimated to make a growing contribution to global power generation; the total share is likely to reach about 5% in 2030[1]. The renewable sector is now growing faster than the growth in the overall energy market. Approximately £15 (US$ 22) billion was invested in renewable energy worldwide in 2003. In comparison, total investment in the electric power sector is likely to be in the range of $120-160 billion/year. Annual investment in renewable energy has grown almost four fold from $6 billion in 1995, while cumulative investment since 1995 is of the order of $110 billion. The 2003 investment shares in the renewable sector was roughly 38% for wind power, 24% for solar PV, and **21% for solar thermal hot water**. Small hydro power, biomass power generation, and geothermal power and heat made up the remaining 17%. Solar collectors for heating water are at present used in the UK to a limited extent. In 2001 it was estimated that they contributed 78.5 GWh for heating swimming pools, while the solar contribution to domestic hot water supply in 2002 was estimated at 55.2 GWh [6]. It is estimated that more than 100 million m^2 of solar thermal collector area were in operation in the world at the end of 2002. The newly installed area during 2002 was more than 10 million m^2 [1].

Despite the abundant wind resources, the erection of wind farms still sparks controversy as they are claimed to stain the landscape. Possible detrimental ecological effects propelled by the wind farms, particularly on migratory birds are also being scrutinized.

To add to the demerits, shadows cast by their huge structures invoke unrest among the population. For the tourism-based economy of Scotland, these factors amalgamate and gain greater importance. Similarly the sea or marine current turbines that cash in on the currents are under examination for any negative effects on marine life. Solar water heaters among the huge tidal and wind resources have carved out their niche particularly in the domestic sector. No adverse effects have appeared in the text, even after nearly 30 years of their implementation in the UK. In Scotland, due to the abundance of sparsely populated areas where grid energy may deface the scenery, solar water heating provides an ideal solution.

This singles solar energy out as the prime renewable energy option. It is an encouraging fact- as depicted by fig.1.2 – that the energy received by the earth over a year is 100 times more than what the world annually consumes. The sun is an inexhaustible source of utilizable energy.

Having gone through the importance of energy, the legislatives of Kyoto protocol and how renewable energy is emerging as the biggest alternative, the question *"why solar water heating?"* has been to an extent, vindicated. It would be appropriate at this point to eye the panorama of Scotland's energy.

1.4 Energy Consumption in Scotland

The total energy consumed and the spectrum of its distribution in various sectors for Scotland is important to monitor to determine the energy need that can be addressed through solar water heating.

The following figures provide a quantitative summary of the energy usage in Scotland and the UK. The total energy consumption of all forms of energy in the UK was around 2,760 TWh in 2001, of which Scotland accounts for roughly 7-8%. The actual energy used at the point of demand was around 1,750 TWh. The remainder was lost in energy

conversion, transmission and distribution of energy [7]. The average annual energy use of a Scottish household is 21.4 MWh. The final energy used in Scottish households is approximately 47 TWh, 9% of the UK total of 523 TWh. 82% of energy used in households is for space heating, 58% of space heating in Scotland is provided by natural gas, while around 30% of households are electrically heated. More importantly, 53% of the total domestic energy goes into space heating and water heating. Thus *out of 47 TWh of the energy used in Scottish households, 24.9 TWh can be addressed through heating water from a renewable resource.* A research by the "Energy Saving Trust" carried out in June 2004 has revealed that £28 million a year could be saved if every house in Scotland had a solar water heating panel fitted. In addition to that it will also reduce the impact on the environment – the average domestic system can reduce carbon dioxide emissions by 0.25-0.5 tonnes per year, depending on the fuel replaced.

Tremendous scope lies in addressing the energy requirement particularly for hot water from a renewable source as indicated in the previous. It is now the question of whether or not this energy can be met by solar energy in Scotland. This can be answered by an overview of Scottish weather conditions, particularly solar radiation data.

1.5 Scottish Weather Conditions

Scotland has been blessed with an awe inspiring landscape, breath-taking scenery, a rich cultural heritage, deep-rooted history and abundant natural resources. Geographically, a sizeable portion of the land is located above the latitude of 55°N, placing it among the countries of northern latitudes. Scotland has huge wind resources at its disposal, alongside enormous the tidal and wave resources. It owns 50% of EU wave and tidal resources. On top of that having 25% of EU wind resources further boosts the energy sufficiency. One sector that is often overlooked is solar energy. A prevailing concept, in and about Scotland, is of a gloomy level of solar energy due to persistent murky conditions. A popular fact pointing out over 300 average rainy days a year is a true yet a misleading statement. On the contrary, Scotland has been blessed with not only ample solar insolation but also resonating heat load requirements. Scotland enjoys 17.5 hours

sunshine on solstice day. Fig1.4 shows the incident solar radiation levels in the South of Scotland [8]. The average daily solar irradiance comes out to be 2.73 kWh/m^2. On an annual basis the total available energy would be ≈991 kWh/m^2. For a crude estimate, using an assumed annual efficiency of 35%, the available annual energy comes out to be 346 kWh/m^2. Although 346 kWh/m^2 might not seem an astounding figure it is nonetheless is sizeable enough to seize the initiative, bearing in mind CO_2 reduction, escalating energy prices and subsidiaries by government add to the impetus.

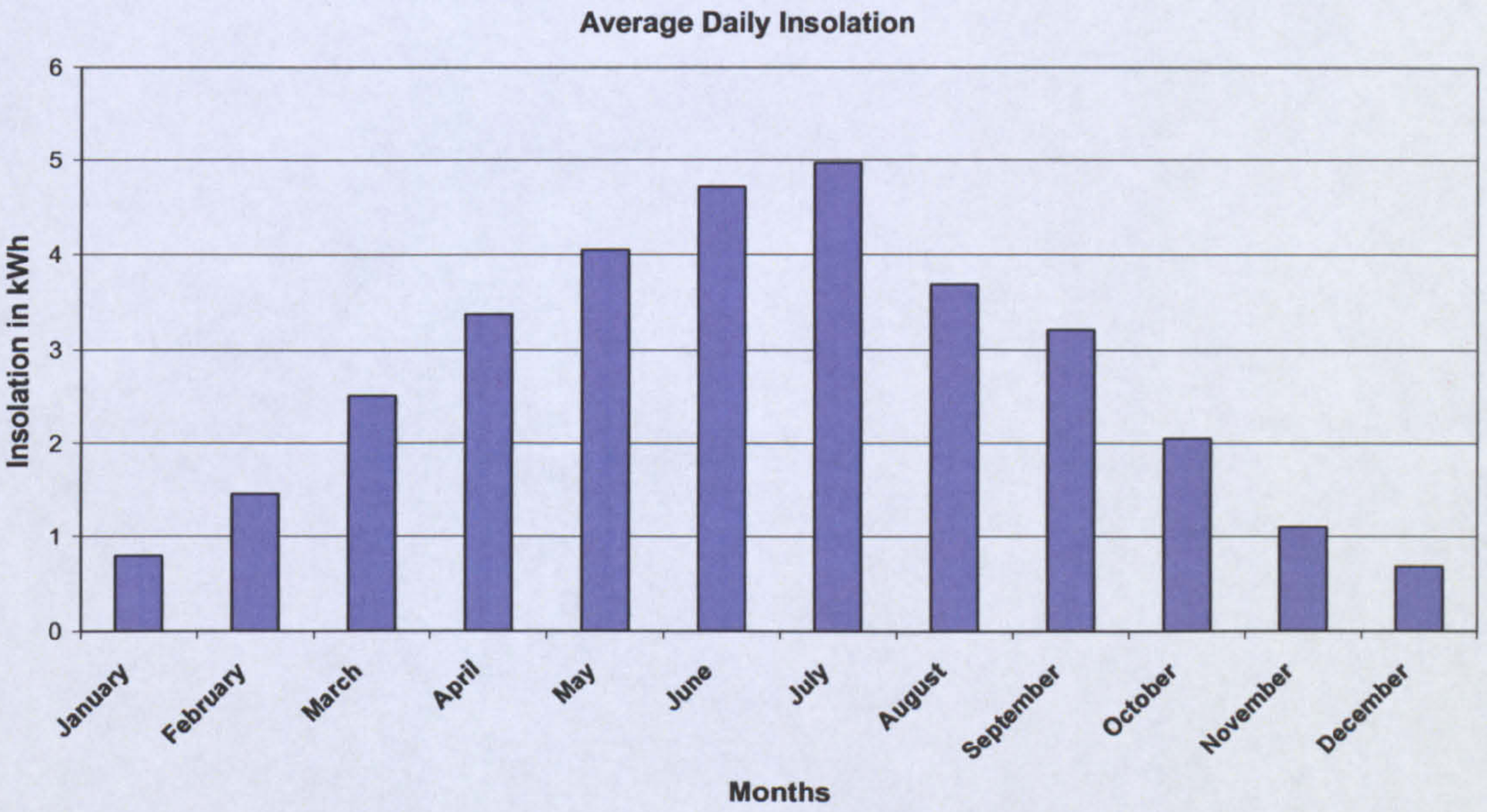

Figure 1.4: Daily average solar insolation in Scotland

Meeting the heating requirement through solar energy in northern countries is a daunting proposition, owing to the inverse relationship between requirement and availability. During winter months, when heating requirements escalate, the scarcity of available solar energy is a major setback. On the other hand during summer months when heating requirements plummet, the surplus insolation is wasted. Inter-seasonal storage has been cited as one of the solutions. The technology however is still in its development phases and so far has not been adopted commercially. For Scotland, it is a different story. In Scotland, an unusually high proportion of annual heating load comes outside 'official'

winter season. Even during the summer time, the main water temperature recorded was a maximum of 22°C. Thus the heating requirements in the summer remain sufficiently high and therefore the available energy can be exploited efficiently. McGregor et al opines Scotland to have one of the best conditions as there is a year round need for hot water [9]. The results from his study carried out for space heating show that solar savings generally increase with latitude, altitude and degree of marimiticity. The best country on these counts is Ireland while the worst being Malta [9]. Similarly, very encouraging results were also provided by a study conducted in Monymusk, Aberdeenshire by Imbabi et al [10].

1.6 Prospects of Solar Water Heating in Scotland

Solar water heating (SWH) in Scotland is not a novel proposition. A fair amount of research on the subject has already been carried out. SWH systems have been available in the UK since the 1970's and the technology is now well developed with a large choice of equipment to suit many applications. The proven success enjoyed by the commercial manufacturers is also a testimony to the viability of the venture. Even at present, the number of SWH installers registered to the SCHRI which is the "Scottish Community and House Holder Renewable Initiative" is a surprising 33 [11].

A crude analysis is presented herein which roughly estimates the feasibility of SWH. It is assumed that a heater accumulates 600 kWh of the incident 1000 kWh/m^2 with collector an assumed collector area of 2m^2, on the basis of an inferred conservative thermal efficiency of 30%. The average cost of a unit of electricity for 2004 is 7.76p per kWh [2]. Based on this would an annual saving of £46.56 can be expected if electricity is replaced as the heating fuel. In light of this, for a new designed collector that has a production cost £1000, the life should span at least 21 years to recover its capital cost. The important guidelines laid by this analysis bring forward that for a new collector, the design should be resilient so as to sustain a period of above 20 years. Secondly, it is imperative to keep the collector cost as low as possible to ensure feasibility well within its life time. As noted earlier, the production cost of the collector should be £1000, which itself is a fairly

stringent target. The other parameter that has room for improvement is the annual thermal efficiency, which should be above 30%. In order to compete, the thermal efficiency of the designed collector should be at least equivalent if not more than that of other existing heaters. A study by the EST [12] claims that solar water heaters could meet half of the annual demand through a collector of 2-5 m^2 .

Looking at the existing commercial designs, the prices of commercially-available collectors came out in the range "£1500- 3000" depending upon the type and capacity of the heater. Similarly, the "Energy Saving Trust" (EST) puts forward costs of "£2000-3000" in their fact sheet [12]. This again dispenses encouragement for a collector that has lower cost. SCHRI provides 30% grants to Scottish households on the installation of any renewable energy device. This is an important initiative to note as it reduces the payback time of the collector. With the trend of escalating energy prices likely to continue in the foreseeable future, the collector return on investment becomes even higher.

Product aesthetics might not be of any relevance in a scientific research; but it is an influential factor setting the wider acceptability of the collector. Domestic solar heaters have to be non-obtrusive and must not devalue the outlook of a property. Ideally, they should integrate seamlessly into the roof structure. For a domestic collector, aesthetics are of considerable importance as opposed to commercial ones, where this might not be a criterion at all. On this basis, the thermosyphon and many of the focusing collector types can be ruled out.

It is for these reasons, that there is a clear need to develop a low cost solar heater that would work efficiently while being aesthetically sound. It should also endure the occasional harsh weather conditions for at least 25 years. The collector should also either withstand or prevent freezing of water during extreme cold that results in expansion and thus damage to the heater. The "Freeze Tolerant System" by Grassie and McGregor [13] is an indigenous idea developed at Napier University that provides the one of the solutions to abate the problem for Flat plate type collectors.

It is apparent that solar water heaters have a niche in the current and future energy scenario even for energy sufficient countries like Scotland. Solar water heating in Scotland is not new; it is a well worked out and well established practice. Nonetheless the idea of an optimal solar heater for Scotland provides the room for research and brings novelty to previous work.

1.7 Summary

The Kyoto protocol underlines the need for carbon dioxide abatement which has enforced the attainment of energy in a manner that is sustainable. Having observed the current world energy scenario and the various energy options at hand, solar energy was found an adequate, inexhaustible and clean resource. Thus solar energy can be tapped for the future energy needs, even in Scotland where surprisingly ample insolation is available and the demand for hot water is appreciable during the summer season.

The foreseeable emergence of carbon based tax systems and constraints on CO_2 emissions are the additional drivers. Therefore the switch to solar water heating for Scottish homes with the passage of time is becoming more a need and less an option. Solar water heating in Scotland is not simply a possibility but a feasible prospect as ascertained by various authors and professional bodies.

Solar collectors are commercially available in Scotland through several installers. However, the cost of the collector is noticeably high, thus pointing to a potentially exploitable market for a low cost collector.

"How this energy can be harnessed in Scotland by cost effective means?" is the question that will be answered in the subsequent chapters.

For the interest of the reader, a timeline illustrating the historical use of solar energy for thermal application has been presented next.

Solar Energy Usage Time-Line

The following timeline indicates an interesting review of the usage of solar energy [3].

7th Century B.C.
A magnifying glass is used to concentrate the sun's rays on a fuel and light a fire for light, warmth, and cooking.

2nd Century B.C.
As early as 212 B.C., Greek scientist Archimedes makes use of the reflective properties of bronze shields to focus sunlight and set fire to Rome's wooden ships, which were besieging Syracuse.

1st to 4th Century
In the first to the fourth centuries, Roman bath houses are built with large, south-facing windows to let in the sun's warmth.

. 13th Century
In North America, the ancestors of Pueblo people known as Anasazi build south-facing cliff dwellings that capture the warmth of the winter sun.

1891
Baltimore inventor Clarence Kemp patents the first commercial solar water heater.

Mid-1950s
Architect Frank Bridgers designs the world's first commercial office building featuring solar water heating and passive design. The Bridgers-Paxton Building is listed in the National Historic Register as the world's first solar-heated office building.

3rd Century B.C.
Greeks and Romans use mirrors to light torches for religious purposes.

A.D. 20
The Chinese report using mirrors to light torches for religious purposes.

6th Century
Sunrooms on houses and public buildings are so common that the Justinian Code establishes "sun rights" to ensure that a building has access to the sun.

1767
Swiss scientist Horace de Saussure is credited with building the world's first solar collector, later used by Sir John Herschel to cook food during his South African expedition in the 1830s

1908
William J. Bailley of the Carnegie Steel Company invents a solar collector with copper coils and an insulated box, which is roughly the same collector design used today.

References

1. Jeremy Leggett, *Half Gone Oil, Gas, Hot Air and the Global Energy Crisis*. 2005, London: Portobello Books Ltd 2005.
2. *2004 Survey of Energy Resources*. 20th ed. World Energy Council. 2004: Elsevier.
3. Scottish Renewable Obligation, *http://www.scottish.parliament.uk/business/research/pdf_res_notes/rn00-29.pdf* 2007.
4. Scottish Executives, *Energy Efficiency and Micro Generation,*, in *Achieving a Low Carbon Future, A Strategy for Scotland*, Energy Efficiency Unit, Editor. March, 2007, Enterprise, Transport and Lifelong Learning Department: 5 Cadogan Street,Glasgow,G2 6AT.
5. Lomborg, B., *The Skeptical Environmentalist:Measuring the Real State of the World*. 2001, Cambridge: Cambridge University Press.
6. Kerr MacGregor, A. Taylor, and J. Currie. *Breathing Sunshine into Scottish Housing*. in *Proceedings of EuroSun'96*. 1996. Freiburg, Germany: 13–18 September.
7. Scottish Energy Environment Foundation, *http://www.scottish.parliament.uk/business/committees/enterprise/inquiries/rei/ec04-reis-scottishenergye.pdf*. Energy Fact Sheet.
8. ESRU, U.S.W.H., University of Strathclyde, *http://www.esru.strath.ac.uk/EandE/Web_sites/01-02/RE_info/active_urban.htm*. 2007.
9. Kerr MacGregor, *A Comparision of EU Capital Cities for Suitability for Solar Space Heating*. Eurosun 2006 Conference Proceedings, Glasgow, UK 2006.
10. Imbabi, M.S. and A. Musset, *Performance evaluation of a new hybrid solar heating and ventilation system optimised for U.K. weather conditions*. Building and Environment, 1996. **31**(2): p. 145-153.
11. Scottish Community and Householder Renewable Initiative (SCHRI), *Accredited Installer List*, in

http://www.est.org.uk/uploads/documents/myhome/LATEST%20Installer%20List13.03.07.pdf

2007.

12. Energy Saving Trust, *Solar Water Heating Fact Sheet*. 2005: http://www.est.org.uk/schri/downloads/Solar%20water%20o_p.pdf.

13. Kerr MacGregor. *The development and testing of a freeze-tolerant solar water heater*. in *North Sun '97*. 1997. Helsinki, Finland.

Chapter 2

Literature Review

Review and Compilation of Established Research Work

A review of the relevant studies is important to perform at the outset for a number of reasons; first and foremost is to get abreast with up to- date advancements, secondly to avoid reinventing the wheel and most importantly to not deviate into paths that result in futile efforts. Thus a thorough literature review can not only establish the dos and don'ts for the research but also pave the way for it.

This chapter reveals the guidelines that were laid down by the previous researchers. Solar water heating being a well established field required a comprehensive review of previous work and therefore the compilation is fairly exhaustive as reflected by the size of this chapter.

CHAPTER MAP

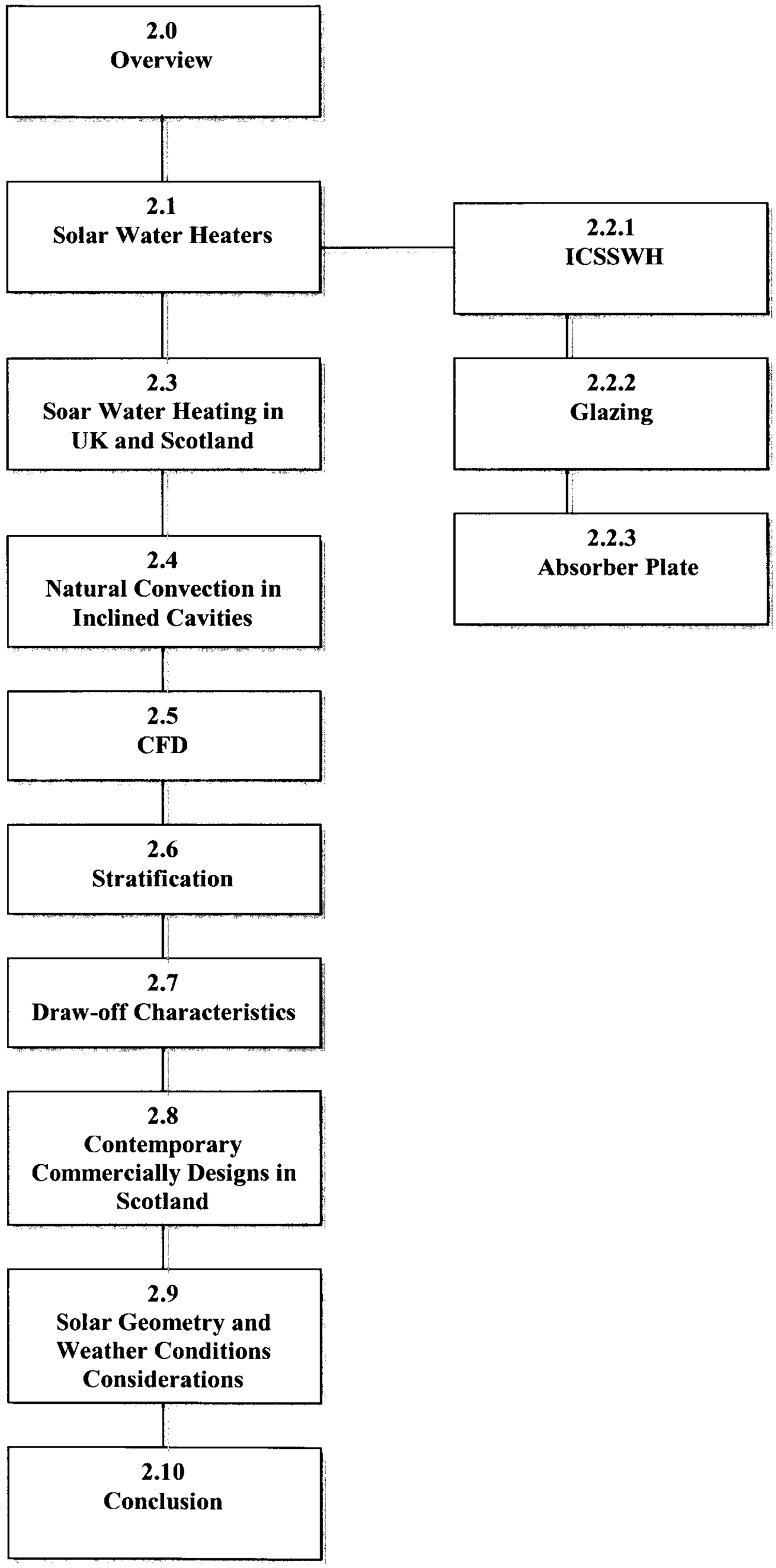
2.0
Overview
2.1
Solar Water Heaters
2.2.1
ICSSWH
2.3
Soar Water Heating in UK and Scotland
2.2.2
Glazing
2.4
Natural Convection in Inclined Cavities
2.2.3
Absorber Plate
2.5
CFD
2.6
Stratification
2.7
Draw-off Characteristics
2.8
Contemporary Commercially Designs in Scotland
2.9
Solar Geometry and Weather Conditions Considerations
2.10
Conclusion

2.0 Overview

To date an extensive amount of literature has been published on the subject of solar water heating. At present, it stands out as a field that is well established and concurrently vibrant. "Optimization of solar water heaters for Scottish weather conditions" has a broad theme encompassing several discrete topics. To effectively grasp the whole spectrum of topics while exploring each of them in-depth requires an atomistic as well as a holistic review. Some of the major topics found enclosed within the title itself are as follows:

- **Solar water heaters**; various types and their corresponding advantages and applications.
- **Convection**; The bulk mode of heat transfer in a collector.
- **Stratification**; Significant for estimating the energy content/solar fraction of the heater (see Textbox 1 for more details).
- **CFD**; Modern analysis tool for providing deeper insight and solving several "what-if" scenarios of optimization.
- **Draw-off characteristics**; Yield of the collector.
- **Solar heating at higher latitudes**; installation, orientation and considerations of the weather-conditions

The diversity of the surveyed literature highlights the complexity of composing of a concise review. The studies on the subject can be broadly categorized in two types, termed herein as macro and micro level studies. The term macro level implies the study on solar water heater year round performance for a particular location whereas micro-level refer to the studies carried out involving component level inspection. A vast amount of macro level studies have been conducted, recording the impact of the load (hot water demand) on the heater performance. Although water consumption bears a strong influence on the performance, geometrical variables such as distance between cover plate and absorber plate, angle of inclination, inlet and outlet pipe locations cannot be totally neglected. The literature review therefore has been sectioned to list the information in a more succinct and orderly fashion.

2.1 Solar Water Heaters (SWH)

A chronological review of the use of solar thermal energy was presented in Chapter 1. The evolution of solar water heaters is presented in this section. The earliest detailed records found were of Baltimore inventor, Clarence Kemp (1891) who patented the first commercial solar water heater. His design was a simple built-in storage heater, more details of which are presented later in the chapter. The increased interest in fossil fuel extraction in the early 20th century proved to be an impediment in the development of SWH. Abundant and low cost fossil fuels made the solar collectors a redundant entity and eradicated the drive for any progress in the field. Solar thermal development activities came to a complete halt in some countries while they were dragged down to sluggish rates in many others. The oil crisis in the late 1970's jolted resurgence and solar water heating was back in business. With the recent oil reserve situation and the Kyoto protocol, the field has been re-galvanized with more motives.
The variation in both the quality and quantity of insolation as well as application specific output requirements has lead to several SWH designs. To cite a few of the active designs; Vacuum tube, Flat plate (with variants: serpentine tubes, Parallel tubes, Built-in storage), Focusing solar collectors and Focusing integrated tank collectors. Each of these collectors has its own niche with respect to application and climate. For instance, in applications where high temperature output is desired, the vacuum tube collector presents a fitting solution. On the other hand in the domestic sector, flat plate and built-in storage have a stronghold owing to lower cost and minimal maintenance issues. McGregor et al [1] conducted experimental study for more quantitative figures on the comparison of energy output from flat plate and vacuum-tube collectors. In his study, the results explicitly indicated that on a typical operating point, the flat plate design provided 20% more useful heat than the vacuum-tube collector with the same aperture area. In fig 2.1 the various types of collectors have been presented.

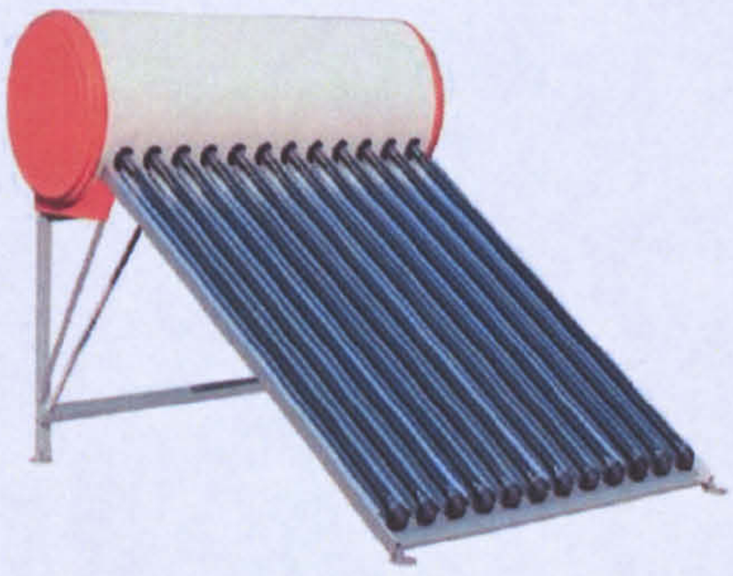

a) Vacuum tube

b) Thermosyphon

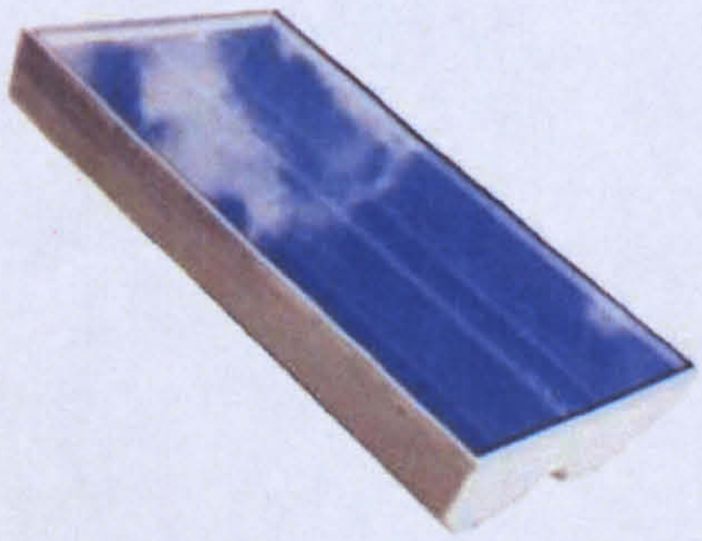

c) Built-in storage

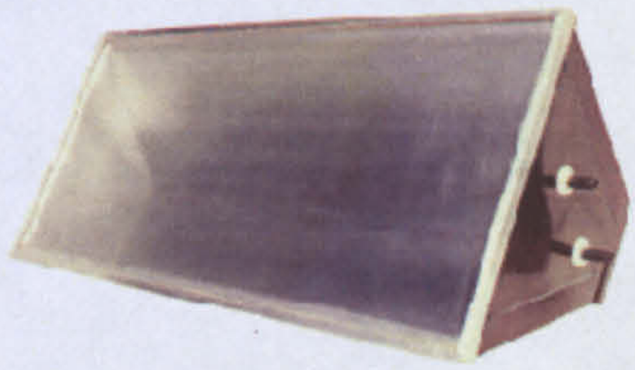

d) Built-in storage

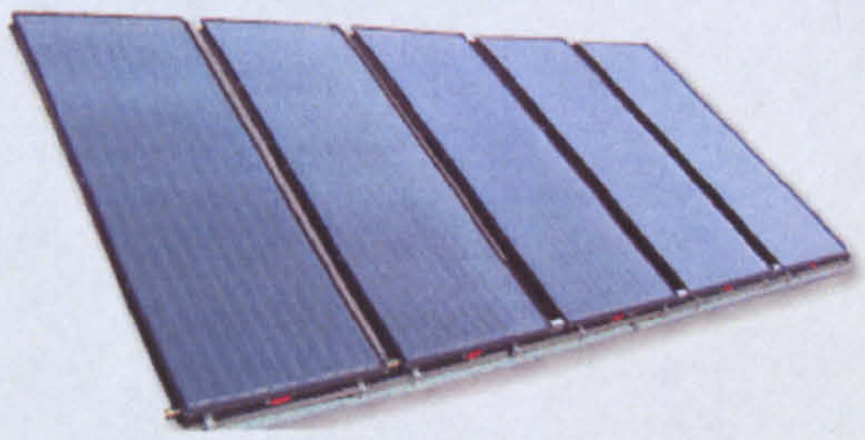

d) Flat plate collector

Figure 2.1: Different types of Solar Water Heaters
Pictures courtesy (a) BTFsolar.com (b) lowestcostenergy.com
(c) sole.gr (d) Thermomax.com (e) shop.solardirect.com

These Built-in storage collectors, for a number of reasons have attracted attention and thus have been presented in more detail in the following section.

2.2.1 Built-in Storage or ICS Solar Water Heater

The Built-in storage SWH- also known as ICSSWH (Integrated Collector Storage Solar Water Heater) - because of its design simplicity and low cost is the oldest heater design that is still popularly used. The first recorded evidence of its deployment was in Maryland and Texas, USA [2]. The heater's geometrical design at that time was based on intuition rather than calculation. In 1936, the first detailed scientific study was carried out on ICCSWH at University of California Agricultural Experimental Station, USA [3]. This study was carried out on single, multiple tanks open and closed ICS systems. In the following period, the investigations were discouraged due to the discovery of oil and natural gas until the 1970s where they came to a complete halt.

The performance of the ICSSWH has an edge over other types for two main reasons. First is the direct contact of the working fluid with the absorber plate (the heating surface). This enables heat to be directly transferred to water, eliminating the need of a heat exchanger resulting in increased system efficiency. The other reason is the absence of conduits and connecting pipes to the storage tank, which are responsible for the bulk of the heat losses in other types. Additional benefits of ICSSWH are its effective use of direct and diffuse radiation, no solar tracking requirements and minimal maintenance. As mentioned in section 1.5, the aesthetics play a vital role in the wider acceptance of any product. A huge advantage of the ICS is its bespoke flexibility. It can be made in designs that seamlessly integrate in the roof structures. This eradicates the concern regarding the defacing of outlook of a property because of any prominent non-structural installations particularly in conservation areas. This is not the case with other collector types such as a thermosyphon or the focusing collectors that protrude considerably.

Numerous designs of the ICSSWH have appeared in the texts over the years. Kemp's design [4] (1891) being the oldest (see fig 2.2) was basically three cylindrical interconnected vessels boxed in a glazed wooden frame. In the 1950s, the closed

membrane or plastic bag ICSSWH, sometimes referred as the 'plastic pillow' type were developed in Japan. This was a large rectangular Polyvinylchloride bag; with the bottom surface a black membrane and the top membrane transparent. Approximately 240,000 units of this type were sold in 1963–64 [5]. Chinnappa and Gnanalingam [6] in 1973 tested a built-in storage heater which consisted of a square coil of 7.5 cm diameter pipe, 13.5 m in length, in a wooden box with heat insulation at the bottom and two glass covers.

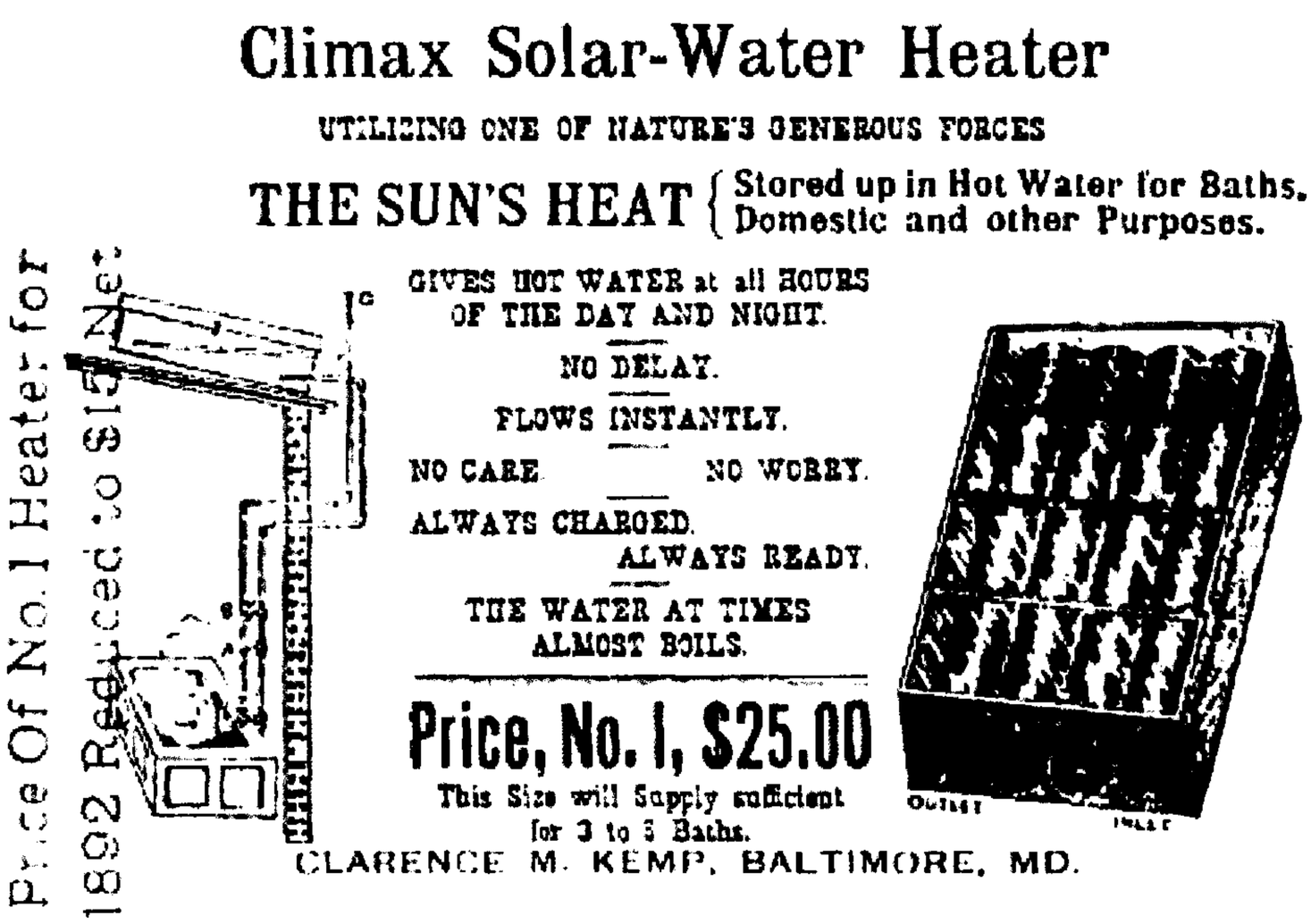

Figure 2.2: Climax solar water heater advert poster

Heaters with triangular storage tanks described by several studies perform better because of increased natural convection. Sokolov and Vaxman (1983) [7] analyzed the performance of an integral compact solar water heater numerically and compared the results with the experimental data. They investigated two solar water heaters, one with a rectangular and the other with triangular shaped tank. A baffle plate in their design separated the absorbing area and the storage tank. An efficiency of 53% for the triangular storage tank system was estimated. The comparative study between rectangular and triangular tank was later conducted by Soponronnarit et al [8] with similar storage volume (75 lt), absorber surface (0.7 m^2) and identical operating conditions. Efficiencies of 63% for the triangular tank and 59% for the rectangular tank were recorded. The triangular design saw added attention by Ecevit et al (1989)

[9] who studied triangular collectors of different volumes. In his research collectors were observed to operate with high efficiency during the heating period and also during the 24-hour cycle.

Mohamad [10] built on previous developments on triangular ICS systems with baffle plates and introduced a simple thermal diode to prevent reverse circulation at night-time. The thermal diode consists of a light weight plastic 'gate' that allows one-way flow only, located at the entry to the baffle at the bottom of the vessel. Mohamad presents vessel storage efficiencies of 68.6% and 53.3% for the vessel with and without the diode, respectively.

More recently, a trapezoidal storage tank design for the Mediterranean climate has been suggested by Cruz [11] (2002). The unique shape of the heater induces thermal stratification in the water store. A thermal network analysis model was used to assess the energy-saving potential of this system. It indicated that a 30–70% reduction in daily load could be obtained in contrast to direct, electrical or gas, heating.

To the best of author's knowledge, the first ever year round performance study of a built-in storage heater was carried out by Garg & Rani (1974) for Jodhpur, India [12]. The tests showed that collector supplied 90 litres of water at a mean temperature of 50 °C to 60°C in winter and 60°C to 75°C in summer. The thermal efficiency (energy received on collector aperture / energy absorbed by water) was found to reach as high as 70%. Year round performance for a similar heater but with different dimensions was recorded for Benghazi, Libya and has been reported by Muneer et al [13, 14]. His studies also included a comparison between ICSSWH and thermosyphon type collectors. It was found that even though simple and low cost, the ICSSWH heater edged out the thermosyphon collector. To enable a valid comparison between the two, the absorber plate areas and storage volumes for both types of heaters were kept the same. The schematics diagrams of different types of ICSSWH are presented in fig. 2.3

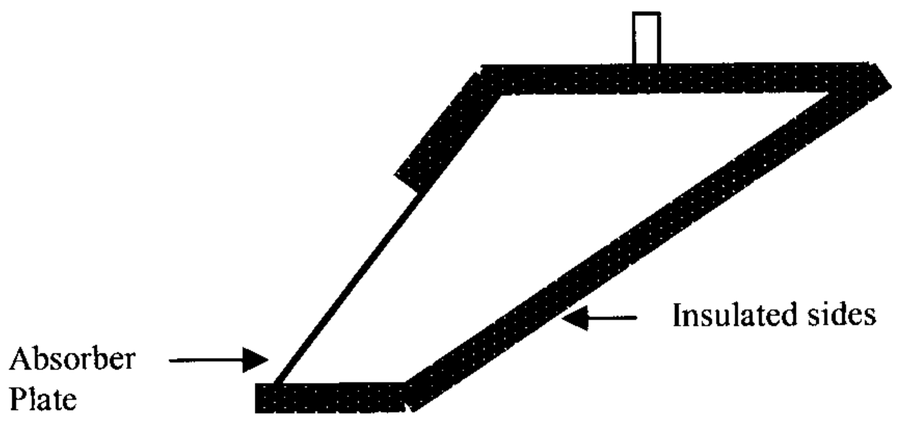

Trapezoidal heater by Cruz et al for Portuguese conditions [11]

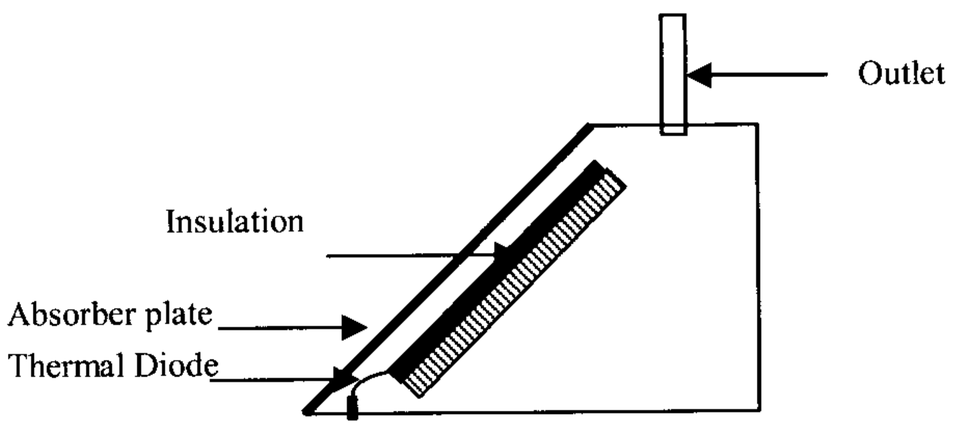

Schematic diagram ICS heater by Mohammad [10]

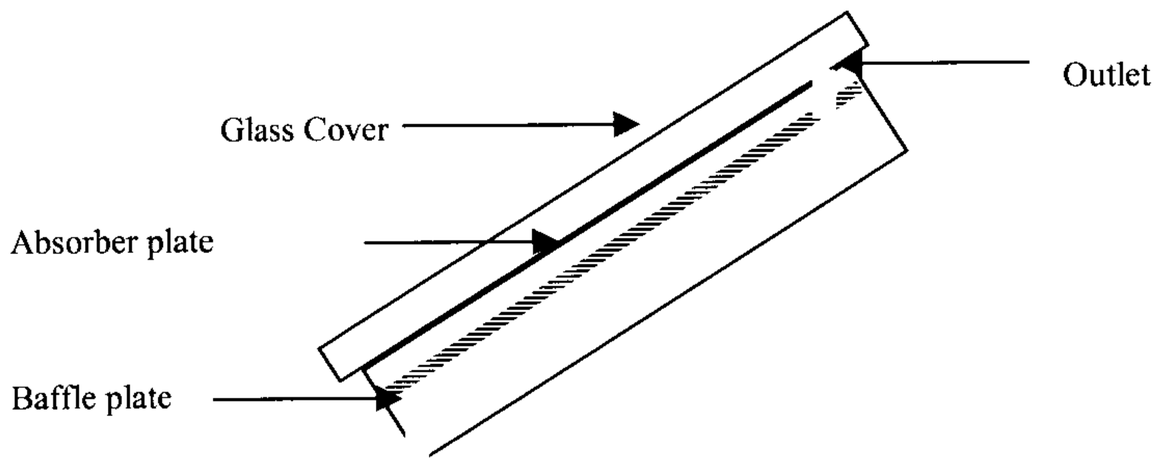

Schematic diagram of heater by Garg and Rani [12]

Figure 2.3: Various designs of ICSSWH

The depth of the storage tank of the ICSSWH is a critical design parameter. Muneer et al [13] in a separate parametric study of built-in storage type computed efficiencies of 65% and 73% for storage tank depths of 6 cm and 8 cm depth respectively. Increase in depth enhances the storage volume which makes the system operate at lower temperatures and so the losses are curtailed. A new design was proposed by Muneer et al [8] having the addition of fins inside the storage tank. The heater was fabricated and field tested in Lahore, Pakistan [8]. It was observed that the fins not only did thermally prove effective but also added to the structural stability. The solar fractions[†] at the time of the tests were found to be 63% and 73%.

More recently Smyth et al (2005) [2] chronologically summarized the development and performance of ICSSWH. In his study, popular collector designs from Japan, Australia, South Africa, USA and Israel were covered. The regional, environmental and economical factors that have shaped the heater design were also reviewed. The article did not take into account the quantification of heat transfer of the reviewed collectors. The performance comparison to gauge the effectiveness of heaters had also been largely neglected. Smyth [2], however has described methods to benchmark performance of all heaters through common performance indices. The development of different designs of SWH over time has propelled the need of a common criterion to measure the effectiveness of a heater. Organizations such has "European Solar Collector System Testing Group (ESCSTG)" came into existence as a result. ASHRAE (American Society of Heating, Refrigeration and Air Conditioning Engineers) has also developed test procedures to asses the heaters. These standards can be referenced in ASHRAE-standard 95[15]. Smyth has outlined various other procedures developed as "add-on" to the mentioned standard. He has also identified the absence of a long term performance solution to SWHs in standard-95.

The most common test procedure is a combination of test methods proposed by the ESCSTG [16] and gives a realistic ICSSWH performance representation which allows direct comparison with other experimentally investigated ICSSWH. The collection efficiency is superficially similar to the Hottel-Whillier-Bliss equation for distributed type solar collectors [17], but applies to diurnal system performance. Plots of

---

[†] For definition of Solar Fraction please look at textbox 1 (page 40)

collection efficiency are made against values of $\Delta T^{\circ}/ I_{ave}$ where ΔT° is the difference between the average vessel water temperature of the heating period minus the average ambient temperature over the same period and I_{ave} is the average insolation on the collector aperture. However, direct comparison of measured system performances is quite simple; predicting the performance of an ICSSWH at another location or different installation set-up is more challenging.

As stated earlier, the major drawback of the ICSSWH is the night time heat loss. Due to high collection area, the losses to the sky are predominant, mainly on cloudless nights. This shortcoming fostered the emergence of thermosyphon heaters. Several solutions to abate this problem have been proposed. A favoured suggestion is the withdrawal of water from the collector at the end of each day. An alternate solution by Muneer et al suggests placing a wooden cover on top of the tank. Rommel and Wagner [18] have suggested the use of transparent insulation material (TIM). Several modern day collector designs incorporate TIM. The use of TIM results in increase of the overall cost of the heater; however the need for daily human activity- for placing and removing cover- is eliminated. The use of a self regulating cover (electro-mechanical system) on the other hand would not only increase the cost of the heater but would also add to the maintenance cost. The overall reliability of the system is also impaired. Kaptan and Kilic[19] have put forward the idea of using an insulated baffle plate or a phase change material as a possible remedy. The use of baffle plate was first suggested Straaten [20]. Garg and Rani (1982) [21] carried out extensive theoretical and experimental studies on 90 litre rectangular tank with dimensions 112 x 80 x 10 cm. They have ascertained that the use of an insulating baffle plate inside the storage tank improved the performance of the system significantly during the day as well as the night time. On the other hand they also concluded that the use of insulation cover performs more efficiently during the night time than the baffle plate.

In a very recent investigation, a novel design of inverted absorber plate built-in storage collector has been proposed by Smyth et al [22]. The novelty of the heater is that it heats from the bottom surface, which due to buoyancy effects is more efficient than heating from the top. An additional advantage is the alleviation in the night time losses. This is attributed to the storage tank mounted in the tertiary cavity of a compound parabolic concentrator with a secondary cylindrical reflector. Smyth also

observed that using partial transparent baffles at the entry to the secondary cavity reduces convective heat transfer from the absorber to ambient without significantly reducing the optical efficiency.

Recent studies by Trinkl [23] confirm better performance (energy yield) of the flat plate collector over the vacuum tube collector for the same gross area throughout the period of observation. This study was carried-out in a Bavarian countryside house in Germany (latitude 48°). The vacuum tube collector shows superior efficiency in lower latitudes and warmer climates. At higher latitudes such as Scotland, Holland or Germany, the built-in storage tank performs comparatively better. It was also mentioned earlier that thermosyphon were ruled out based on earlier comparative studies by Muneer et al [14].

2.2.2 Glazing / Covers

Duffie and Beckman [24] suggest the use of additional covers to minimize heat losses incurring through radiation and convection. Charts for single, double and triple glazed collectors against the top-loss coefficient have been computed to provide a measure of the collector performance. Encouraging results of using additional glazing were observed by Muneer [13] in his parametric study of the Built-in storage type. He compared similar vessels with single and double glazing and found a difference of 1-10 °C in the temperatures values throughout the period of observation. Similarly, the effect of up to six glazing layers in freezing climate was checked by Bishop [25]. The results indicated 2.88m^2 of glazing produced enough water for a family of four in January in the climate of Denver, USA.

Addition in glazing layers reduces mainly the convective losses to the ambient; however it has to be kept in mind that the increase in glazing also increases the transmission losses. A possible solution to offset this problem is the use of selective coating on the glass cover itself. The increase in shading of the absorber plate with the increase in glass covers is too an associated adverse effect. Higher glazing hinders the collection of diffuse radiation as it tends to channelize the incident radiation. For longest life and maintained transmissivity, the most appropriate glazing material is tempered plate glass. Of the various grades of tempered plate glass, low-iron glass has

the highest transmission and lowest reflection of sunlight as explained by Symth et al [2] and used by Bishop et al [25]. The most important property required of a glazing material is high transmittance of solar radiation, as any loss in transmittance will lead to a direct reduction in collection efficiency.

The cost of the collector goes up with the number of glazing layers which incites the need to strike a balance for optimal solution. The spacing of covers or glazing has sparked a lot of interest in the research community. It had been a general practice to employ a distance of 2.5 cm (1 inch) between the first glazing layer and absorber plate. Hottel [26] has suggested through his experiments that increasing the air space beyond 1.27 cm had little effect on reducing the conductance, while Buchberg [27] has shown that the spacing between the tilted hot solar absorber and successive glass covers should be in the range 4-8 cm to assure minimum gap conductance.

The literature review for glazing /covers has revealed the prospect of significant improvement in the heater performance if the number of glazing layers is increased. Setting the right distance between the absorber and the cover is also a factor of paramount importance. The fact that the nature of heat transfer is a function of aspect ratio and the angle of inclination, leaves room for evaluating optimal parameters for Scottish conditions.

2.2.3 Absorber Plate

The foremost criterion for the absorber plate material is the high value of absorptance which can be achieved by applying coatings or dark colour paint. The other important feature is the non-corrosive nature. The use of metallic as well as non-metallic (polymer) absorber plates have been cited in the literature [24]. In a recent study of solar collector, a polymer storage vessel has been suggested by Liu et al [28] . In applications where the absorber plate temperature remains low, polymer absorber plates provide an effective low cost solution. The coating on the surface of the absorber plate is critical for the performance of the collector. The research in this area has given birth to the physics of selective and non-selective coatings.

The absorber plate should have high absorptance for insolation and at the same time low emissivity value. Duffie and Beckman [24] have given a detailed account of the effect of selective and non-selective surfaces. They conclude that "the temperature of the absorber plate in most flat-plate collectors is less than 200 °C (473k) while the effective surface temperature of the sun is approximately 6000K. Thus the wavelength range of the emitted radiation overlaps only slightly the solar spectrum. Ninety eight percent of the extra terrestrial solar radiation is at wavelengths less than 3.0μm, whereas less than 1% of the blackbody radiation from a 200°C surface is at wavelengths less than 3.0 μm. Under these circumstances, it is possible to devise surfaces having high solar absorptance and low long-wave emittance, i.e. selective surfaces. Many of the coating materials used are metal oxides and the substrates are metal. Examples are copper oxide on aluminium and on copper. A nickel-zinc sulphide coating can be applied to galvanized iron. Selective surfaces have been in use in Israeli solar water heaters since about 1950. Black chrome selective surfaces, have been widely adopted in the United States. It was found by Moore [29] that the average properties of production run collector plate with black chrome coating had α (absorptance) = 0.94 and ϵ (emissivity) = 0.08. Through vacuum sputtering processes metal and metal carbide coatings have been produced with extremely low emittance ϵ = 0.03"

As explained by Duffie and Beckman[24], "Burton and Zweig [30] have compared systems with a selective absorber with those painted a dull black. Although providing no quantitative results they found that the system with the selective surface coated absorber always produced the warmest water. The type of selective absorber used was a metallic nickelchrome type with an absorptance of 0.97 and an emittance of 0.10. A similar study by Duff and Hodgson [31] revealed that the efficiency of the collector with the non-selective absorber was substantially lower than the collector with the selective absorber. The application of selective coating is a regular practice in Australia, where the coating process is claimed to be cheaper than painting [32]"

To summarize, the absorber can be made from one of a wide range of materials, including copper, stainless steel, galvanised steel, aluminium and even polymers. While choosing an absorber material, it is important to ensure that it is corrosion resistant. It should not toxicate the heat transfer fluid used particularly in ICS where

there is direct contact of potable water. If a polymer is used, the absorber must be able to withstand the high temperatures that are reached on sunny days while stagnation (no draw-off from the collector). More importantly, the absorptance of the plate should be high.

2.3 Computational Fluid Dynamics (CFD)

In the last two decades, CFD has emerged as an effective tool for solving complex flow problems. It provides an insight to flow details that in the past was unachievable through experimental means. The technology has been well received by the industry. CFD now caters for a wide range of industrial applications from HVAC to Aerospace. The technology nonetheless is prone to errors due to numerical instabilities. Therefore the utter reliance on CFD alone is inappropriate and results should be validated through experiments. This drawback, poses a question on the advantage of the tool. A fitting answer in adjudication to the technology is that although CFD may not have entirely eliminated the need for experiments but has substantially reduced its amount. Figure 2.4 has been extracted from a recent report, it illustrates the use of CFD for product concept, product development and virtual prototyping to reduce the design cycle time [32].

Recent studies indicate an upsurge in the use of CFD for analyzing solar collectors design/ performance. Groenhout et al for example [33]- in a study on advanced collector design- has used CFD to compute the "h (convective heat transfer coefficient) value" as well as the dimensionless numbers (Nusselt number, Rayleigh number) for the collector.

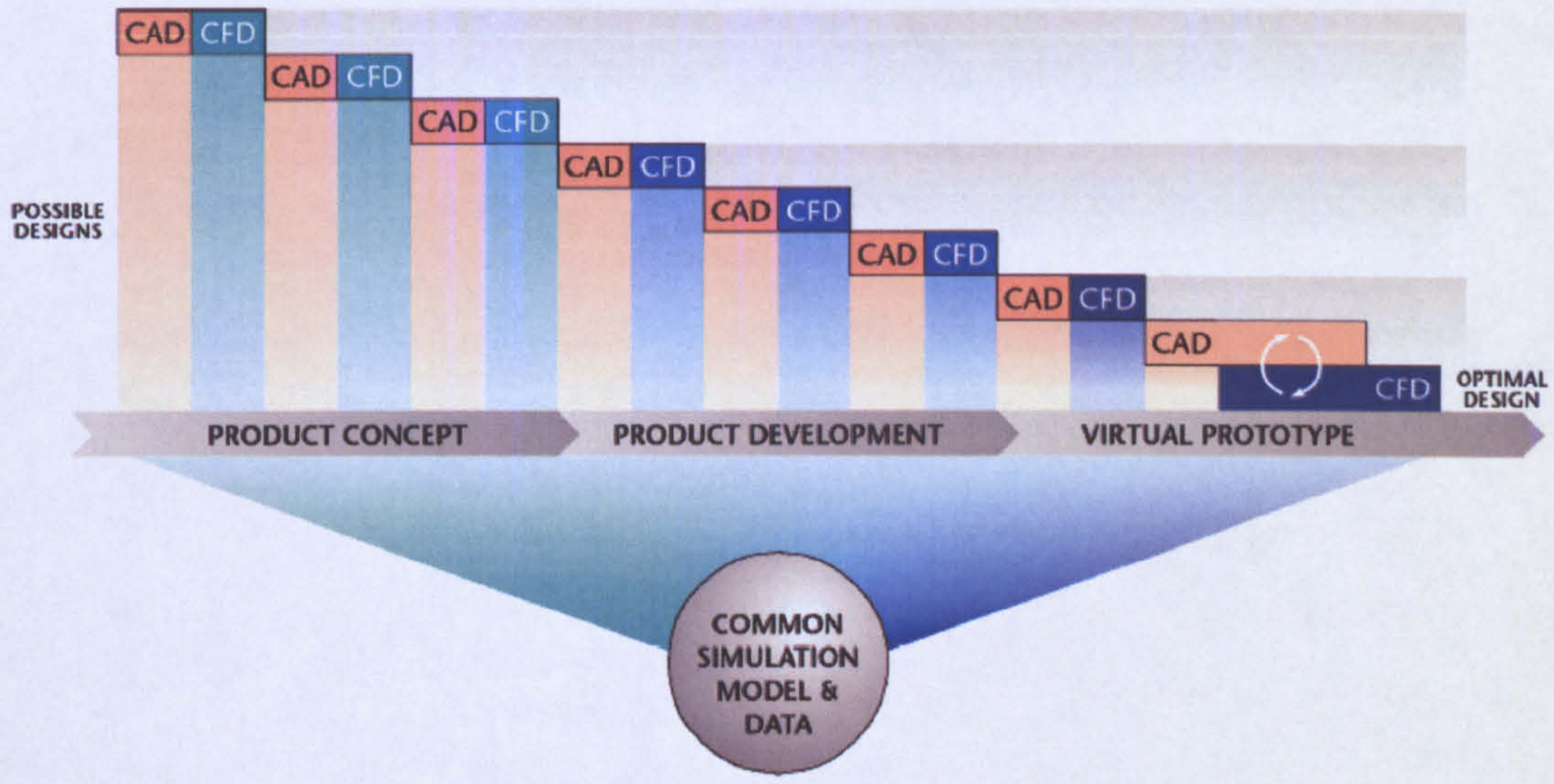

Figure 2.4: The use of CFD in the product concept, product development and virtual prototyping stages.

CFD analysis of solar water heaters can be divided into two distinct areas; the studies that involve natural convection between the absorber and cover and the convective heat transfer to the fluid side (water or anti-freeze). The latter has witnessed sparse interest. Numerical studies on the air-gap (the space between the absorber plate and collector) have seen more vigorous efforts, mainly for its usage in several other applications.

A CFD analysis can be done in two ways; an in-house CFD code (developed indigenously) or the utilization of available off-the-shelf software. For the current study, *Fluent* software was chosen as it has been the choice of several other research institutes in academia as well as commercial R & Ds. The exclusion of in-house development of CFD code can be explained. The option was ruled out to save time and effort. The proven success enjoyed by many commercial software a testimony to their high degree of accuracy. In addition to that the continual research for robust schemes, added stability and optimal usage of computational resources has catapulted the available software to technological levels that are simply unachievable by indigenous development. It was also foreseen that the analysis had to be done in 3D, thus another reason that prompted the usage of existing software.

Although thermocouples are reliable for measuring point temperatures, their use in high number generally hinders the flow and moreover is a costly measure. CFD on the other hand can generate a complete thermal map of the system. Not only can the temperatures be evaluated, but the velocities throughout the computational domain can also be computed. CFD has therefore its own niche when it comes to deeper insight which is a key requirement for optimizing the solar heater.

One of the first relevant numerical studies was that by Ozoe et al (1983) [34]. Employing a finite difference technique, he calculated the longitudinal roll pattern for a cavity heated from the bottom and calculated the changes with different angles. His study was a generic and did not specifically target SWH application. An even earlier numerical study on cavities was that by Gill (1966) [35]. His pioneering study used a finite element method and solved for the flow in a square cavity. To the best of author's knowledge, this is the first CFD study after the Courant Frederic and Levy condition (CFL) was established. The CFL was a breakthrough development that provided a stability criterion for hyperbolic equations. The CFL condition dates back to 1928 [36]. The work by Gill led to subsequent work which was more closely related to the solar water heater. Zhong (1985) [37] improvised on the work by Ozoe and probed deeper by monitoring the effects of varied fluid properties.

The work on the flow pattern inside the water tank or storage tank of a built-in storage tank is still largely an unexplored avenue. Groenhout et al [33] conducted a 2-dimensional CFD analysis to experimental results. He employed a conjugate analysis method involving both radiation and convection in CFD. The results show undershoots of CFD data when compared to the experiment values.

2.4 Stratification

Thermal stratification plays a vital role in regulating the total heat absorbed and delivered by the heater. It is a desirable natural phenomenon which is required to be sustained inside the storage tank. Several studies on stratification have been done for vertical storage tanks that are connected separately to the collector. For integrated

collector storage, the occurrence of stratification has been reported but not analyzed. Experimental study of stratified hot water storage tanks was undertaken by Zalman and Thompson (1976) [38]. They asserted that even at very large flow rates, thermal stratification improves with increasing L°/D°, ΔT^{1} and the inlet and outlet port diameters and it decreases with the increasing flow rates. The merits of stratification have been thoroughly described by van Koppen et al in 1979 [39]. The study was carried forward by Furbo and Mikkelsen (1987)[40] and later by Hollands and Lightstone in 1989[41]. They have all highlighted the thermal benefits of high stratification and emphasized the use of low flow rates, which enhance the collector performance.

Several multi-node stratified tank models have been developed and have been compiled by Duffie and Beckman[24]. These models though are only applicable to vertical storage tanks that are a part of the solar heaters where the collector and water storage tank are separate components e.g. Thermosyphon collectors. For integrated collector storage, having the storage tank at a titled position, no thermal stratification model has been suggested as yet. Stratification bears the key to evaluating the actual heat content inside the heater, which is vital for estimating the efficiency. The only study on stratification in the built-in storage was reported by Muneer [13] showed no significant influence of performance with a change in depth. The study involved vessels of 6cm and 8cm depths. This however might not be the case for heaters installed at higher angles such as in Scotland.

To maintain and promote stratification in storage tanks, several methods have been suggested. These include the utilization of sleeves, partitions, baffles, and porous intake manifolds, and low flow rates. A water storage tank will naturally remain stratified until water is supplied to the load. As the hot water leaves the tank and fresh cold water is infused, mixing occurs -as a result of flow circulation - which leads to de-stratification. The degree of stratification in an ICS depends upon the angle, the exposure time and the incident solar insolation. Convective heat transfer helps the fluid to settle to the top corners of the tanks and thus aids layering of water inside the tank. During night times or when the collector is shaded, losses incur which leads to stratification decays.

In light of previous studies, it was concluded that stratification in the tank is a crucial state that holds the key to efficient design. The location of the outlet and inlet pipes should be designed in accordance to the stratification studies.

2.5 Draw-off Characteristics

Water is not normally drawn from a water heating system uniformly throughout the day. The patterns of use may vary considerably between households. This poses a need to establish an average pattern for the demand of hot water for Scottish homes. The rate and amount water drawn is crucial to the performance of the heater. More explicitly, the greater the quantity of the fluid displaced, the lower the system temperature and consequently the higher the thermal efficiency. Higher flow rates ensure overall low temperatures of operation which keeps losses to a minimum. However, higher draw off also result in low grade energy output by the collector. Therefore a balance has to be struck between the flow rate and lowering collector temperatures.

The draw-off characteristics help sizing the storage tank. In an ICS, the heater storage capacity can be increased by increasing the either the surface area or the depth of the heater. Shallow heaters result in giving high grade energy output on a low efficiency while the opposite is true for heaters with deeper storage tanks. Increase in the surface area is also coupled with the night time losses. Storage volume / surface area ratio is the determining factor when designing a tank for any specific location. Previous studies suggest that high flow rates during draw-off are detrimental to the heater performance.

In a study carried out in Benghazi, Libya; Muneer et al [13] tested four different modes of water draw-off. Efficiency as low as 53.8% and as high as 95% by the variation in the flushing patterns was recorded.

Sodha et al. (1984) [42] analyzed the thermal performance of several built-in storage water heaters connected in series. The study again was carried out to provide a solution to counter the adverse effect of cold water induction in the storage tank.

Holland and Lightstone [41] claim that by using low collector flow rates (roughly one seventh of those that have been generally used) and by taking measures to ensure the water in the storage tank remains stratified, the energy delivered by a forced-flow solar system can be increased substantially. In addition, the lower collector flow rates permit substantial savings in system cost, mainly through reduction in plumbing costs. The influence of collector and heat exchanger flow rates on the performance of the heater have been investigated by Fanney and Klein [43]. In their experiments, substantial improvement was observed in side by side testing as a result of lowering the collector fluid flow rate for direct systems. The improved thermal performance was attributed to better stratification within the solar storage tank and a significant reduction in mixing, which occurred between the solar and auxiliary heated portions in a single tank system.

Courtney et al [44] has carried out a multinomial analysis of water demand for the UK. The aim of the study was targeted to water usage in domestic properties. It was concluded that the multinomial distribution is well suited to the synthesis of combined demand on building services from a group of users. Cruz et al [11] has utilized hot-water demand for simulation using the British Standard 'domestic heating-load profile' standard for his study involving trapezoidal heater. In a subsequent study by Courtney [45] the pattern of water use on the calculated heat output was investigated. Three alternative usage patterns were employed each taking a daily total of 170 lt. The effect was found to be clearly not insignificant and an evening peak in consumption will maximize the contribution of the solar system. A change in the daily total to 250 lt while keeping the hourly proportions of the standard pattern increased the annual heat output of the reference system from 5.26 GJ to 6.3 GJ and with this increased water consumption, 6m^2 of collector area supplied 7.77 GJ.

2.6 Natural Convection in Inclined Cavities

Natural convection in inclined cavities is important to study, particularly from the perspective of a solar collector. It epitomizes the principal heat loss from the collector. Over five decades of research on the topic classifies it as a well documented

and widely explored area of research. The dimensionless analysis on inclined cavities reveal that the average Nusselt number[‡] (Nu) depends upon the Rayleigh number (Ra), Prandtl number (Pr), vertical and horizontal aspect ratios, angle of inclination ϕ and the end wall boundary condition. In the case of solar collectors, air is the working fluid for the heat losses from top surface for which the Pr is nearly constant (0.71). This simplifies the behaviour to some extent. The studies on vertical air layers and horizontal slots have been studied far more than inclined cavities.

A brief history of cavity behaviour is presented herein. The principal investigation on inclined cavities was carried out by De Graaf and Van der Held in 1952 [46]. Dropkin and Somerscales (1965) [47] followed the research and conducted numerous experiments involving liquids, for which Ra range was 10^5-10^9. Increasing popularity of solar heaters in the early 1970's encouraged Hart [48] to explore stability of the flow in inclined cavities, he did not however quantify the heat transfer. In the late 1970's and early 1980's experimental research was performed by a number of researchers for determination of critical Ra and critical angle for cavities with high aspect ratios (H/L)[37, 49-53]. The following decade saw a boost in progress, owing to the increase of computing power. Initially, only low Ra and small aspect ratios were investigated. More complicated studies, involving higher Ra numbers and aspect ratios, were picked up as passage of time gave way to more robust computing machines. In the 1980's the knowledge of flows was extended by numerical investigation of 3D aspects [34, 54-56]. The influence of variable fluid properties and radiation was later inspected by Zhong (1985)[37] Recently the study of cavities has been broadened by additional variations that include electromagnetic effects [57], variations of geometry such as effect of curved wall [58], addition of partitions, shallow or long cavities with aspect ratio less than 1 [59], changes in the boundary conditions such as spatially varying temperatures[60]. The wide-ranging work of Ozoe et al (1974-1983)[34, 54-56] is a proven cornerstone of the subject. His work includes theoretical (2D, 3D), experimental and photographic proof of the long rolls generated.

[‡] For definition of dimensionless numbers see textbox 2 (see page 74)

To date heat transfer in air cavities has been examined experimentally up to Ra = 10^8 [61]. Areas related to turbulent behaviour for high aspect ratios of cavities still remain vague and unexplored. Higher values of both the aspect ratios and Ra number lead to instabilities, the numerical solution of which also becomes complicated, if not impossible.

For three dimensional study of the inclined cavity, two aspect ratios have been defined (see Fig.2.5). The vertical aspect ratio is the height to length ratio (A= H/L) and has been the focal geometrical parameter for nearly all previous studies. The other aspect ratio is the cavity width to the cavity length (A_H= W/L) ratio, more commonly referred as the horizontal aspect ratio [13]. As long as the horizontal ratio is large, the dependence of flow on this parameter is negligible. The term 'aspect ratio' (A) unless defined, hereafter would imply a vertical aspect ratio. Flat plate collectors generally have an aspect ratio (A = H/L) above 12 for the air cavity. Focus was kept on studies close to these ratios which are classified as medium and large ratios.

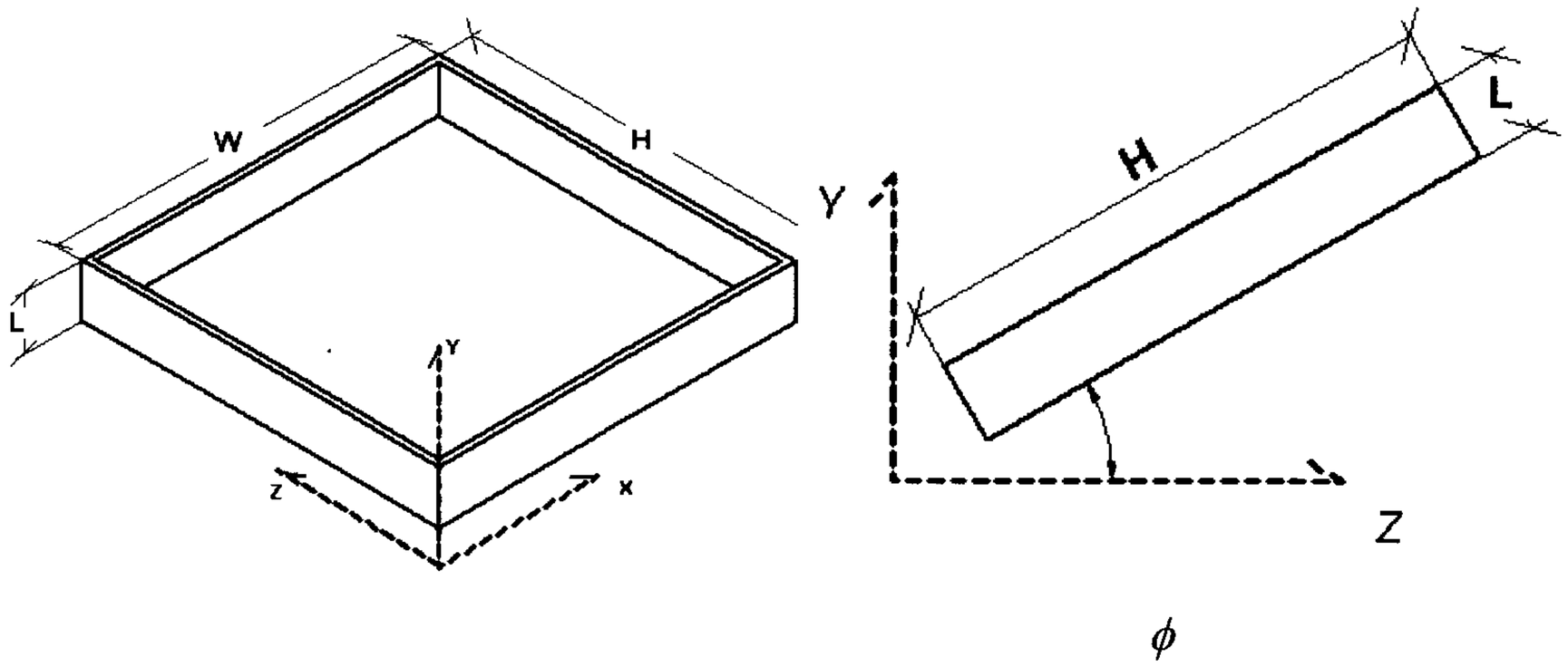

Figure 2.5: Cavity shown in 3D with the coordinate axis. The inclination angle remains in the Y-Z plane

The previous research on cavities is summarized and has been split into two sections. The first section examines the cavity behaviour in the range of angles $\phi = 0^\circ$ to 90°, while the subsequent section epitomizes behaviour in the range $\phi = 90^\circ$-180°. A

comprehensive review on inclined cavities can also be referenced from the review report of Yunhua Yang [62].

2.6.1 Cavity Behaviour in Range ϕ = 0° – 90°

The flow behaviour between ϕ 0° to 90° is intricate and therefore has been subjected to extensive research. In this range, two types of flow instabilities exist, one is the static top heavy instability associated with the horizontal case when the angle is near 0° and second is the gravitational buoyancy associated with the vertical case. The cavity is termed as horizontal when ϕ= 0° and vertical when ϕ= 90°. At vertical orientation, the direction of the temperature gradient is perpendicular to the gravity force and any finite Rayleigh number would cause the circulation motion of the flow in the cavity. However, for small Ra i.e. ⊴000, the buoyancy driven flow is weak and heat transfer is primarily by conduction, thus implying the Nusselt number value again is unity [63].

For horizontal cavities (heated from below), the Ra has to reach a certain value before advection begins. This value is also termed as the critical Rayleigh number, which is reported by Holland and Konicek [32-33] as $\mathbf{Ra_c}$= **1708** for H/L, W/L>>1. Another value for horizontal cavities, $\mathbf{Ra_c}$ = **1080,** has also been suggested [34]. For lower values than critical, heat transfer takes place through diffusion (conduction) only as viscous forces overcome any advection. When the Ra exceeds the critical value, the flow becomes unstable and series of convective three dimensional rolls are formed. These rolls are more commonly known as Bénard cells. In case of inclined cavities the multi-cellular convection arises when the Ra exceeds **1708/cos** ϕ. Ozoe et al [56] have photographically shown, using aluminium powder as a tracer that each of these rolls is confined to a rectangular volume whose dimensions do not change with inclination i.e. each fluid particle remains within the cell. These cells not only appear along the length but also the width of the cavity. The width of the cell is experimentally shown by Dubois and Berge to remain equal to cell height for a Ra up to 10 times the critical value in the case of large-Pr fluids [23, 35]. Oertel [64] carried out experiments for nitrogen (Pr = 0.7) and found that the number of roll cells in a 4 x

10 x 1 horizontal box changed from 10 to 9 at Ra =2300, to 8 at 5680 and to 7 at 8900. On the other hand, for silicone oil (Pr =1780), the number remained at 10 up to Ra =12000. Each cell rotates with a sense of rotation counter to its adjacent cell. As the angle of inclination is increased, the strength of rolls with an axis parallel to the x-axis increases. Cells with axes parallel to the height– axis (up slope axis) tend to get weak and finally break up with increasing inclination. Ozoe et al has given a detailed account on the nature of the flow through the finite difference solution of cell. The streak lines resulting from finite difference calculation for reduced domain give a noteworthy picture of the 3D nature of the flow (See Fig 2.6).

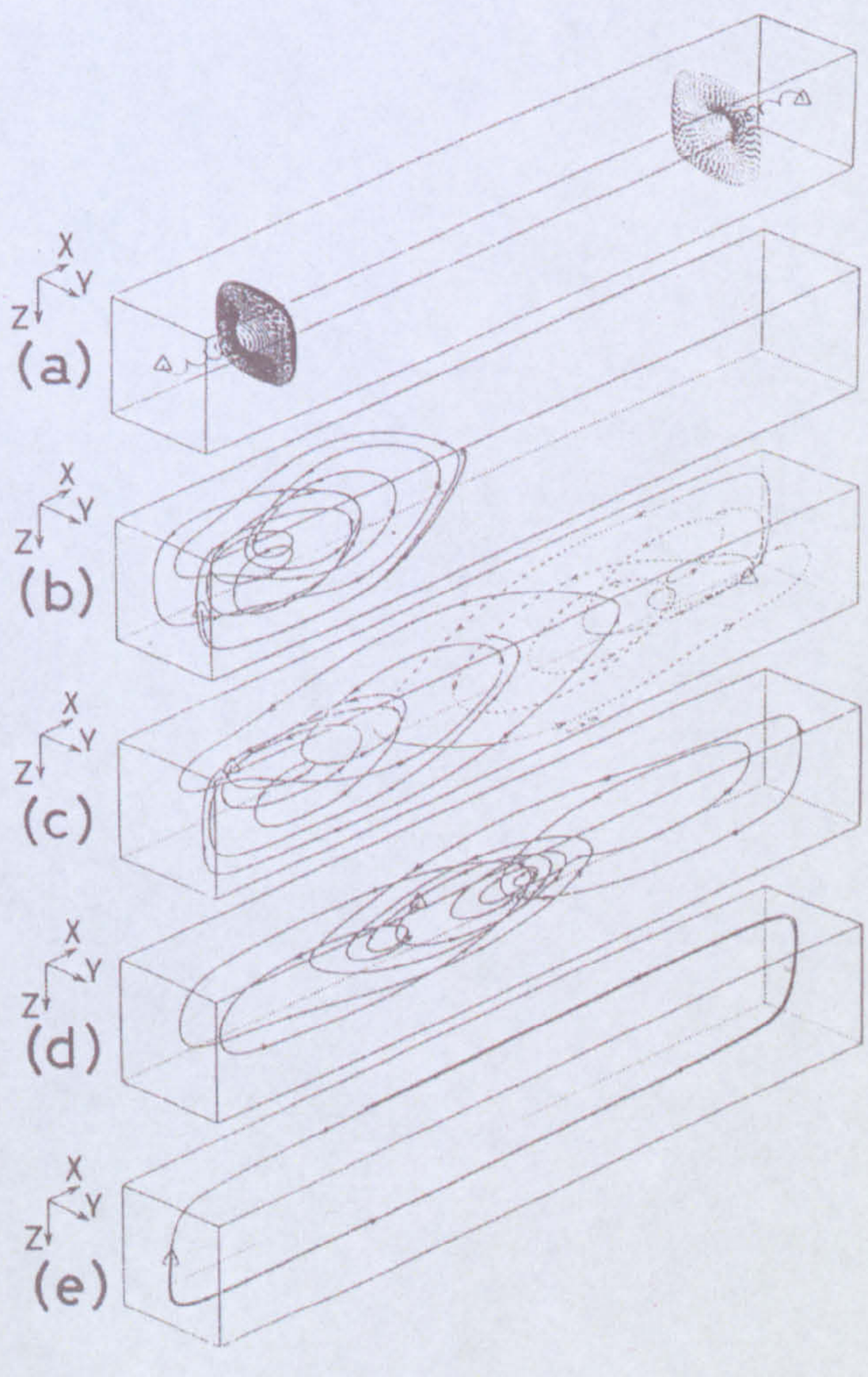

Figure 2.6: Perspective view of streak line from 3D finite difference calculation of Ozoe et al with free-free cell boundary condition, The angle of inclination lies in the X-Z plane (a) $\phi = 0^\circ$ (b) $\phi = 20^\circ$ (c) $\phi = 30^\circ$ (d) $\phi = 40^\circ$ (e) $\phi = 90^\circ$

Original figure reproduced from [33]

It was also found that the minimum heat transfer is associated with the angle where the flow characteristics change from multiple cells to a single cell. This angle is called the critical angle. The critical angle is dependent on both the Ra and the aspect ratio. It has been confirmed however that the aspect ratio has far more influence on the critical angle as compared to the Ra. Increasing aspect ratio shifts the critical angle towards the vertical orientation 90°. In an article by Soong [65], it has been validated that the transition point of the flow also moves to a higher angle as the Ra increased.

Table 2.1 lists the values of critical angle at various aspect ratios. As the angle is increased from horizontal to vertical it is found that the flow nature is 3D before the critical angle is reached, reliance on CFD results from 2D analysis therefore is inappropriate. Yang [62] has given comprehensive detail on the 2D CFD analysis compared with the results of experimental testing. After crossing the critical angle, the flow converts itself into single circulation roll with an axis parallel to the depth (in-page) axis. The flow rising along the hot wall joins the flow descending down the cold wall and vice versa to make a complete loop along the walls. The nature of this flow is two dimensional which can be tackled using 2D CFD analysis. Turning to Table 2.1, it can be noticed that for an aspect ratio >12 the critical angle is 70°, which implies that only the angular span of 20° between 70° and 90° can be analyzed using 2D CFD analysis. As most solar collectors would have an aspect ratio above 12, 3D CFD studies are essential for conclusive analysis.

Table 2.1: Critical angle for various aspect ratios [66]

A (H/L)	1	3	6	12	>12
ϕ_C	25°	53°	60°	67°	70°

For medium to large aspect ratios cavities with vertical orientation, the effect of high aspect ratio is the delay in the departure of Nu from unity to larger values of Ra. Hollands et al has also reported that for increasing aspect ratio, the contribution of convective heat transfer to the average Nu becomes vanishingly small so that the average Nu reaches unity.

Summarizing all the results, the established trend in a cavity with high aspect ratios would be the steady decrease in the Nu with increasing angle till a local minimum is reached. This point marks the critical angle. The Nu from this point onwards escalates, but with a gentle slope. This general trend for high aspect ratios is depicted in Fig. 2.7.

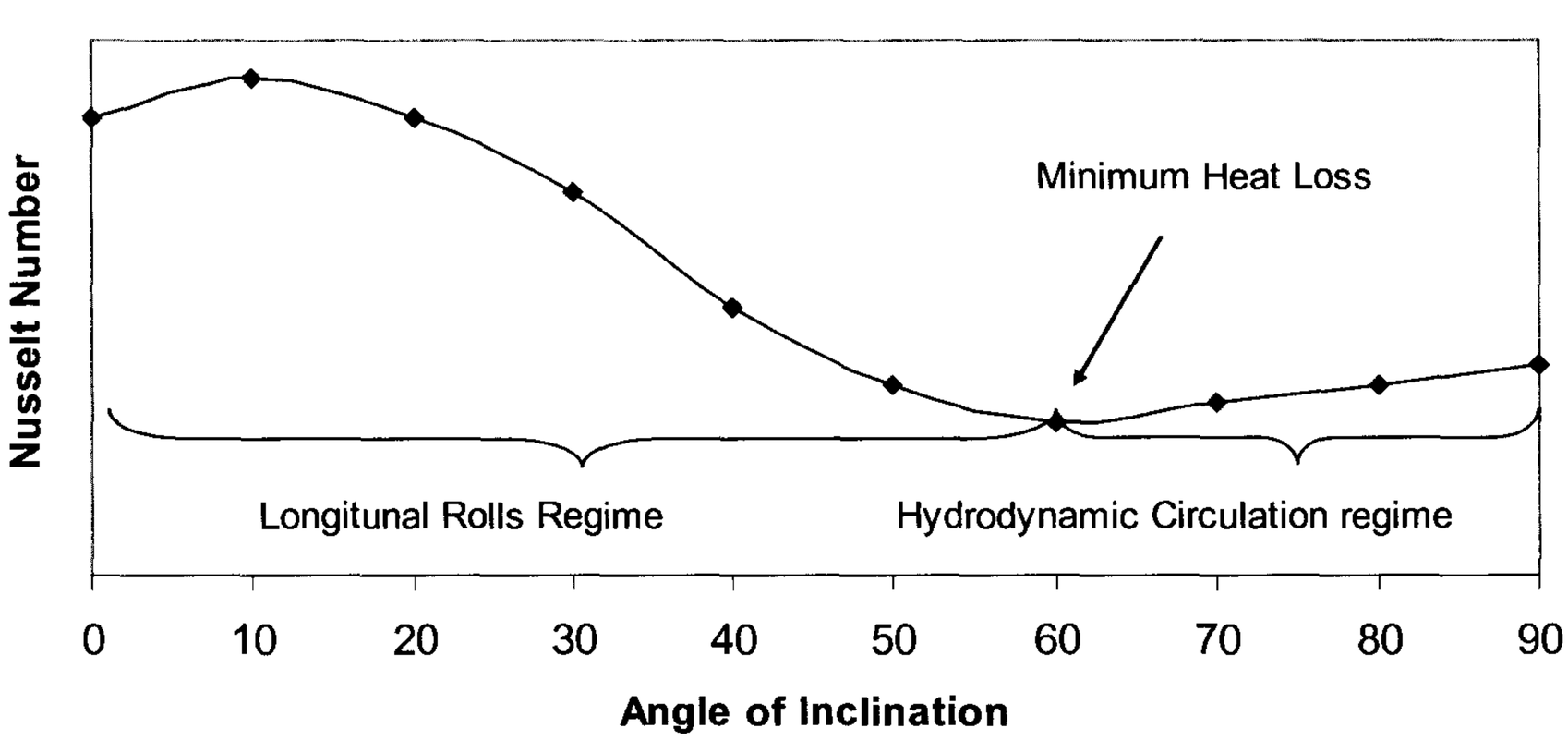

Figure 2.7: The Nusselt number trend (hypothetical) at high aspect ratios

2.6.2 Cavity Behaviour in Range $\phi = 90^{\circ} - 180^{\circ}$

To date the work done on cavities for $90^{\circ} \leq \phi \leq 180^{\circ}$ has witnessed lesser attention as compared to the previous range. From the perspective of current research, it is important to examine the behaviour in this range as it gives a clue to the water tank performance an ICSSWH (which functionally resembles an inverted cavity).

The cavity at 180° indicates "inverted horizontal cavity" i.e. being heated from the top. In terms of convection strength, this position is indicative of the worst case scenario. The Nu for a cavity at $\phi = 180^{\circ}$ is "1" according to study by Hamady [51]. This value implies pure diffusive heat transfer. The Nu remains unity at this angle, irrespective of the strength of the Ra for ZHF (Zero Heat Flux) boundary conditions. For LTP (Linear Temperature Profile) boundary conditions, however the Nu values

depart from unity for Ra $\approx 10^5$, as suggested by Elsherbiny in his experimental study of A=20 & 80 [67]. Advection begins with the slightest of rotation of the cavity towards the vertical position. Previous studies have shown velocity along the walls to increase as the cavity is rotated from "inverted horizontal" (180°) to a vertical position (90°). This increase in velocity accounts for the increase in Nu. Studies by Ozoe and Elsherbiny have shown this increase being sinusoidal. The rate of increase of the Nu with the Ra also depends upon the angle of inclination. The higher the angle the lower is the slope.

In general for the range of the $\phi = 180°$ to 90° the behaviour has marginal intricacy as compared to its mirror range. The nature of the flow all along is a 2-dimensional hydrodynamic circulation with axis of rotation parallel to the depth of the cavity (x-axis).

It is also a feature of flow in this range that for any given value of Rayleigh number, the departure of Nusselt number from unity is delayed with the increase in the angle (90°-180°). For any given angle and Rayleigh number the Nusselt number decreases with the increase in the aspect ratio. The results of Elsherbiny are depicted in Fig. 4 - 6 and sum-up the activity in this range. The increase in the delay in departure of the Nusselt number from unity with increasing angle can be noticed in Fig. 2.8 & 2.9. The effect of the increasing aspect ratio is the reduction of Nusselt number for the same operating conditions (Rayleigh number and angle of inclination) [67]. As ϕ is increased the change to turbulent flows occurs at higher values of Rayleigh number.

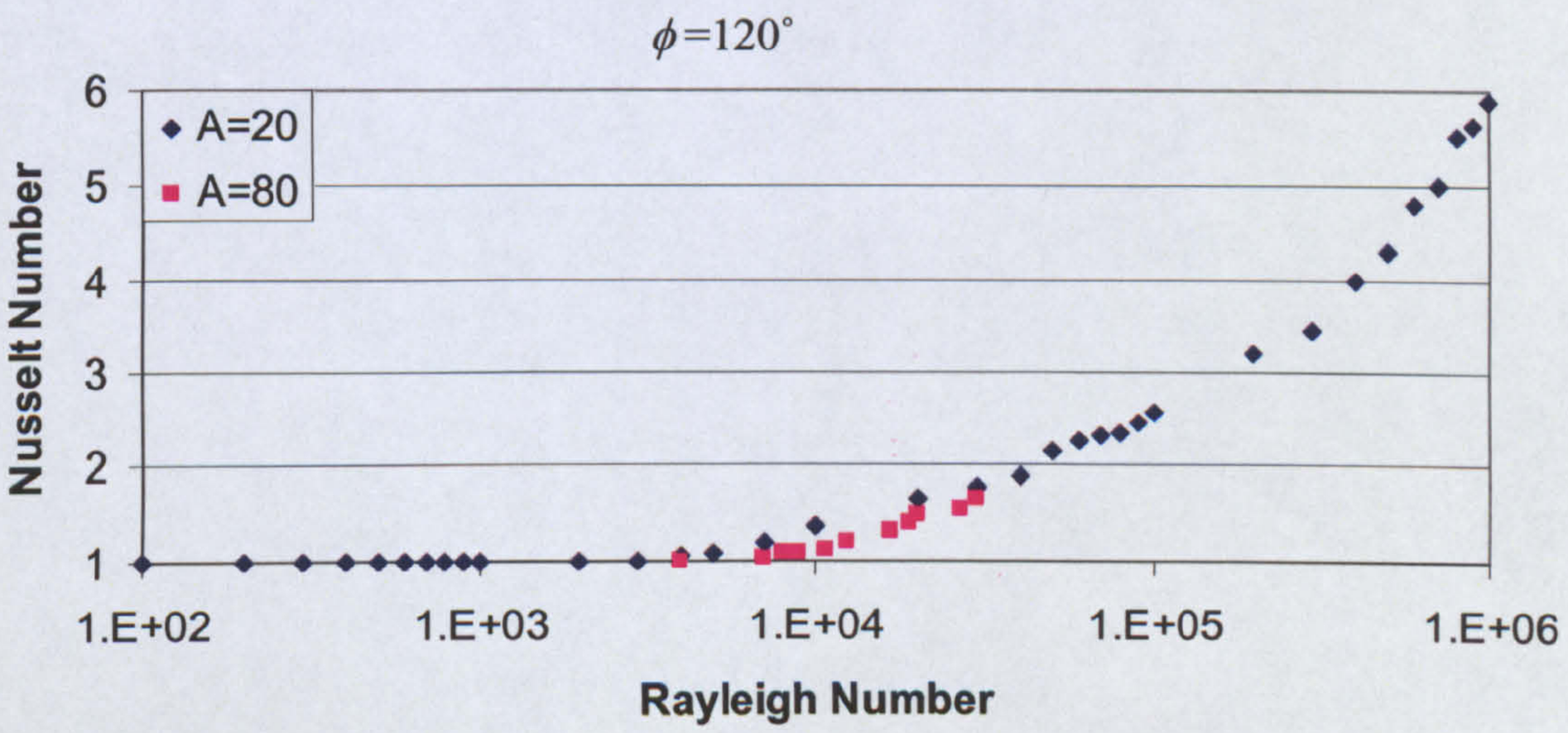

Figure 2.8: Experimental results for A = 20, 80 by Elsherbiny (1996) for different values of Ra at ϕ=120°

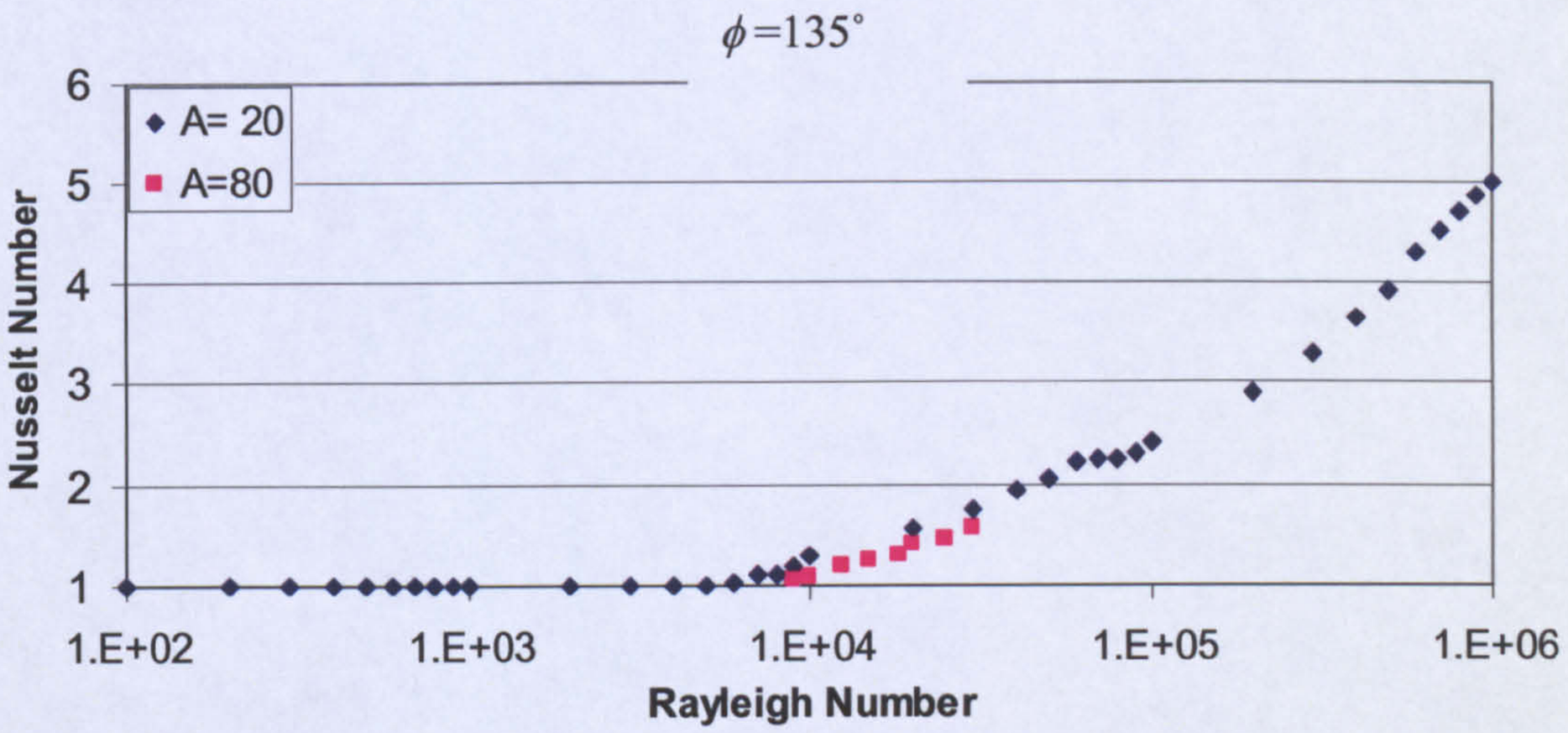

Figure 2.9: Experimental results for A = 20, 80 by Elsherbiny (1996) for different values of Ra at ϕ=135°

2.7 Solar Water Heating In Scotland

The incentives available for solar water heating Scotland were briefly reviewed in section 1.5. The studies done for solar water heating in Scotland are few and many of them are available as unpublished work. The work of Courtney which is primarily for UK and work of Imambi for housing society in (Moneymusk) Aberdeenshire, Scotland were used for guidelines. Similarly, the work of Kerr McGregor [1] is also utilized. In his opinion, Scotland is one of the best places for solar water heating.

The mains water supply in Scotland varies from 10°C during peak winter to 22°C during peak summer. Considering that the water temperature ideally for washing as well as shower purposes is about 40°C (18°C degree difference between the mains supply and required). Hence even in summer there is plenty of room for heating potable water. Furthermore, the occasional requirement of space heating in Scottish summer enhances the utility of hot water additionally. The detached homes are more likely to benefit from solar heating. As Scotland has a significant amount of rural dwellings, the benefit can be realized.

Imbabi and Musset [68] concluded that with careful construction, good thermal insulation, moderate thermal mass and properly controlled ventilation, the collector system can meet the space and domestic hot water heating requirements almost entirely. The annual total heating bill, with full price electricity, could be less than £50 per dwelling at 1994 price. Similarly, Courtney et al has put forward a number of points after his exhaustive study of solar water heating in the UK.

McGregor and Balmbro [69] showed that although solar availability was lower, as the heating season was longer, solar water heating systems provided a greater annual energy saving at higher latitudes. This is illustrated in fig 2.10.

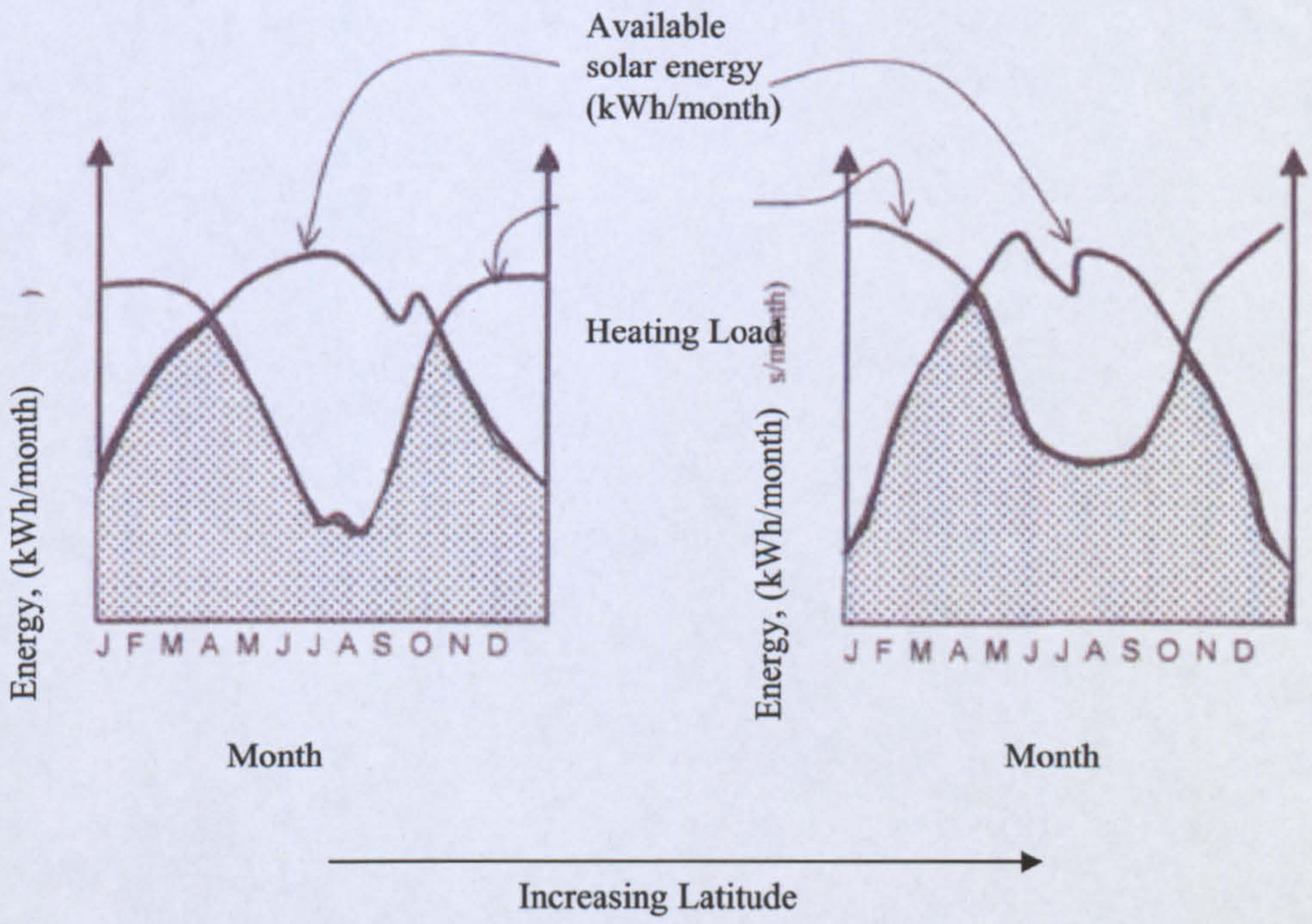

Figure 2.10: The available seasonal energy plotted against available solar energy increasing latitude [69]

All these studies and the commercial success enjoyed by the commercial concerns indicate the healthy prospect of solar water heating in Scotland.

2.8 Contemporary Commercial Designs in Scotland

In addition to the academic research it is also vital to observe some of the popular commercial solar hot water systems as substantial information can be obtained from

them regarding feasibility factors, constraints, common practices and preference of general public. Furthermore these systems indicate proven success and would lead to guidelines that are tested. There are several commercial concerns that provide solar water heating solutions in Scotland. At present, the number of SWH installers registered to the SCHRI which is the "Scottish Community and House Holder Renewable Initiative" is 33. Installers for solar hot water systems accredited by DTI (Department of Trade and Industry, UK) for Scotland regions is a staggering figure of 90 [70]. To study the design by each installer would lead to an exhaustive review in its own right. For these reasons, only three major installers in Scotland namely *Solar Twin*, *Solar Harvester* and *AES solar system designs* were included. A brief summary of their collector designs is presented herein although additional information and the common practices by these installers will appear throughout the dissertation where found appropriate.

In the UK several types of collectors are commercially available most of them being flat plate types. *Sol Heat,* on the other hand install vacuum tube heaters. It is therefore appropriate to look into studies that include side by side testing of flat plate, built-in storage and vacuum tube heaters

Solar Twin [71] collectors are flat plate type collector but use flexible pipes systems to prevent freezing of water. The technology termed FLEXOL was developed at Napier University. The collector piping has a normal serpentine tube configuration. The system plumbing is simple and avoids the use of an additional storage tank, thus cutting costs. The panel dimensions are of 2m x 1m and are double glazed to reduce the top losses. The installation is simple enough to be done without professional installers and so the units are also sold in DIY kits. The *Solar Twin* system has received the DTI SMART Achievement Award for its innovative attributes.

Sun Harvester solar heating systems [72] claim over 400 units a year installation in Scotland and occupy a major share in Scottish market. The panels have a declared life of over 20 years and are sold in sizes of 1892 mm x 978 mm and also 2063 mm x 1063 mm. The height of each collector in each case was 80mm.

AES solar systems [71] similarly provide flat plate tube type collector of both serpentine or header and riser. The system used anti-freeze (water and 30% propylene) for freeze protection and have a claimed life in excess of 25 years. AES systems recommend a 1 m^2 of collector area per person with a minimum of 2 m^2. The collector height with AES solar system was 100mm. The other notable features put forward by the manufacturer were the instantaneous efficiency of 82%.

There are installers that provide vacuum tube collectors in the UK. The cost of these collectors is nearly twice the flat plate types. Owing to higher costs, these collectors have a higher payback time. Moreover, it was earlier noted in a study by Trinkl et al [23] that the additional energy yield that was expected from the vacuum tube design for its high cost and intricate design was not recorded during the observation period. Furthermore, it was also noted that the design showed a conceptual weakness during winter times.

(a)

(b)

(c)

Figure 2.11: Collectors in operation
(a) Solar Twin (b) Sun Harvester (c) AES system

2.9 Solar Geometry and Weather Conditions Considerations

Solar geometry comes into play as the transmittance, absorptance and the reflectance all depend upon the angle between the sun and the plane of the collector. Some of the parameters of solar geometry are illustrated in fig 2.12. The best optical efficiency is expected when the position of the sun and the normal to the plane of collector is zero. The angle of inclination of collector is similarly important. A general rule of thumb suggests 0.9 times the latitude of installation. For instance Edinburgh having latitude 55°, the optimum angle of inclination comes out to be 49.5°. It has also been suggested, that in areas of higher latitude, the angle of inclination can be increased by up to 20° (northern hemisphere) [24] during the winter and decreased by 20° during the summer for maximizing the solar gain.

Although it seems futile to discuss the change in the angles as the designed solar water heating would be at a fixed inclination depending upon the roof pitch, it would be however worthwhile to look into how much seasonal solar gain can be increased by changing the angle. If the increase is substantial, provision for varying angles in the collector design can be considered.

The windy conditions in Scotland compel a few design changes that might not have been considered in collectors at less windy sites. The high winds result in increasing heat losses therefore measures have to taken to ensure the heat loss from the top is curtailed.

A glance at the yearly weather data for Edinburgh (see Appendix A) points out the fact that the temperatures do go below the freezing temperatures. From a design perspective a more conservative approach of taking the freezing temperature 4°C is appropriate. This increases the hours in which the collector is susceptible to freezing. Therefore measures for tackling the freeze problems should be addressed.

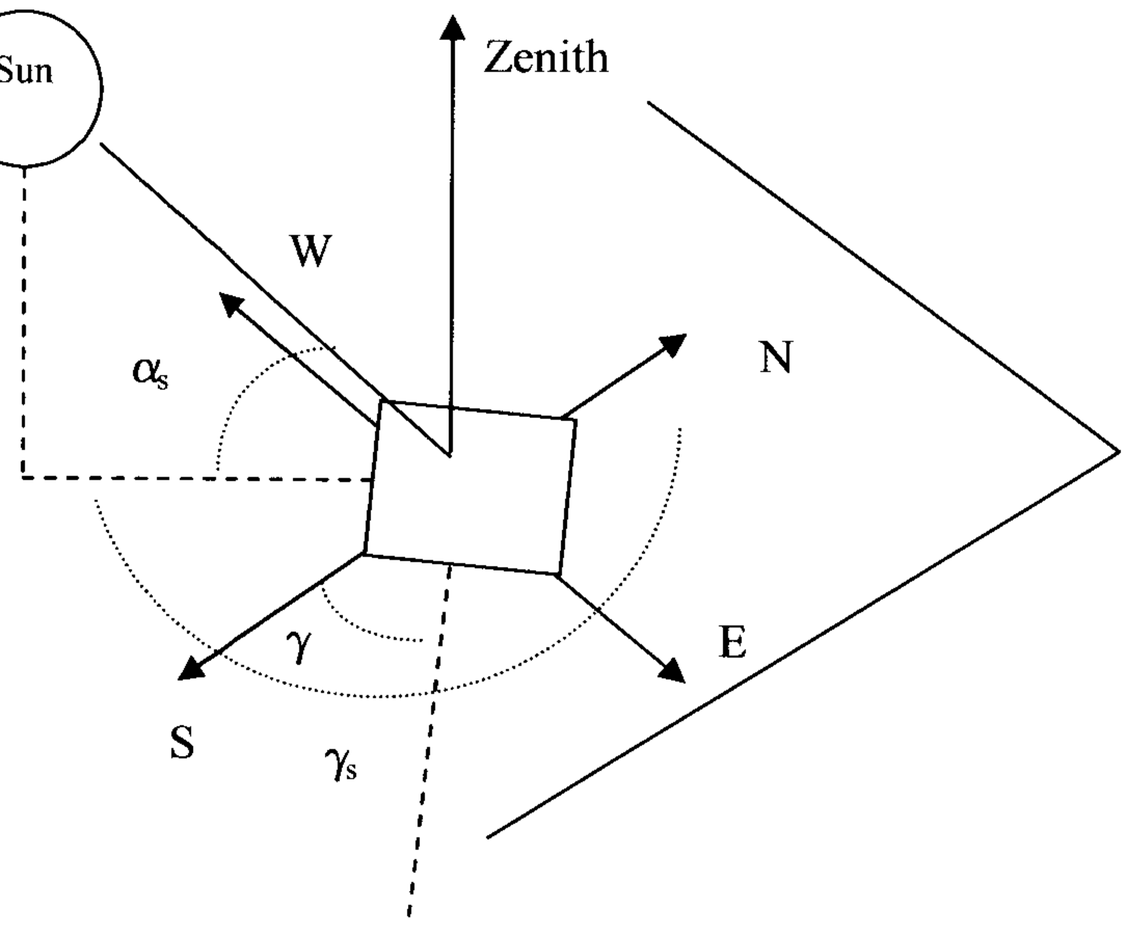

Figure 2.12: Solar Geometry

2.10 Summary

In order to compose a literature review- with vast amount of literature to be surveyed and a wealth of information in each area- it was considered appropriate to section the review and list separately the notable research in each area. This has produced a more concise framework.

From the overview of information on solar water heating it was noted that, over the time, novel solar water heater designs have frequently occurred in paper as well as in practice. Similarly the modifications in the existing designs for enhancing the performance have also been recurring.

Owing to the manufacturing complexities associated with the flat plate type collector that lead to higher costs, it was concluded that ICSSWH design is the way forward. ICSSWH designs are the lowest in cost, easily manufactured and maintenance free thus providing substantial grounds for their selection as the prototype design. Various

commercial designs were also inspected with the sole reason to look at the popular choice and successful product alongside the reasons of their popularity.

Solar Engineering of Thermal Processes; by Duffie and Beckman [24], considered the bedrock of all documented work on the subject, has helped producing the core body of the research and thus has been referenced frequently in this as well as the following chapters.

It was noted that macro level studies on solar collectors were ample in contrast to micro level studies that were rarely found. The published CFD studies on the collector were also limited while the areas related to CFD work on ICSSWH, to the best of author's knowledge were vacant.

Stratification and its maintenance have been studied comprehensively but again these studies were done on detached storage tanks.

In all, the literature review highlighted the opportunities for a positive contribution to knowledge in the areas where information was found lacking such as CFD analysis on the collector, aesthetically designed ICS collectors, quantitative study of the absorber plate and the stratification inside the ICS collector.

Textbox 1

Stratification: Stratification is the layering of a fluid, where the portion of fluid at a certain temperature adjusts itself in the layer with the corresponding density.

Solar Fraction: Solar fraction is the fraction of the energy provided by the water heater to the total load. Since it is a ratio, it can take values from 0 to 1, the latter being the ideal condition.

Transmittance, Absorptance, Reflectance: Incident solar radiation on any surface can be split into three components. Transmittance is the portion of light that is transmitted through the surface/media. For an opaque media, the transmittance is low. For transparent media, the transmittance is higher.
Reflectance is the component of light that gets reflected while absorptance is the portion of light that is absorbed by the surface.
Symbolically it can be represented as:
$\alpha + \tau + \rho = 1$

Zero Heat Flux (ZHF) and Linear Temperature Profile (LTP):
The two boundary condition represent extreme cases where Zero heat flux (ZHF) represent perfect adiabatic conditions it is also called perfect insulation condition whereas perfectly conducting or linear temperature profile (LTP) represents a linear profile variation on the walls of the cavity that represent it depth or "L" (see fig 2.5 for dimension)

References

1. Kerr MacGregor, *A Comparision Between Flat-Plate and Vacuum-Tube Solar Collectors*. 1996, Napier University, 10 Colinton Road: Edinburgh. p. 2.
2. Smyth, M., P.C. Eames, and B. Norton, *Integrated collector storage solar water heaters.* Renewable and Sustainable Energy Reviews, 2006. **10**(6): p. 503-538.
3. Brooks FA, *Solar energy and its use for heating water in California.* Agricultural Bulletin 602. California, 1936. **Agricultural Experiment Station**(University of California).
4. Butti K and Perlin J, *A Golden Thread*. 1981, London, UK: Marion Boyars Publishers Ltd.
5. Tanishita I. *Present situation of commercial solar water heaters in Japan*. in *Proceedings of the ISES Conference*. 1970. Melbourne, Australia.
6. Chinnappa J.C.V. and Gnanalingam K, *Performance at Colombo, Ceylon, of a pressurized solar water of the combined collector and storage type.* Solar Energy, 1973. **15**: p. 195-204.
7. Sokolov M and Vaxman M, *Analysis of Integral compact solar water heater.* Solar Energy 1983. **30**: p. 237-246.
8. Soponronnarit S, Taechapiroj C, and T. S., *Comparative studies of built-in-storage solar water heaters.* RERIC International Energy Journal, 1994. **16(1)**: p. 11–26.
9. Ecevit A., Al- Shariah A.M, and A. E.D., *Triangular Built-in storage solar water heater.* Solar Energy, 1989. **42**: p. 253-265.
10. AA., M., *Integrated solar collector-storage tank system with thermal diode.* Solar Energy, 1997. **61(3)**: p. 211–8.
11. Jose´ M.S. Cruz, Geoffrey P. Hammond, and Albino J.P.S. Reis, *Thermal performance of a trapezoidal-shaped Solar collector / energy store.* Applied Energy, 2002. **73**: p. 195-212.
12. H.P. Garg, *Year round performance studies on a built-in storage type solar water heater at Jodhpur, India.* Solar Energy, 1975. **17**(3): p. 167-172.

13. T. Muneer, *Effect of design parameters on performance of built-in storage solar water heater.* Energy conservation and Management 1985. **25**(3): p. 277-281.
14. T. Muneer and M.M. Hawas. *Experimental study of the thermosyphonic and built-in storage type solar water heaters.* in *Energex 84 conf.* 1984. Regina, Canada.
15. Anon, *ASHRAE Standard-95,* . 1981, ASHRAE, New York, USA.
16. ECSTG, *Recommendations for performance and durability tests of solar collectors and water heating systems*, in *The European Collector and Systems Testing Group;Commission of the European Communities*. 1989, Directorate-General for Science Research and Development, Joint Research Centre: Ispra, Italy.
17. Hottel, H. and A. Whillier. *Evaluation of flat plate collector performance.* in *Transactions of Conference on the use of Solar Energy.* 1958. Tucson, Arizona, USA.
18. Matthias Rommel and Andreas Wagner, *Application of Transparent Insulation Materials in Improved Flat Plate Collectors and Integrated Collector Storages*, Fraunhofer Institute for Solar Energy Systems: Oltmannsstr. 22, D-7800 Freiberg, Germany
19. I.N. Kaptan and A. Kilic, *A Theoretical and Experimental Investigation of a Novel Built-in Storage Solar Water Heater.* Solar Energy, 1996. **57**(5): p. 393-400.
20. J.F. Van Straaten. *Solar Energy research and application with special reference to solar water heating in Southern Africa.* in *2nd Southeastern Conference on Application of Solar Energy.* 1976. Baton Rouge, Louisiana, USA.
21. H.P. Garg and Usha Rani, *Theoretical and experimental studies on collector / Storage type solar water heater.* Solar Energy, 1982. **29** (6).
22. M. Smyth, P.M., P.C. Eames , B. Norton,, *Experimental comparison of alternative convection suppression arrangements for concentrating integral collector storage solar water heaters.* Solar Energy, 2005. **78**: p. 223–233.
23. Christoph Trinkl, W.Z., Claus Alt,Christian Stadler. *Performance of Vacuum Tube and Flat Plate Collectors Concerning Domestic Hot Water Preparation*

and Room Heating. in *2nd European Solar Thermal Energy Conference (ESTEC2005)*. 2005. Freiburg, Germany; 21-22/06/2005.

24. Duffie, J.A. and W.A. Beckman, *Solar Engineering of Thermal Processes*. 2nd Edition ed. October 1991: John Wiley & Sons Canada, Ltd.
25. Bishop, R., *Superinsulated Batch Heaters for Freezing Climates.* Proceedings of the eighth National Passive Solar Conference,Sante Fe,New Mexico, USA, 1983: p. 807–10.
26. Hottel Hoyt C. *Performance of Flat- Plate Solar Energy Collectors,*. in *Space Heating With Solar Energy, Proceedings of a Course Symposium,*. 1954: MIT Press.
27. Buchberg;, H., I. Catton;, and D.K. Edwards, *Natural Convection in Enclosed Spaces – A Review of Application to Solar Energy Collection.* Journal of Heat Transfer, Transaction of ASME, 1976. **98**(Series C. No. 2).
28. W. Liu, J.H.D. and F.A. Kulacki, *Thermal Characterization of Prototypical Integral Collector Storage Systems with Immersed Heat Exchangers.* Journal of Solar Energy Engineering,, February 2005 **127**(1): p. 21-28.
29. Moore, S.W. *Results obtained from Black Chrome Production Run of Steel Collectors*. in *AES coatings for Solar Collector Symposium,American Electroplater's Society*. 1976. Winter Park, Florida.
30. J.W. Burton and P.R. Zweig. *Side by side comparison study of integral passive solar water heaters*. in *Proceedings of the sixth national passive solar conference*. 1981. Portland, Oregon, USA
31. William S. Duff and D. Hodgson, *Testing of a Flat Plate Collector with Selective and Non selective Absorbers that are otherwise Identical* in *Colorado State University, Fort Collins CO 80523, USA*, Colorado State University, Fort Collins CO 80523, USA
32. Fluent Inc, *Achieving Engineering Breakthroughs in Early Stages of Product Design Process*, www.fluent.com.
33. Groenhout, N.K., M. Behnia, and G.L. Morrison, *Experimental measurement of heat loss in an advanced solar collector.* Experimental Thermal and Fluid Science, 2002. **26**(2-4): p. 131-137.

34. Ozoe, H.a.K.F., N. Lior and S.W. Churchill; , *Long Rolls generated by natural convection in an inclined, Rectangular enclosure.* International Journal of Heat and Mass Transfer, Oct, 1983. **26**(10): p. 1427-1438.

35. A. E. Gill, *The boundary-layer regime for convection in a rectangular cavity.* Journal of Fluid Mechanics 1966. **26**(515- 536).

36. Courant, R., K. O. Friedrichs and H.Lewy;, *Uber die partiellen Differenzengleichungen der mathematischen Physik.* 1928, Math. Ann. p. 32.

37. Zhong, Z.Y., K.T. Yang and J.R. Lloyd,, *Variable property natural convection in tilted enclosure with thermal radiation.* Numerical Methods in Heat Transfer, 1985. **III**: p. 195-214.

38. Thompson, Z.L.a.J., *Experimental Study of Thermally Stratified Hot Water Storage Tanks.* Solar Energy. **19**: p. 519-524.

39. Van Koppen, C.W.J., Thomas, J.P.S and Veltkamp, W.B,. *The actual benefits of thermally stratified storage in a small medium size solar system.* in *Proceeding of ISES Solar World Congress*. 1979. Atlanta U.S.A.

40. Furbo, S. and S.E. Mikkelsen. *Is low flow operation an advantage for solar heating system?* in *Proceeding of ISES World Congress*. 1987. Hamburg, Germany.

41. Hollands, K.G.T. and M.F. Lightstone, *A review of low-flow, stratified-tank solar water heating systems.* Solar Energy, 1989. **43**: p. 97-105.

42. Sodha M.S., S. S.N., and Tiwari G.N. , *Thermal performance of built-in storage solar water heaters (or shallow solar ponds) in series.* Solar energy 1984. **32**: p. 291-297.

43. A.H. Fanney and S.A. Klein;, *Thermal performance comparision for solar hot water systems subjected to various collector and heat exchanger flow rates.* Solar Energy, 1988. **40**(1): p. 1-11.

44. Coutney, R.G., *A Multinomial Analysis of Water Demand.* Building and Environment,Pergamon Press, 1976. **11**: p. 203-209.

45. R.G Coutney *A Computer Study of Solar Water Heating.* Building and Environment. **12**: p. 73-80.

46. De Graaf, J.G.A. and E.F.M. Van der Held, *The relation between the Heat Transfer and Convection Phenomena in Enclosed Plane Air Layers.* Appl. Sci. Res, 1953. **3**: p. 393-409.

47. Dropkin, D. and E. Somerscales, *Heat Transfer by Natural Convection in Liquids Confined by Two Parallel Plates Which are Inclined at Various Angles With Respect to Horizontal.* Journal of Heat Transfer, Transaction of ASME, 1965. **Series C,Vol 87,** : p. 74-84.

48. J. E. Hart, *Stability of the flow in an differentially heated inclined box.* Journal of Fluid Mechanics. Fluid Mech, 1971. **47**: p. 547-576.

49. Elsherbiny, S.M., G.D. Raithby, and K.G.T. Hollands, *Heat Transfer by Natural Convection Across Vertical and Incline Air Layers.* Transaction of ASME, Journal of Heat Transfer, 1982. **104**: p. 96-102.

50. S.M. Elsherbiny, K.G.T. Hollands, and G. D. Raithby, *Nusselt number distribution in vertical and inclined air layers.* J. Heat Transfer, 1983. **105**: p. 406-408.

51. Hamady. F.J.. H.R. Lloyd.. H.Q. Yang and K.T. Yang, *Study of local natural convection heat transfer in an inclined enclousure.* . International Journal of Heat and Mass Transfer, 1989. **32**: p. 1697-1708.

52. Linthrost, S.J.M., W.M.M. Schinkel, and C.J. Hoogendorn., *Flow Structure with natural convection in inclined Air filled Enclousures.* Journal of Heat Transfer, Transaction of ASME, 1981. **103**: p. 535-539.

53. Yang, H.Q., K.T.Yang and J.D. Lloyd., *Flow transition in Laminar buoyant flow in three dimensional tilted rectangular enclosure.* Proceedings of the International Heat Transfer Conference, 1986. **4**.

54. Ozoe, H., K. Yamamoto, H. Sayama and S.W. Churchill., *Natural Circulation in an inclined rectangular channel heated on one side and cooled on the opposing side.* International Journal of Heat and Mass Transfer, 1974. **17**: p. 1209-1217.

55. Ozoe, H.K., Yamamoto, H., Sayama and S.W. Churchill., *Natural circulation in an inclined rectangular channel at various aspect ratios and angles, experimental measurements.* International Journal of Heat and Mass Transfer, 1975. . **18**: p. 1425-1431.

56. Ozoe, H.K., H., Sayama and S.W. Churchill., *Natural convection in an inclined rectangular box heated from below. Three directional photography. International Journal of Heat and Mass Transfer.* 1977. **20**(2): p. 123-129.

57. W. Bian.. P. Vasseur, E. Bilgen, and F. Meng;, *Effect of an electromagnetic field on natural convection in an inclined porous layer.* International Journal of Heat and Fluid Flow, 1996. **17**(1): p. 36-44.

58. L. Adjlout.. O. Imine, A.A. and M. Belkadi, *Laminar natural convection in an inclined cavity with a wavy wall.* International Journal of Heat and Mass Transfer, May 2002. **45**(10): p. 2141-2152.

59. Polat, O. and E. Bilgen, *Laminar natural convection in inclined open shallow cavities.* International Journal of Thermal Sciences, April 2002. **41**(4): p. 360-368

60. Dalal, A. and M.K. Das, *Laminar natural convection in an inclined complicated cavity with spatially variable wall temperature.* International Journal of Heat and Mass Transfer, August 2005. **48**(18): p. 3833-3854.

61. Kuyper, R.A., Th. H. Van Der Meer, C.J Hoogendorn and R.A.W. Henkes., *Numerical Study of laminar and turbulent natural convection in an inclined square cavity.* International Journal of Heat and Mass Transfer, 1992. **36**(11): p. 2899-2911.

62. Yunhua Yang, *Laminar natural convective flow in inclined rectangular glazing cavities.* CEERE, University of Massachusetts, Department of Mechanical Engineering and Industrial Engineering, 2002.

63. Frank P. Incropera; David P.DeWitt, *Fundamental of Heat and Mass Trasnfer.* 2002: Wiley. .

64. H. Oertel, J., *Three-dimensional convection within rectangular boxes.* ASME HTD 8, 1979. **Thermische Zellularkonvection, Habilitationschrift, Universitat Karlsruhe**(11-16 (1980)).

65. Soong, C.Y., P. Y. Tzeng, D.C. Chiang, and T.S. Sheu., *Numerical study on mode-transition of natural convection in differentially heated inclined enclosures.* International Journal of Heat Transfer, 1996. **39**(14): p. 2869-2882.

66. Tariq Muneer; Jorge Kubie and Thomas Grassie, *Heat Transfer; A problem solving approach.* . 2003: Taylor & Francis.

67. SAMY M. Elsherbiny, *Free convection in inclined air layers heated from above.* International Journal of Heat and Mass Transfer., 1996. **39**(18): p. 3925-3930.

68. Imbabi, M.S. and A. Musset, *Performance evaluation of a new hybrid solar heating and ventilation system optimised for U.K. weather conditions.* Building and Environment, 1996. **31**(2): p. 145-153.

69. MacGregor Kerr. and Balmbro D. *Why North is best for solar heating of buildings.* . in *Northsun 1984.* 1984. Napier University, Edinburgh, Scotland.

70. Department of Trade and Industry(DTI). *Installers for Solar Hot Water System; Low Carbon Buildings Programme.* [Webpage] 2007 23 March, 2007 [cited.

71. Solar Twin, *www.solartwin.com*. 2007, 9 Abbey Square, Chester, CH1 2HU

72. Solar Harvester, *http://www.sun-harvester.co.uk/*. 2007, Imex Business Centre, Broadleys Industrial Estate,Craigleith Road Stirling,FK7 7LQ

CHAPTER 3

Design & Engineering

Materials, Fabrication and Experimental Setup

This chapter encapsulates the details of fabrication of the collector, the experimental tests and the scaling of error. The chapter starts with the detailed inspection of all elements that assemble to form the collector. Not only their physical and thermal properties have been reported, but more importantly their utility as collector components has been discussed. To gauge the quality of the collected experimental data, it is imperative to construe an uncertainty analysis. The details of this analysis are scripted in the penultimate section and rightly qualify as the main crux of this chapter. Furthermore, the physics epitomizing the heat transfer in the collector has been included.

In this era of price driven human behavior, the economics of materials cannot be ignored and so the commercial aspects have been briefly touched on. Techniques for productive manufacturing - that came as hindsight in wake of the indigenous fabrication - have also been included for the benefit of the reader.

To summarize, this chapter has been written to carry an essence of "Engineering" rather than projecting a holistic scientific approach.

Chapter Map

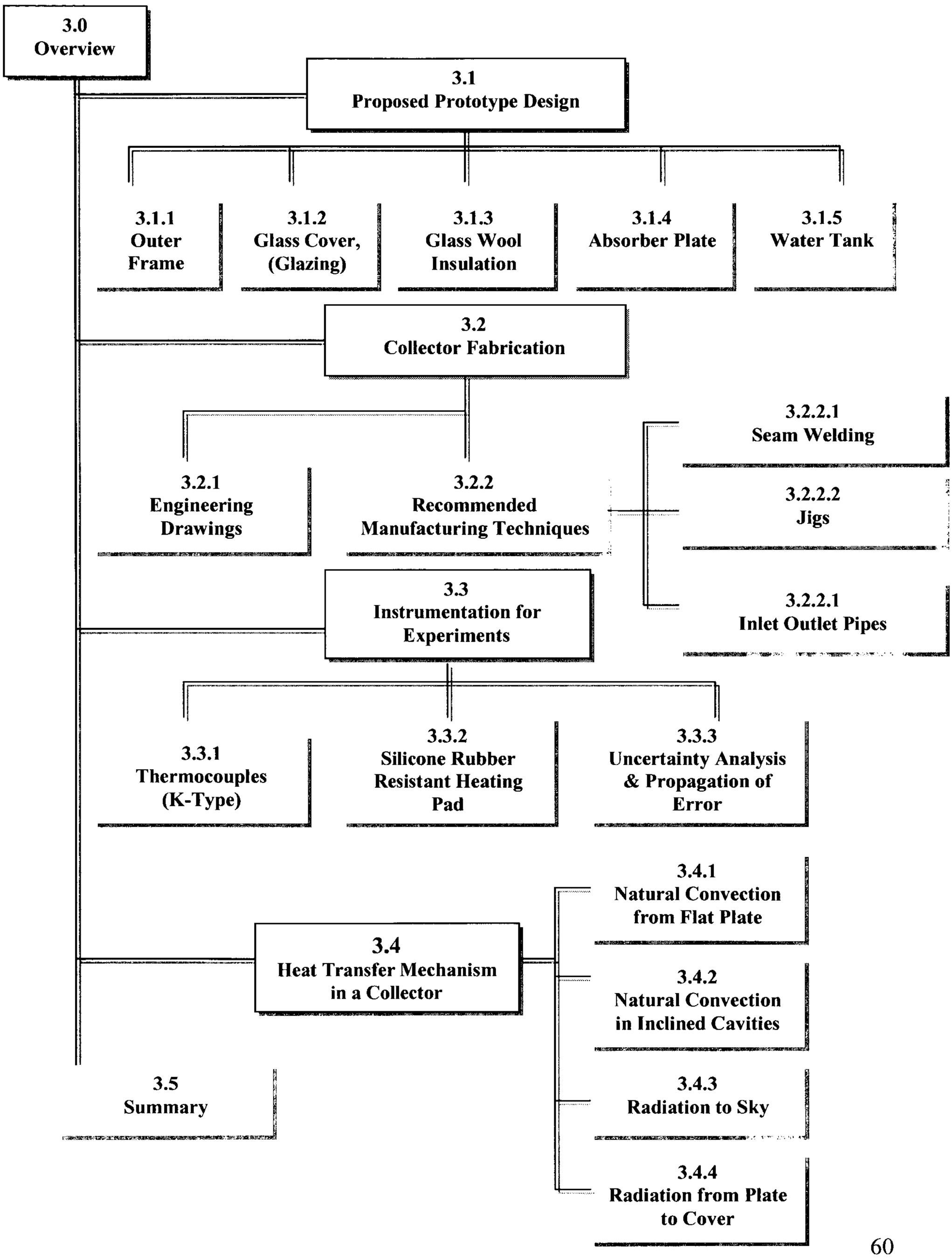
3.0
Overview
3.1
Proposed Prototype Design
3.1.1
Outer
Frame
3.1.2
Glass Cover,
(Glazing)
3.1.3
Glass Wool
Insulation
3.1.4
Absorber Plate
3.1.5
Water Tank
3.2
Collector Fabrication
3.2.1
Engineering
Drawings
3.2.2
Recommended
Manufacturing Techniques
3.2.2.1
Seam Welding
3.2.2.2
Jigs
3.2.2.1
Inlet Outlet Pipes
3.3
Instrumentation for
Experiments
3.3.1
Thermocouples
(K-Type)
3.3.2
Silicone Rubber
Resistant Heating
Pad
3.3.3
Uncertainty Analysis
& Propagation of
Error
3.4
Heat Transfer Mechanism
in a Collector
3.4.1
Natural Convection
from Flat Plate
3.4.2
Natural Convection
in Inclined Cavities
3.4.3
Radiation to Sky
3.4.4
Radiation from Plate
to Cover
3.5
Summary

3.0 Overview

Solar water heaters, owing to their wide variety of design and construction, enlist several materials in components. However the simplicity of an ICS design eliminates the presence of pipes, headers, connectors, pumps, tracking devices and evacuated tubes. As the collectors have to withstand testing weather conditions and endure lengthy time scales (20-30 years), it is imperative that the component materials are resilient, non-corrosive and long lasting. In addition to these properties, it is vitally important that the cost of the collector is kept as low as possible. It is the price of the collector that manipulates the interest among the general public as well as settles the feasibility figures.

3.1 Proposed Prototype Design

As established in the previous chapter, within the domain of interest i.e. a collector meeting domestic hot water requirements utilizing Scottish weather conditions, the merits of the ICS collector outweigh all the other types of collectors. Therefore an ICS was settled as the logical choice for the prototype design. Out of the several types of ICS, for instance the triangular tank, trapezoidal storage and focusing collector storage, the rectangular tank was chosen mainly for its aesthetic design and easy integration in roof structures. Rectangular tank ICS designs have been around for decades and many variants of this type have been quantitatively tested. However, one of the disadvantages of this design is that heating of water is carried out by an overlaying surface. It is a well established fact that heat transfer is most effective if the heating surface is kept below the media to be heated. The addition of fins-perpendicular to the heating surface in this regard is anticipated to improve heat transfer to the tank. This novelty in rectangular tank ICS heater has been reported in the earlier study by Muneer et al has been tested in the field [1] showing encouraging results. However, the mentioned heater was not tested with an objective of evaluating the heat gain/loss characteristics. Thus for the testing of the modification (fins) and to assess its effectiveness, two collectors (finned and non-finned) were fabricated and tested side by side (fig. 3.2)

The ICS heaters were fabricated indigenously with an eye to explore methods of keeping costs to a minimum. As an initial reference, a collector cost of £1000 per unit was set as a target limit. This figure was settled after reviewing the costs of collectors in the UK market (See section 1.6 for details). As has been highlighted in section 2.9, most solar panels available in the UK have absorber plate areas of over 2 m^2 whereas the fabricated collectors had collection areas of only $1m^2$. Two reasons can be cited to adjudicate the absorber size. Firstly, the main purpose of the exercise was to enumerate the collector efficiency from a statistical standpoint rather than gauging the collector from a utility point of view. Nonetheless, evaluating the utility of the collector is an important aspect that will be gradually construed through the course of this thesis. Secondly, the fabricated collector is an ICS as compared to flat-plate types. Thus it was envisaged that the smaller collector size would make up for the hot water demand owing to its higher conversion efficiency.

The properties of the materials that were used in the fabrication of the prototype collectors alongside their costs are individually described in the subsequent sections.

3.1.1 Outer Frame

In an ICS heater (such as shown in fig 3.1), an outer frame normally made of wood is employed for housing the water tank. For the prototype collectors, they were made using yellow pine wood. Although yellow pine is the hardest of the available soft woods, it still has to be used with a surface treatment (varnish or coating) to cope with changing weather conditions. In order to stuff glass wool insulation at the bottom of the water tank, slots were made using wooden panels. These panels also served to strengthen the outer frame and provided both longitudinal and lateral structural stability. Technical drawings for the outer frame are presented in the annexure (Appendix-B).

Although the anisotropic nature of wood suggests varied thermal conductivity in different directions, a general value of k= 0.147 W/m-K – as suggested in literature [4] -was used

for calculations. The outer frame for the prototypes was made in two portions, the top cover and the main section. The top cover held the glazing as well as the toggle clamps. The water tank was placed inside the main section, and was packed all-around with thermal insulation. A closed cell foam air seal was used between the top cover and the main section to ensure that the air leakage is minimized. In the UK and Scandinavia it is a general practice to paint the wooden windows for increasing life (protection from rain, air moisture and ultra violet radiation). This practice can be adopted for the outer frame. Varnish is also used along with wood-staining for weather proofing. One practice suggests that by covering wood with vinyl, the need to ever paint or replace the wood again is eliminated [2]. The use of either paint or varnish results in marginal increase in the cost (£20). The cost of the outer frame depends primarily upon the type of wood used. A ball park figure of the total cost (material and labour) of the manufactured outer frame for the prototype collector is estimated to be £115.

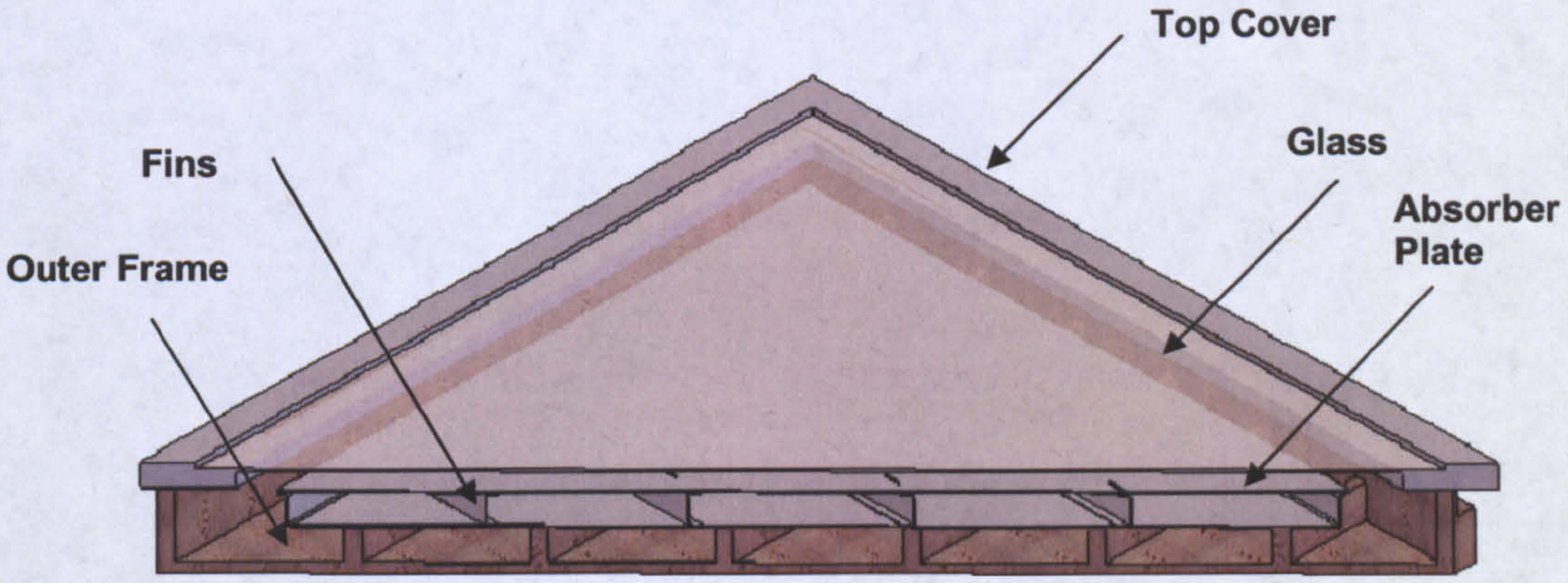

Figure 3.1: Cut away view of the fabricated collector

Table 3.1: Thermal properties of various types of wood [4]

Type of Wood	Temperature °C	Thermal conductivity k=W/mK	Density ρ (kg/m^3)	C, kJ/kgK	A m^2/s
Balsa	30	0.055	140		
Cypress	30	0.097	460		
Fir	23	0.11	420	2.72	0.96
Maple or Oak	30	0.166	540	2.4	1.28
Yellow pine	**23**	**0.147**	**640**	**2.8**	**0.82**
White pine	30	0.112	430		

3.1.2 Cover (Glazing)

The choice of a particular type of glazing is crucial as it governs the optical efficiency that in turn dictates the collector's performance. Plastic (polymer) glazings have gained popularity in recent times due to lower costs but are used in applications of low temperature range. A glass cover is the normal choice that has been employed on the outset and is used because of its availability, negligible degradation (over time) effects and higher transmittance values. The transmittance (τ) of a glass depends upon its thickness, composition as well as its angle of incidence (ϕ). The table 3.2 explicitly enumerates the effect of the angle to transmission losses.

Table 3.2: Beam Transmittance of a glass cover at various angles [3]

ϕ	0°	60°	70°	80°	90°
$\tau(\phi)$	0.9	0.8	0.65	0.35	0

A 4mm thick float glass of dimensions 1200 mm x 1200 mm was used in the prototype collectors as the covering. The other optical property that also plays a vital role in the collector performance is the emmisivity (ϵ). Higher emmisivity values result in higher heat losses to the ambient. For smooth glass, emmisivity values of 0.94 (at T = 22°C) has been reported in literature [4].

The glazing in the prototypes was adjusted such that it maintained a distance of 35mm from the absorber plate thus giving the air-gap a vertical aspect ratio of A = 28.57 (1000 mm/35mm). As the absorber plate and the glazing were geometrically square in shape, the same value holds true for the horizontal aspect ratio (A_H =28.57). These aspect ratios are important design parameters as they strongly influence the convective heat transfer. Their coupling to heat losses will be covered extensively in the subsequent chapters. The price of the glass depends primarily on the composition, thickness and the size.

3.1.3 Glass Wool Insulation

Several types of thermal insulations have been developed over time for different applications. The choice of insulation is mainly governed by the range of temperatures of exposure. In the case of a domestic collector - with the range 10-80˚C, air is the best available cost free insulator (k= 0.02495 - 0.0302 W/m-K), however the slightest bulk movement in air triggers convection which can significantly augment the heat losses. Insulation, particularly glass wool insulation, fills up space and creates air pockets, where movement of air is confined. The thermal conductivity of general purpose glass wool varies slightly with temperature. It is usually evaluated at mean temperatures when tested in accordance with ASTM C177. For higher precision, the values of thermal conductivity may be obtained from fig 3.2 [5].

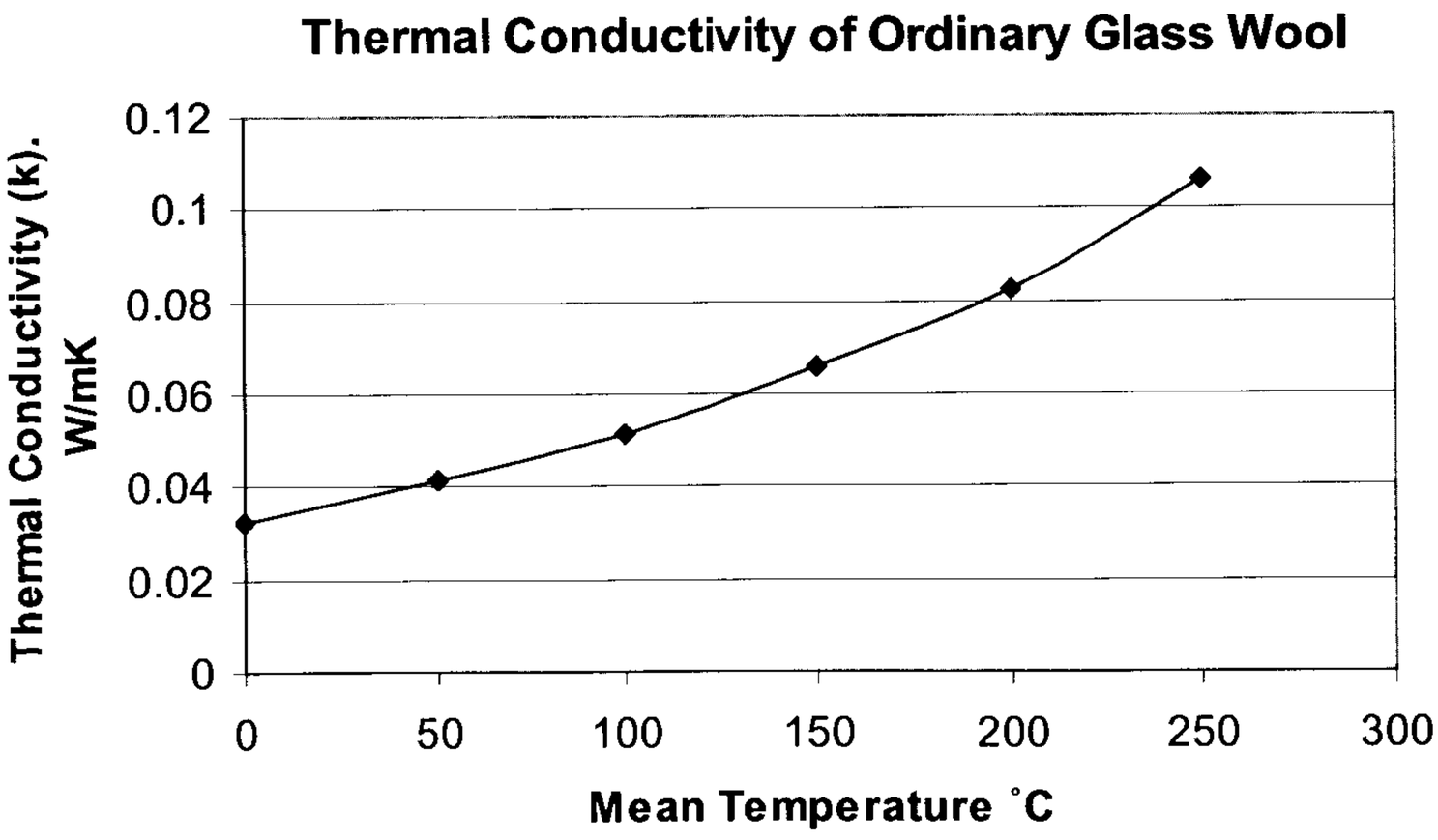

Figure 3.2: Variation of thermal conductivity of ordinary glass wool with temperature

Mean Temperature = $(T_1 + T_2)/2$

Where T_1 = temperature of hot side of insulation (°C)

Where T_2 = temperature of cool side of insulation (°C)

Glass wool insulation of 100mm thickness was packed around the three sides of the prototype collector. A roll of insulation is priced £31.2[1] (100 mm thickness) that is enough to cater for up to six collectors of the proposed size.

3.1.4 Absorber Plate

Being functionally the driving component of a collector, the design of the absorber plate requires added attention. The outer face of the plate is generally painted matt black to maximize absorption. The size of the collector is often categorized by area of the absorber plate. The larger the area, the greater is the collection of solar energy. Nonetheless it has also to be accounted that in the case of an ICS collector larger exposure area can lead to higher heat losses. ICS heaters in the past have been designed with specific absorber plate to storage tank ratios, unique for each location. Rules of thumb on these ratios are presented in the section 3.1.5.

Similar to glass cover transmittance, the absorptance values are also a function of the angle of inclination of the collector. Table 3.3 elucidates the typical values of absorptance of the absorber plate with changing angles.

Table 3.3: Absorptance (α) of an absorber plate at various angles [3]

ϕ	**0°**	**60°**	**70°**	**80°**	**90°**
$\alpha(\phi)$	0.92	0.85	0.75	0.60	0
$\tau(\phi).\alpha(\phi)$	0.83	0.68	0.49	0.21	0

[1] Please note that mentioned price is quoted for period December 2004 and it may vary subject to inflation

The water storage tank was made out of stainless steel sheet type 304 2B, the emmisivity values for which range from ϵ = 0.54-0.63 [4]. As the emmisivity in general is directly related to absorptance of a surface, the mentioned emmisivity value for steel suggests a low absorptance. This necessitates the painting of the absorber plate to dull black colour so that the absorptance is enhanced. As a resistant heating pad was used for imposing the heat flux for the laboratory tests, the absorber plates on the prototype collectors were not painted as this would not have any effect.

1.5 mm gauge thickness stainless steel 304-2B was used for forming the absorber plate and the water tank. Stainless steel type 304- 2B is an austenitic stainless steel, the thermal properties of which are given in table 3.4

Table 3.4: Thermal properties of 304 2B stainless steel [6]

Properties		**T** (°C)
Thermal Expansion (10^{-6}/°C)	16.2	0-100 more
Thermal Conductivity (W/m-K)	15.9	100 more
Specific Heat (J/kg-K)	500	0-100

As mentioned, the transmittance of a glass cover and the absorptance of the absorber plate both are coupled to the angle of incident radiation, it is important here to determine the product of the two values $(\tau\alpha)$ to evaluate the total energy gain. As the angle of incident solar radiation keeps changing with the traverse of the sun, a mean value of $(\tau\alpha)$ has to be calculated. This mean value is normally defined with the following relationship [3].

$$(\tau\alpha)_m = \frac{\int_{\phi=0}^{\phi=2\pi} \tau(\phi)\alpha(\phi).\sin\phi.\cos\phi.d\phi}{\int_{\phi=0}^{\phi=2\pi} \sin\phi\cos\phi.d\phi} \qquad (3.1)$$

For a single glass cover the result is approximately $(\tau\alpha)_m = 0.70$ [3]

3.1.5 Water Tank

The water tank design in an ICS is intricate to balance as it is linked to a number of interlinked parameters that can significantly augment the advantage as well as drastically curb the performance. The size of the tank determines the thermal inertia, which is important to build up a freeze tolerance. The higher the thermal inertia, the lower the possibility of freezing. Higher thermal inertia also results in increased efficiency of the heater. On the other hand it also produces a low grade output i.e. lower water temperatures at the outlet are obtained. The size of the tank also determines the weight of the heater. If the ICS heater is to be mounted on the roof, it should have a weight that is bearable by the roof trusses. The other parameters that influence the size of the water tank are the hot water demand and availability of solar insolation.

Using 1.5 mm stainless steel sheet, the same as that was used in the absorber plate, the water tank was fabricated. Stainless steel was chosen for its corrosion resistant properties. The tank depth was kept 50 mm giving the water storage tank a capacity of 50 litres (absorber plate dimensions being 1m x 1m). The optimal ratio for the absorber plate to the collector volume has been evaluated primarily on the basis of the amount of incident radiation.

Smitty and Chuck [7] have put forth generally accepted rules of thumb for solar thermal collector sizing based on different climatic regions. Although the regions (USA states) mentioned are of little significance to Scottish weather conditions; however for the interest of the reader, and review in general, they have been presented herein.

- In the Sunbelt, 0.09 m^2 (1 square foot) of collector per 7.6 litres (2 gallons) of tank capacity.
- In the Southeast and mountain states, 0.09 m^2 of collector per 5.7 litres (1.5 gallons) of tank capacity.
- In the Midwest and Atlantic states, 0.09 m^2 of collector per 3.8 litres (1.0 gallon) of tank capacity.

- In New England and the Northwest, 0.09 m^2 of collector per 2.8 litres (0.75 gallons) of tank capacity.

The water tank sizes mentioned above were sized keeping in view of the domestic daily consumption which has been assumed to be 75 litres per person per day.

The figures mentioned above are ballpark calculations that will be affected by incoming water temperature, hot water temperature set point, actual usage, and the intensity of the solar resource on site. 1 m^2 for 50 litres (13.15 gallons) was used in light of Scottish condition, where the intensity of radiation is much lower than the places mentioned in the above thumb rules.

3.2 Collector Fabrication

The fabrication of collector was carried out indigenously at Napier University. It was made certain that specialized and complicated manufacturing processes were not utilized as they lead to increase the cost of the production models. This section closely examines the details of fabrication of both collectors (finned and non-finned). The assembly diagram showing exploded view of each collector are given in fig. 3.3

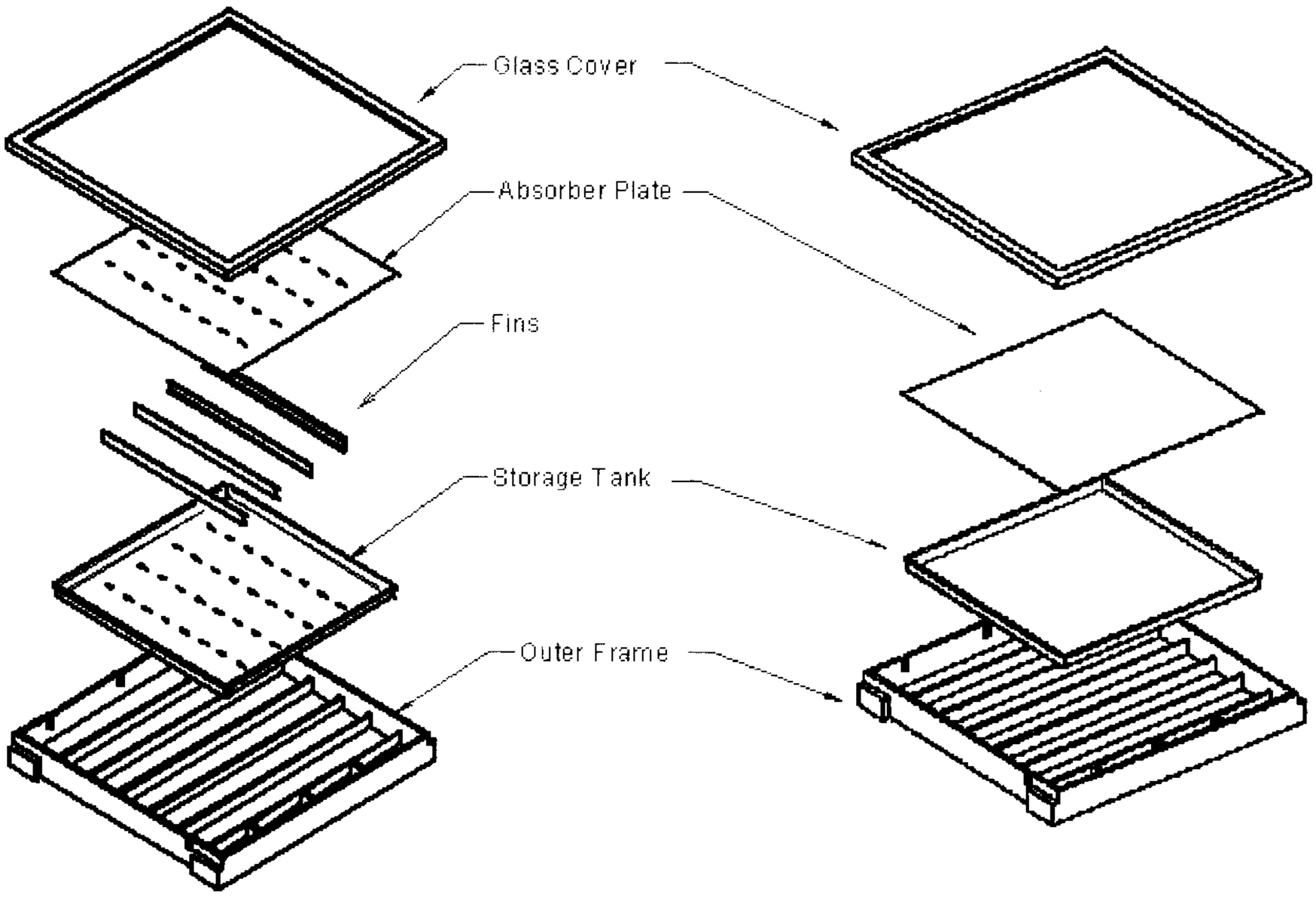

Figure 3.3: Side-by-side exploded view of the fabricated prototype collectors

OUTER FRAME

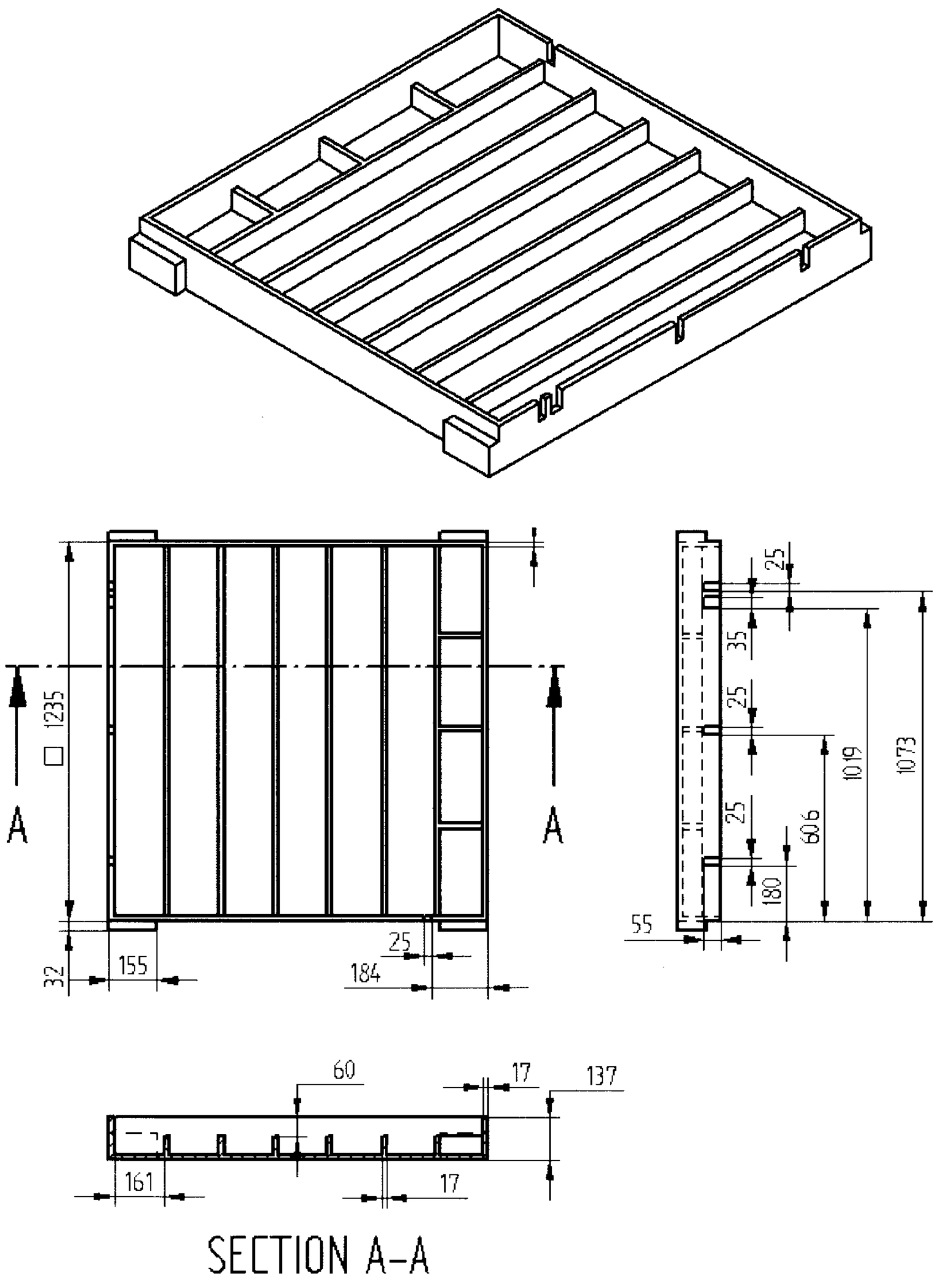

SECTION A–A

[2] The Technical drawings for the cover are given in appendix B

Process Flow Diagram of Finned Heater

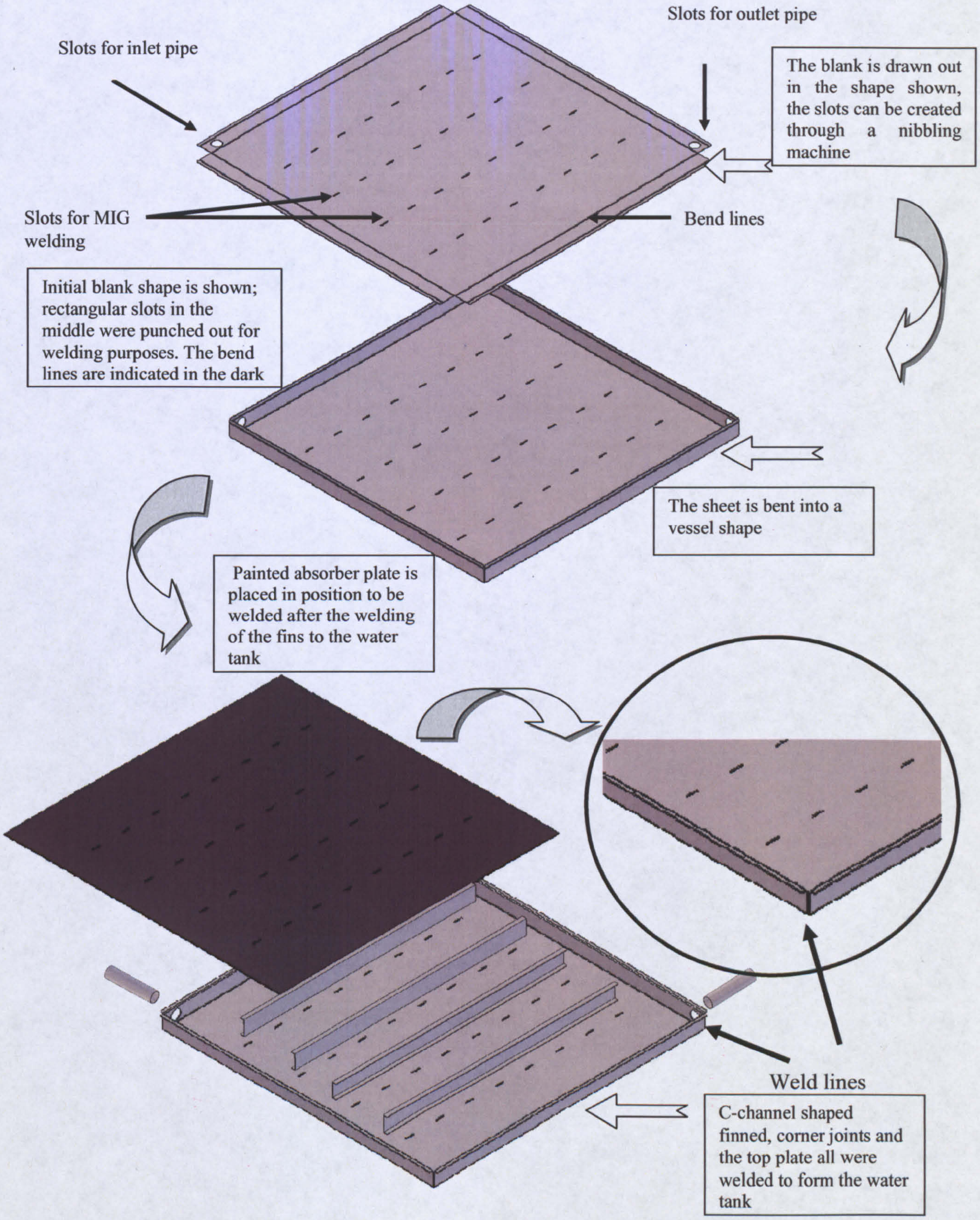

Figure 3.5: Process flow diagram

In order to avoid buckling of the collectors under hydrostatic pressure particularly when inclined at angles closer to vertical, buckles can be additional added as a measure of safety. The orientation of these buckles is given in figure 3.5

3.2.1 Weldability of Steels

As welding was the sole method used for producing joints in the water tank, it would be appropriate at this point to discuss some of the weldability issues with sheet metal steel. The weldability of steels is inversely proportional to a property known as the hardenability of the steel. Hardenability is linked to the chemical composition. The greater the amount of carbon and other alloying elements, the greater will be hardenability as it is a measure of the ease of martensite formation during heat treatment. Thus it is difficult to weld alloys with higher values of hardenability [8].

In order to be able to judge alloys made up of many distinct materials, a measure known as the equivalent carbon content is used to compare the relative weldabilities of different alloys by comparing their properties to plain carbon steel. The effect on weldability of elements like chromium and vanadium, while not as great as carbon, is more significant than that of copper and nickel, for example. As the equivalent carbon content rises, the weldability of the alloy decreases. The disadvantage to using plain carbon and low-alloy steels is their lower strength - there is a trade-off between material strength and weldability [8].

Figure 3.6: The finned heater after bending and before the welding process

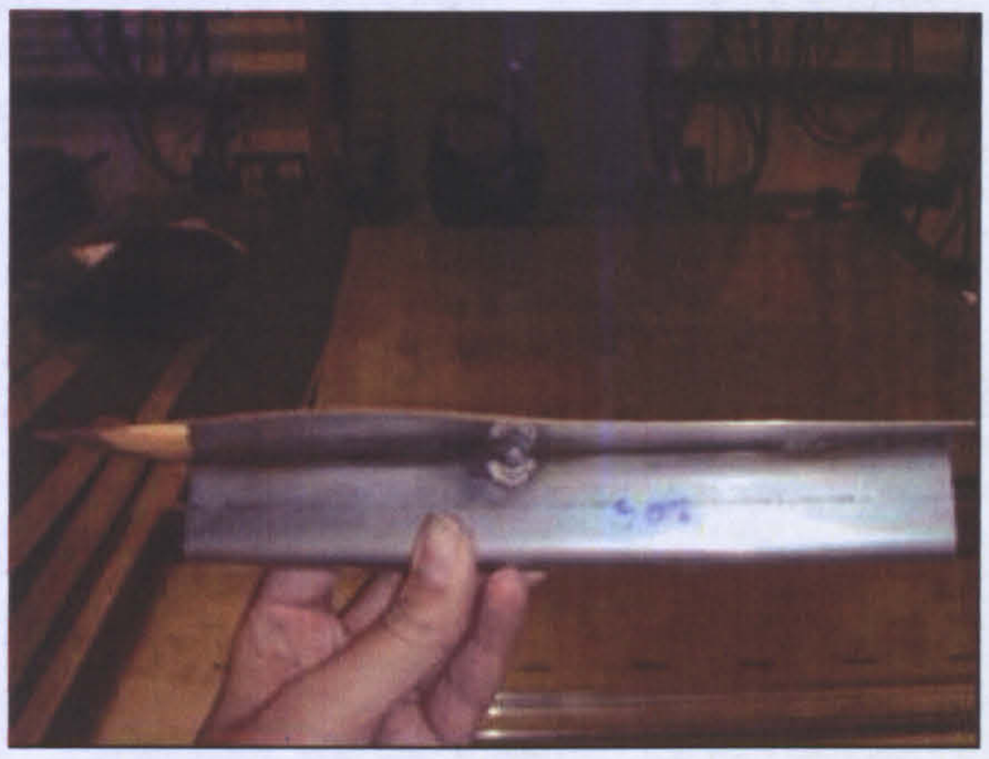

Figure 3.7: Picture highlighting the welding distortion encountered using normal arc welding

Stainless steels, because of their high chromium content, tend to behave differently with respect to weldability than other steels. Austenitic grades of stainless steels tend to be the most weldable, but they are particularly susceptible to distortion due to their high coefficient of thermal expansion. Some alloys of this type are prone to cracking and reduced corrosion resistance as well. Hot cracking is possible if the amount of ferrite in the weld is not controlled- to alleviate the problem, an electrode is used that deposits a weld metal containing a small amount of ferrite [8].

The 304-2B grade of steel falls in the category of austenitic steel. Severe distortion was encountered initially, when the electric arc welding method was used. It was determined that as the temperatures in an arc welding process reach sufficiently high values, the base metal, being of thin cross-section expands to a high degree which results in distortion. The coefficient of thermal expansion of austenite is 30 to 40% greater than that of ferrite.

Other types of stainless steels, such as ferritic and martensitic stainless steels, are not as easily welded, and must often be preheated and welded with special electrodes [8]

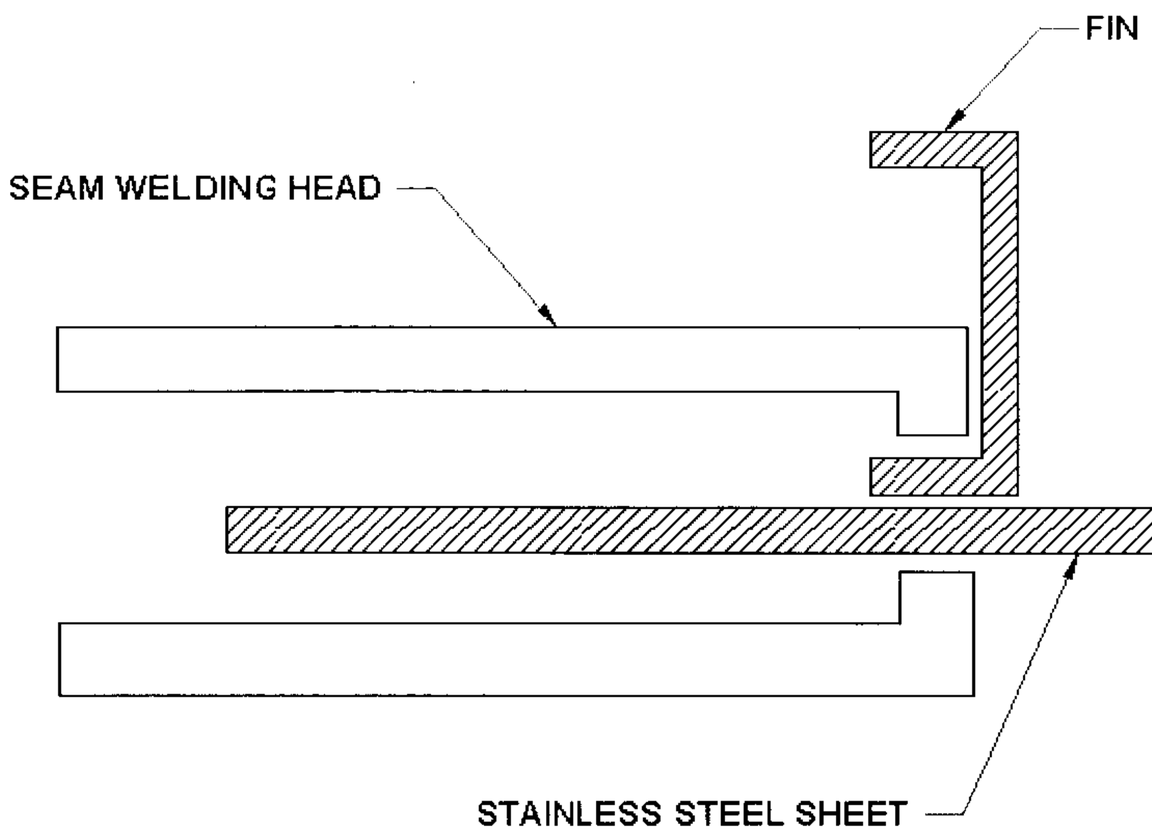

Figure 3.8: The use of *seam welding* for attaching the fins to the base metal sheet

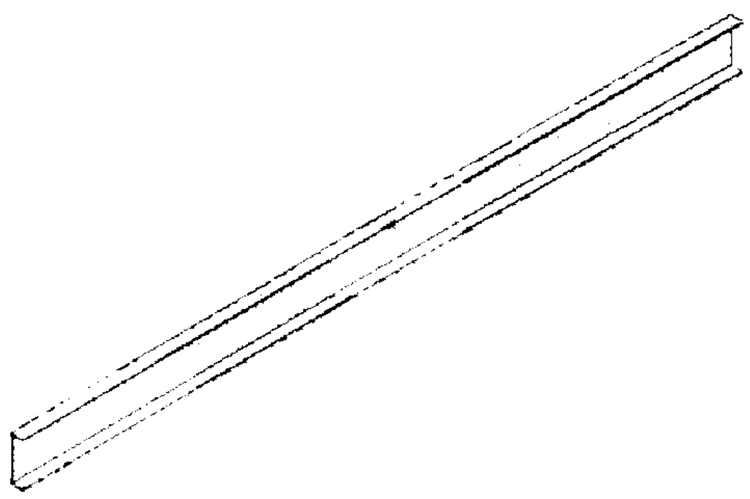

Figure 3.9: Steel sheets bent into C-channel bar to make fin

3.2.1.1 MIG Welding

Metal inert gas welding (MIG) is a semi automatic welding technique that is employed when the base metal cross-section is very thin. As 1.5mm gauge thickness stainless steel sheet was used to make the water tank, MIG welding ideally suited the joining procedure. Due to the low conductivity of the base metal, heat dissipation becomes critical issue as it can manifest itself in distortion, a problem that is encountered when normal welding procedures (arc and gas welding) are employed. Fig.3.7 illustrates the metal distortion problem encountered during arc welding. MIG welding abates the problem through higher control and low heat inputs. The welds require almost no cleanup.

3.2.2 Recommended Manufacturing Techniques

The following section presents the manufacturing techniques for high quality, low cost and fast production of collector units identical to the prototypes.

3.2.2.1 Seam Welding

Seam welding is a resistance welding technique that produces quality welds at faying surfaces of overlapped parts along the length of a joint. Like spot welding, seam welding relies on two electrodes to apply pressure and current to join metal sheets. However, instead of pointed electrodes, wheel-shaped electrodes roll along and often feed the work piece, making it possible to make long continuous welds [9].

A convenient method to attach fins to the water tank would be through seam welding as its automatic procedure requires minimal skill and effort level. Moreover, the welds produced through seam welding are uniform and maintain a higher contact surface of the fin with the absorber plate. In case of the MIG welding, the contact is established only at the slots which were cut in the metal plate. Seam welding would ideally suit any batch production because of its automatic nature. Moreover the slots that were cut into the sheet for MIG welding are not required in case of seam welding thus reducing the nibbling cost. The use of seam welding is illustrated in fig 3.8. For connecting the inlet and outlet pipes, gas welding was employed.

3.2.2.2 Jigs

Jigs can be created for the bending of the sheet to form the collector water tank. This could enable faster and easier production and reduce the skill level required. Similarly, jigs can also be setup for bending the plate to form C or Z channel bars which are easier to weld as they provide overlapping surfaces.

3.2.2.3 Inlet and Outlet Pipes

The inlet and outlet pipes can be soldered to the body of the water tank, resulting in a reasonable strength joint. As the pipes used are normally of different materials (other than steel), soldering is the only option for joining. The circular cut-outs for placing the pipes

can be created through a nibbling machine. To enable the ability to change to angle the use of expandable polymer pipes are suggested at the inlet and outlet to be used connected by means of non toxic adhesives.

3.3 Instrumentation for Experiments

The equipment setup for the experimentation of both the collectors is described in this section. A total of 16 thermocouples were used for measurements. 12 of them measured the temperature inside the water tank at positions shown in the fig.3.12 (pg 65). Ambient temperature inside the lab was measured by one thermocouple while 3 were placed on the glass cover. In the later scheme of experiments, transparent insulation material was used inside the air cavity and four thermocouples were used for experiments.

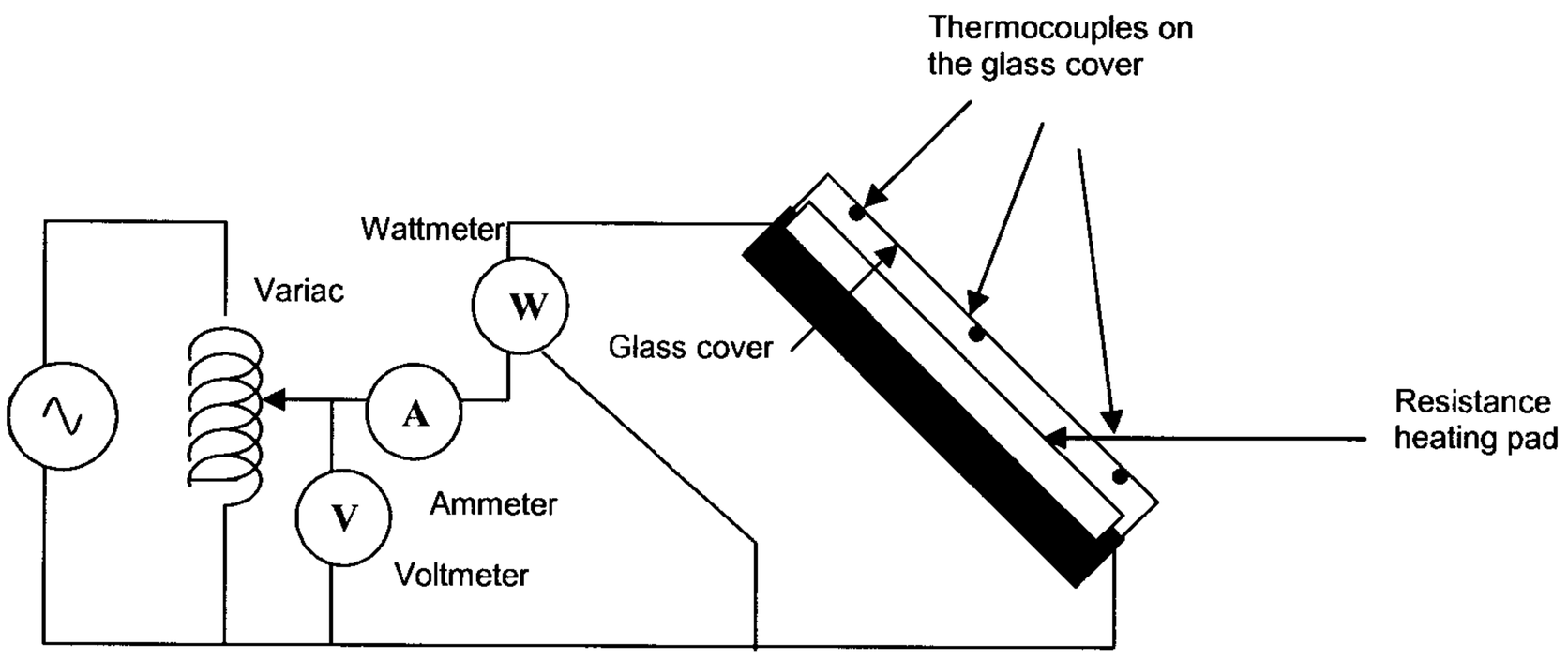

Figure 3.10: Circuit diagram of the electrical equipment for control & measurement of the heat flux.

3.3.1 Thermocouples (K-type)

Several types of thermocouples have been developed, each type customized to perform in different conditions or more discretely, different temperature range. K-type thermocouples[3] are the most popular and use nickel-chromium and nickel-aluminium

[3] TC LTD; website: http://www.tc.co.uk

alloys to generate voltage. Table 3.5 illustrates the various types of thermocouples; their corresponding temperature ranges and resolution [10].

Table 3.5: Range of temperatures for different thermocouple types

Thermocouple Type	Overall Range (°C)	0.1 (°C) Resolution	0.025 (°C) Resolution
B	100..1800	1030..1800	-
E	-270..790	-240..790	-140..790
J	-210..1050	-210..1050	-120..1050
K	**-270..1370**	**-220..1370**	**-20..1150**
N	-260..1300	-210..1300	340..1260
R	-50..1760	330..1760	-
S	-50..1760	250..1760	-
T	-270..400	-230..400	-20..400

The relationship between the temperature and current is not linear and hence a polynomial relation is used for conversion. Grant SQ800 series data loggers were used for recording the temperature. The logger used the following relationship as defined by the British Standards (BS EN 60584.1),

$$\text{Temperature conversion equation: } T = a_0 + a_1 x + a_2 x^2 + \ldots + a_n x^n \qquad (3.2)$$

Where the coefficients a_0 –a_5 are presented in table 3.6 while "x" is the current in amperes. For the common type- K thermocouple[4], the voltmeter must be able to resolve 4 μV to detect a 0.1 °C change. The calculation of high-order polynomials is a time consuming task for a computer. Time can be saved by using a lower order polynomial for a smaller temperature range. In the software for one data acquisition system, the thermocouple characteristic curve is divided into eight sectors, and each sector is approximated by a third order polynomial.

[4] Resistance Technology Limited, 8 Worrall Street, Salford, Manchester, M5 4TH, England, UK http://www.resistance-technology.co.uk

Table 3.6: Polynomial coefficients for K- type thermocouples [10]

Polynomial Coefficients	Type K 0°C to 1370°C ± 0.7°C 8th order
a_0	0.226584602
a_1	24152.10900
a_2	67233.4248
a_3	2210340.682
a_4	-860963914.9
a_5	4.83506E + 10
a_6	-1. 18452E + 12
a_7	1.38690E + 13
a_8	-6.33708E + 13

3.3.2 Silicone Rubber Resistant Heating Pad

A resistant heating (silicone rubber) pad was used for imposing heat flux. The pad heat output was controlled through a variac attached to it (see fig.3.10). Silicon rubber can withstand exposure temperatures of up to 230˚C. The fibreglass reinforced silicone rubber layers sandwiched a pre-formed heating element made from fine resistance wires. The heating pad was checked by means of a thermal imaging camera and was found devoid of any hotspots. Silicon rubber has high emmisivity for long wave length radiation and a value of (ϵ =0.86 to 0.95)[11]. The rubber pad dimensions were 1000 x 960 mm.

Figure 3.11: Silicone rubber resistance heating pad for applying the desired heat flux

3.3.3 Uncertainty Analysis and Propagation of Error

In order to gauge the quality of any data and the consequent results from analysis of data, it is vital to carryout an uncertainty analysis and to evaluate the likelihood of error propagation to downstream processes. Apart from the errors that cannot be accounted and eradicated such as human errors, it is important that all systematic or instrument errors should be measured, scaled and adjusted in calculations to improve the quality of the data acquired through experiments.

All measuring instruments, regardless of their precision have a certain domain of measurement termed as range, and a least possible value that can be measured called resolution. In most cases the range of instrument is inversely related to resolution of measurements. The uncertainty in the resolution herein is referred to as the accuracy. It is important to estimate the range of the variable to be measured during the operation and the requirement of accuracy beforehand, so that appropriate measuring instruments are selected. Temperatures in a collector can reach values as high as 76˚C according to Muneer et al [12] from his tests on rectangular tank ICS in Benghazi, Libya. This provided a clue to what the outer limit of temperature might be for the developed collectors. As the volume of the water tank for the fabricated collectors was sufficiently large i.e. 50 litres and the temperature measurements were to be taken after 10 min intervals, it was judged that temperature accuracy of 0.1 ˚C would suffice. Therefore K-type thermocouples were chosen on this basis.

The K-type thermocouples were calibrated using distilled water and carrying out ice and boil tests to set temperatures of 0˚ and 100˚C respectively. As Edinburgh is a coastal city, slightly above sea level, it was reasonable to assume of 100˚C as boiling temperature. Due to the limitation of the resolution of the data loggers, a final least count of 0.1 ˚C was attained. As mentioned earlier, this resolution was sufficient for the experiments as the range of expected temperatures was 15˚-85 ˚C. The limits of error, for the K-type thermocouples is reported[13] ± 2.2°C or 0.75% above 0°C (whichever is greater). As described earlier, the relation between the current produced at the junction of a

thermocouple and the temperature is not linear and therefore a polynomial function to accurately define the temperature is used. This polynomial (8^{th} order) is highly accurate and thus the uncertainty due to the polynomial-accuracy can be neglected.

For the voltmeter (AC voltage) for the range of 200V, a resolution of 100mV ± (3% reading + 5digits) was listed in the data specification sheet. Similarly, the ammeter for the AC current range for up to 2000mA was ± (1% reading + 2digits) was also noted. The electrical circuit (Fig. 3.10) although measured the heat flux both through the volt + ammeter as well as watt (power) meter; however the uncertainty in the power output culminated to + 4.5% or -3.5% of reading, assuming that both the ammeter and the voltmeter would have negligible influence over each other (this in reality depends upon their internal resistance).

It would be appropriate at this point to segregate the system input and output uncertainties. The heat flux provided to the system is the input, while the thermocouple readings can be classed as system outputs. In order to estimate the mean temperature or more importantly, the energy absorbed by the system, thermocouple readings cannot be readily used. A control volume should be defined that describes the reason of influence of each thermocouple inside the tank. The average temperature of this control volume determines the temperature at which average energy inside the heater is stored.

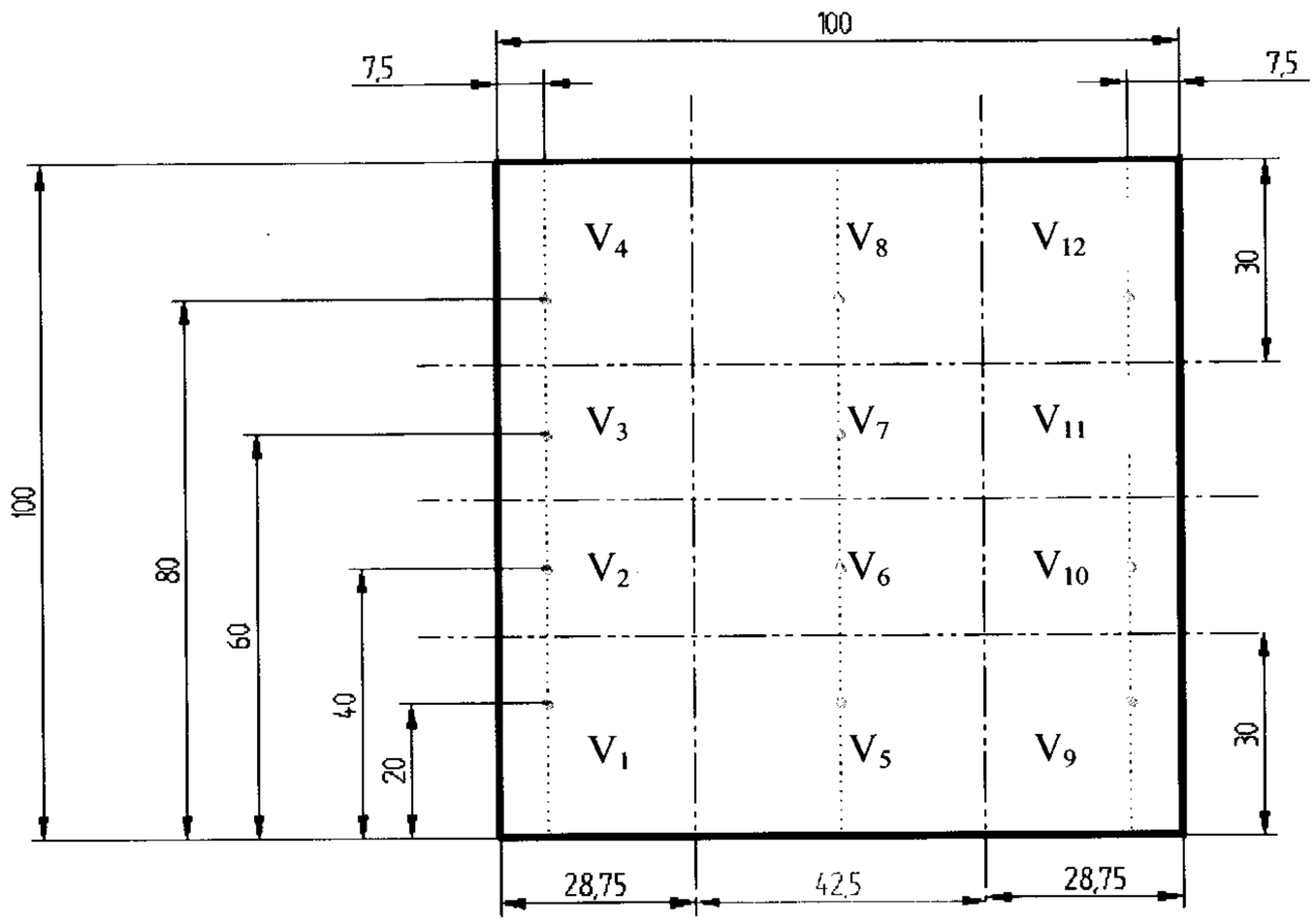

Figure 3.12: The position of the thermocouples inside the tank. The dashed lines indicate the control volumes. Blue dots represent the thermocouples. All the dimensions are given in cm

The volume average temperature therefore takes the form:

$$T_{av} = \frac{[(0.0043125)(4)(T_1 + T_4 + T_9 + T_{12}) + (0.002875)(4)(T_2 + T_3 + T_{10} + T_{11}) + (0.006375)(2)(T_5 + T_8) + (0.00425)(2)(T_6 + T_7)]}{0.05} \quad (3.3)$$

Where: $V_1 = V_4 = V_9 = V_{12}$; $V_2 = V_3 = V_{10} = V_{11}$; $V_6 = V_7$; $V_5 = V_8$

For a pilot test, the output of the thermocouples using the control volume was compared to simple averages for 4 and 12 thermocouples and is shown in table 3.7. It was noted that the simple average for both 4 and 12 thermocouples under predicts the results.

Table 3.7: Comparison of the control volume approach vs average of 4 and 12 TC

TC 5	TC 6	TC 7	TC 8	Average of TC 5-8	Average of TC 1-12	CV Approach	% Difference CV -4 Average	% Difference CV -12 Average
19.9	20.0	19.9	20.5	20.1	19.8	21.12	-4.95	-6.45
20.0	20.3	20.2	20.9	20.4	20.0	21.37	-4.78	-6.42
20.2	20.5	20.4	21.2	20.6	20.2	21.63	-4.87	-6.49
20.3	20.7	20.7	21.4	20.8	20.4	21.88	-5.05	-6.65
20.4	20.8	20.8	21.7	20.9	20.6	22.13	-5.43	-6.93
20.7	21.0	21.0	21.9	21.2	20.8	22.39	-5.53	-7.06
20.8	21.2	21.3	22.3	21.4	21.0	22.57	-5.20	-6.97
20.9	21.3	21.4	22.4	21.5	21.2	22.84	-5.85	-7.16
21.0	21.5	21.7	22.7	21.7	21.4	23.05	-5.75	-7.34
21.2	21.7	21.8	22.9	21.9	21.6	23.24	-5.76	-7.23
21.3	21.8	22.0	23.0	22.0	21.7	23.45	-6.06	-7.37
21.5	22.0	22.2	23.3	22.3	21.9	23.70	-6.10	-7.51
21.7	22.2	22.3	23.5	22.4	22.0	23.90	-6.16	-7.76
21.8	22.4	22.5	23.8	22.6	22.3	24.05	-5.93	-7.49
21.9	22.5	22.7	23.9	22.8	22.4	24.30	-6.36	-7.63

As the temperature was measured at 12 different points inside the heater, the total uncertainty of enthalpy of the system could be as much as ± 5538.72 kJ arising from 50 x 4.196 x 26.4 for a worst case scenario. Where 26.4 is the cumulative uncertainty of 12 TC (each TC uncertainty being ± 2.2°C).

Thus for 100W of applied heat flux, the percentage of uncertainty in the total energy content after 1 hour can be as much as 354.46 kJ. The percentage difference of energy absorbed by the system increases initially with time and settles around 7-8% of the 12-TC average. This is because the system moves towards attaining equilibrium with the surroundings and the magnitude of the change in temperature drops with time.

The control volume approach helps to reduce the error associated with evaluating the average temperature. A normal average means considering equal control volumes. It was noticed through the temperature profile of a similar ICS heater by Liu et al [14] that the has a sharp change in temperature occurs at the top and the bottom end of the collector. Similar profile was also confirmed through a basic CFD analysis (details will be presented in the following chapter). However in the middle portion of the heater, the temperature change is fairly linear. Therefore the top and the bottom thermocouples in the case of control volume approach are given the length of 0.3 meters instead of 0.25 m. This gives the average temperature a more accurate value as shown in Fig 3.12.

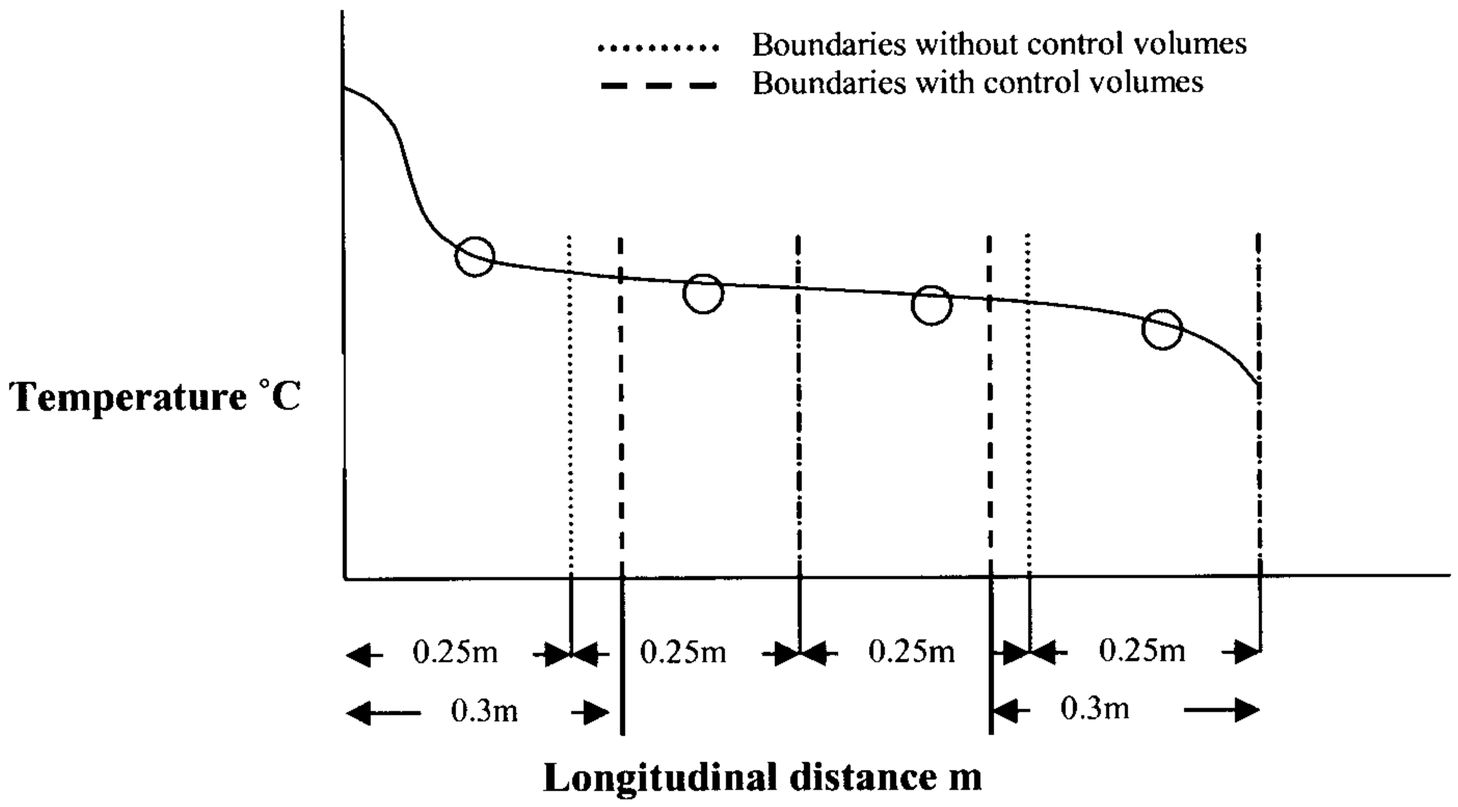

Figure 3.13: Hypothetical diagram depicting a normal temperature profile plotted against control volumes

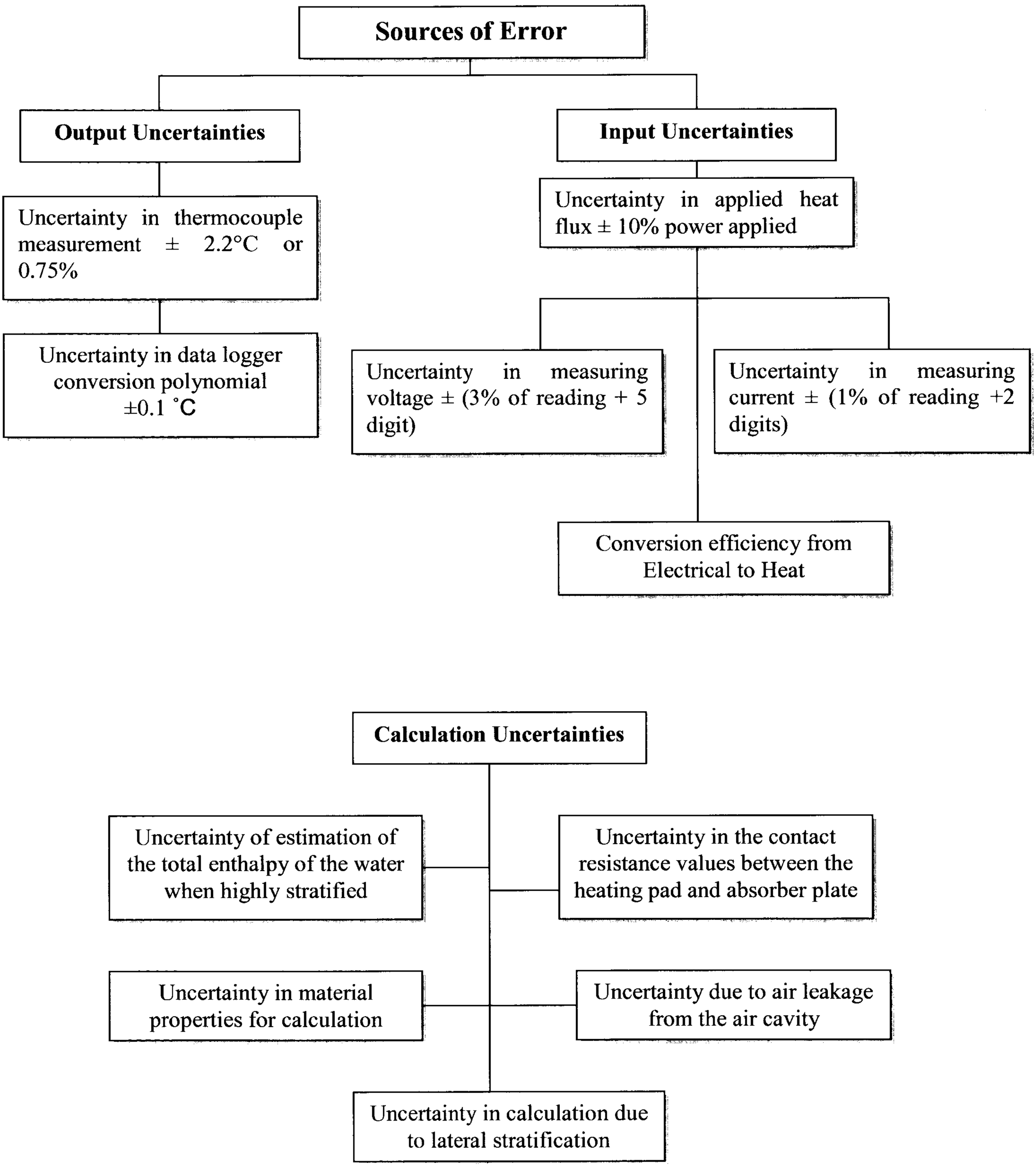

Figure 3.14: Sources of error & uncertainties

3.4 Heat Transfer Mechanism in a Collector

Heat loss/gain through a solar water heater ensues and emanates through all three modes of heat transfer i.e. conduction, convection and radiation. The latter two constitute the bulk of the heat transfer. Radiative heat losses in particular are difficult to measure with any degree of certainty through experimental means. At higher temperature levels, the radiation losses can be of the same order as the convection losses, or even higher, depending upon the characteristics of the cover and absorber plate. Convection and radiation losses both can be suppressed through well established techniques. Convection suppression can be carried out by using materials such as honey comb structure or transparent insulation material. Radiation losses can be controlled by employing selective surfaces (Section 2.2.3).

Focusing back on the integrated collector storage, we now turn our attention to the individual mechanisms of radiation and convection that occur inside the collector and result in heat loss or heat gain. Interestingly, all these different mechanisms have been studied in great detail and are as follows:

- Convective heat transfer from an inclined flat plate
- Convective losses from two parallel plates at different temperature (air cavity)
- Convective losses from flat plate to ambient
- Radiative heat transfer between two plates
- Radiative losses from a flat plate to sky

In the following section each of these modes are studied individually along with their effect on the design of the collector. All of these mechanisms of heat transfer are mainly influenced by the temperature of the absorber plate temperature. Therefore throughout the course of this thesis, the absorber plate temperature has been taken as the driving parameter, while the cover temperature and other parameters are considered a function of the absorber plate temperature.

3.4.1 Natural Convection from (Inclined) Flat Plates

Inclined heated plates have been studied in detail and a good amount of literature is present on angles ranging from horizontal ($\phi = 0^{\circ}$) to vertical ($\phi = 90^{\circ}$). Regressions are available for both upward facing and downward facing heated or cooled plates. The following regression for the lower surface of heated plate or the upper surface of a cooled plate is commonly used [1]:

$$\overline{Nu}_L = 0.27\,\mathrm{Ra}_L^{1/4} (10^5 \le Ra_L \le 10^{10}) \qquad (3.4)$$

For the above equation, the fluid properties are determined at T_f, and the characteristic length L = A/P, where "A" and "P" are respectively, the area and the perimeter of the plate. Another regression for upward facing cooled plates or downward facing heating plate is the one developed by Fuji and Imura (1972) [2], this regression can be used for both isothermal and constant heat flux horizontal plates.

$$\mathrm{Nu_L} = 0.58\mathrm{Ra_L}^{1/5},\ 10^6 < \mathrm{Ra_L} < 10^{11} \qquad (3.5)$$

For the case of a vertical plate, Churchill and Chu (1975) recommended the following regression for an isothermal vertical plate for Laminar flow ($\mathrm{Ra_L} \le 10^9$).

$$Nu_L = 0.68 + \frac{0.67 Ra_L^{1/4}}{[1+(0.492/\mathrm{Pr})^{9/16}]^{4/9}}, 10^{-1} < Ra_L < 10^9, \qquad (3.6)$$

For a uniform heat flux Churchill and Chu [3] recommend that the following regressions can be applied (the only change is the denominator value of 0.492 replaced by 0.437).

$$Nu_L = 0.68 + \frac{0.67 Ra_L^{1/4}}{[1+(0.437/\mathrm{Pr})^{9/16}]^{4/9}}, 10^{-1} < Ra_L < 10^9 \qquad (3.7)$$

For the case of inclined heated downward facing plate (fig 3.5), equation 3.6 can be used but the Rayleigh number has to be evaluated as:

$$Ra_L = \frac{g(\cos\theta)\beta(T_s - T_\infty)L^3}{\upsilon\alpha} \qquad (3.8)$$

Where the angle θ is measured from the vertical and L is the length of the plate in the flow direction. If θ>88°, the regressions for the horizontal plate can be used. The incorporation of angle in the Rayleigh number term for the regression suggests that a sinusoidal increase can be expected in the heat transfer with the increase in angle.

Regression for an inclined plate with the heated surface facing down, for uniform heat flux, Fussey and Warneford (1978) [4] recommended the use of the following equations:

$$Nu_x = 0.592(Ra^*{}_x \cos\theta)^{0.2}, 0 < \theta < 86.5, Ra_x^* < Ra_{x,CR} \qquad (3.9)$$

$$Nu_x = 0.889(Ra^*{}_x \cos\theta)^{0.205}, \theta < 31, Ra_x^* > Ra_{x,CR} \qquad (3.10)$$

Where $Ra^*_x = g\beta qx^4/k\nu\alpha$ (3.11)

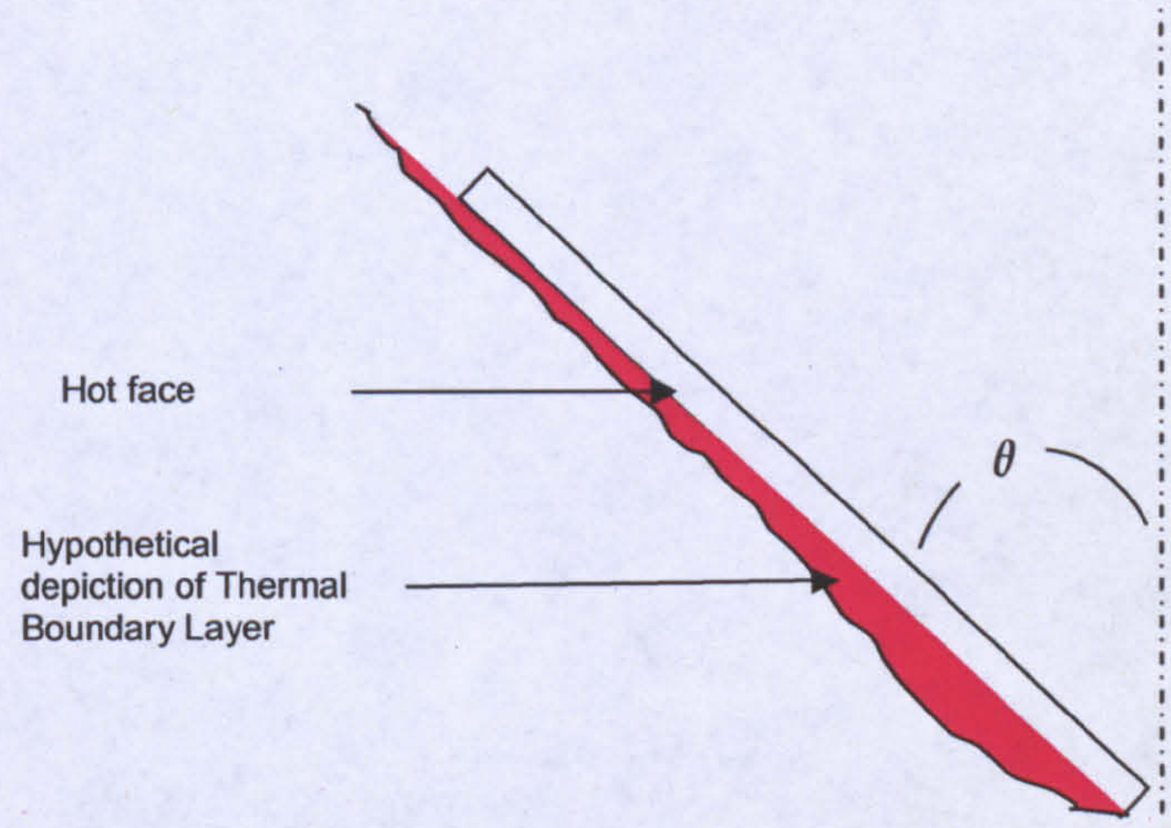

Figure 3.15: Heated plate facing down. Angle is measured from the vertical

3.4.1.1 Considerations for Collector Design

- It is apparent from the study of inclined plate that a downward facing heated plate is the worst case scenario for spread of heat with the Nusselt number poised at unity. As the angle increases, the Rayleigh number increases which results in an increased heat transfer. It is worth noting that the best case for convective heat transfer (highest heat lost) is when the plate is vertical.

- It is important to know the state of the natural convection flow (laminar or turbulent). Turbulence, if artificially induced, can substantially increase the heat transfer. Roughening the water side surface for promoting heat transfer is an important prospect.

3.4.2 Natural convection in Inclined Cavities (Air Layers)

The literature review for inclined air layers or air cavities has already been presented in chapter 2. The area of natural convection in an air-cavity is well established and has been picked up by various researchers around the globe. The widely accepted and used regression is that of Hollands [15]

$$Nu_L = 1 + 1.44\left[1 - \frac{1708}{Ra_L \cos\theta}\right]^*\left[1 - \frac{1708(\sin 1.8\theta)^{1.6}}{Ra_L \cos\theta}\right] + \left[\left(\frac{Ra_L \cos\theta}{5830}\right)^{1/3} - 1\right]^* \quad (3.12)$$

The notation * implies that, if the quantity in brackets is negative, it must be set equal to zero. The relation holds for H/L $\geq$12 and $0° < \phi \leq \phi_c$. The mentioned equation has been found to give excellent results inside the regime of longitudinal rolls, when these rolls collapse at higher angles, the equation fails to deliver accurate results.

The angle depends upon the orientation of the hot surface. 0° is taken as the angle when the air cavity is bottom heating, while 180° is the angle when the heating surface is the top surface. Fig 3.16 illustrates the definition of the aspect ratio and the angles, while fig 3.17 shows the variation of Nu with the increase in angle.

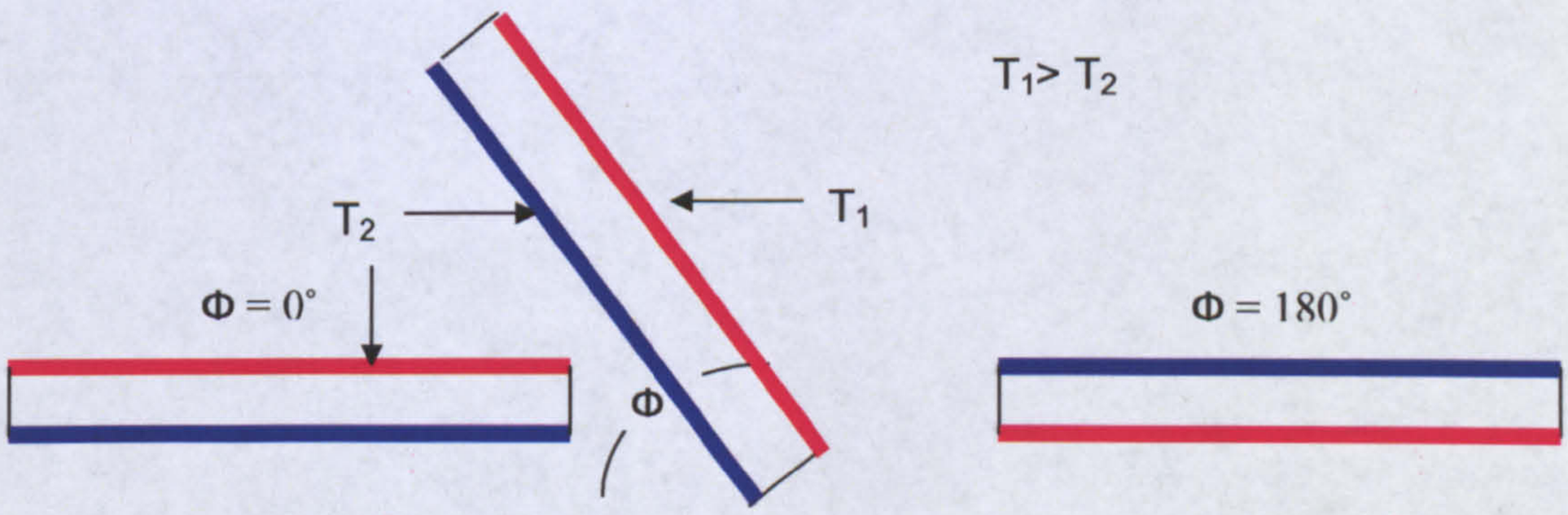

Figure 3.16: Air-cavity showing the orientation of the angle with respect to the position of the hot and cold plates

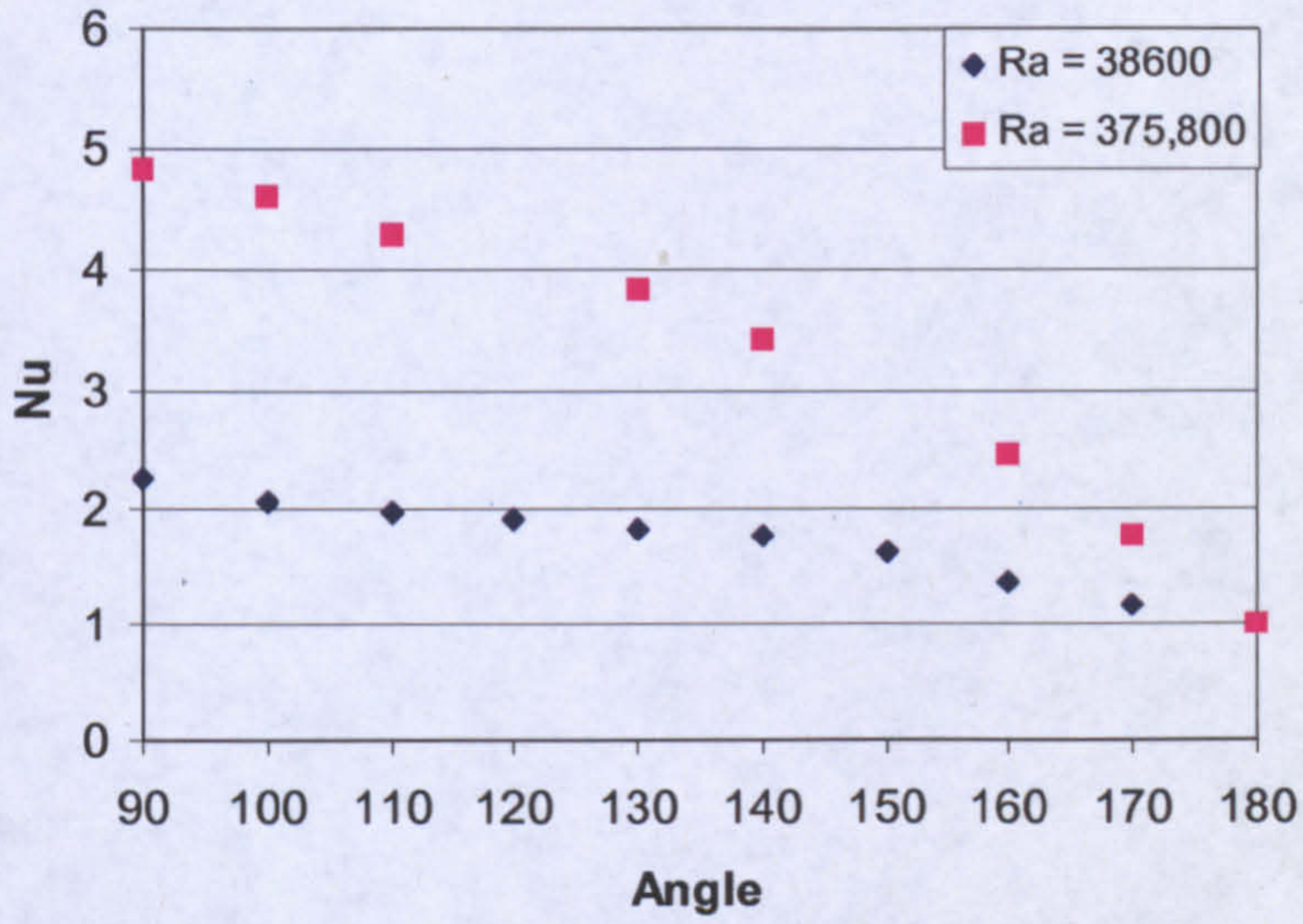

Figure 3.17: Results of Elsherbiny showing variation of Nu with increasing angle of inclination ($\phi = 90° - 180°$)

3.4.2.1 Findings for Collector Design

- Losses through the top portion (air-cavity) make up a significant portion of the overall collector losses and ensue via convection and radiation. The design of a properly designed air cavity could lead to substantial reduction in the heat losses. It has been noticed that apart from the temperature difference, the tilt angle the thickness of the air gap is vitally important to collector design.

- For the cavity of 35 mm thickness- as in the case of prototype collectors- a temperature difference of less than 0.5 °C is enough to propel the Rayleigh number beyond the critical limit (Ra =1708) and hence convective losses take over conduction

- For the experiments on prototype collectors (details of which are presented in the following chapter) Rayleigh number for the air cavity was found to be in range[5] Ra $= 0 - 10^5$

3.4.3 Radiation to Sky

Radiative losses make up a major fraction of the total losses and thus cannot be ignored. Depending upon the temperature range, they can amount up to half, or even more, of the total losses. Radiation to the sky can be calculated through the equation 3.14.

$$q = \sigma \epsilon A (T^4 - T_a^4) \qquad (3.13)$$

Where σ is the Stefan- Boltzmann constant $\sigma = 5.67 \times 10^{-8}$ $Wm^{-2}T^{-4}$

Where T_a represents the ambient temperature. For calculating the radiative losses to the sky, it should be noted at this point that the ambient temperature is not equal to sky temperature (sky temperature being slightly lower). The following relationship has been suggested to calculate the sky temperature if ambient temperature is known.

$$T_{sky} = 0.0552\ T_a^{1.5} \qquad (3.14)$$

The above equation was proposed by Swinbank [16] for estimating more accurate values of radiative heat loss to the sky. To estimate the radiative heat loss from the collector, experiments for which were conducted inside the laboratory, equation 3.14 was not used. Nonetheless this equation is important will be used for calculating the losses when predicting the field performance of the collector.

---

[5] The mentioned range of Rayleigh number was computed from the experiments on the prototypes as mentioned in section 4.1.2

3.4.3.1 Key Findings for Collector Design

- As evident from equation 3.13 the collector glass should be made out material that has low emissivity ϵ and higher transmissivity. As discussed earlier, tinted glass with higher iron oxide content would serve the purpose.

3.4.4 Radiation from Plate to Cover

The heat transfer between the cover and the plate is through both radiation and convection. In the case of two covers, the heat exchange through radiation is higher between cover 1 and cover 2. The standard expression for net radiation exchange between two parallel plates is:

$$Q = \frac{\sigma \varepsilon_1 \varepsilon_2 A_c (T_1^4 - T_2^4)}{(1 - \frac{1}{\varepsilon_1} - \frac{1}{\varepsilon_2})} \tag{3.15}$$

Where T_1 and T_2 are the temperatures of the hot and the cold plate respectively

ϵ_1 and ϵ_2 are the emissivity for the same.

3.4.4.1 Key Findings for Collector Design

- The use of selective coating on the absorber plate can curb the emmisivity and thus reduce the radiation exchange. In some places such as Australia [17], where selective surface coatings are cheaper than painting the surface matt black, reduces the cost and thus the payback time.
- The collector cover should be opaque to high wavelength radiation.

3.5 Summary

The proposed collector design was inspected with a bottom up approach. The collector components were examined for the thermal properties that affect the performance as well as parameters that influence the cost. It was noted that special care and specific methods have to be adopted for the welding of steel as the proposed design utilizes stainless steel sheets of thickness of only 1.5mm. Although MIG welding can be employed it was however suggested that seam welding is a better proposition for higher weld quality and productivity. The fins were made in "C" channel bars to provide a contact overlapping surface for the welding procedure. The requirement of slots cut on the top (absorber plate) and the bottom sides of the tank – that was used for MIG welding- is eliminated with seam welding.

The physical and thermal properties of the individual elements that make up the heater were examined in detail. Steel, as anticipated, was the biggest contributor to the cost. However it was encouraging to find the overall collector cost remained within £700 for 1 m^2, 50 litre capacity collector.

Uncertainties in the instrumentation and in calculation were examined. It was noted that there were several different sources that contributed towards the error. For the experimental tests, the measuring instruments had measurement tolerances, where as in calculations error induction was due to assumptions. The magnitude of each error was calculated. It was noted that due to stratification inside the tank and the contact resistance between the heating pad and the absorber plate, the uncertainty in applied heat flux going to the tank was not possible to estimate unless thermal analysis was carried out. It was for this reason, that the temperatures on the cover were measured. These temperatures have been used (in the later chapters) to evaluate the heat losses and were extrapolated to find out the heat flux going in the water tank.

Finally the mechanisms of heat transfer that occur inside the collector were examined in detail along with the developed mathematical expressions for their behaviour.

Although this chapter encapsulates the details pertaining to fabrication of a low cost and durable collector- that can be referenced for manufacturing process- the details on manufacturing an optimized collector will be presented in the chapter 6. With the details of the experimental setup now presented the next chapter deals with estimation of collector performance.

The break up of the cost of the collector components is provided in table 3.8 for the interest of the reader.

TEXTBOX 2

Rayleigh Number (Ra)

Rayleigh Number is the dimensionless number associated with the heat transfer within the fluid. When the Rayleigh number is below the critical value for that fluid, heat transfer is primary in the form of conduction; when it exceeds the critical value, heat transfer is primarily in the form of convection.

$$Ra = Gr.\Pr = \frac{g\beta(\Delta T)L^3}{\upsilon\alpha}$$

Prandtl Number (Pr)

The Prandtl number is a dimensionless number approximating the ratio of momentum diffusivity (viscosity) and thermal diffusivity. It is named after Ludwig Prandtl. It also gives a measure of the velocity boundary layer thickness to the thermal boundary layer thickness.

$$\Pr = \nu / \alpha$$

Peclet Number (Pe)

It is the ratio of heat advection to heat diffusion.

$$Pe = \frac{VL}{\alpha}$$

$$\alpha = \frac{k}{C_p \rho}$$

Nusselt Number (Nu)

The Nusselt number is a dimensionless number used in convective heat transfer calculations. It is the ratio of conductive heat transfer resistance to convective heat transfer resistance in a fluid media on the surface of a body.

$$Nu = \frac{hx}{k}$$

Table 3.8: Price break-up for the fabricated collector

Items		**Cost**
Stainless Steel sheet 304 2B	Material	£ 230[6]
Drawing, Nibbling process	Process	£ 30
Welding Process	Process	£ 30
Glass wool insulation	Material	£32/per roll[7]
Outer Frame (Wood)	Material	£ 65
Outer Frame Manufacturing	Process	£ 50
Glass Cover	Material	£ 104[8]
Coating and painting	Process	£ 50
Connecting pipes and fittings	Material	£ 50
Miscellaneous (Seal, Gasket, paint)		£ 50
Total		**£ 691**

[6] Price for July 2004 (when it was purchased)
[7] One roll can be used for insulating 6 collectors
[8] The glass prices are significantly lower if they are imported, (£ 8.525/m^2 from Shenzen China)

References

1. Muneer, T. and M. Asif, *Prospects for secure and sustainable electricity supply for Pakistan.* Renewable and Sustainable Energy Reviews, 2007. **11**(4): p. 654-671.
2. John Rocco, *Weatherproofing wood window sills and trim*. 6/18/2007, http://www.buzzle.com/articles/weatherproofing-wood-window-sills-and-trim.html.
3. R. H. B. Exell, M.A., D. Phil. (Oxford); Hon. D. Sc. (KMUTT). *Flat Plate Solar Collectors*. 2000 [cited 2007 15th March]; Available from: http://www.jgsee.kmutt.ac.th/exell/Solar/FlatPlate.html.
4. Holman, J.P., *Heat Transfer*. 7th ed. 1992: McGraw-Hill Book Co.
5. Glaser, P.E., I. A. Black, and P. Doherty „ *Multilayer Insulation*, in *Mechanical Engineer*. 1965. p. 23.
6. Engineering Fundamentals Website, *Thermal properties of stainless steel 302 B* 2007, www.efunda.com. p. http://www.efunda.com/materials/alloys/stainless_steels/show_stainless.cfm?ID=AISI_Type_302B&prop=all&Page_Title=AISI%20Type%20302B.
7. AAA Solar Supply Inc, *Solar Design Guide*. 2007: 2021 Zearing NW, Albuquerque, NM 87104. p. http://www.aaasolar.com/AAASolar2004WebCatalog.pdf.
8. Lincoln Electric, *The Procedure Handbook of Arc Welding*. 1994, Cleaveland.
9. Weman Klas, *Welding processes handbook*. 2003, New York: CRC Press LLC.
10. Pico technology, *Thermocouple catalogue*. 2007.
11. Carl Salvaggio and D.P. Miller;. *Temporal variations in the apparent emissivity of various materials.* in *Sensory Data Exploitation and Target Recognition, Algorithms and Technologies for Multispectral, Hyperspectral, and Ultraspectral Imagery X.* April 2004: Proceedings of the SPIE.
12. T. Muneer, *Effect of design parameters on performance of built-in storage solar water heater.* Energy conservation and Management 1985. **25**(3): p. 277-281.
13. National Institute of Standard and Technology, *Monograph 175,Revised to ITS-90.* reference tables for K-type.
14. W. Liu, J.H.D. and F.A. Kulacki, *Thermal Characterization of Prototypical Integral Collector Storage Systems with Immersed Heat Exchangers.* Journal of Solar Energy Engineering,, February 2005 **127**(1): p. 21-28.
15. K.G.T Hollands, T. Unny; G.D.Raithby, and L Konicek, *Free Convective Heat Transfer Across Inclined Air Layers.* Journal of Heat Transfer, Transaction of ASME, 1976. **98**(Series C): p. 189-193.
16. Swinbank, W.C., *Long-wave radiation from clear skies.* Quarterly Journal of the Royal Meteorological Society, 1963. **89**: p. 339-348.
17. Courtney, R.G., *An Appraisal of Solar Water Heating in the UK.* 1975.

CHAPTER 4

Research Methodology

Analysis, Calculations and Results

In the previous chapter, the collector components were studied individually along with their costs and physical properties. The optimization of the solar water heater requires gauging the influence of various design parameters individually as well as evaluating their cumulative effect. For this purpose, different analysis techniques are required that would incorporate these parameters and examine various cause and effect scenarios.

This chapter epitomizes the details of the analysis and calculations carried out on the prototype collectors. Primarily, the behaviour of the collector with various levels of imposed heat fluxes and different angles of inclination is examined. To understand the behaviour of the collector, a three pronged approach, comprising of experimental testing, abbreviated thermal analysis and CFD analysis was adapted for attacking the problem. Each mode individually would not have sufficed as the presence of several unknown parameters shroud the technicalities of the collector. The ultimate objective of this chapter is to establish the overall "U" value (heat lost coefficient) for both the finned and the non finned heaters.

Chapter Map

- 4.0 Overview
  - 4.1 Experimental Testing
    - 4.1.1 Experimentation Schemes
    - 4.1.2 Experimental Results
    - 4.1.3 Discussion on Experimental Results
  - 4.2 Abbreviated Thermal Analysis
    - 4.2.1 Complexity of the Absorber plate
    - 4.2.2 Assumptions for ATA
    - 4.2.3 Mathematical Expressions
    - 4.2.4 Simulation Flow Chart
    - 4.2.5 Results from ATA
    - 4.2.6 Discussion on ATA
  - 4.3 CFD
    - 4.3.1 Benchmarking natural convection
      - 4.3.1.1 Mesh Size Criterion
      - 4.3.1.2 Flow over a flat plate
      - 4.3.1.3 Flow on a Vertical Plate
      - 4.3.1.4 Flow in an Air Cavity
      - 4.3.1.5 Hindsight from benchmarking
    - 4.3.2 Details on CFD of Collector
    - 4.3.3 Discussion on CFD Results
  - 4.4 Discussion on U value
  - 4.5 Summary

4.0 Overview

The analysis of the collector behaviour is the first task on the road to optimization. The collector behaviour /characteristics herein refer to the response of the system to measured levels of irradiance. For a conclusive investigation, this response has to be measured and calculated at various levels of heat flux as well as various angles of inclination for both the finned and the non-finned prototypes.

The adopted research methodology is based on a three legged approach that comprises of experimental testing, abbreviated thermal analysis and CFD. Individually, each of these methods would not have sufficed for accurate and certain set of results. Prevailing uncertainties in each method due to either unavailability of data, precision of measuring instruments or even system errors undermine the accurate resolution of the collector. Therefore all three of them had to be used in conjunction to obtain a conclusive set of results. Furthermore the deficiency in the results from one method is in many cases countered by output of the other. For instance, through the experimentation, accurate data for collector was gathered only at a small number of points whereas through CFD, temperature and velocity data was available for the whole domain. However, the possibility of numerical errors in CFD presented an uncertainty. Thus, the results of all three methods have to be intertwined so that the outcome of each of the methods is verified and validated by the other. The situation is depicted in the fig 4.1.

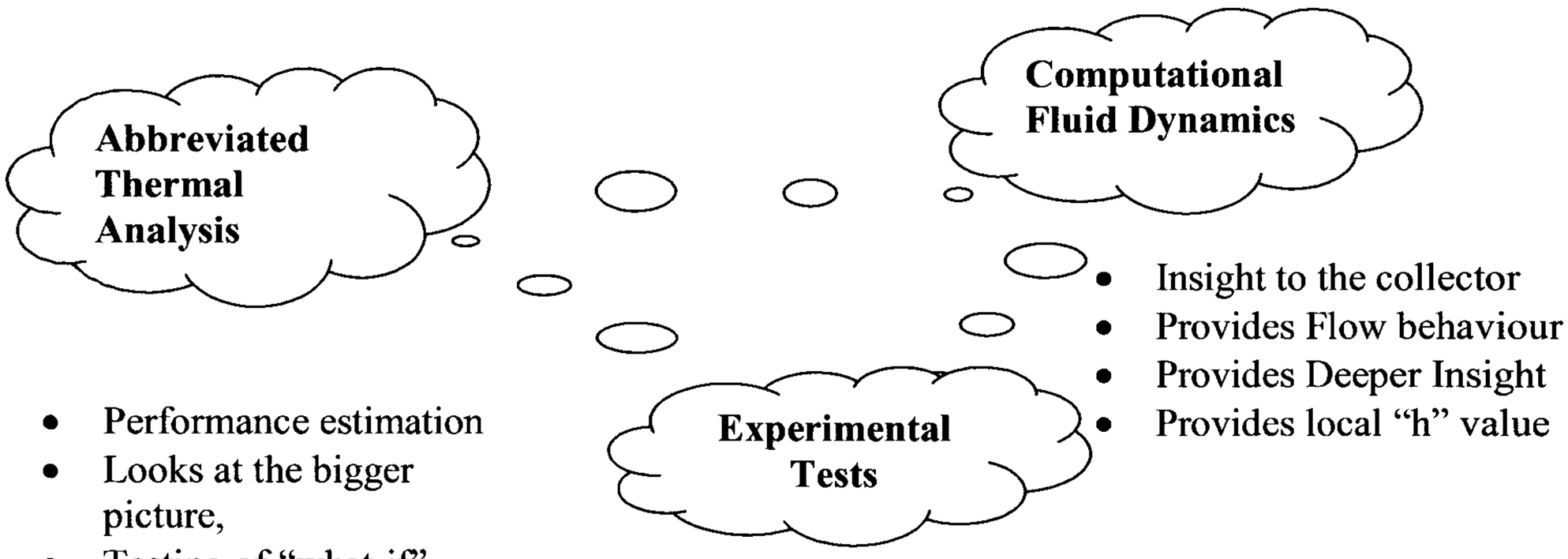

Figure 4.1: The Triumvirate Method

On similar grounds, an alternate method to CFD was also needed. CFD provided intricate details of the collector's temperatures and velocity, however it was computationally intensive and therefore could not be utilized for chronologically long transient simulations. Furthermore, to check several "what-if" scenarios an alternate method was required that would model the collector focusing at the "bigger picture", leaving aside the intricate details. This method should also be capable of handling different input parameters (changing of imposed heat flux) as well as design variables. Abbreviated thermal analysis was thus carried out for macro modelling of the collector. In the following section details of each method and results have been presented.

4.1 Experimental Testing

Experiments are the most reliable mode of recording the collector response because it is based on the actual performance of the collector therefore does not exclude any physical phenomenon that might be neglected when modelling the system mathematically. The

experimental measurements however include uncertainty as was noted in the previous chapter. This uncertainty manifests itself in the form of an error about the actual value. The scale of this error can be calculated as shown in the previous chapter. In case of abbreviated thermal analysis or CFD the scale of error is unknown and therefore the results are not as reliable. Furthermore, as mentioned earlier, experiments account for every occurring physical phenomenon that can possibly be neglected while modelling. In light of this, the results from the experimental tests are herein used as yardstick for benchmarking both the ATA and the CFD results. Therefore it can be rightly said that the experimental testing is the core while the other two are peripheral methodologies.

Experiments were done on both prototypes (details of the setup were presented in section 3.3) using identical schemes the details of which are noted in the next section.

4.1.1 Experimentation Schemes

To workout the collector response at various inputs, different series of experiments were devised. These schemes can be divided in five categories, the objectives of which are as follows.

a) The comparison between the finned and the unfinned heater
b) The performance of the collector at various angles of inclination
c) Cooling test and effect of transparent insulation material (TIM)
d) Draw-off characteristics
e) Thermal Imaging

Bearing in mind the Scottish weather conditions, an imposed heat flux of 400 W was assumed to be an adequate value for the maximum limit. This heat flux was imposed till the heater reached equilibrium temperature values i.e. no further temperature increase in the water was recorded. The temperature stagnation in most cases was achieved over a time period of over 1440 minutes (1 day). It can be argued- owing to the intermittent

nature of solar radiation- that imposing constant heat flux for the diurnal period is of little value. However the objective of the exercise was not to emulate the field conditions but to quantify the collector's behaviour (heat gain and heat losses) for which it was necessary to impose controlled conditions for a long duration. The measurements were taken in 50W increments starting from 100W. For every value of the applied set of heat flux, the heaters were tested at inclination angles of 0°, 30°, 45° and 60°.

Draw-off experiments were done with the heater inclined at an angle of 45°. Hot water was drawn-out from the heater at different flow rates in order to evaluate an optimal flow rate for maximum throughput of hot water. All measurements were logged at 10 minute intervals. However, for the draw-off experiments more frequent measurements were made, with interval time 10 sec to monitor the system response to the sudden change in water temperature.

Apart from the experiment on the heat gain by the collector, cooling tests were also performed to evaluate the "U"[1] (W/m^2k^{-1}) value of the heater before carrying out field tests. The reduction in "U value" using transparent insulation material was also recorded through experiments. Thermal images using an infrared thermal imaging camera were acquired to see the heat dissipation in detail. In the next section the results have been presented as well as the discussion for the same have been presented. The draw-off results are not discussed in this section and will be presented later in Chapter 5 where they are more relevant.

4.1.2 Experimental Results

This section discusses the various results that were obtained from the experiments. The conclusion drawn from these results is taken forward for modelling as well as suggestion for design improvements. As mentioned earlier, temperatures were recorded every 10 minutes. The complete datasets for the results can be referenced from annexure (Appendix C) as not all the datasets have been presented herein to maintain brevity.

---

[1] The term "U" value is define in textbox 3 page 133

4.1.2.1 Collector Response on Imposed Heat Flux

The response of the system to an imposed heat flux is examined first. In fig 4.2, the temperatures in the collector for an imposed heat flux 200 W are shown. The imposed heat flux was increased to 250 W after a period of 1 day. The system was kept at the same heat flux for the period of 67 hours after which it was allowed to cool down to ambient temperature. The position of thermocouples can be referenced from fig 3.12.

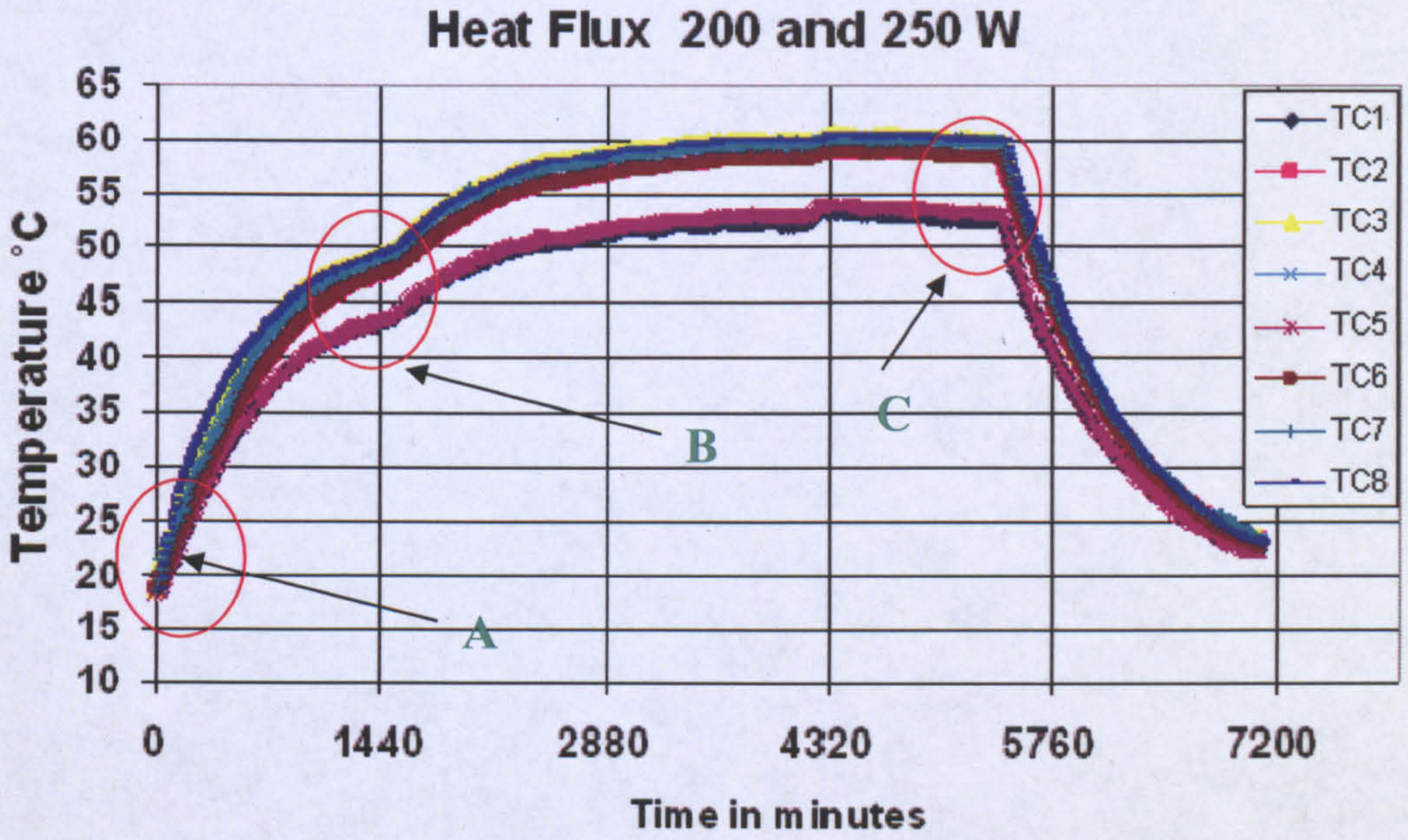

Figure 4.2: The temperatures inside the collector for 200W-250W for finned collector at $\phi = 45^{\circ}$ plotted against time

The temperatures in fig 4.2 were obtained from the experiment on the finned collector inclined at an angle of $\phi = 45^{\circ}$. There are three distinct regions of interest in the chart, marked A, B & C. The region "A" highlights the initial stage where the temperature can be noticed to rise sharply, the rate of increase gradually decreases thereby following an asymptotic profile. Region "B" encompasses two important points; the stagnation temperature (for 200 W) is nearly achieved as indicated by the slope of the temperature curves that are near horizontal. Secondly, another rise in the curve can be noticed which indicates when the collector heat flux was increased from 200 W to 250 W. Region "C" highlights the logarithmic decrease in the temperature after the removal of heat flux with

a profile depicting Newton's law of cooling. It has to be kept in mind that the rubber pad results in a slower rate of drop because it shields the absorber plate from the air inside the air-cavity. Hence the actual collector temperature drop-rate would be higher. This situation practically can arise when the collector is shaded.

4.1.2.2 Rise in Temperatures and Equilibrium Temperatures

It was noticed in fig 4.2 that a stagnation temperature was achieved for both 200W and 250W. In light of this, further tests were conducted to evaluate the stagnation temperatures for a particular value of heat flux.

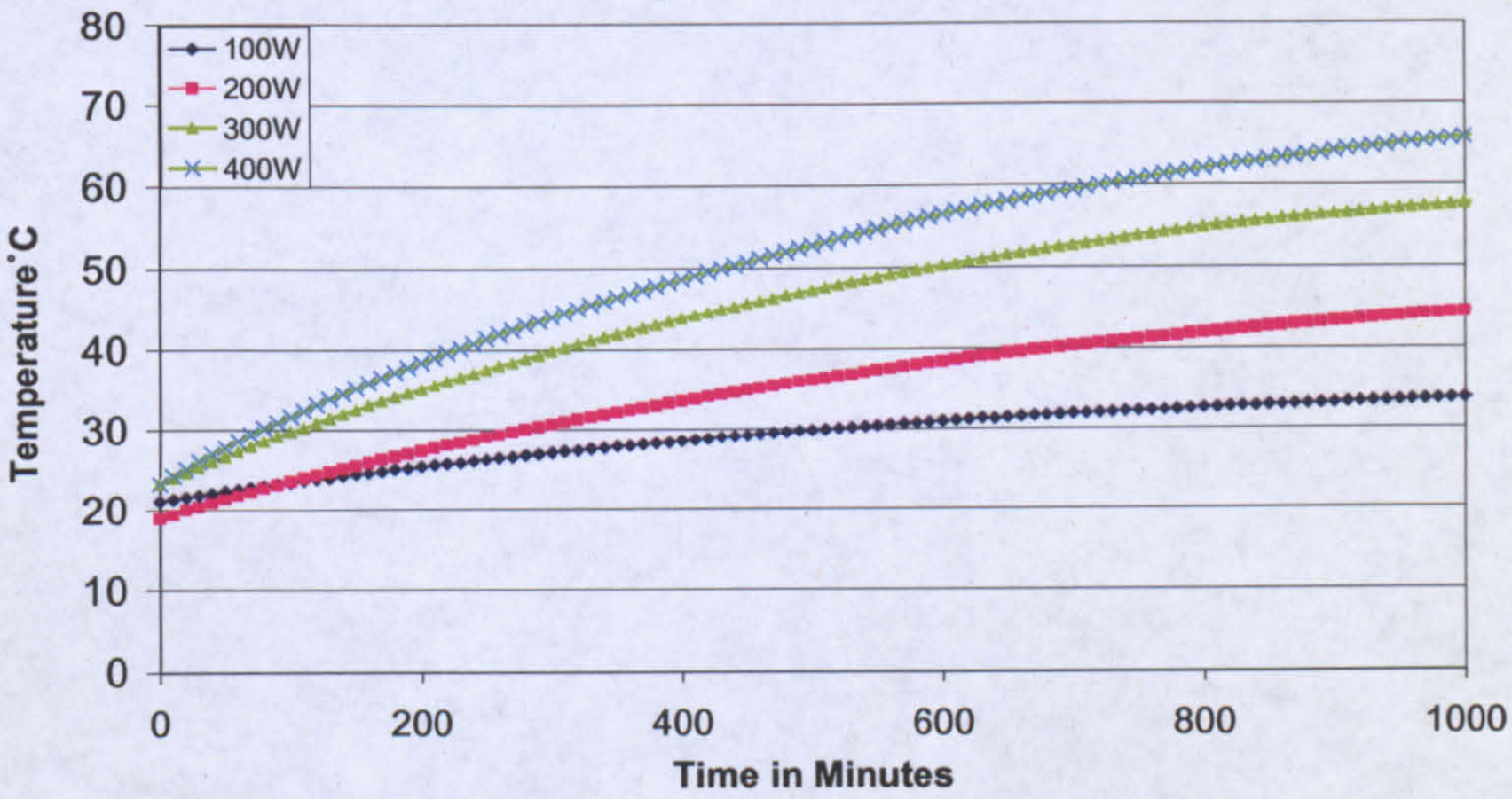

Figure 4.3.a: The average temperatures inside the collector for 100, 200, 300, 400 W for the finned collector at $\phi = 45^{\circ}$

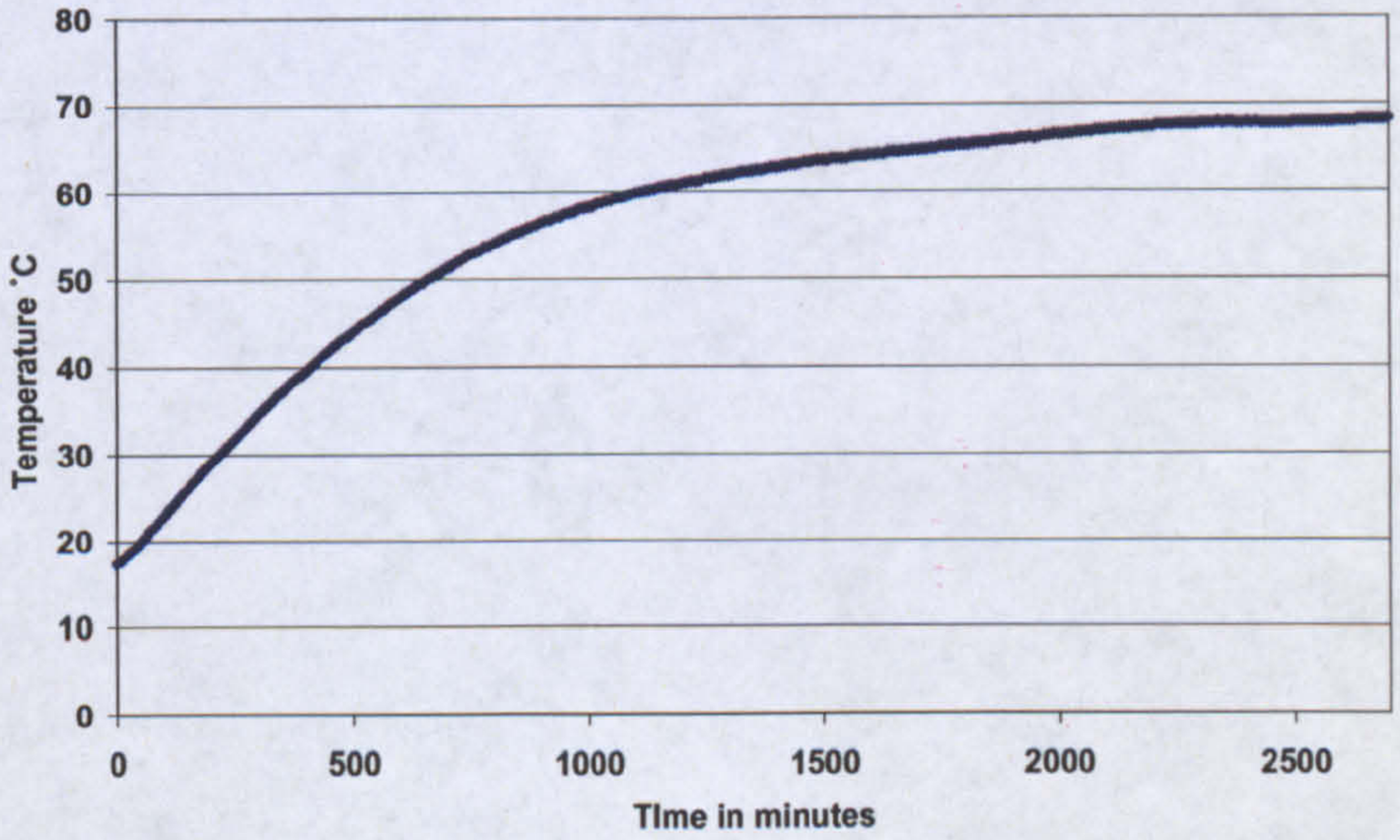

Figure 4.3.b: The average temperatures for 300W at $\phi = 45^{\circ}$

It can be seen from fig 4.3.a that for each value of imposed heat flux there is a specific rate of increase in temperature as well as a "stagnation" temperature value. The term stagnation herein implies the peak value of mean water temperature inside the storage tank. Once this condition is achieved, all the imposed heat flux goes into losses. The temperatures depicted in the figure are average temperatures evaluated from the constant volume approach mentioned in section 3.3.3. It can also be noticed that the temperatures achieve a near horizontal slope after the first 1000 minutes of exposure. This is more explicitly indicated in fig 4.3.b An increase of only 4.5 °C was for the later 1000 minutes of exposure was noticed i.e. less than 10% of the total temperature rise. Although there is an increase in temperature after this time, this increase is marginal. From a practical point of view, this relatively long time period is of little value owing to the intermittent nature of solar radiation, nonetheless to compare with the results from the simulation these results are important as will be shown in section 4.2.

4.1.2.3 Comparison of Finned and Unfinned Collectors

The comparison of finned and unfinned collectors is of particular interest as it provides a clue to the quantity of heat transferred by fins, and more importantly, the rate at which it is transferred. In fig 4.4 the datasets are compared from similar conditions on the collector. As mentioned earlier, a total of four fins were added in the finned collector. It should be noted that the efficiency of system is tied to a number of factors; these include stratification in the tank, inlet water temperature, average temperature and ambient temperature.

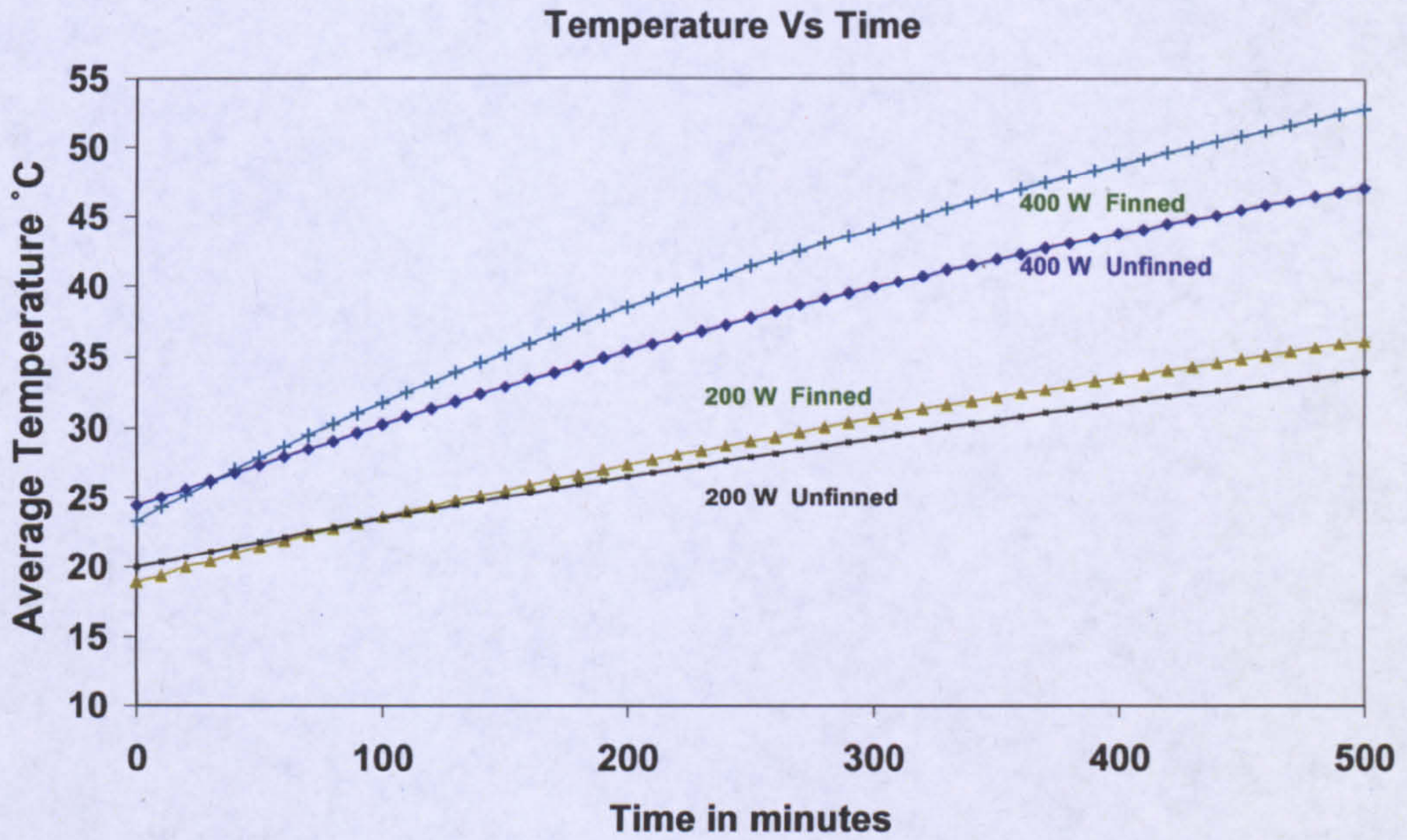

Figure 4.4: Comparison of fin and unfinned collectors at 200 W and 400 W

Fig 4.4 compares the finned and unfinned collectors. It is evident that the finned collectors outperform the unfinned collector. It can be further noticed that the rise in temperature is steeper for finned collectors. With the passage of time, the unfinned collector catches up with the finned counterpart and the temperatures become nearly the same after 1000 min (16.6hr). It is important to understand that it is the early difference in rise of temperature that is of critical for the performance. This is an encouraging fact as the collector would not be allowed to stagnate for such a long period. In other words before a time lapse of 16 hrs water will be tapped. Thus the fins do result in an increase in heat transfer. It is important at this point to examine quantitative difference between the two collectors.

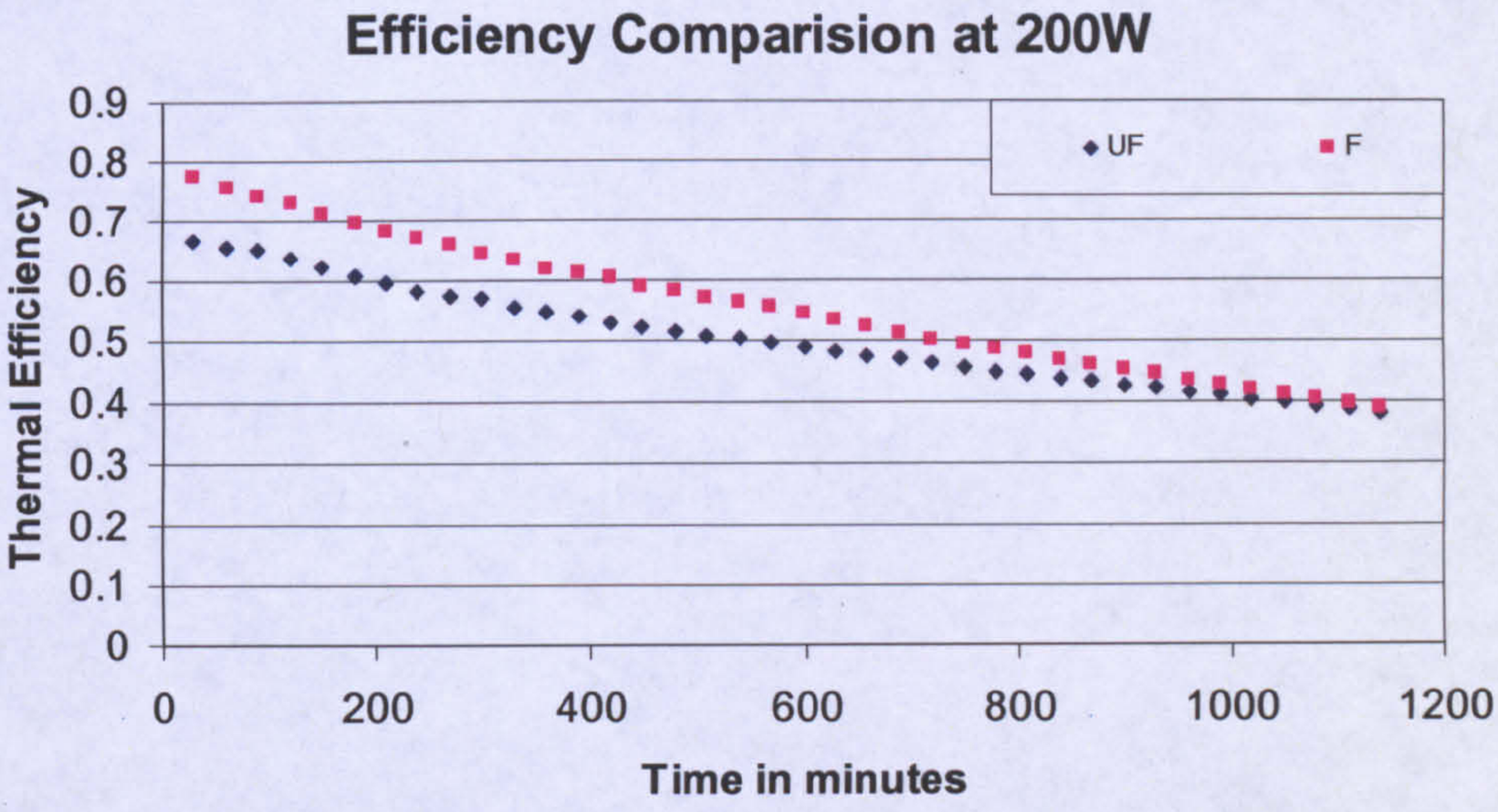

Figure 4.5.a: Comparison of efficiencies for finned and unfinned collector at 200W

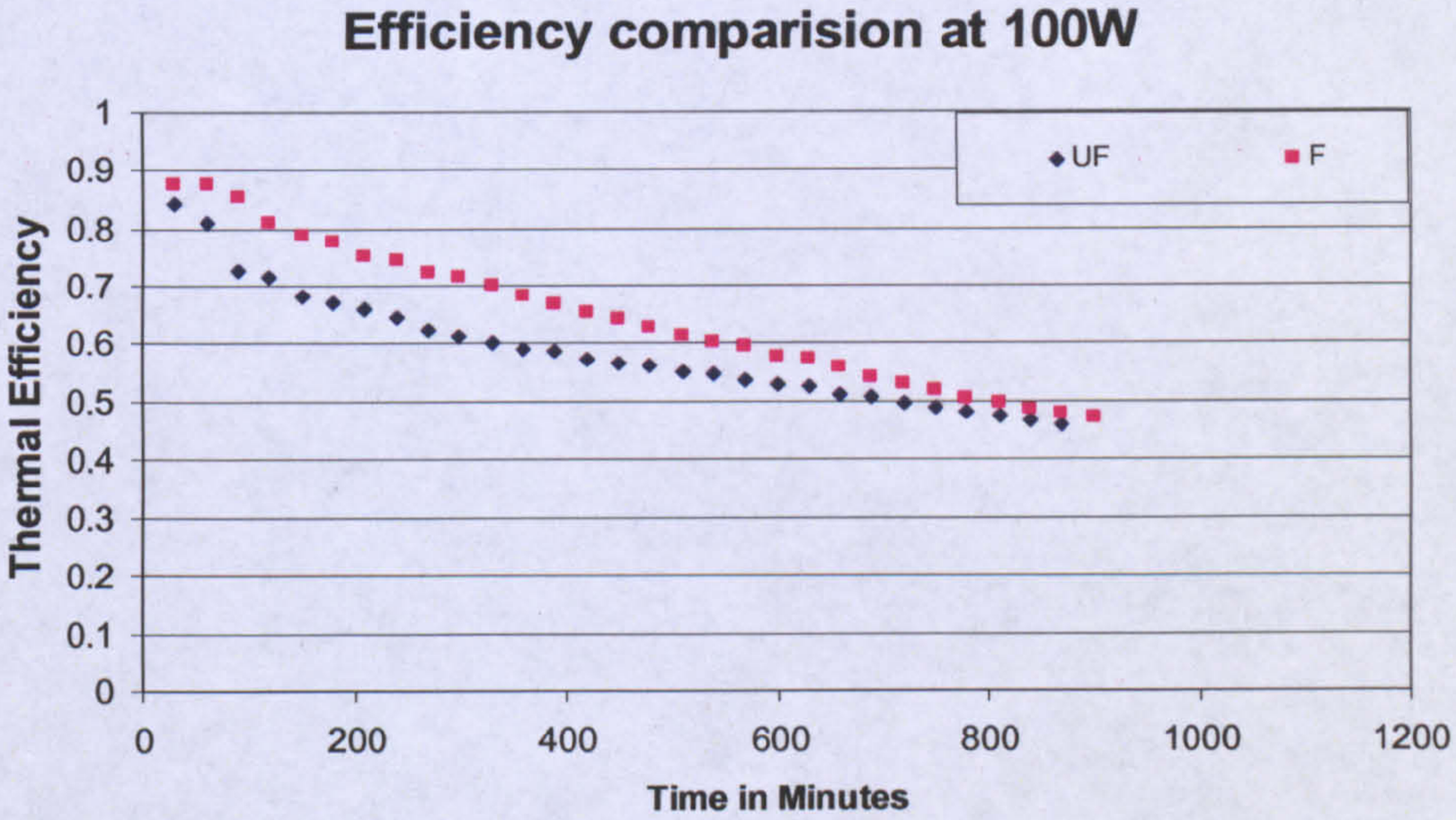

Figure 4.5.b: Comparison of efficiencies for finned and unfinned collector at 100W

The difference is elucidated in fig 4.5.a and 4.5. b. The efficiency was evaluated using the control volume approach given in section 3.3.3. It is evident that the difference in the efficiency is at its peak at the starting period (up to 10%). Both the efficiency values eventually terminate at the same level. These efficiencies were computed for readings after the first 60 minutes of exposure for the heater at $\phi = 45^{\circ}$ to avoid the initial capacitance effects in system. The efficiency was defined as the energy absorbed on the system to the total amount of energy imposed on the system in that particular interval.

4.1.2.3 Collector Response at Various Angles

The study of inclined cavities provided an idea on the behaviour of the collector with increasing angle of inclination. From the previous studies, it was noticed that heat losses decreases with the increasing angle whereas the heat transfer rate to the water-side increases with the angle. The expected net effect should therefore be an overall increase collector efficiency with increase in angle. This behaviour was observed for the tested prototype collectors and is shown in fig 4.6.

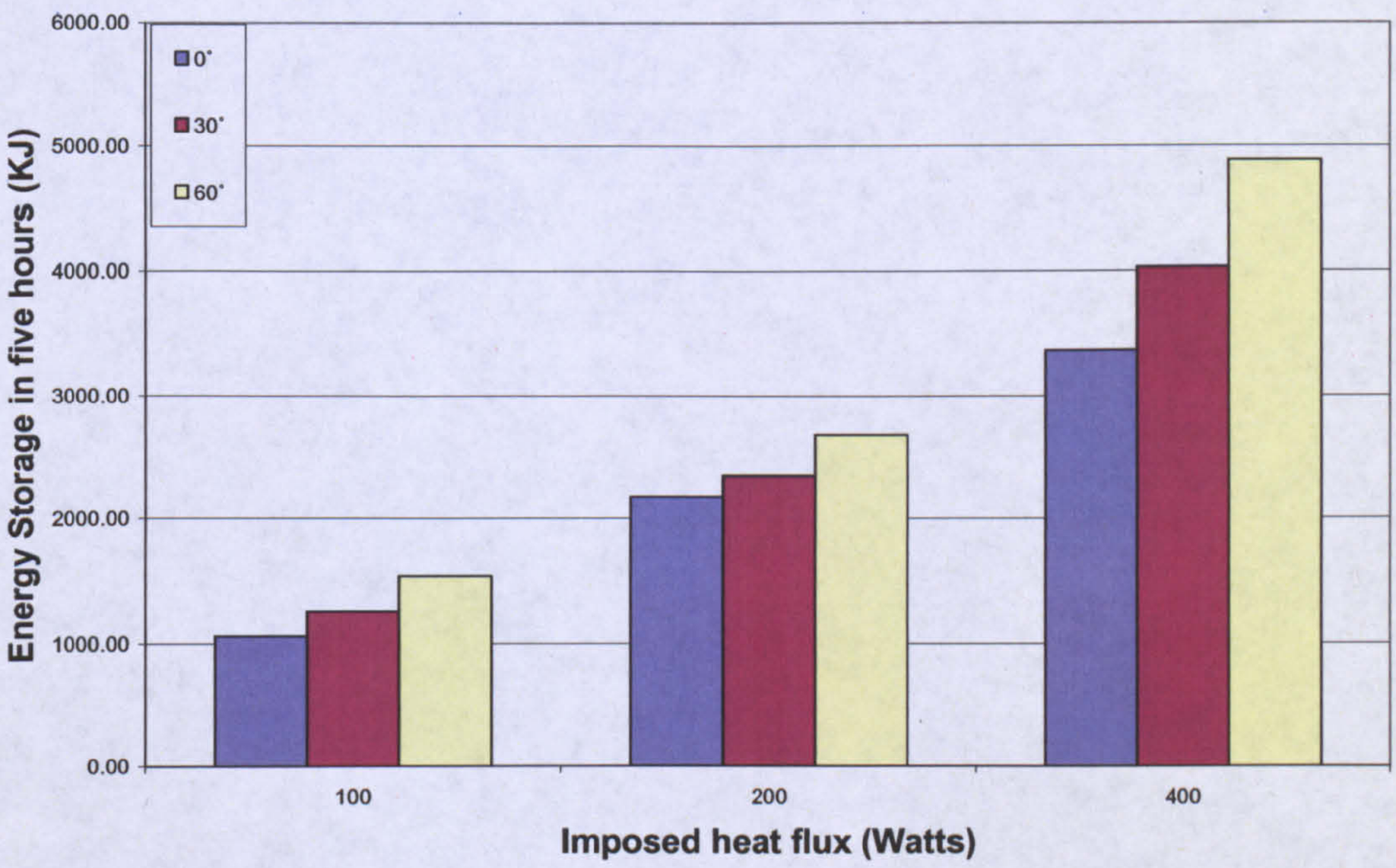

Figure 4.6: The energy gain for angles 60°, 30° and 0° for different values of imposed heat flux.

Fig 4.6 clearly illustrates that for any value of imposed heat flux, more energy is stored when the collector is at a higher angle of inclination.

4.1.2.4 Collector Cooling Profile

After reaching the stagnation temperature values for an imposed heat flux the collectors were allowed to cool under laboratory conditions. The main objective of this exercise was

to evaluate the overall U value. Region "C" in fig 4.2 presents the cooling temperature profile. The collector followed a logarithmic decrement in accordance with Newton's law of cooling. This implies that the cooling profile $\ln(T_m-T_a)$ should be a straight-line. This is clearly depicted in fig 4.7. Although this curve was evaluated by cooling the collector in the laboratory conditions, and may not emulate the cooling in windy field conditions, nonetheless this condition can also arise practically during a clouded day with little or no wind.

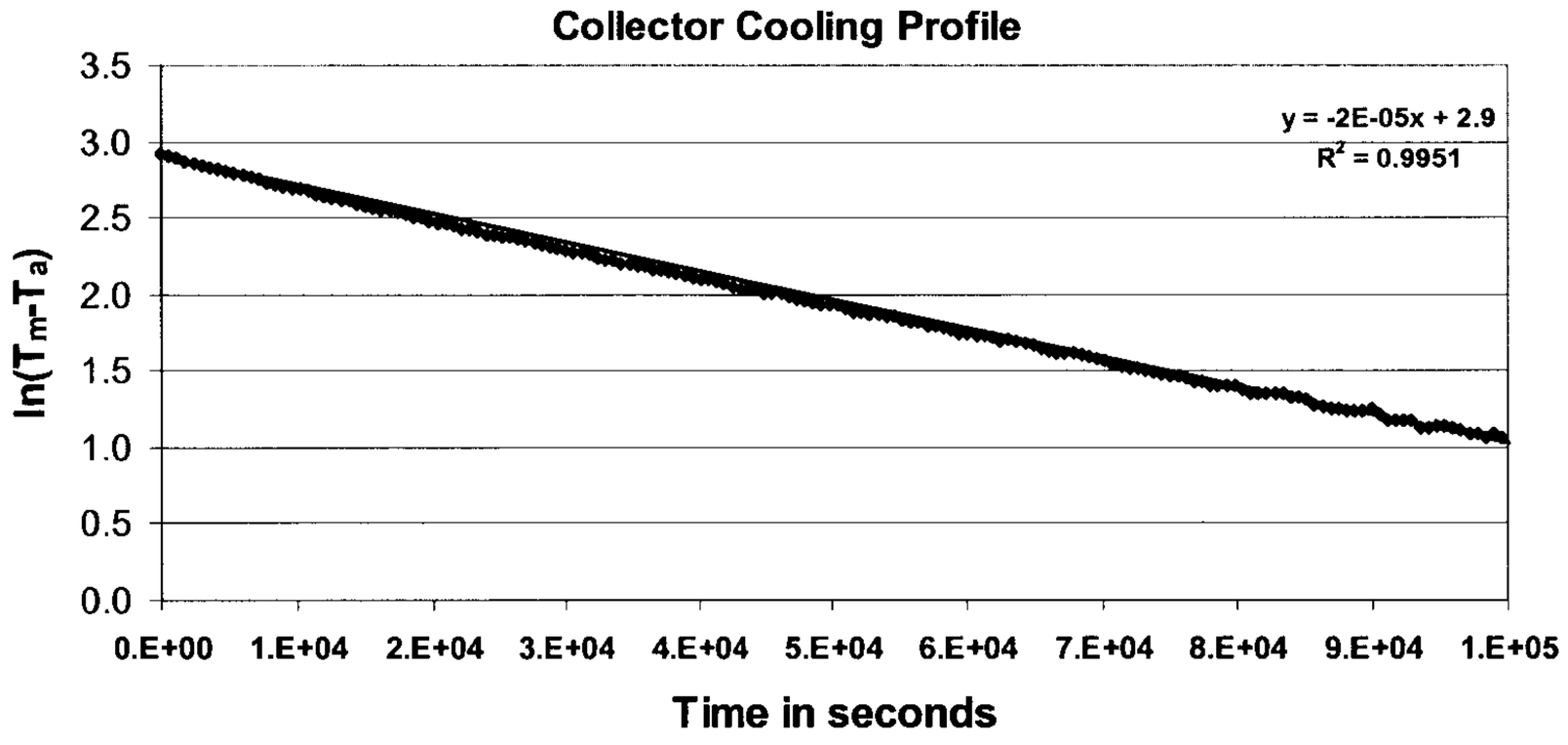

Figure 4.7: Logarithmic decrement of the cooling curve

4.1.2.5 Effect of TIM

As mentioned in chapter 2, through previous studies it was recognized that the use of TIM (Transparent Insulation Material) has a reasonable influence in reducing the cooling of the collector. TIM has also been recommended for ICSSWH collectors to prevent night-time losses.

Experiments were carried out for cooling profiles with TIM. Polycarbonate TIM was used (shown in fig 4.8.a) placed at the top 20% (200mm) of the collector length. Although not considerable, the evidence of reduction in heat loss was witnessed as shown in fig 4.8.b.

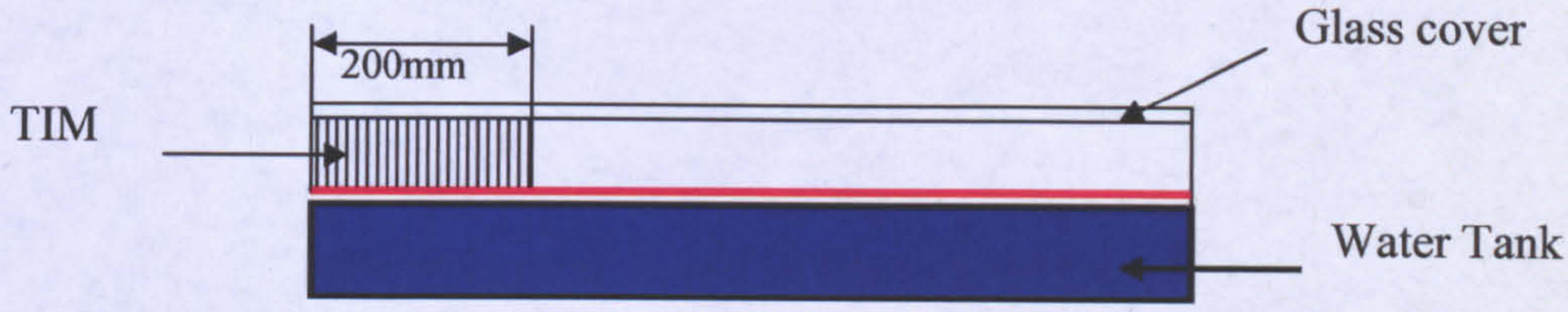

Figure 4.8.a: Position of TIM in the air-gap

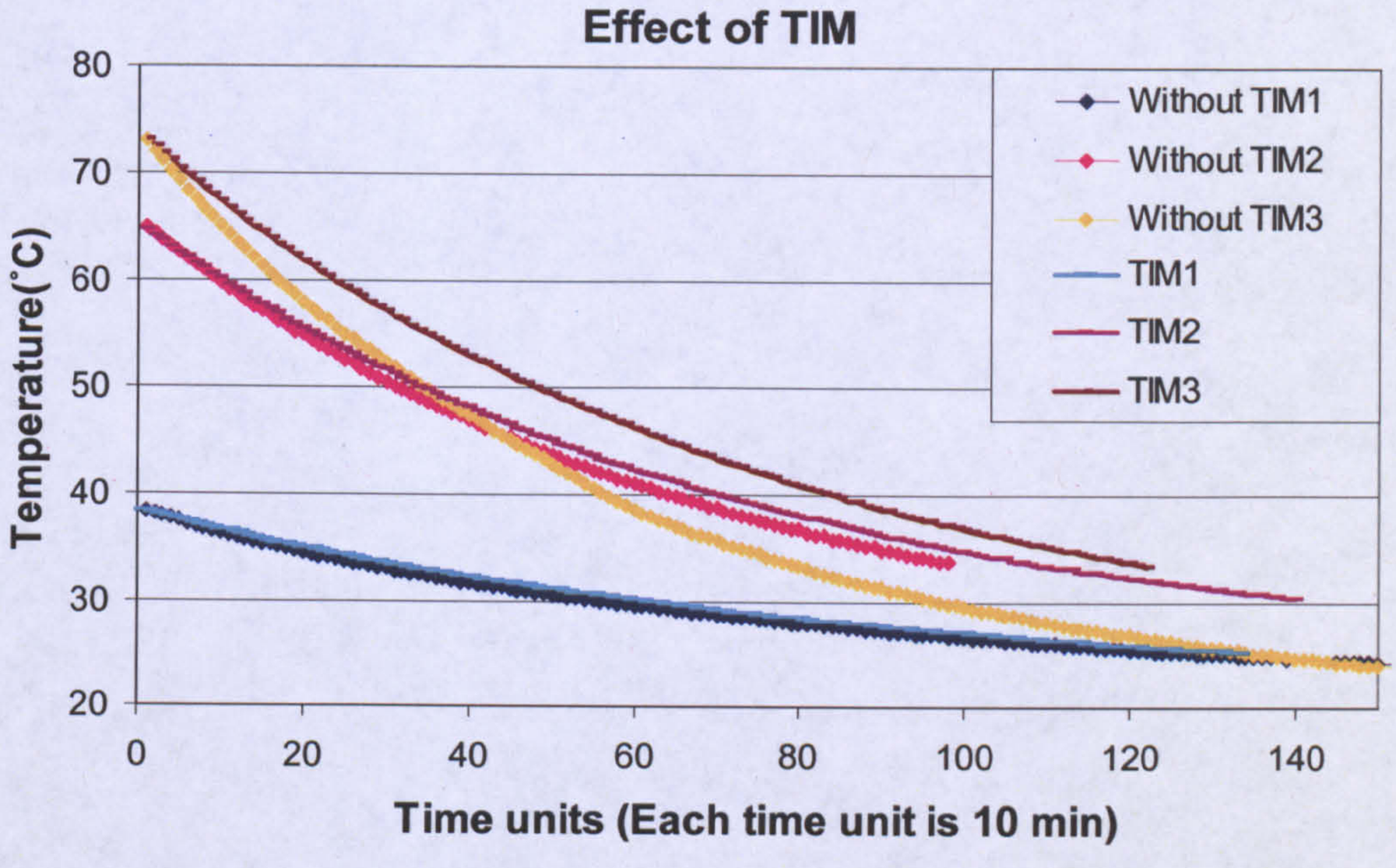

Figure 4.8.b: Comparison of cooling with and without TIM

Cooling curves were obtained (for collector with & without TIM) by allowing the collector to cool starting at different temperatures (38°C, 65°C, 73°C). It can be noticed (fig 4.8 b) that in each case the use of TIM cover retains more heat than a normal cover. The difference at higher temperatures is more prominent. A significant reduction in losses would have pointed out to a straight forward use of TIM in the optimal design; this however is not the case. It has to be bear in mind that the use of TIM results in reduction of the optical efficiency[2] of the collector. Therefore a detailed analysis has to be carried out to compute if the loss in optical efficiency is worth the reduction in the U value.

---

[2] For explanation of optical efficiency please refer to textbox 3

4.1.2.6 Stratification and De-stratification

In this section the evidence of stratification is reported which is important as it reflects on the yield of the collector. This aspect is dealt in detail in chapter 5. To effectively gauge stratification, the difference of average temperatures at the top and the bottom portions of the collector has been plotted. Where the average temperature at the top was measured by thermocouples 4,8,12 while bottom portion temperature was found through thermocouples 1,5,9 (see thermocouple map fig. 3.12) . The temperature difference with the passage of time has been plotted in fig. 4.9.a with the collector charging at various levels of imposed heat flux. It can be noticed that stratification increases with time as well as heat flux. Similarly when the collector is allowed to cool, stratification shows a logarithmic decrement as shown in fig 4.9.b. It is worthwhile noting that although no heat flux was imposed while measuring destratification, however the curves (in fig 4.9.b) have been labelled to indicate the previous stratification that was achieved while charging the collector at the mentioned power.

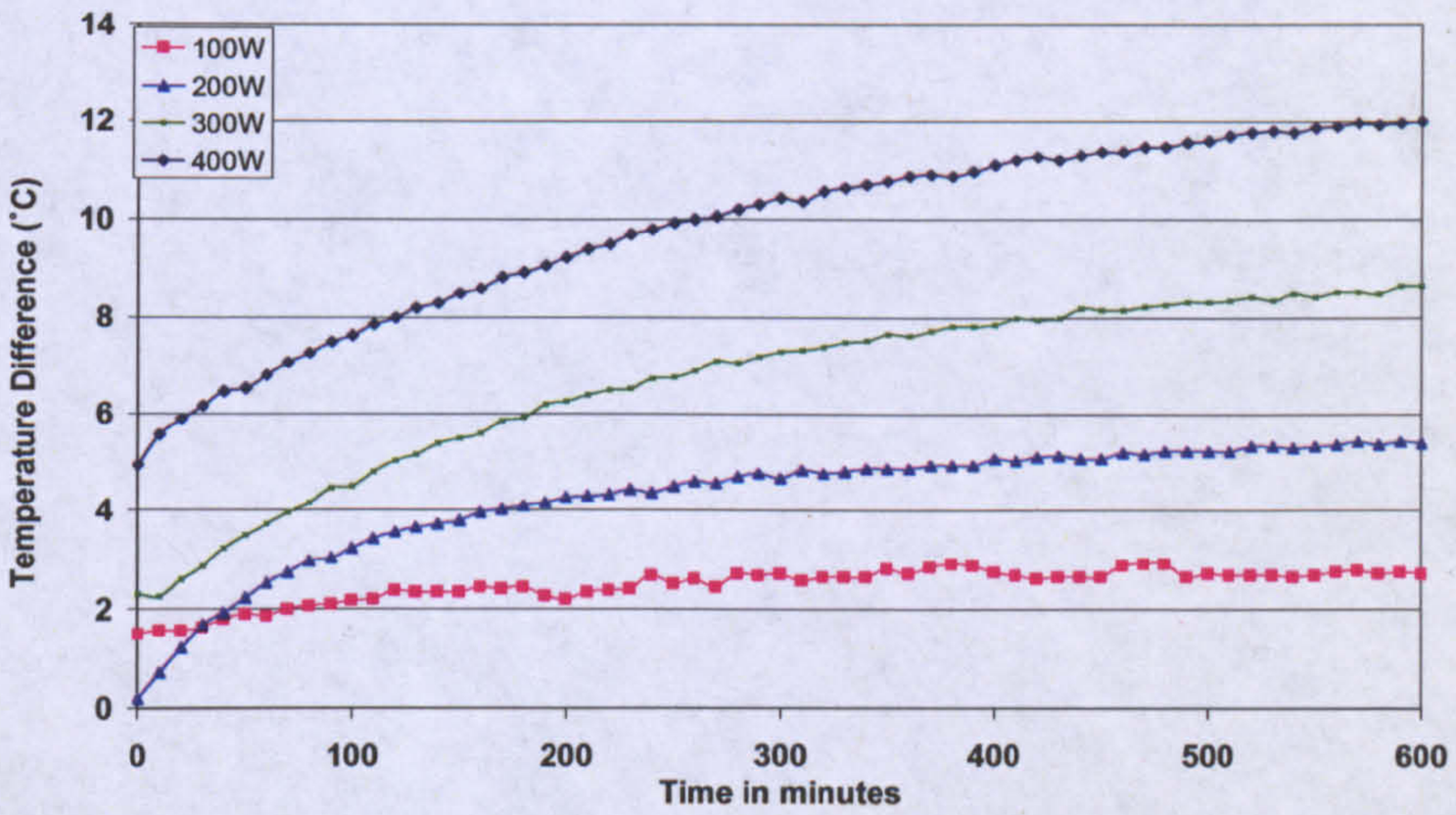

Fig 4.9.a: Temperature difference between tank's top and bottom portions showing stratification during charging of collector

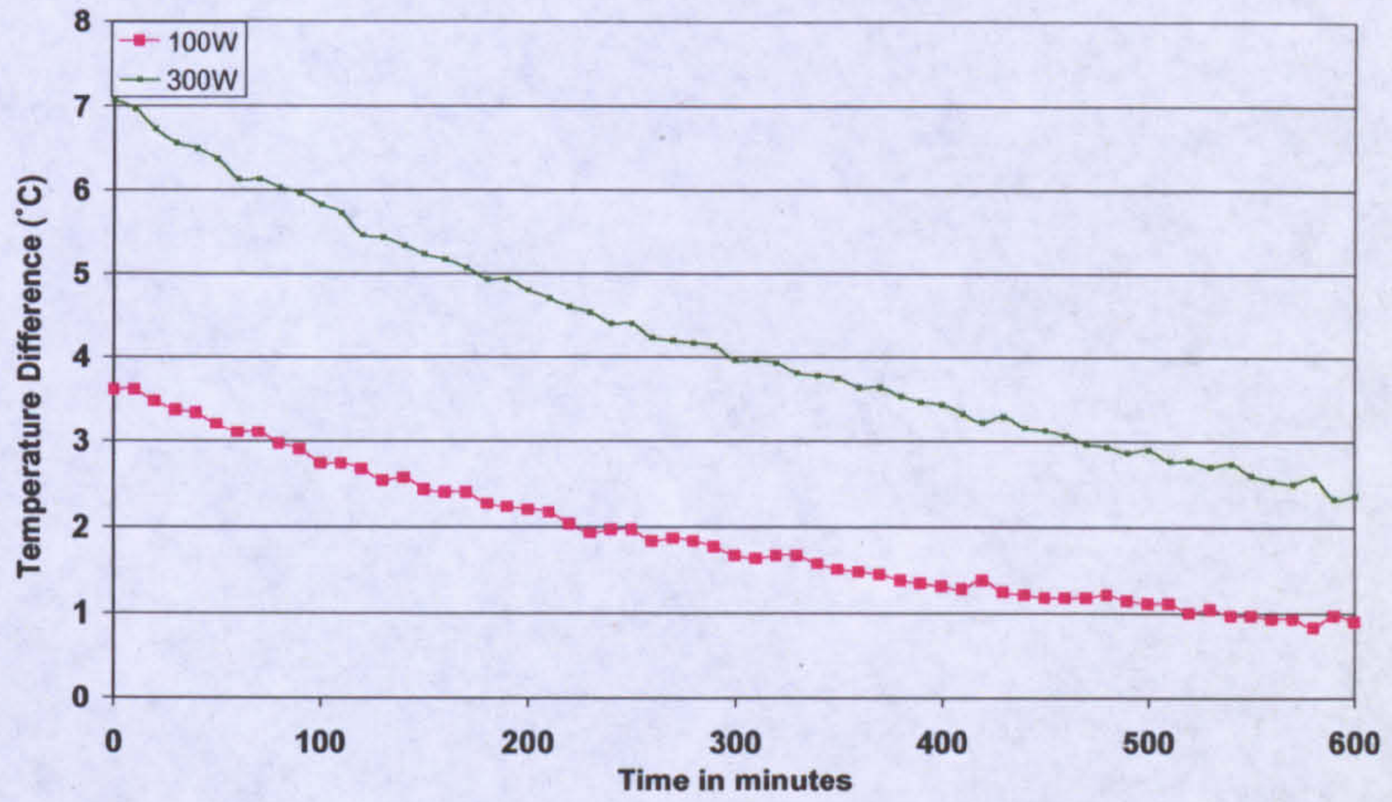

Fig 4.9.b: Temperature difference between tank's top and bottom portions showing destratification during cooling of collector

4.1.2.7 Change in Stratification with Time and Angle

It was noted in the previous section that stratification does increase with the increasing heat flux. In this section the increase of stratification with time and angle is observed. The dimensionless temperature $\frac{T_x}{T_{max}}$ has been plotted along the longitudinal length of the collector to check the variation with the change in angle (fig 4.10-12). Where T_x is the local temperature and T_{max} is the maximum temperature in the collector at the same instant. The temperatures used for the plots were obtained from thermocouples 5-8 (see fig 3.12 for positions of thermocouples)

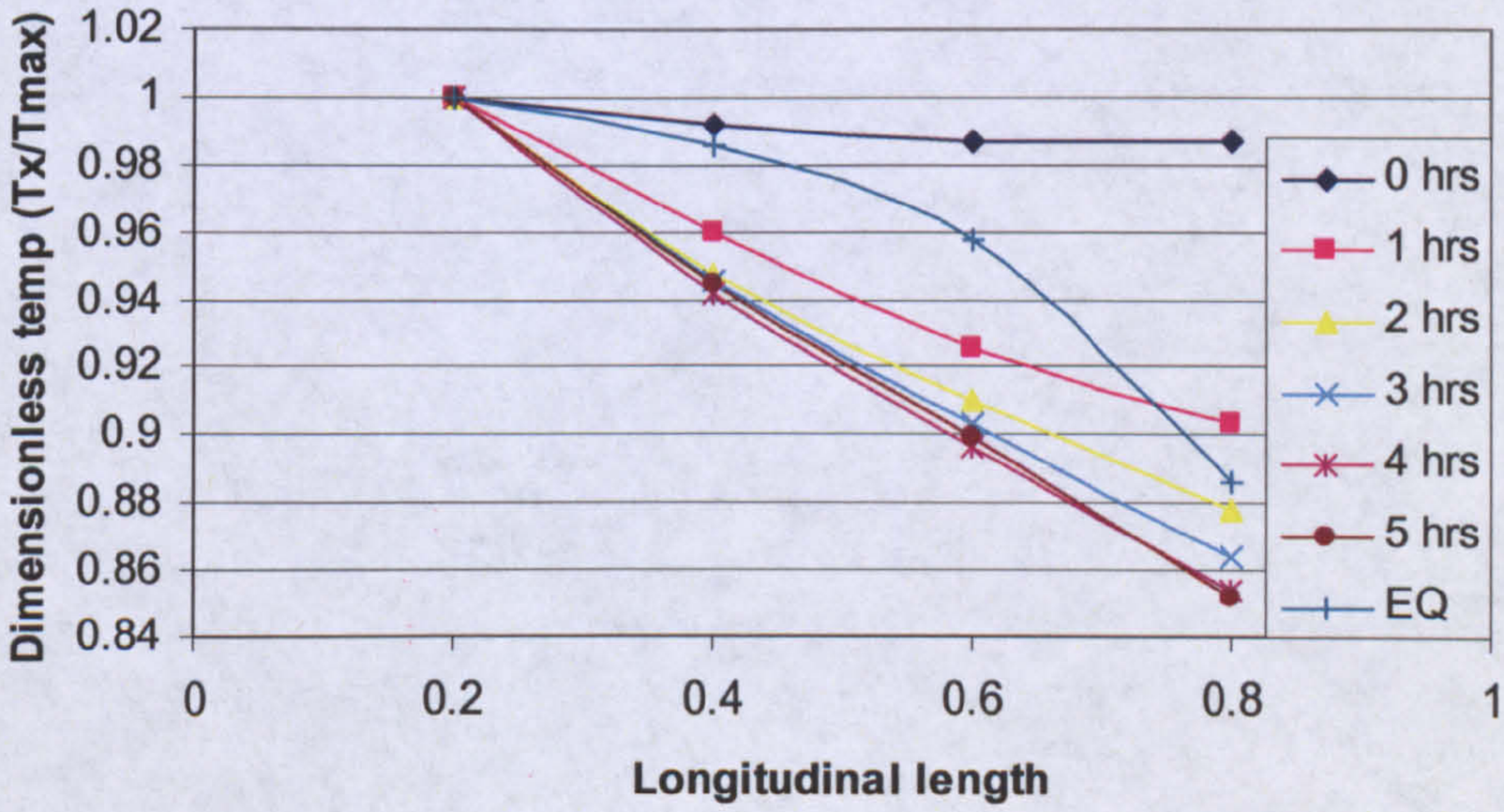

Figure 4.10: Dimensionless temperatures along the longitudinal length for $\phi = 30^{\circ}$, 200 W

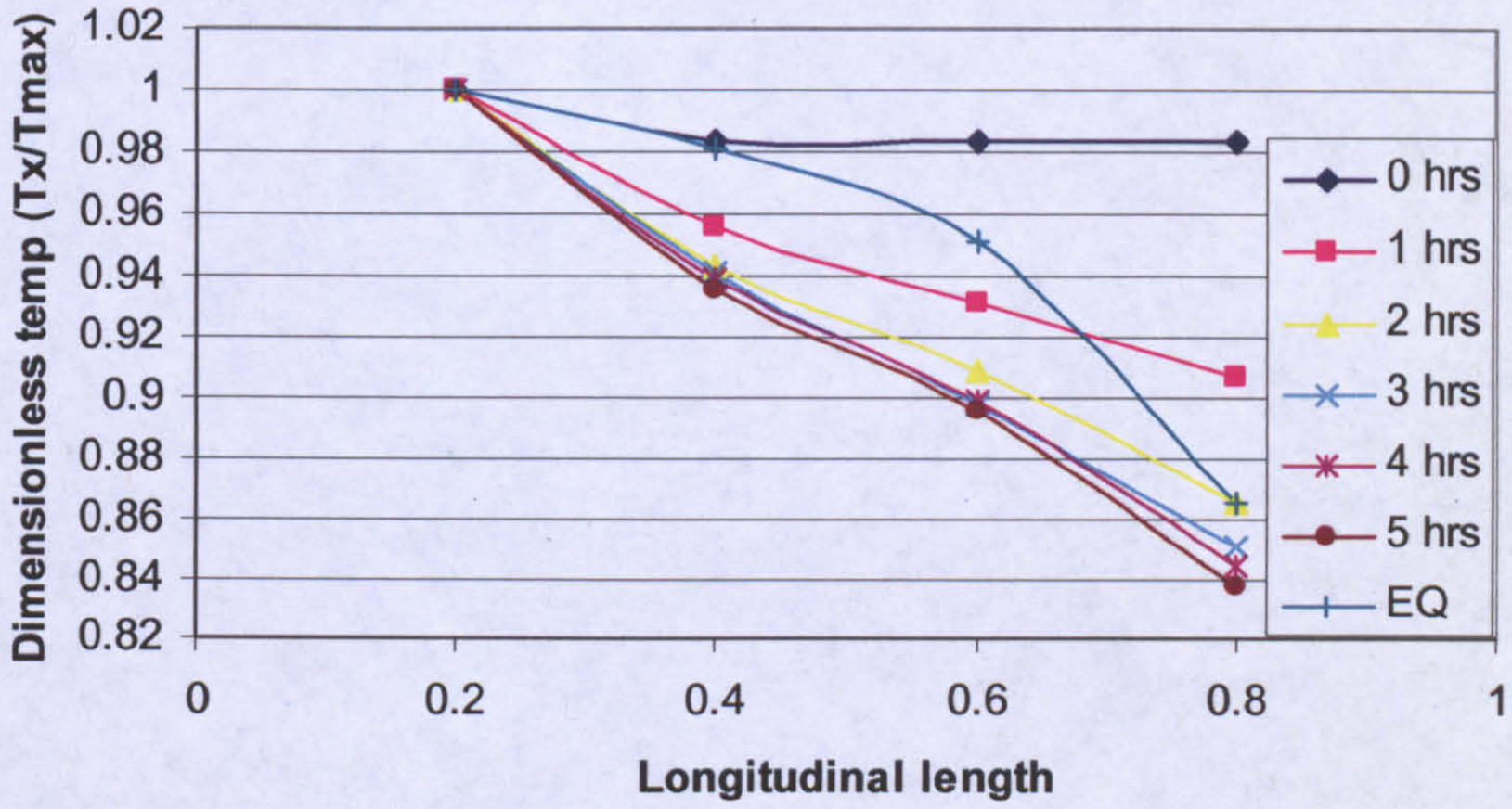

Figure 4.11: Dimensionless temperatures along the longitudinal length for $\phi = 45^{\circ}$, 200 W

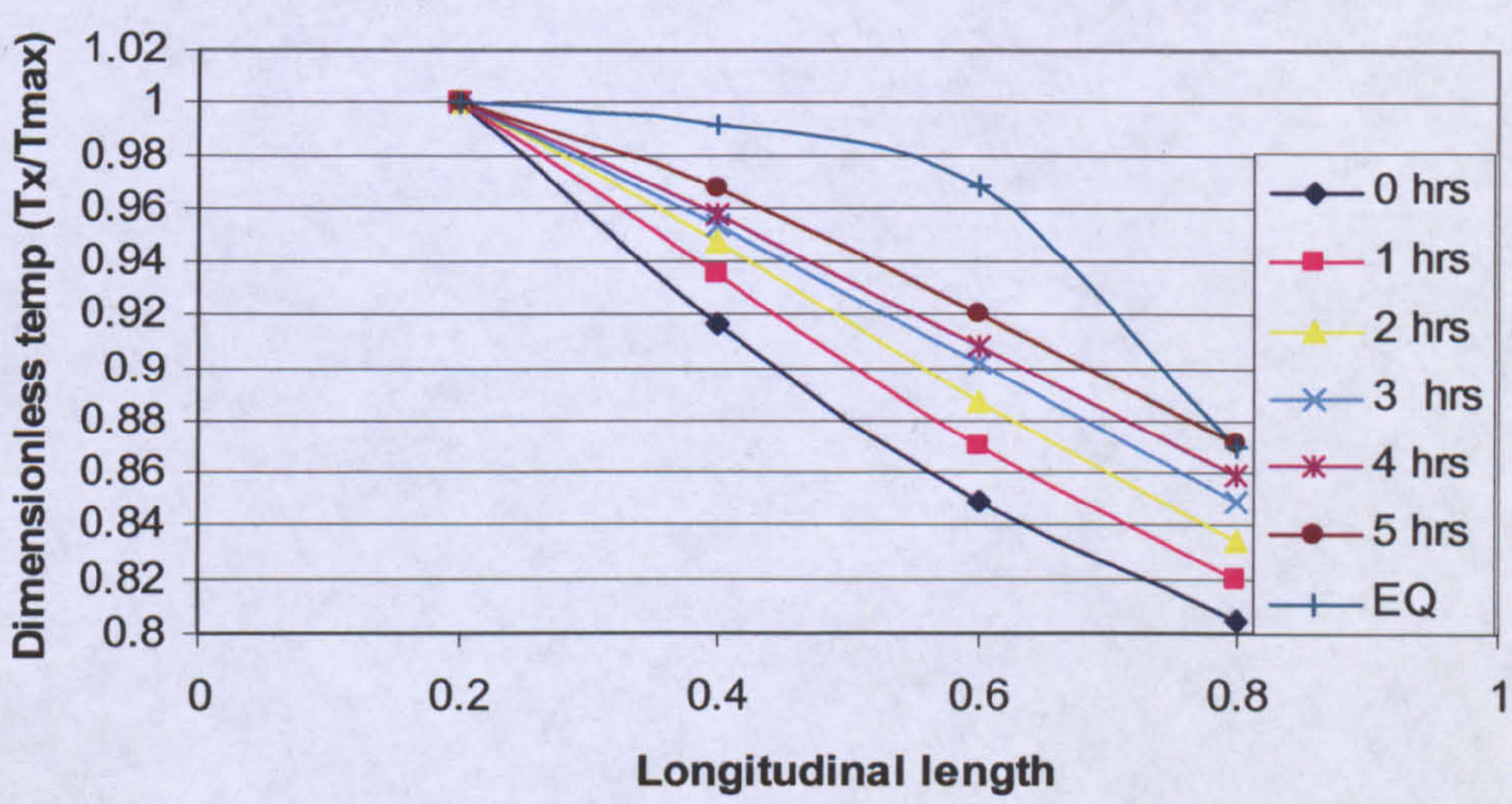

Figure 4.12: Dimensionless temperatures along the longitudinal length for $\phi = 60^{\circ}$, 200 W

It can be noticed stratification profile in all cases changes with time. The term "EQ" in the charts represents the equilibrium profile which can be seen to be convex which was obtained when the system reached equilibrium. The temperature profile also depends upon the initial level of stratification in the tank, however the overall trend is that the profile tends to get convex with the passage of time as the heat flux is imposed. It can

also be noticed that the degree of stratification increases with the increase in the angle. For $\phi = 60°$, a value of $\frac{T_x}{T_{max}} = 0.8$ can be seen where as for lower angle the minimum value of $\frac{T_x}{T_{max}}$ is slightly higher.

4.1.2.8 Thermal Imaging Results

The thermal imaging of the collector was also carried out. This was done for the collector orientated at 0° as well as 60°. These results provide a clue to the nature and magnitude of heat transfer from various sections of the collector. It was observed that the wooden outer frame contributed negligible heat loss as compared to glass surface. On the glass itself, the top portion lost more heat compared to the bottom half.

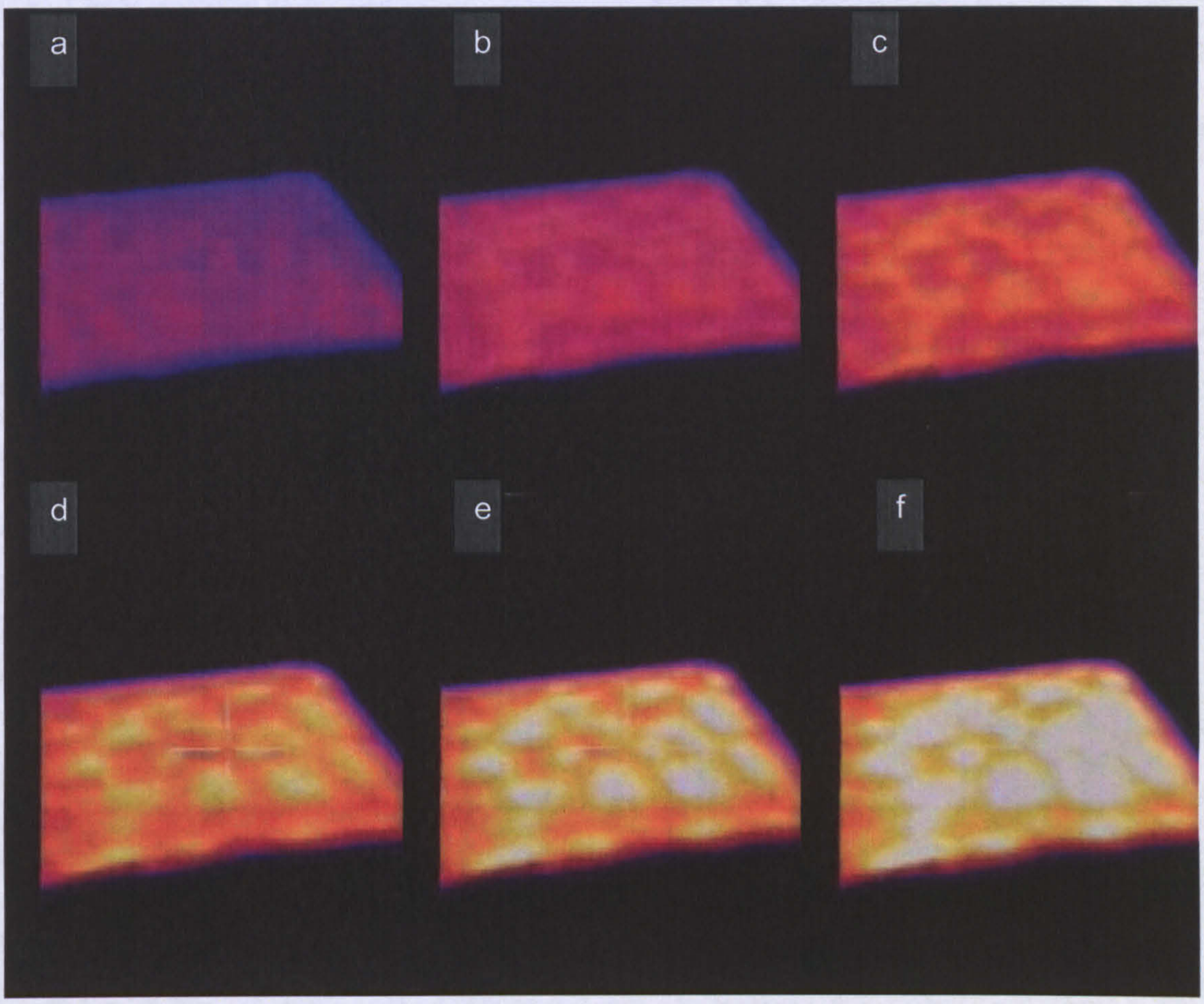

Figure 4.13: Thermographic images of the collector air-cavity at 0° (a) 100 Sec (b) 200 Sec (c) 300 Sec (d) 400 Sec (e) 500 Sec (f) 600 Sec

From fig 4.13 hot spots can be seen at various positions on the glass cover indicating an uneven heat loss patterns. Bénard cells[3] are a possible explanation for this behaviour.

---

[3] Details on Benard Cells can be found in textbox 3

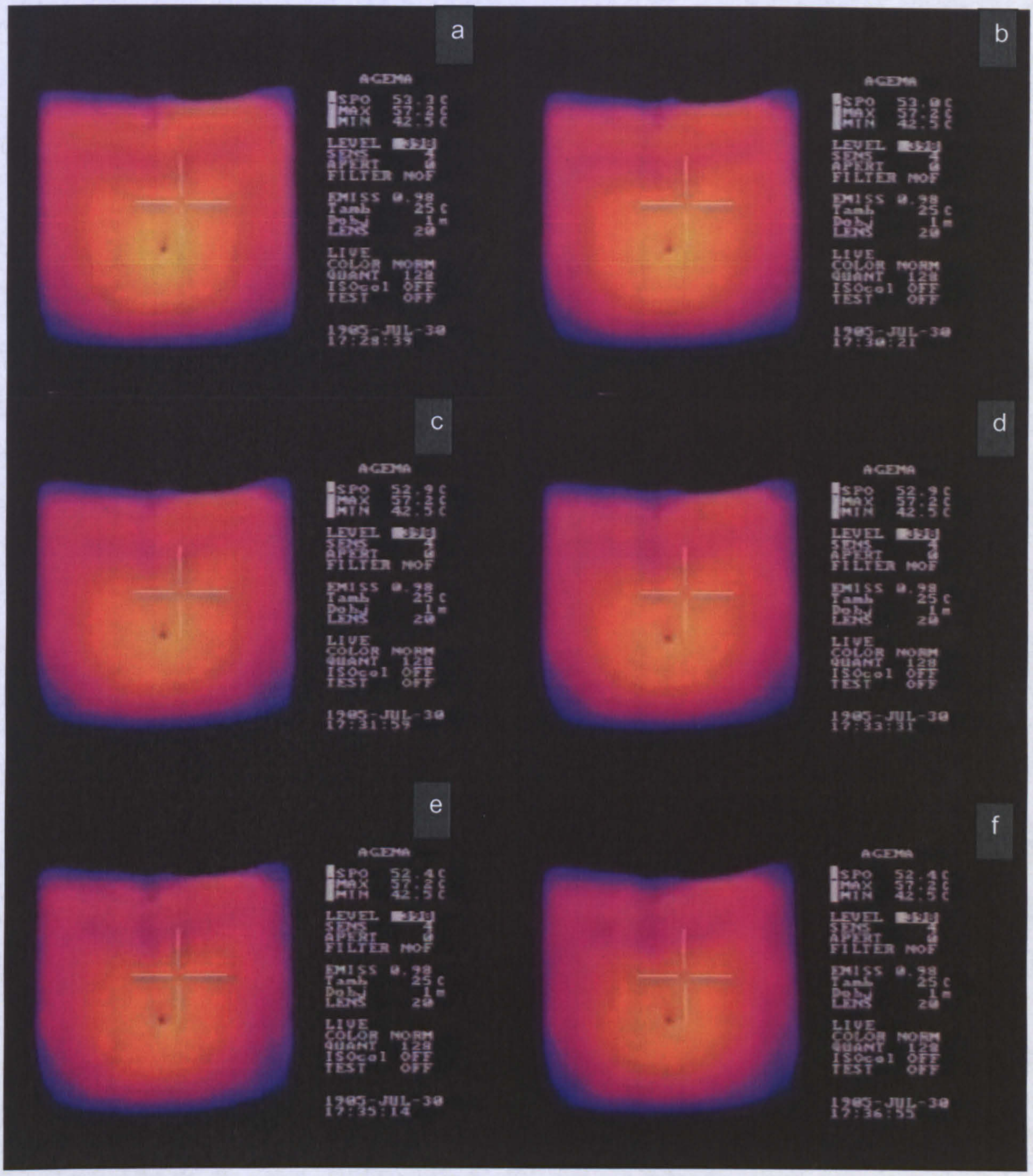

Figure 4.14: Thermographic images of the air cavity at 60° (a) 100 Sec (b) 200 Sec (c) 300 Sec (d) 400 Sec (e) 500 Sec (f) 600 Sec

For the collector at $\phi = 60^{\circ}$, the thermal image in fig 4.14 shows a much more uniform even convective heat transfer from the glass as compared to the hot spots seen at 0°.

4.1.3 Discussion on Experimental Testing

Experimental tests revealed many facets of the collector behaviour. This included the collector response to the change in angle, imposed levels of heat flux and stratification. The recorded data followed an anticipated pattern of results. The magnitude of the recorded parameters was more important.

Experimental tests took significantly long periods of time. Moreover, the results gathered were for only a small number of points depending upon the number of thermocouples used. This implied that alternate methods to probe deeper in the collector behaviour should be developed.

As the data from experiments was available for the behaviour of collector, modelling the collector could now be carried out to predict the performance. For modelling purposes two methods were used. ATA analyzed the collector on a macroscopic scale while CFD modelled deeper, micro aspects of the collector.

4.2 ABBREVIATED THERMAL ANALYSIS (ATA)

The ATA herein implies the resolution of a thermal network for the collectors (finned and unfinned) by utilizing the established mathematical relations/regressions for the elements of its electric analogue. The thermal network diagram for the prototype collector is depicted in fig 4.15:

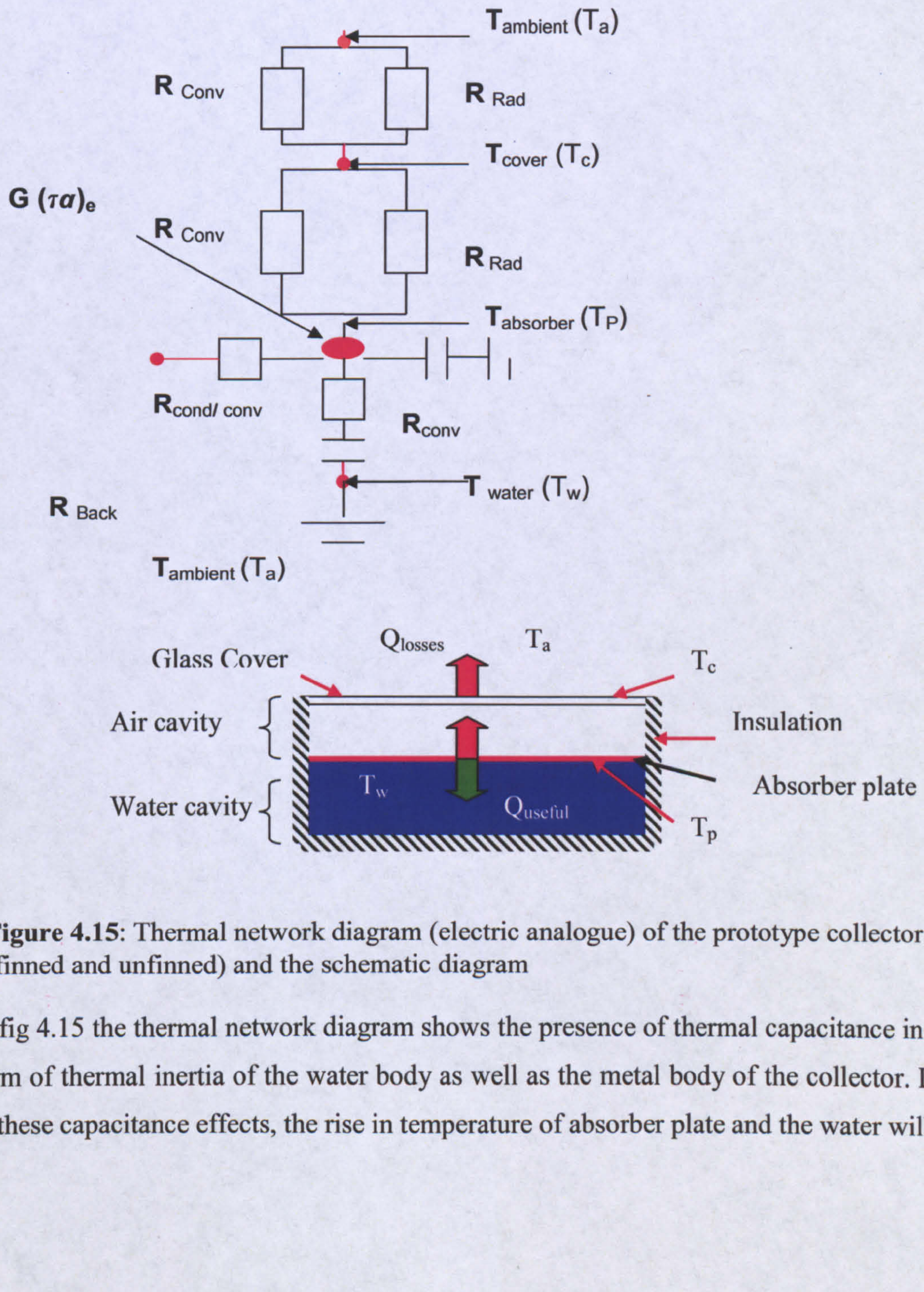

Figure 4.15: Thermal network diagram (electric analogue) of the prototype collector (finned and unfinned) and the schematic diagram

In fig 4.15 the thermal network diagram shows the presence of thermal capacitance in the form of thermal inertia of the water body as well as the metal body of the collector. Due to these capacitance effects, the rise in temperature of absorber plate and the water will be

slower than that of the air inside the air cavity as the capacitance effects of the trapped air are negligibly small.

The abbreviated thermal analysis has been carried out for several different collectors in earlier studies. Similarly this analysis is done with an aim to look at the "big picture" by only focusing at the one dimensional heat transfer to the collector. Leaving aside the intricate details (such as temperature at various points inside the collector), the collector performance for long periods of time can be analysed.

4.2.1 Complexity of the Absorber Plate

A challenging aspect of resolving the thermal network of the ICS (fig 4.15) was the absorber plate that is in contact with both the air and water sides. The absorber plate can be assumed as a heat source with the energy being split between water and air that surround its two faces. The ratio of the split depends upon the temperature differences and the thermal network resistance on both faces. As the temperature difference as well as the thermal resistance is changing with time, the problem in hand is essentially transient. What further compounds the problem is the fact that the absorber plate realistically has a constant heat flux boundary condition rather than an isothermal boundary condition which is simpler to resolve. This coupling of the absorber plate can only be resolved by adapting an iterative procedure. For this reason, a computer program was written using Visual Basic Application (VBA) in a Microsoft Excel spread sheet. The VBA program code can be found in print in Appendix-D. The flow chart of the program can be referenced in section 4.2.4.

4.2.2 Assumptions for ATA

A number of assumptions had to be made to advance the analysis. The reasons were either the unavailability of data from exactly matching conditions/properties or in some cases to simplify the problem i.e. compromising marginally higher accuracy for reducing computation. Similarly some values were assumed only to initialize the simulation; these

were later recalculated by the program. Care has been exercised that the assumptions adhere to the actual process and do not render the analysis inappropriate.

1) The transient analysis was carried out in a series of small time steps. During each step the process was assumed to be essentially steady state.
2) The plates on the air cavity were assumed isothermal.
3) Heat flow is considered one dimensional.
4) Dust on the collector is negligible.
5) Thermophysical properties are taken at the film temperature.
6) The specific heat capacity of water as well as the density is assumed to be constant.
7) Heat flow from the sides as well as the back of collector has been accounted, however it has been considered one dimensional
8) The temperature of the absorber plate has been considered 2-4˚C above the water initialization temperature.
9) The analysis was carried out for the angle of $\theta = 45^{\circ}$. The angle and the emissivity of the cover and plate (ϵ_c & ϵ_p) were taken as variables that could be changed later in the simulation.
10) Similarly provision was made in the program to account for the convective heat transfer coefficient "*h*" in the case of wind. Although for the laboratory tests the wind factor and the sky temperature wouldn't be used, programming was done to keep this value flexible by making it a user input.
11) Stratification inside the tank was neglected. The water temperature inside the tank was considered uniform represented by T_w.

4.2.3 Mathematical Expressions for Modelling

The following section elucidates the mathematical relations that were used to create the simulation program. Considering the collector a control volume, the simple equation 4.1

encapsulates the overall collector mechanics. Each term of this expression is later examined individually in detail.

$$\mathbf{Q_{useful} = Q_{input} - Q_{loss}} \tag{4.1}$$

Where Q_{input}[4] is the known entity while both Q_{loss} and Q_{useful} are to be estimated.

To evaluate Q_{loss}, it is known that 95% of the losses in similar heater occur through the top [5]. The top loss that includes both radiative and convective losses can be given by the following standard expression:

$$Q_{Toploss} = h_{c,p}(T_p - T_c) + \frac{\sigma(T_p^{\,4} - T_c^{\,4})}{\frac{1}{\varepsilon_p} + \frac{1}{\varepsilon_c} - 1} \tag{4.2}$$

As mentioned earlier, for a steady state time step, the heat loss from the plate to the cover would be equal to that from the plate to the ambient. Taking into account both the radiative and convective losses, the losses can be related as:

$$h_{c,p}(T_p - T_c) + \frac{\sigma(T_p^{\,4} - T_c^{\,4})}{\frac{1}{\varepsilon_p} + \frac{1}{\varepsilon_c} - 1} = h_{ca}(T_c - T_a) + \sigma\varepsilon(T_c^{\,4} - T_{sky}^{\,4}) \tag{4.3}$$

Where the sky temperature is calculated as mention in chapter 3 as:

$$T_{sky} = 0.0552 T_a^{\,1.5} \tag{4.4}$$

Now, the more important aspect of the simulation is to calculate the useful heat that results in the increase in temperature of both water and the steel tank casing. The useful heat gain can be related as:

---

[4] Note that for field tests $Q_{input} = G_{in}$

$$\Delta Q_{useful} = m_w C_{pw}(Tw_1 - Tw_o) + m_s C_{psteel}(Ts_1 - Ts_0) \quad (4.5)$$

Where,

ΔQ_{useful} = The energy in joules absorbed by the tank and steel body for each time step

Tw_1 and Tw_0 denote the final and initial temperatures of water.

Ts_1 and Ts_0 denote the final and initial temperature of steel.

It would be appropriate at this point to introduce the heat loss coefficients. The heat loss coefficient for radiative and convective heat losses are given as:

$$U_{pc} = h_{pc}{}^{r} + h_{pc}{}^{c} \quad (4.6)$$

Similarly,

$$U_{cs} = h_{ca}{}^{r} + h_{ca}{}^{c} \quad (4.7)$$

Here $h_{ca}{}^{c}$ *(Convective heat transfer coefficient)* can take two values.

a) When outside in the field conditions, it can be evaluated using the relationship provided by Duffie and Beckman[1]:

$$h_{ca}{}^{c} = 2.8 + 3V_{\circ} \quad (4.8)$$

Where "V_o" is the wind velocity.

b) For laboratory conditions, as the heat loss occurs mainly through natural convection the following expression can be used:

$$\overline{Nu}_L = 0.27\,\mathrm{Ra}_L{}^{1/4} (10^5 \le Ra_L \le 10^{10}) \quad (4.9)$$

$$h_{ca}{}^{c} = \frac{\overline{Nu}_L(k)}{L} \tag{4.10}$$

Equation 4.8 can also be used for laboratory conditions where the velocity can be taken as V= 0.1 m/s for a confined space room such as laboratory condition [11].

The Rayleigh number in this case again would be evaluated using the Rayleigh number expression for angular plate as mentioned earlier in chapter 3 (eqn 3.8)

Similarly, the convective heat transfer coefficient for the convective losses through the air gap ($h_{cp}{}^{c}$) are calculated using Hollands' regression given below.

$$\frac{h_{cp}{}^{c} L}{k} = 1 + 1.44\left[1 - \frac{1708}{Ra_L \cos\theta}\right]^{*}\left[1 - \frac{1708(\sin 1.8\theta)^{1.6}}{Ra_L \cos\theta}\right] + \left[\left(\frac{Ra_L \cos\theta}{5830}\right)^{1/3} - 1\right]^{*} \tag{4.11}$$

Where the Rayleigh number in equation 4.11 is calculated at film temperature, which is described by the following equation:

$$T_f = \frac{T_c + T_p}{2} \tag{4.12}$$

Solving the thermal network diagram, the cover plate temperature T_c can be given as:

$$T_c = \frac{(U_{pc}T_p + U_{ca}T_a + U_{cs}T_{sky})}{U_{pc} + U_{ca} + U_{cs}} \tag{4.13}$$

Similarly, the expression for the plate temperature T_p was found to be:

$$T_p = \frac{(G_{in} + U_{pc}T_c + U_w T_w)}{U_{pc} + U_w} \tag{4.14}$$

The losses that occur through the sides and back losses are important and amount to a sizeable fraction that cannot be neglected. The heat loss coefficient for the back and side loss combined can be given as:

$$h_{back} = 0.72 \text{ W/°C} \tag{4.15}$$

Note that the value for h_{back} was evaluated using the conductive resistance values for wood, steel and insulation as mentioned in chapter 3 and using the combined area for the back and the sides.

The water temperature T_w similarly can be explicitly given as:

$$T_{w1} = \frac{T_{w0} + Q_{useful}}{mC_{pw} + mC_{psteel}} \qquad (4.16)$$

The U_w value mentioned in equation 4.14 is a crucial parameter as it defines the heat transfer coefficient to water. It would be different for finned and unfinned heater. The expression for U_w would be dependent on the temperature level as well as the temperature difference of the bulk fluid with the absorber plate. The work of Cruz [2]here has been used here as the foundation brick. For trapezoidal heaters (similar to the prototypes), Cruz has defined the following expression for the Nusselt number on the water side (See fig 4.16 for Cruz's collector design).

$$Nu_L = 0.56(Ra\cos\phi)^{\frac{1}{4}}(\frac{D}{U})^{\frac{1}{9}}(\frac{H}{U})^{\frac{1}{6}} \qquad (4.17)$$

Where D, U and H are the collector dimensions described in fig. 4.16

For comparison, Fuji and Imura relation mentioned earlier in Chapter 3 is revisited.

$$Nu_L = 0.58Ra_L^{1/5},\ 10^6 < Ra_L < 10^{11} \qquad (3.2)$$

The uncertainty for the expression 4.17 was found to be 7%. This expression has also been reported to agree well with the Fuji and Imura correlation mentioned in chapter 3 when $\phi = 45°$. This according to Cruz indicates that geometric parameters[5] (D/U and H'/U) have only a small influence in comparison with the modified Rayleigh number, $Ra.\cos\phi$.

---

[5] The geometrical parameters for Cruz collector D, U & H' can be referenced from fig 4.16 and should not be confused with similar annotations used prior or later in the text (reference from nomenclature).

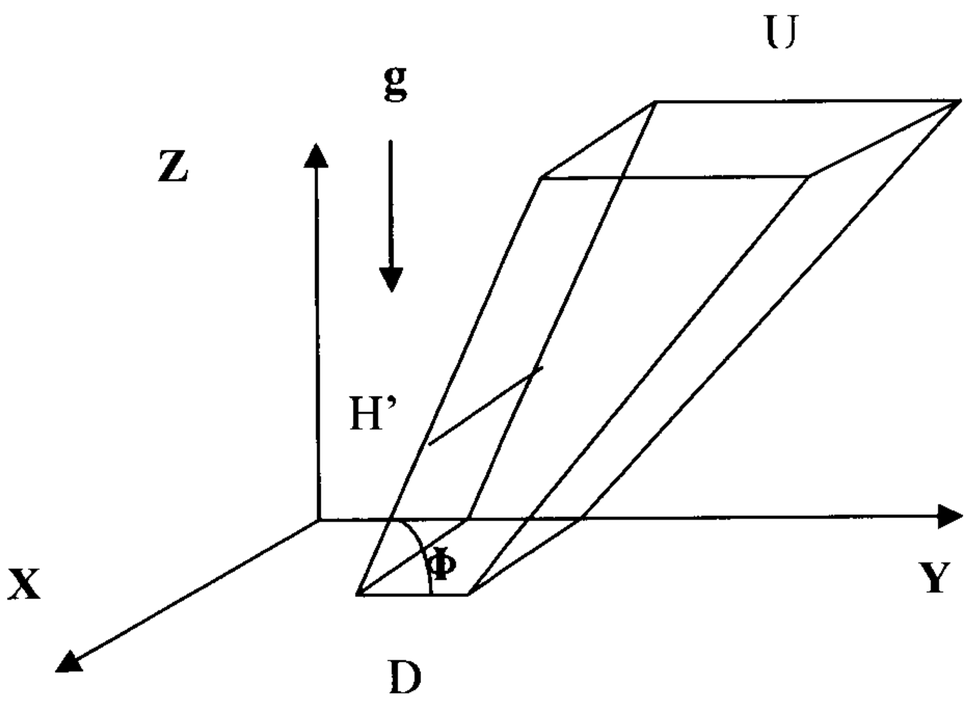

Figure 4.16: Geometrical configuration of trapezoidal heater by Cruz [1]

For the prototype heater D=U= 50mm, therefore D/U =1; likewise H'/U = 1000/50 =20

This reduces equation 4.13 to

$$Nu_L = 0.56(Ra\cos\phi)^{\frac{1}{4}}(1)^{\frac{1}{9}}(20)^{\frac{1}{6}}$$

$$Nu_L = 0.56(Ra\cos\phi)^{\frac{1}{4}}(20)^{\frac{1}{6}}$$

$$Nu_L = 0.92(Ra\cos\phi)^{\frac{1}{4}} \qquad (4.18)$$

It is worth noting that in the above equations, fins have not been accounted for. Therefore undershoot in the predicted temperatures from the simulation to the experimental results is expected. The Nu relation for the finned heater would be developed later in the chapter. To initiate the simulation, a couple of assumptions were made which are listed below:

$$T_p = T_w + 4 \qquad (4.19)$$

The equation 4.19 implies that the plate temperature is 4 ˚C above the water temperature.

Similarly;

$$T_c = T_p - \frac{(T_p - T_a)}{3} \qquad (4.20)$$

(The cover temperature is closer to the plate temperature than the ambient)

These equations were only used for the initialization of the simulation. After the first time step, the values of T_p, T_c and T_w are calculated by the program and are used as an input for the next time step.

4.2.4 Simulation Flow Chart

The following flow chart illustrates the simulation:

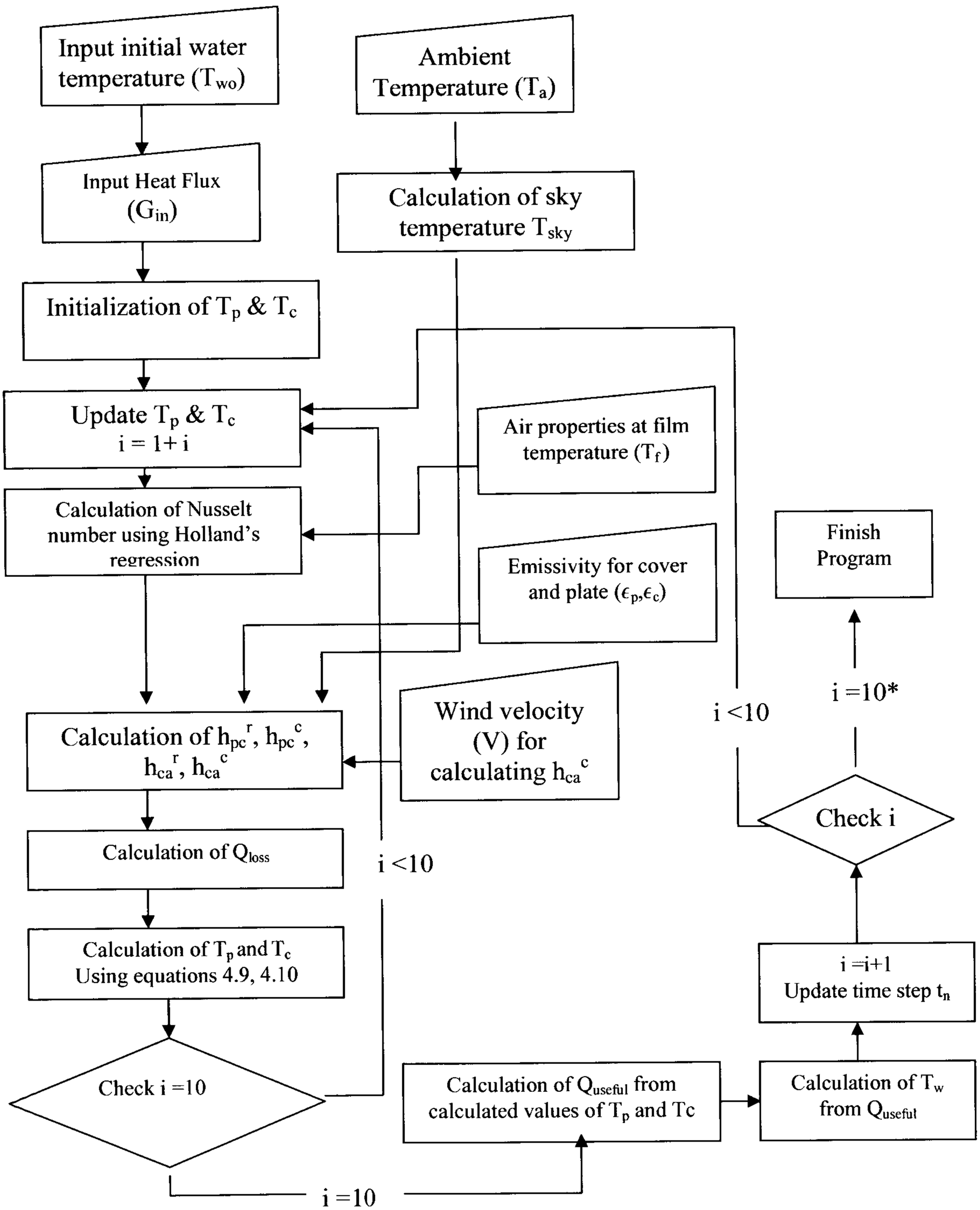

* i =10 because the time step taken was 360 sec (6min), therefore i =10 would report results after every hour

4.2.5 Results from the ATA

The values for the water and the cover temperatures obtained from ATA were compared with the experiments. Surprisingly close conformance was noted; a few of the results obtained from the ATA are given in 4.17-20

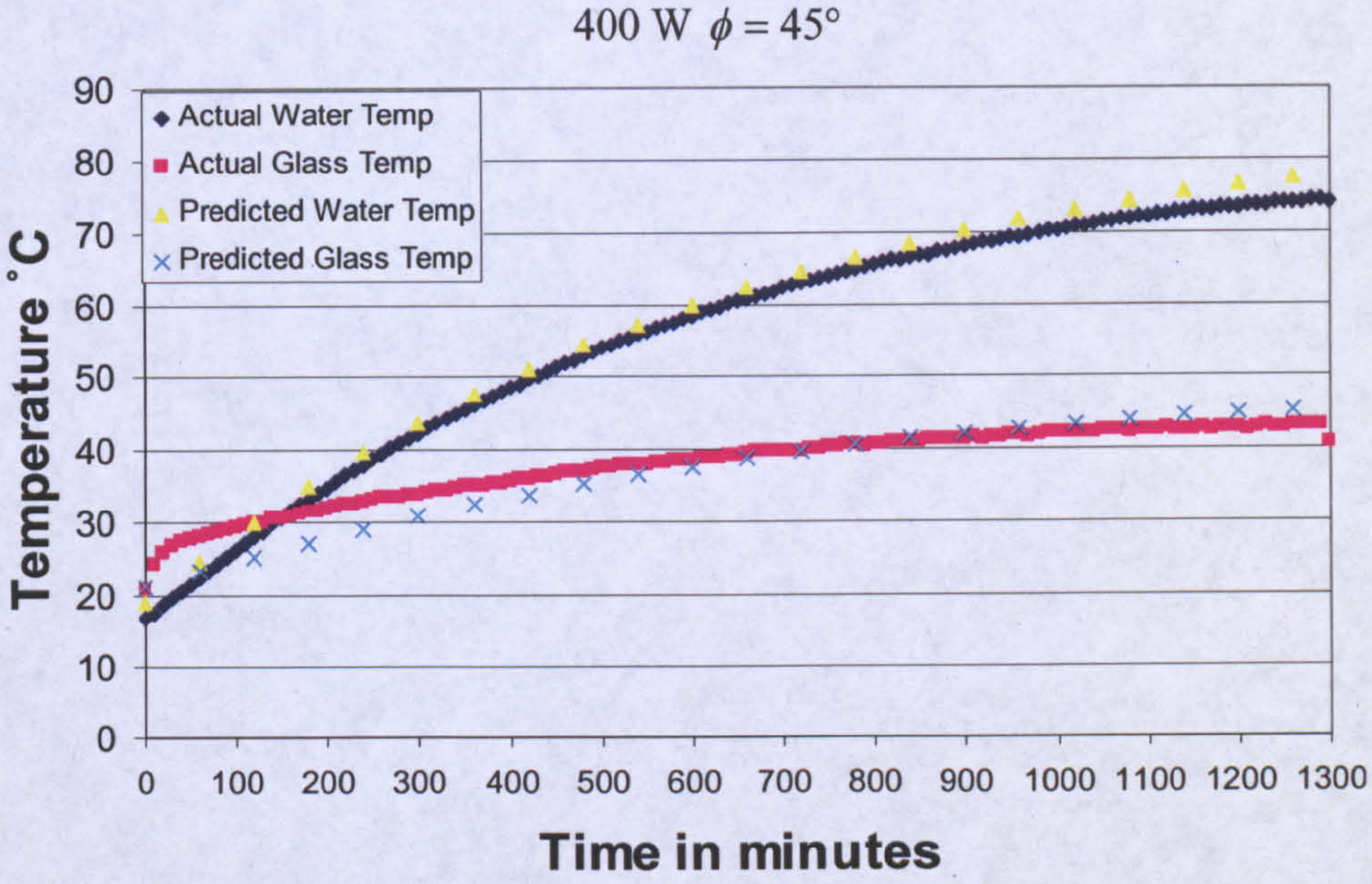

Figure 4.17: Comparison of simulation results & the experimental results (400W)

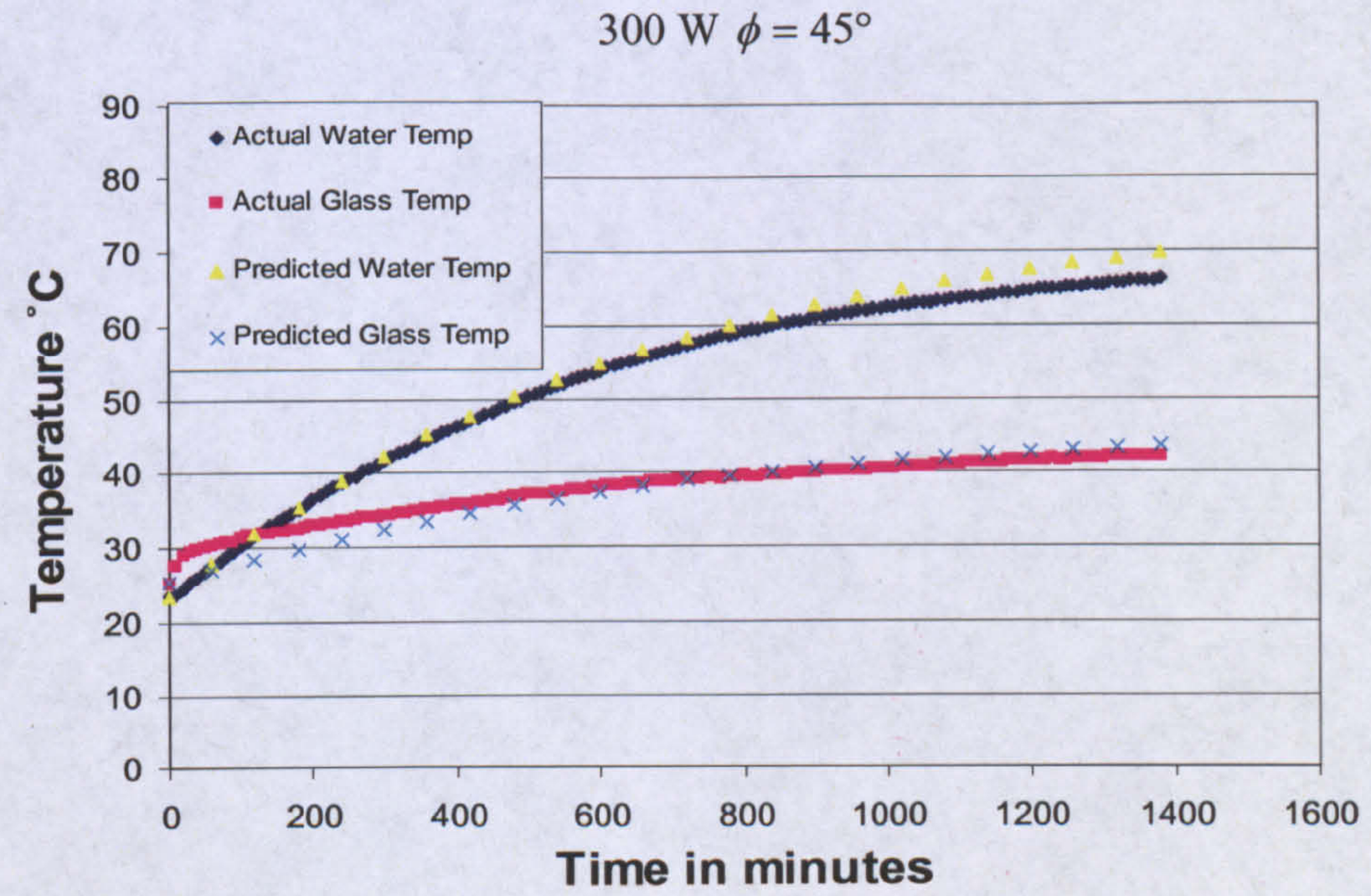

Figure 4.18: Comparison of simulation results & the experimental results (300W)

As can be seen in figures 4.17 and 4.18, that experimental water temperature is followed up very closely by predicted water temperature. The predicted cover temperatures however, at the initial hours do not closely match experimental values. Nonetheless it is only the water temperature that if of importance for predicting the yield of the collector.

It was also found that the convective heat transfer follows an asymptotic behaviour where it increases rapidly at the start and with the passage of time settle for an increasing but more steady values (fig 4.19.a). Radiative losses follow a similar trend (fig. 4.20.b). They remain lower than convective losses but have comparable values. With the increase in the imposed heat flux, the convection to radiation loss ratio also changes. This behaviour influences the selection of cover(s) and thus has been revisited and inspected more deeply in chapter 6.

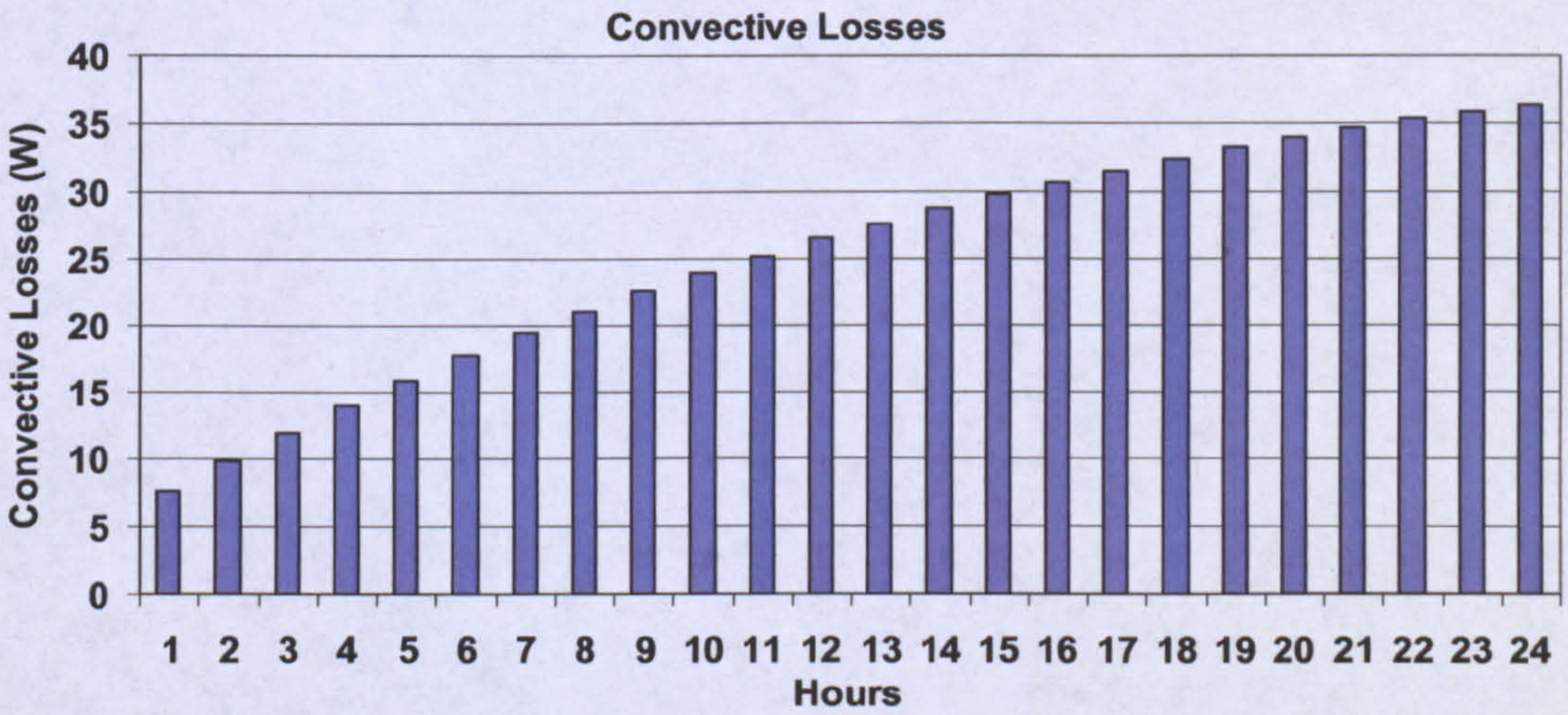

Figure 4.19.a: Convective losses computed from ATA for 24 hrs for 100 W

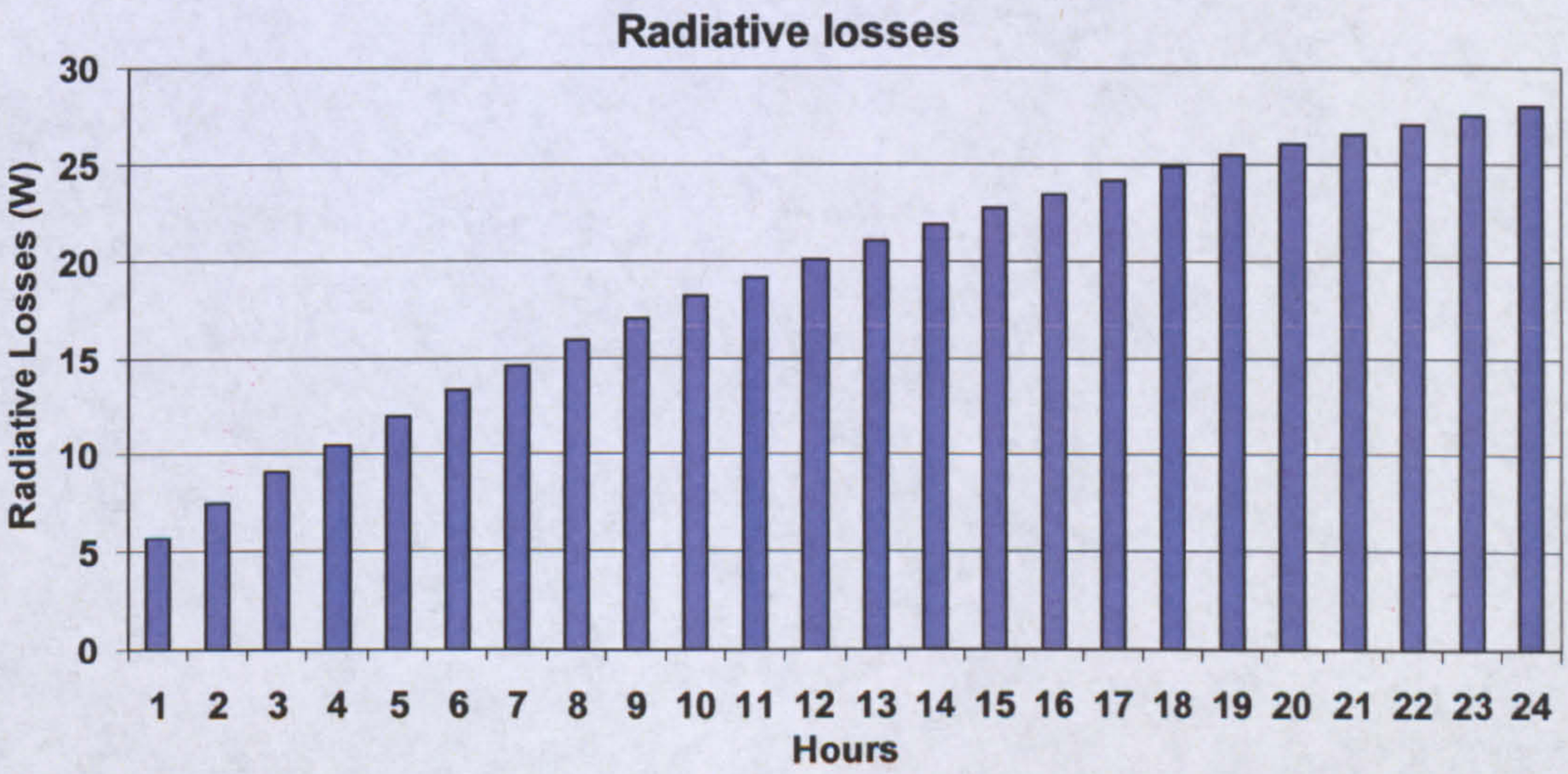

Figure 4.19.b: Radiative losses computed from ATA for 24 hrs for 100 W

4.2.6 Discussion on ATA

The main advantage of using ATA is that in a short span of time, various scenarios can be analyzed. The program can be provided with the daily radiation data as an input and the corresponding temperatures inside the tank can be estimated. The simulation cannot only be run for a time period of a day but extended to a whole year. Thus ATA is a useful tool for estimating the yearly performance of the collector.

The drawback of this method it is based on regressions that have a band of error/ uncertainty. The use of a series of regressions results in the propagation and thus magnification of uncertainty/error in the final result. The other disadvantage is that the ATA gives only mean values for the absorber plate and the water temperature. In reality, it was seen through experiments that water and absorber plate temperature vary along the longitudinal height of the collector.

4.3 COMPUTATIONAL FLUID DYNAMICS (CFD)

As mentioned earlier in Chapter 2, the recent upsurge in the use of CFD has reduced design cycle times to a great degree and provides deep insight into flow behaviour.

In order to proceed with the CFD analysis of the collector, it was anticipated that simple cases of natural convection should be solved for which correlations are available. This would help setup the software accurately as well as provide a benchmark for the results before proceeding with the more complex analysis of the collector.

Fluent 6.2 and Gambit 2.2 were used for CFD analysis. Fluent is a leading multipurpose CFD package and has been successful tool for modelling various flow and thermal scenarios.

Initially, flows involving natural convection were solved for establishing benchmarks. The exercise was later extended to solve forced convective flows. The work was productive as it helped identify the degree of grid dependence for solving problems of such kind. It also helped chalking out the various discretization schemes and options for solving natural convection flow. In a recent article, Zhai [3] has quantified the degree of error when a coarse grid is employed for a finite volume method. However his study was focused more towards the estimation of heat losses from the walls of buildings. A fair amount of literature is available on numerical solution to the classic natural convection problems. These include the flow over a flat plate, flow over a vertical plate, flow past a cylinder, and flow across an inclined channel. Collectively, these studies indicate the advantage of using a structured mesh and the importance of grid size in the boundary layers or the regions of high gradients. Setting up the boundary conditions (BC) accurately is a challenging task in itself. In some cases it is impossible to measure the true boundary conditions through measuring instruments while in the other cases the BC might be known but it is difficult to incorporate in the CFD software. A similar problem was encountered when analyzing the prototype collector. As the experimental testing was

carried out using the heating pad, it was not possible to enumerate the exact amount of heat flux going into the collector though the total applied heat flux was known.

To setup a problem in CFD, is time consuming particularly for 3D domains. However, once a converged solution is obtained, the operating conditions can be changed and the response of the problem domain over new conditions can be calculated easily. Details such as fluid velocity, temperature, density, pressure, Peclet number and convective heat transfer coefficients can be obtained at several points in the computational domain.

4.3.1 Benchmarking Natural Convection Cases

Modelling of natural convection in CFD is a complicated affair due to the presence of buoyant forces. Natural convection cases of even the most elementary types are difficult to resolve due to their intricate nature. Even the regressions for natural convection flows are available only for a small number of cases.

The case studies that were solved are briefly presented herein.

4.3.1.1 Criterion for Mesh Size

To construct an accurate mesh, the boundary layer thickness is required to be known. The main reason is that the mesh size should not exceed the boundary (thermal and velocity) layer thickness.

Analytical studies in many cases provide relationships for boundary layer thickness. One such example is the Blasius solution for flow over a flat plate [4] presented in equation 4.19.

$$y_p\sqrt{\frac{U_\infty}{\nu x_o}} \le 1 \qquad (4.19)$$

4.3.1.2 Flow over Flat Plate

Forced convection from a flat plate is a well studied phenomenon owing mainly to its numerous practical applications and in particular the fins in air cooled engines. 2D flow analysis over a flat plate was carried out. The widely used regression for it gave good results particularly in the low Reynolds numbers and is presented in 4.20.

$$Nu_x = h_x x / k = 0.664 \,\mathrm{Re}^{1/2}\, \mathrm{Pr}^{1/3} \; for \; \mathrm{Pr} \geq 0.6 \qquad (4.20)$$

Table 4.1: Comparison of Regression and CFD results

	Regression	**CFD**	**% Difference**
Q (Watts)	42.5	42.7	0.47
h (W/m^2K)	5.10	5.16	1.17

4.3.1.3 Flow over a Vertical Plate

The study of natural convection flow on a vertical plate has been one of the elementary studies in natural convection. The velocity profile in this case is particularly interesting. The velocity increases while moving away from the plate till it reaches a maximum and thereon decreases back to stagnation generating a parabolic profile. The study on over vertical plate has several applications most common of which is the heat loss that occurs from building walls.

Table 4.2: Comparison of Regression and CFD results

	Regression	**CFD**	**% Difference**
Q (Watts)	172	167.4	2.6%
h (W/m^2K)	3.4	3.3	2.9%

4.3.1.4 Flow inside an Air-Cavity

As mentioned earlier, the work on air-cavities is fairly exhaustive owing to its diverse application. Four cases of air-cavity were modelled in CFD to compare the results with regression for the same. The value of critical Rayleigh number at which transition to turbulence occurs is 2 x 10^4 for two dimensional cavities as has been described by Yin et al, [5]. In light of this, for all the cases for CFD analysis, the value of Rayleigh number was kept less than the critical value. Thus the flow modelled, was laminar in all cases. The cases solved were only vertical cavity cases with H/L ratio of above 50 (details present in table 4.3). Further details of these cases have been described in table 4.4.

Table 4.3: Details of the air-cavity cases solved

Cases	Cavity Dimensions	In Filled Gas	Wall Temperatures	Rayleigh Numbers
A	0.6m x 0.012m	air	0 and 20°C	4.10 x 10^3
B	0.6m x 0.02m	air	0 and 20°C	1.90 x 10^4
C	1m x 0.05m	air	0 and 20°C	2.97x 10^5
D	0.6 m x 0.012m	air	0 and 20°C	4.10 x 10^3

Table 4.4: Results from CFD of air-cavity

Case	h_{exp}	h_{CFD}	% Difference
A	2.20	2.20	0
B	1.90	1.88	1.05
C	1.80	1.78	1.11
D	1.47	1.42	3.4

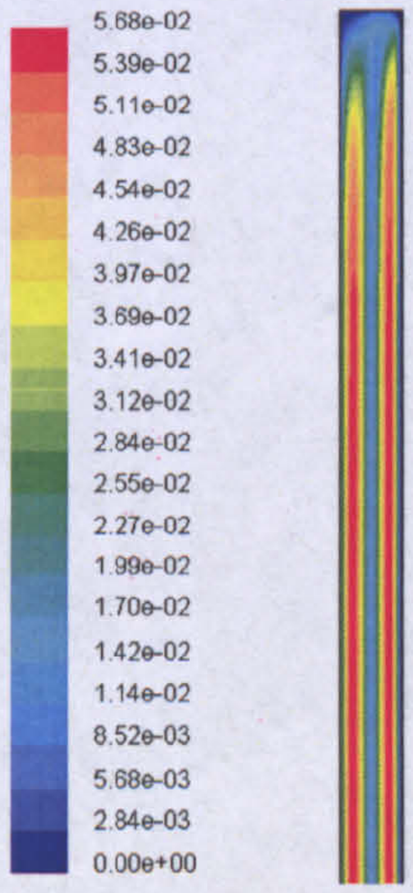

Figure 4.20: Contours of velocity in a cavity Dimensions 0.6m x 0.012m

4.3.1.5 Hindsight from Benchmarking

The exercise of solving simple natural convection cases yielded several important results that helped in the later analysis of more complex collector behaviour and are listed below:

- Benchmarking of CFD analysis provided assurance for the next step i.e. resolution of the whole collector. It was established through benchmarking that QUICK (Quadratic Upstream Interpolation scheme for Convective Kinetics) was the best scheme for the natural convection cases along side the Boussinesq method for density. Quad mesh was used in all cases which has been reported to give 3rd order accuracy when used in conjunction with QUICK interpolation scheme[6].
- The most important outcome was the size of the mesh. It was found out previously by Gill [7] that at least one node should remain inside the boundary layer, to accurately resolve temperature and in the velocity fields.
- Through repeated tests and literature review it was ascertained that a boundary layer of 1 mm is the optimum.
- The convergence criteria of 10^{-3} for the directional (x, y and z) velocities and 10^{-6} for temperature was found to give reasonable results. Shifting the criteria to lower values would have required more iterations for convergence.
- Segregated scheme works better as compared to coupled scheme. The use of coupled scheme resulted in divergence in most cases and singularity errors.
- The thermophysical properties (such as viscosity, Prandtl number, conductivity, specific heat) were modelled as constants –values determined at the film temperature- and yielded good results. This also kept the solution computationally less expensive.
- It was also noted that for some cases a steady state solution from the onset did not work. Therefore, a transient approach was adopted for this case. The details of this approach are mention in the Chapter 8 of Fluent Users Guide [10].
- All the benchmark cases done were 2D.

- In cases of forced convection, the mesh size becomes critical and extremely mesh sensitive after Re= 3200 [8]

4.3.2 Details on CFD of Collector

Initially, the collector components were analyzed individually (air-cavity and water tank). Although these analyses did provide fine details of the collector behaviour, it was realized that unless a conjugate (combined) analysis is carried out, the results would be inconclusive, owing to the coupled nature of heat transfer from the absorber plate.

One of the challenges for using CFD was the unknown value of the heat flux going into the waterside of the absorber plate. Through experiments it was observed that the fraction of imposed heat flux going into the storage tank changes with time. This changing flux was to be set as one of the boundary conditions for the analysis.

Experiments had revealed that the quantity of heat going in the system was dependent upon the absorber plate temperature as well as the energy content of water, the tilt angle and stratification. Providentially, through ATA, the heat flux going into the storage tank with the passage of time could be determined. The results were evaluated and are depicted in fig 4.21 and fig 4.22.

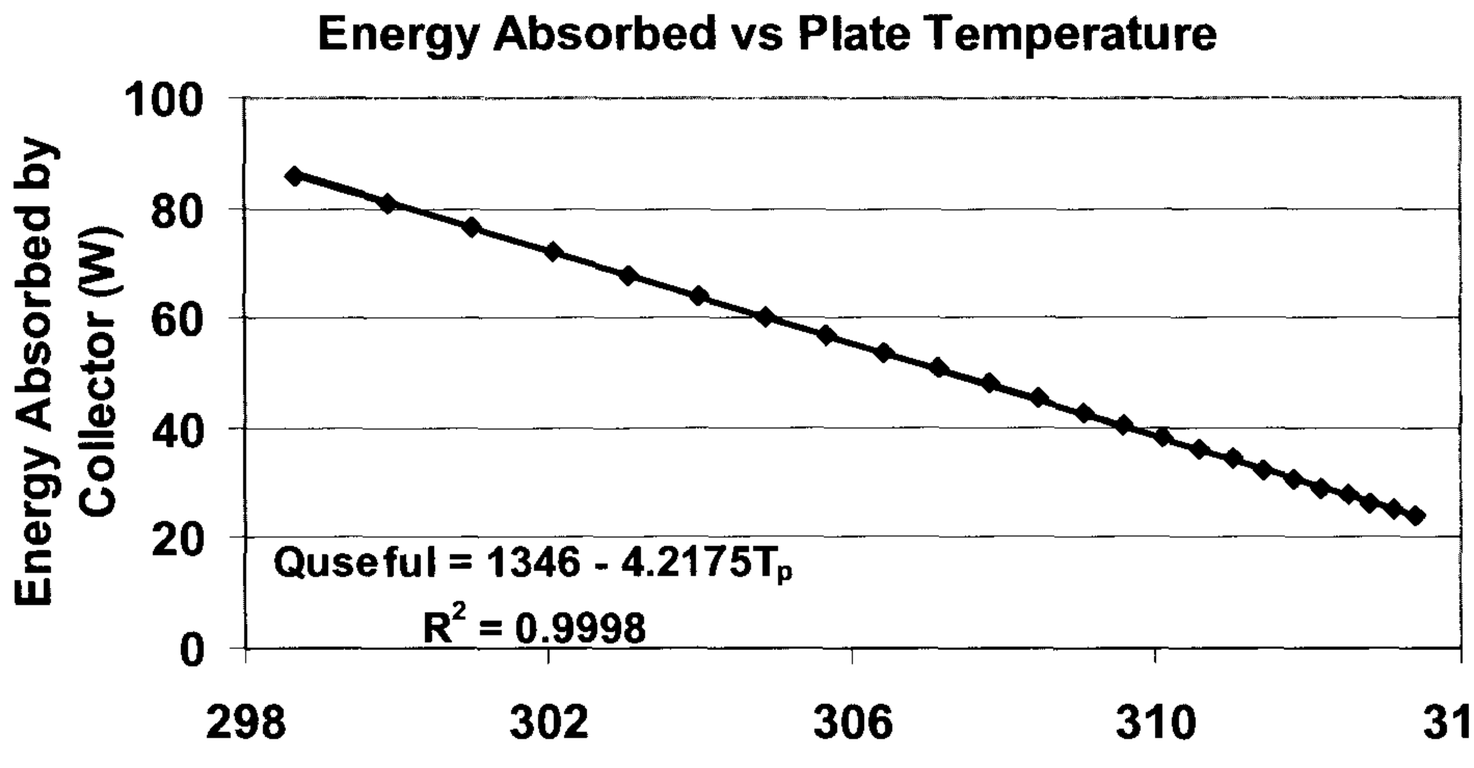

Figure 4.21: Energy absorbed by the collector plotted against the plate temperature

Where,

$$Q_{useful} = 1346 - 4.2175T_p$$

The plot for Q_{useful} against T_p is almost linear. It gives a highly conforming fit for linear equation as evident by R- squared value $R^2 = 0.9998$

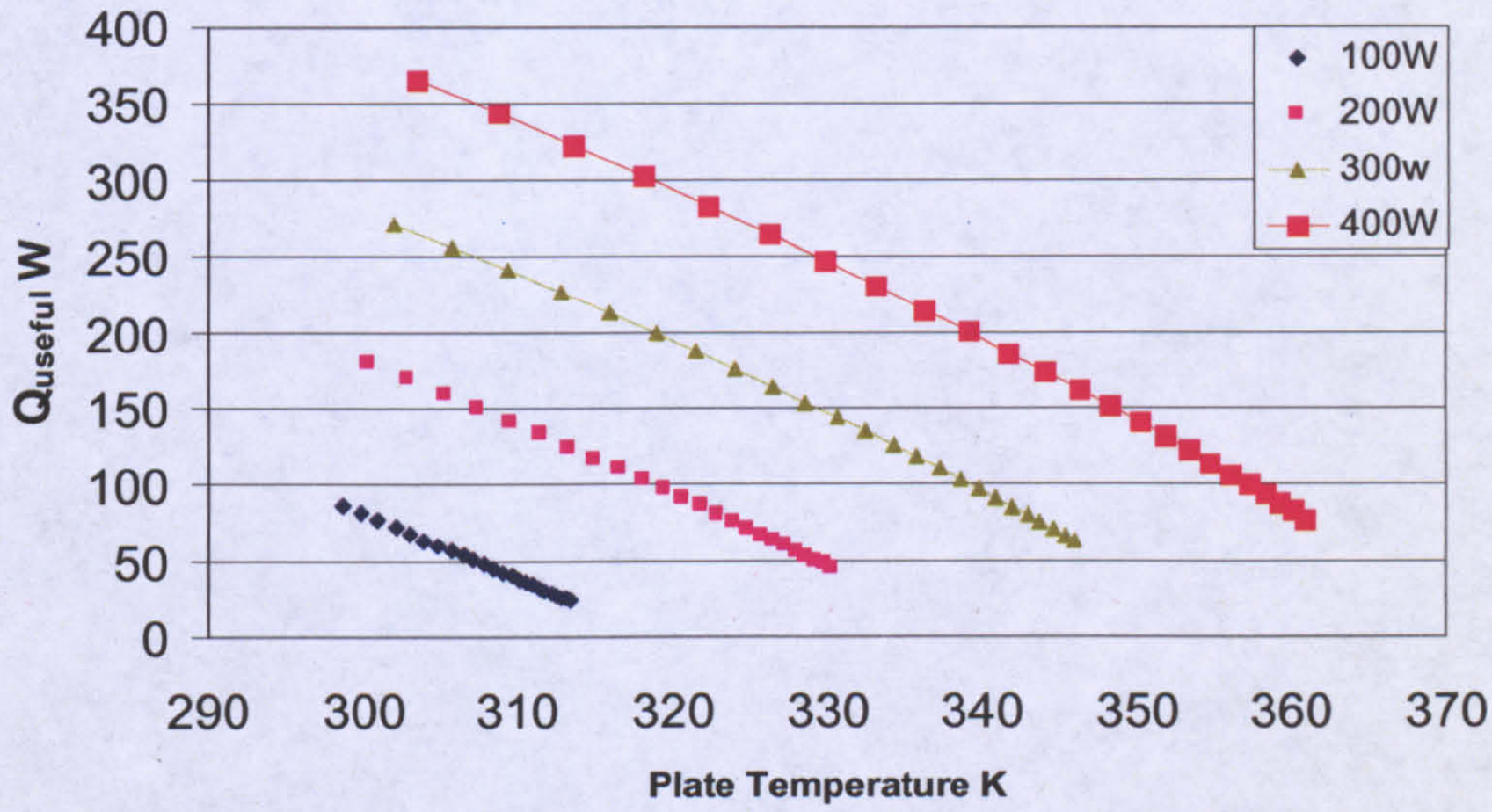

Figure 4.22: Energy absorbed by the collector plotted against plate temperature for various values of heat flux

It can be noticed that Q_{useful} not only depends upon the applied plate temperature but also the level of imposed heat flux. It is also dependent on the energy content inside the collector as will be revealed later in the chapter. Nonetheless, what is important is the relationship that was obtained for Q_{useful} with the plate temperature. This has been utilized to carry out CFD.

One of the collector characteristics that remained obscure after ATA was the stratification inside the collector. A hint on the stratification on the collector was provided by experimental data. Therefore in the CFD analysis for collector, particular emphasis was placed on observing the stratification of the collector. The details of all the CFD analysis is presented in the following sections.

4.3.2.1 CFD Analysis for the Collector Air-Cavity

In the prototype collector the space between the absorber plate and the cover of dimensions 1m x 1m x 0.035m (air-cavity) was subjected to CFD analysis. From the review studies it was realized that 2D analysis is not appropriate and does not predict the true behaviour. The work of Yunhua Yang [8] has reported the discrepancy of 2D analysis.

Mesh size for the storage tank was kept at 200 x 200 x 15. This implied a cell count of 600,000. In normal practice, for a PC, up to 1 x 10^6 cells, is a suitable number. The computing machine used for processing was an Intel Pentium 4 CPU 2.8 GHz, with 1 GB RAM.

A total of three types of CFD tests were performed for estimating the heat loss coefficient against increasing tilt angle. Initially a 2D analysis was carried out, results of which are presented in fig 4.23. The 3D analyses were done for both the air-cavity identical to the earlier study of Elsherbiny and the prototype collector air-cavity. The experimental results of Elsherbiny were available for an aspect ratio of A = 40 and Ra = 9650. These were the closest available results in the reviewed literature to the dimensions of the prototype air-cavity. A high degree of conformance was observed between the CFD results and the experimental results by Elsherbiny. A MBD (Mean Bias Difference) of only 0.083 and RMSD (Root Mean Square Difference) of 0.0136 was observed between the two. Therefore on this basis, the results obtained for the prototype collector air-cavity can be used with confidence.

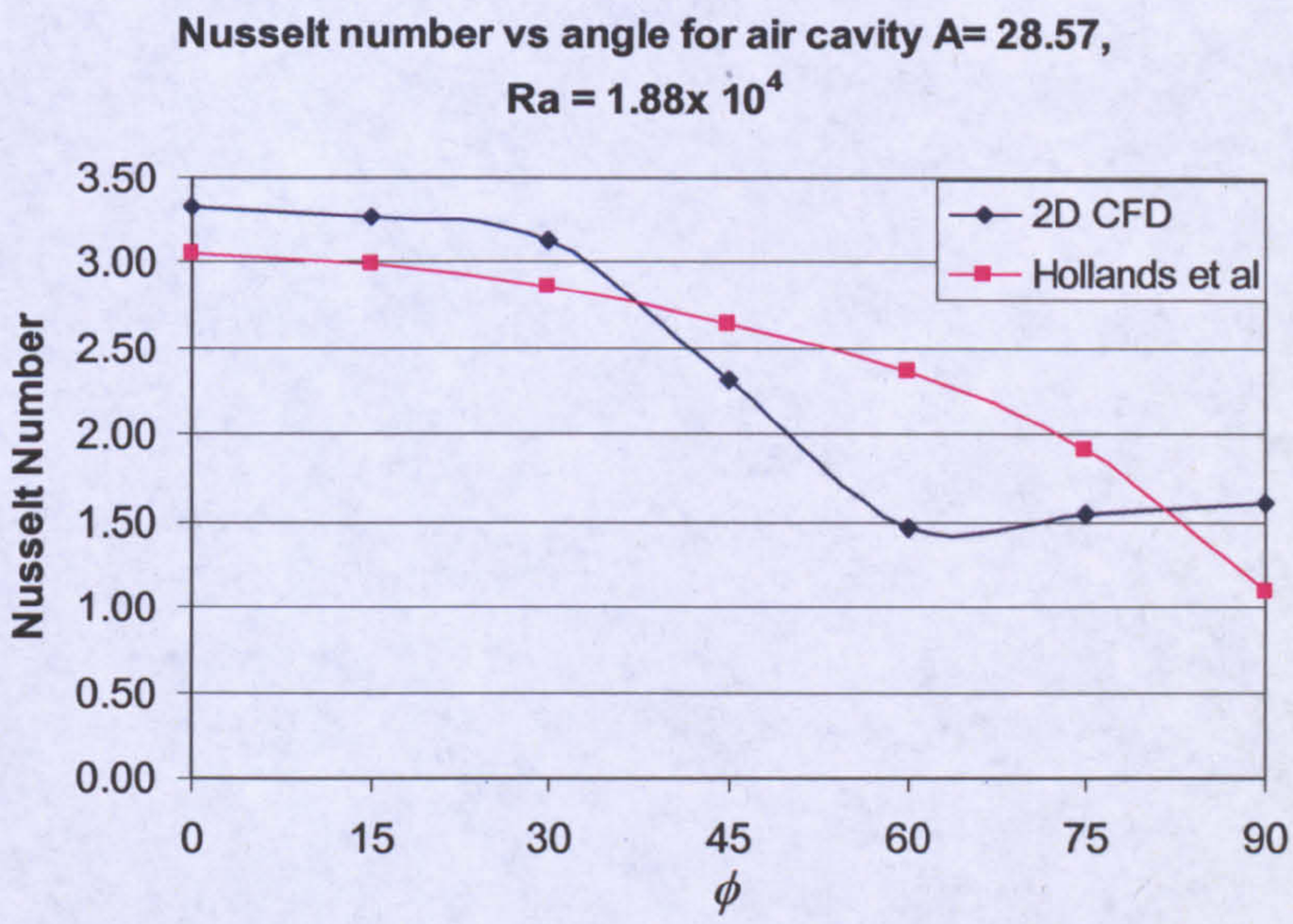

Figure 4.23: CFD results from 2D analysis showing the behaviour of Nu with the tilt. The results from regression from Hollands has also been plotted

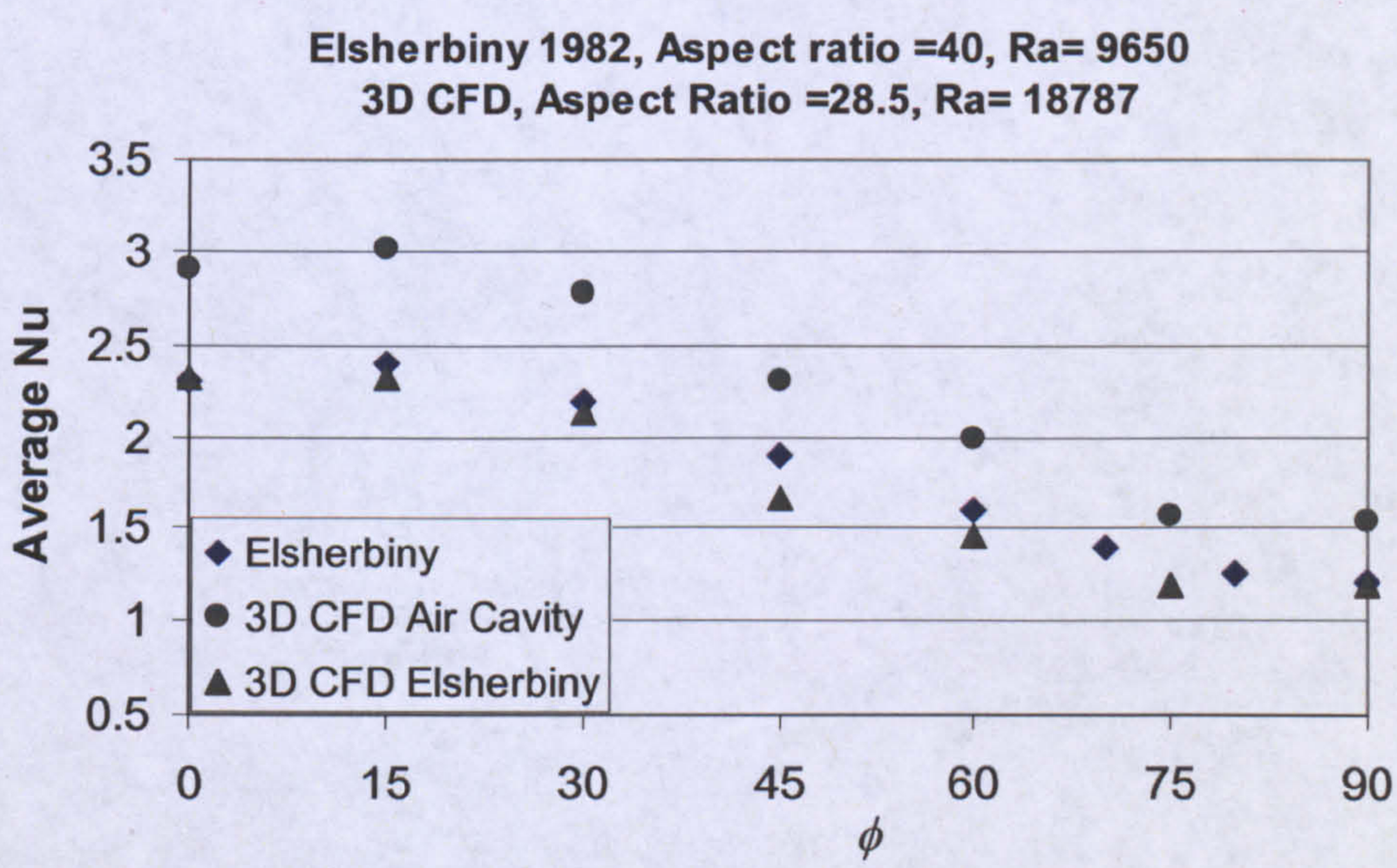

Figure 4.24: Results from the study of Elsherbiny, 1982 showing a steady decline in the Nusselt number

In fig 4.24 it can be noticed from Elsherbiny's experimental results that the Nu gradually declines with increasing angle of inclination. This is very closely matched by the results from 3D analysis. Examining 2D analysis (fig 4.23) also reveals an overall decline however a sudden drop in the middle of the curve is also observed. The widely used

regression by Hollands et al generates a sinusoidal (convex curve). This confirms the claim of Yunhua Yang that 3D analysis being the only infallible way forward. Another conclusion that can be drawn from the results is that 2D analysis is accurate up to $\phi =$ 30°. The increasing angle results in a slump in the convective heat transfer. This asserts that the increase of angle is favourable to the overall performance of the collector as it lowers the heat losses.

The streak lines from the 3D analysis of Elsherbiny's have been shown in fig 4.25.a –c. The 3D nature of the convective rolls has as traced by particles that were released from the middle of the cavity (17.5mm) along "z" and "x" as indicated by various points of the domain have been shown in fig 4.25.a, which is when the collector is at $\phi = 0°$. Streak lines of the rolls appear with axis perpendicular to lateral as well as longitudinal direction. When the tilt angle is increased, the strength of the longitudinal rolls can be seen to be increasing (see fig 4.25.b). The trend continues and longitudinal rolls gain strength while the lateral rolls disappear (fig 4.25.c-d).

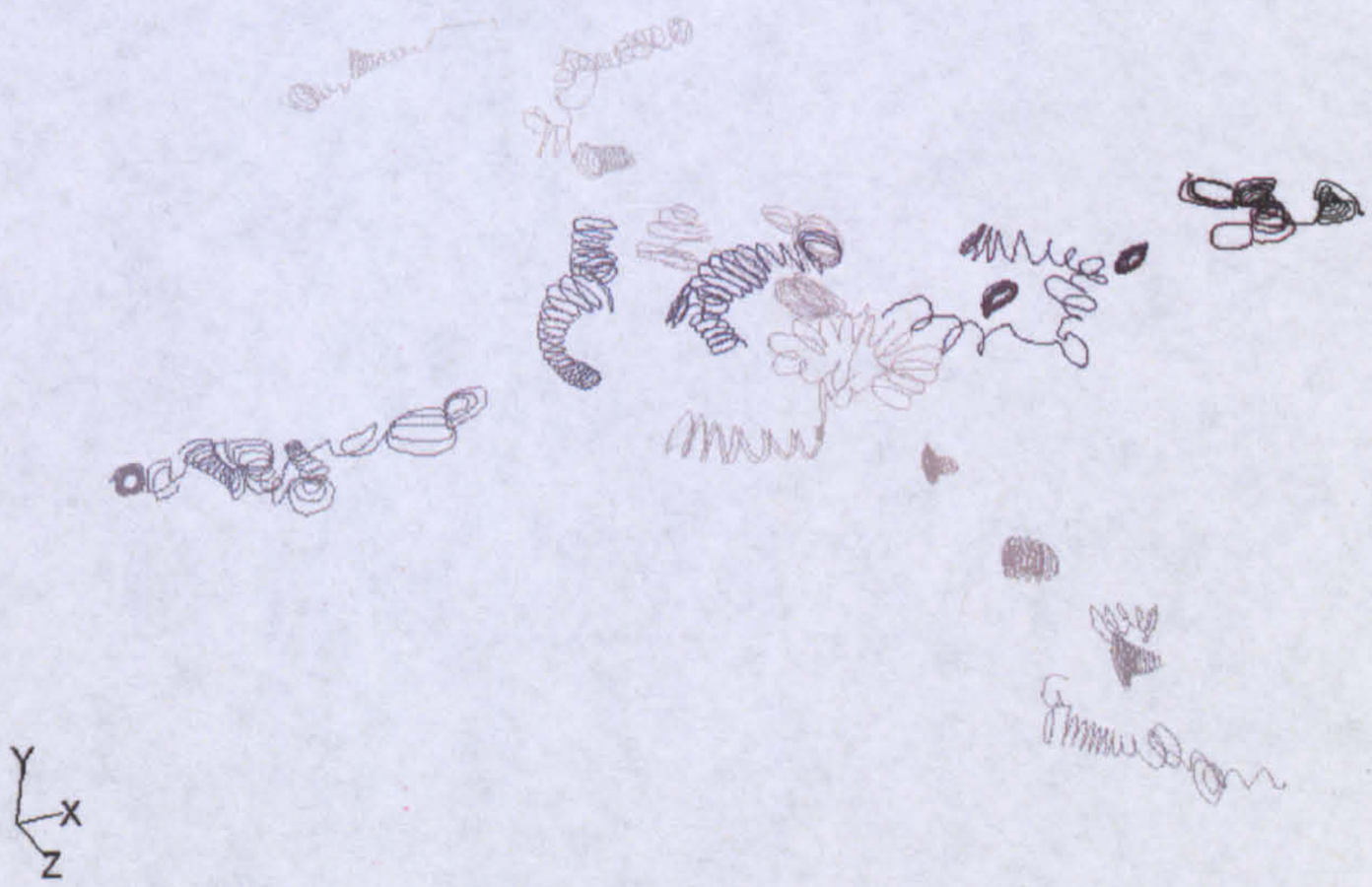

Figure 4.25.a: 3D CFD analysis of Elsherbiny's case. Streak lines for $\phi = 0°$

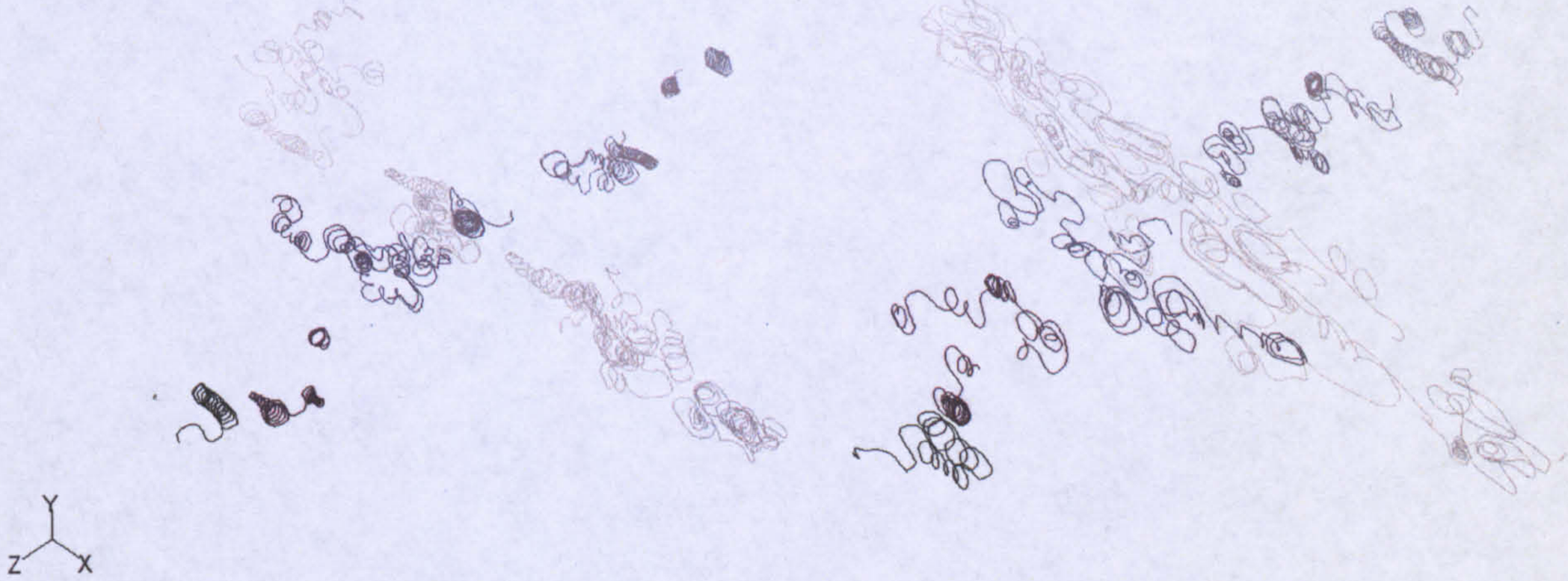

Figure 4.25.b: Streak lines for $\phi = 15^{\circ}$ and 30°

Figure 4.25.c: Streak Lines $\phi = 45^{\circ}$ and 60°

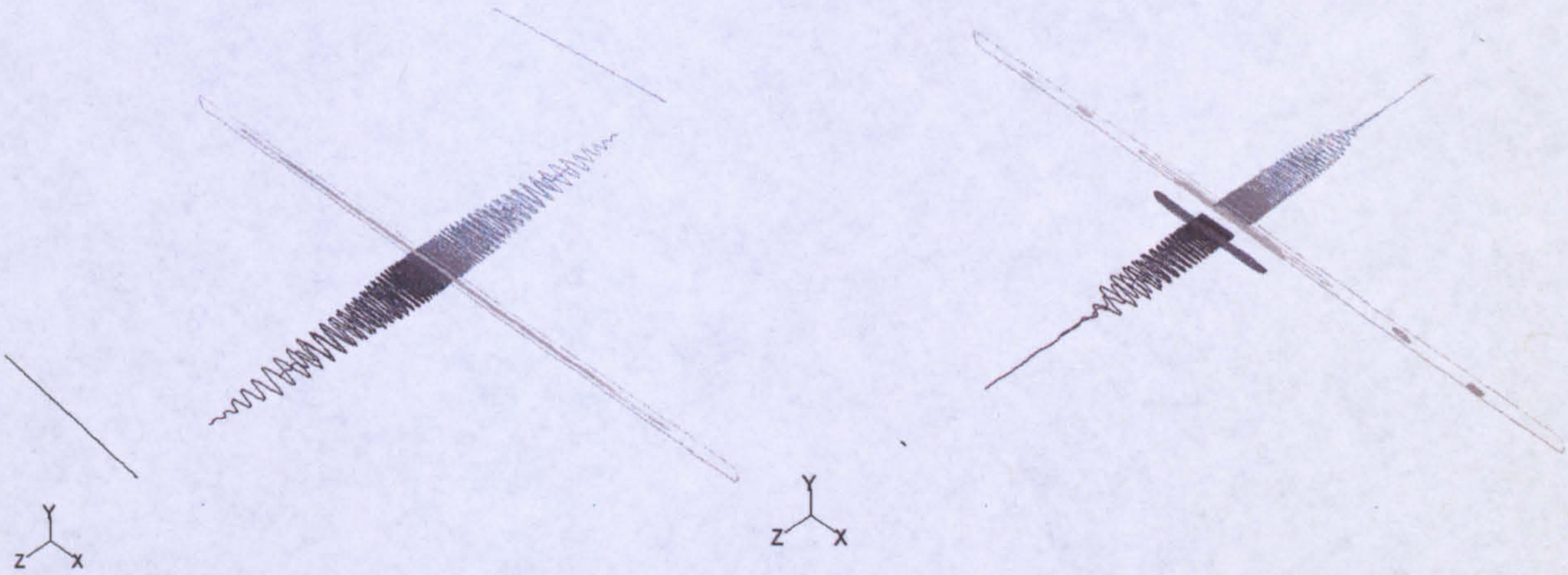

Figure 4.25.d: Streak Lines ϕ=75° and 90°

4.3.2.2 CFD Analysis of the Water Tank

A 2D CFD analysis of the water cavity was carried out by only modelling the longitudinal section of the collector. As only the section with dimension 1m x 0.050m was modelled, the domain does not encompass the fins. Nonetheless the domain adequately represents the unfinned collector. The mesh size was kept 1000 x 50 thus laying out a 1mm x 1mm mesh all-around. The analysis was transient with 100 W of heat flux applied on the absorber plate. The results show that the stratification varied slightly with the angle. It also showed that with the passage of time, the hot water starts accumulating at the top. This results in the reduction of overall flow movement in the tank and consequently weakens the heat transfer coefficient with time. Although in the 2D analysis may not be matching the actual collector geometry, the results produced are important. The fig 4.26.a-j show the contours of velocity and temperature after 10 minutes of exposure to 100W heat flux.

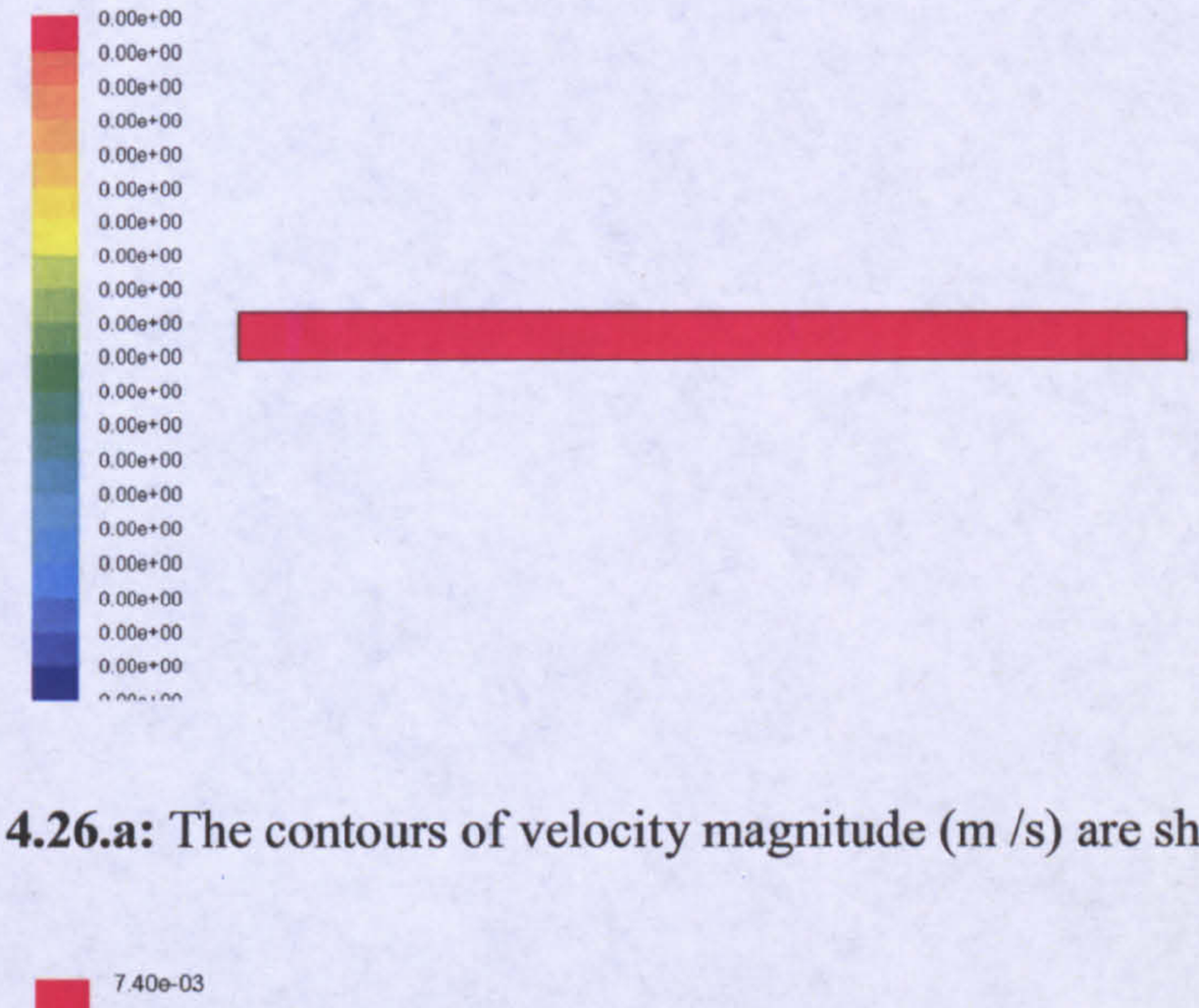

Figure 4.26.a: The contours of velocity magnitude (m /s) are shown for $\phi = 0^{\circ}$

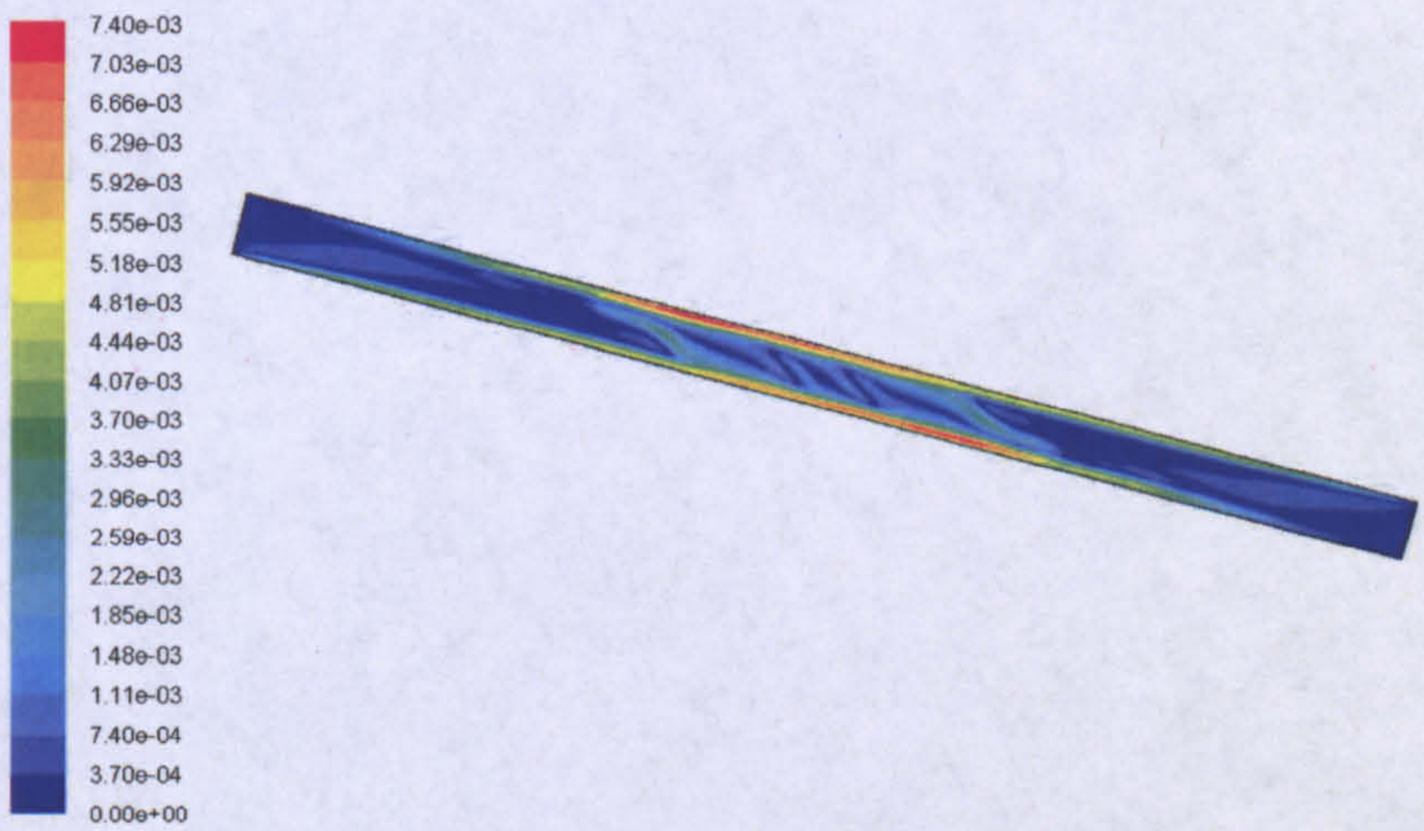

Figure 4.26.b: The contours of velocity magnitude (m/s) are shown for $\phi = 15^{\circ}$

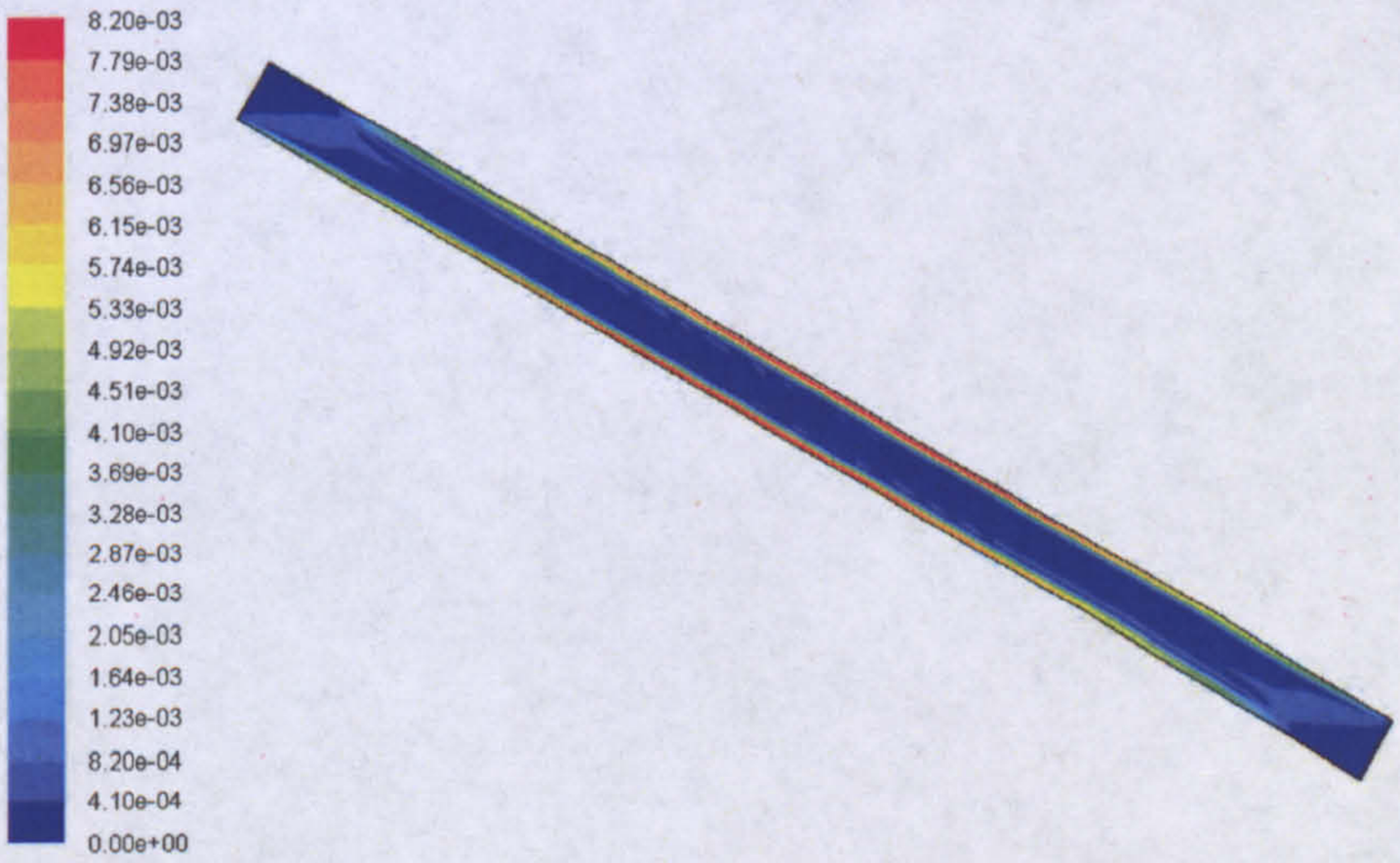

Figure 4.26.c: The contours of velocity magnitude (m/s) are shown for $\phi = 30^{\circ}$

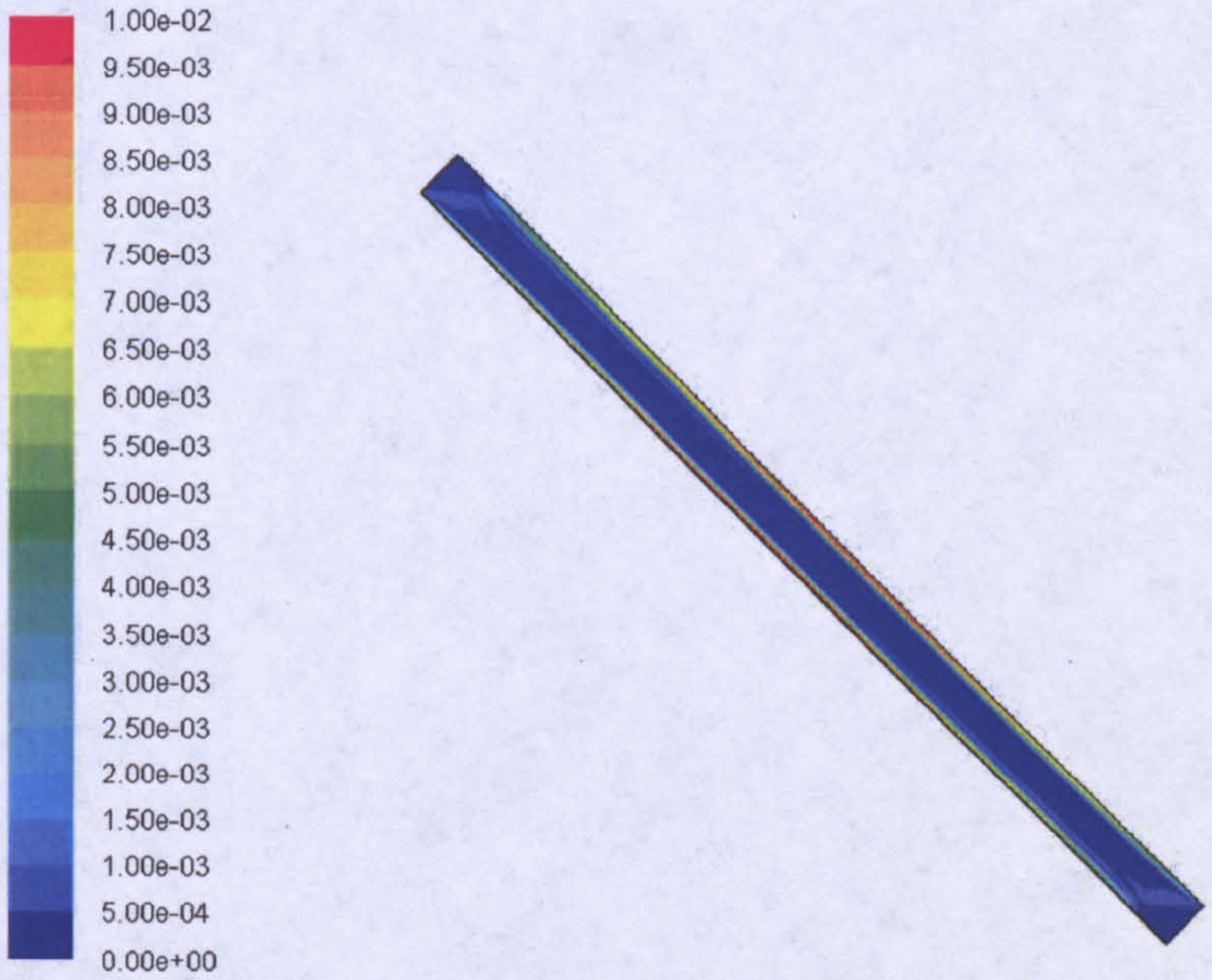

Figure 4.26.d: The contours of velocity magnitude (m/s) are shown for $\phi = 45^{\circ}$

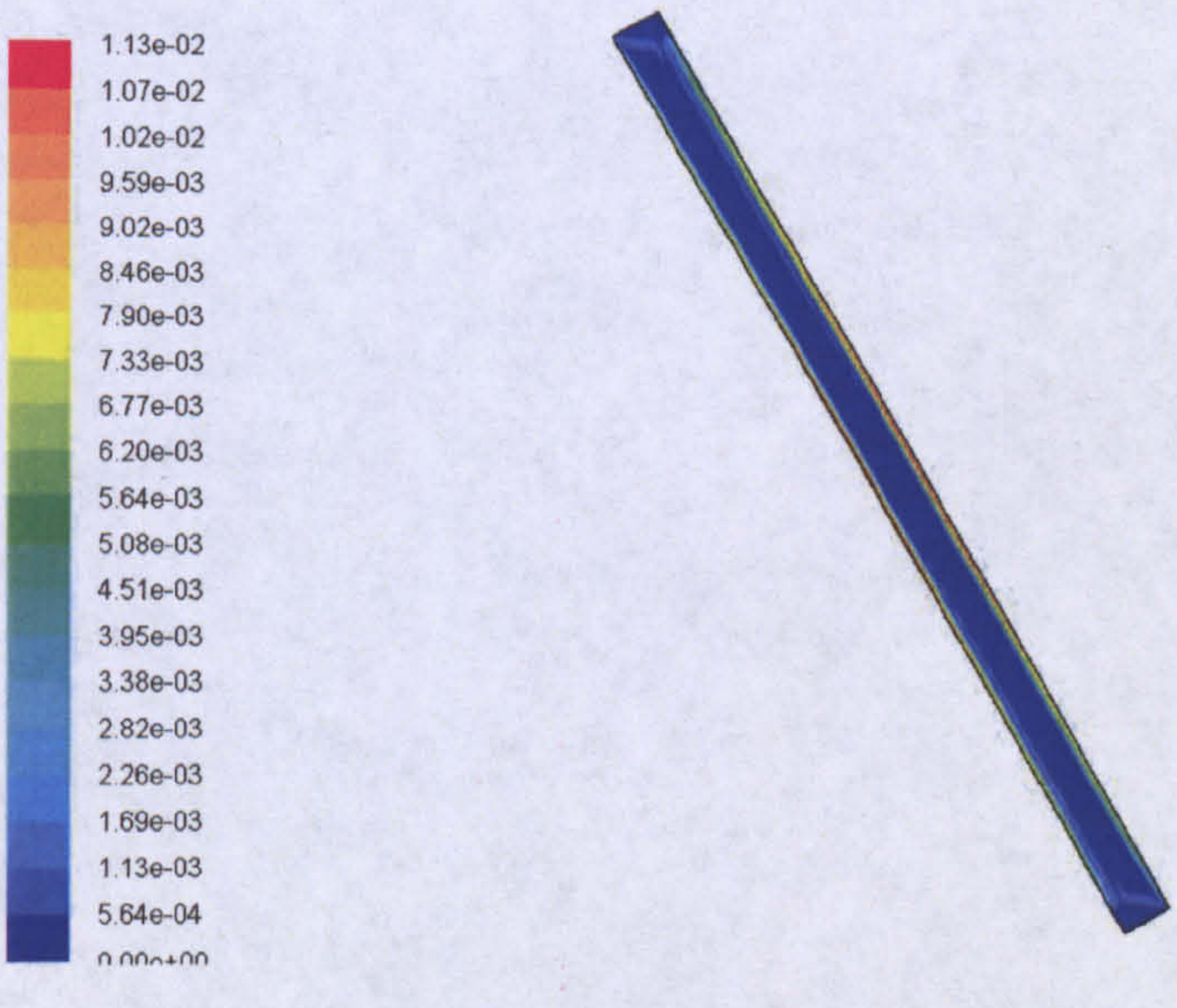

Figure 4.26.e: The contours of velocity magnitude (m/s) are shown for $\phi = 60^{\circ}$

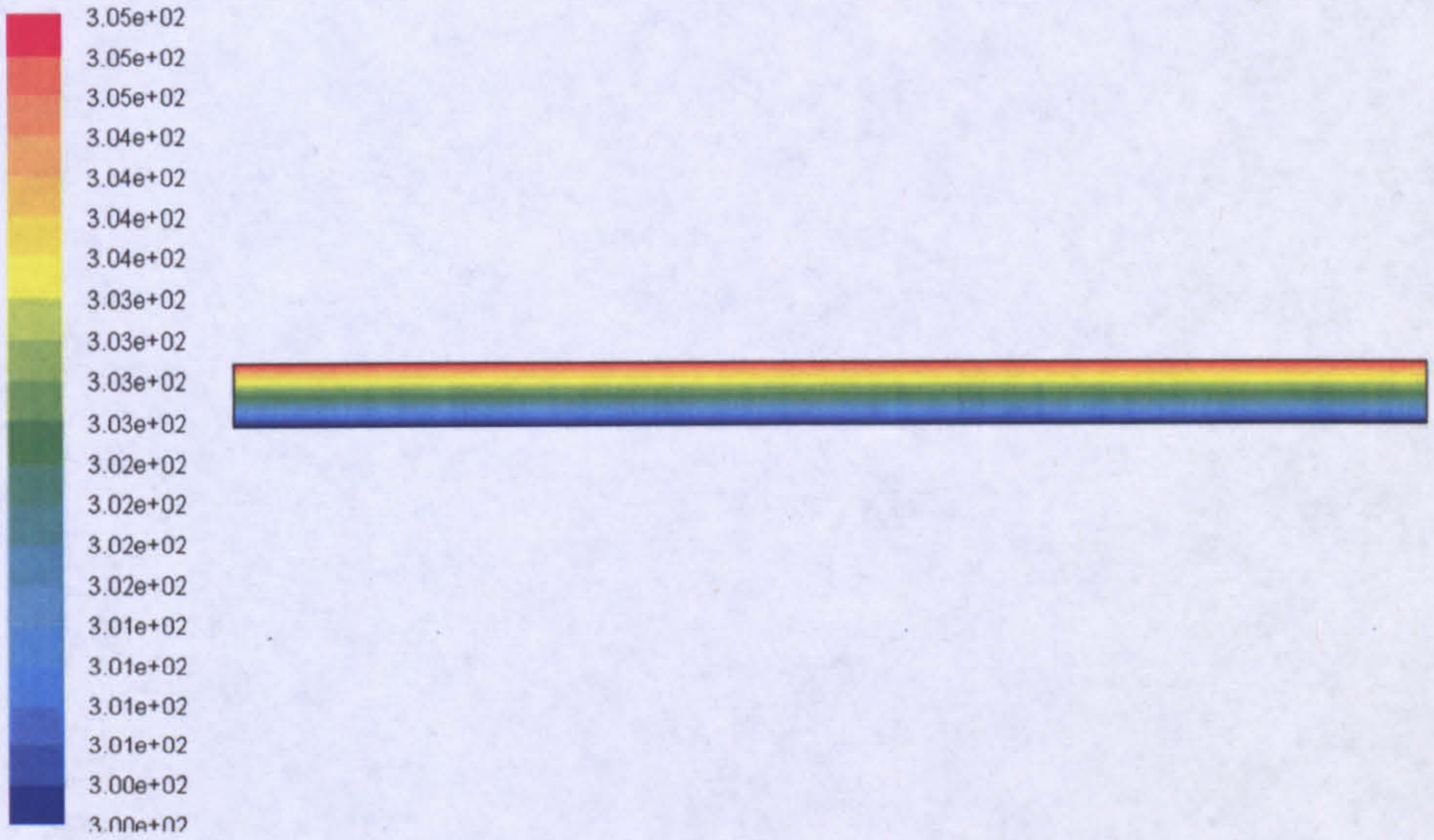

Figure 4.26.f: The contours of temperature (K) at ϕ =0°

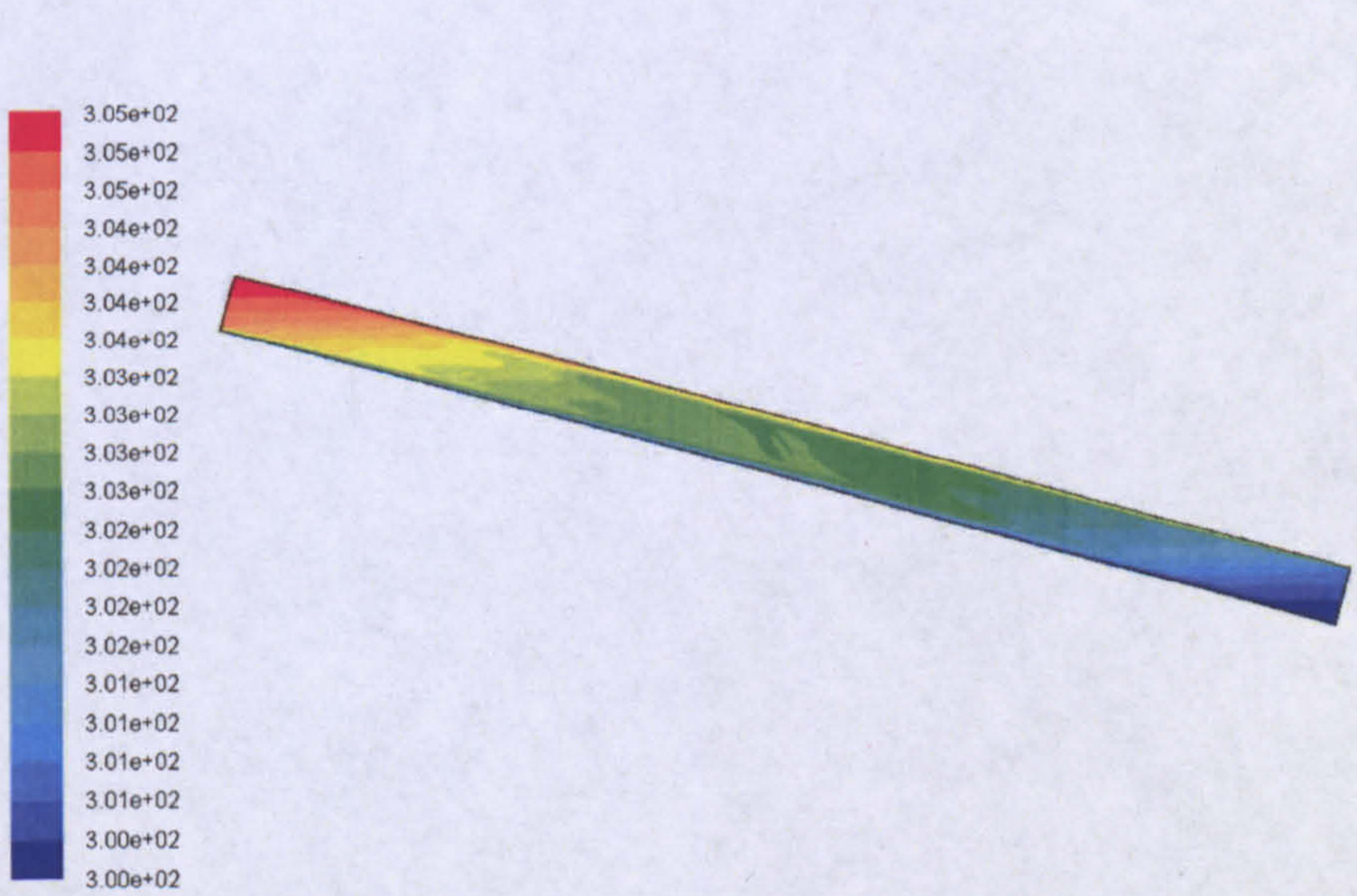

Figure 4.26.g: The contours of temperature (K) at ϕ=15°

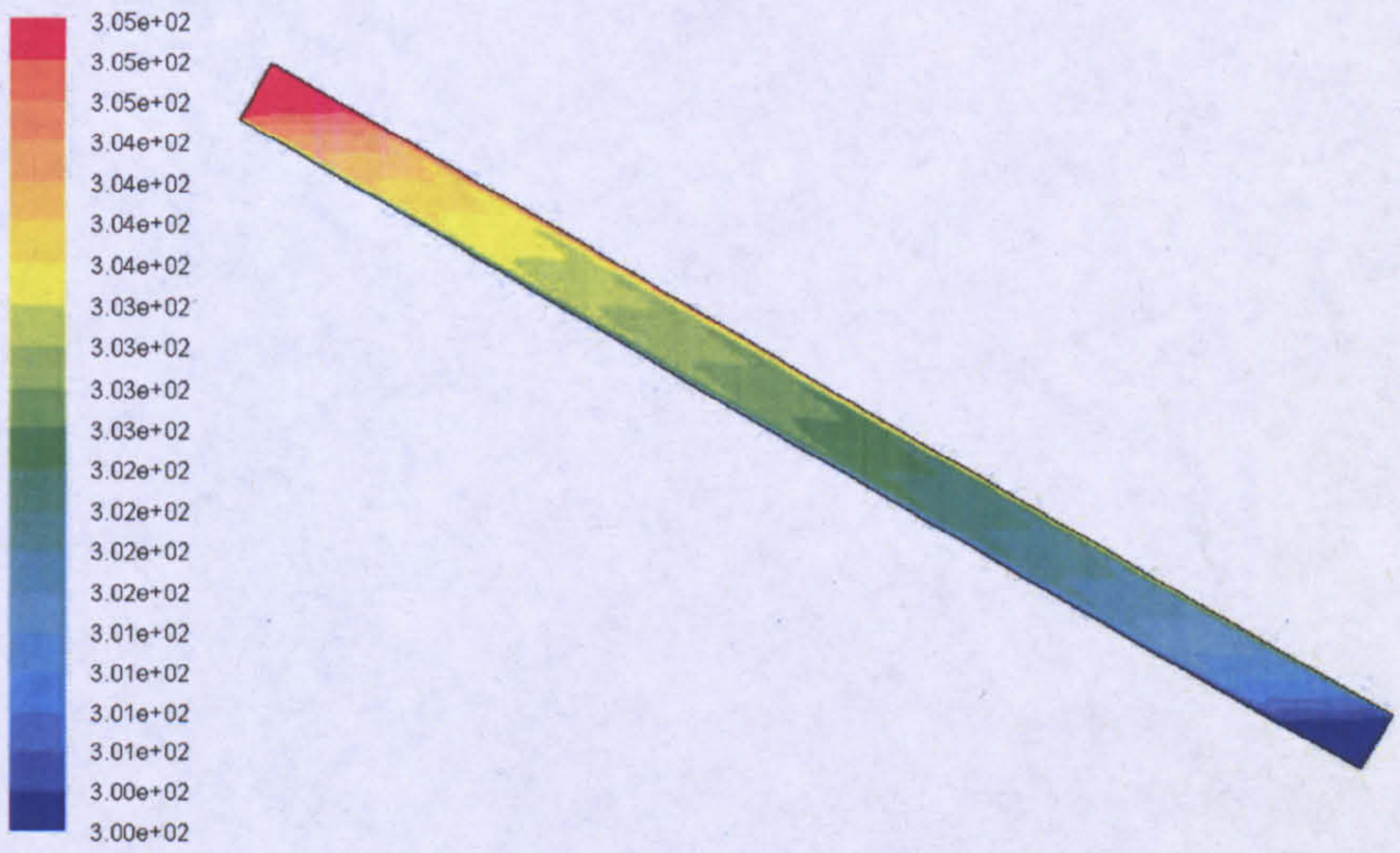

Figure 4.26.h: The contours of temperature (K) at $\phi = 30^{\circ}$

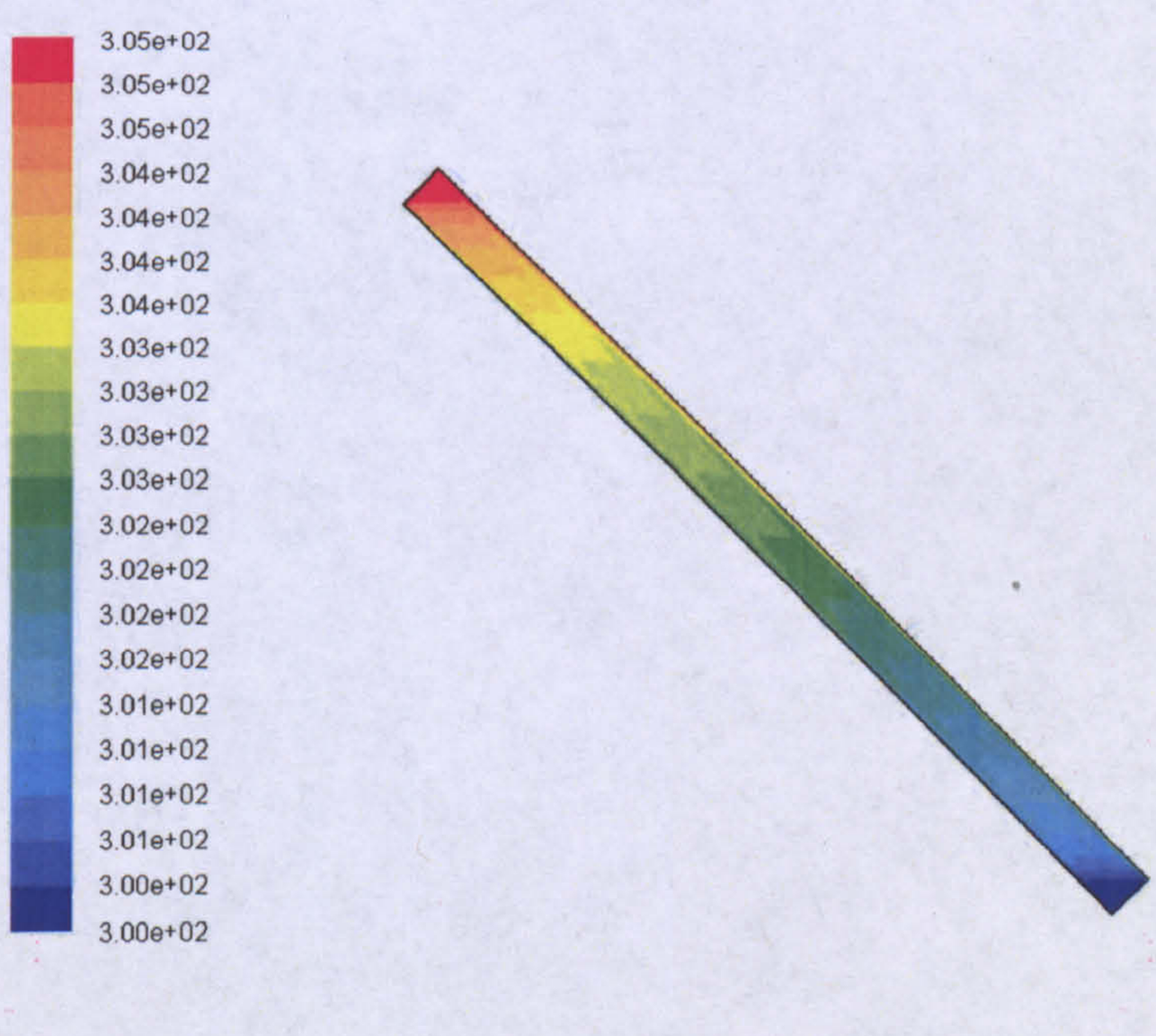

Figure 4.26.i: The contours of temperature (K) at $\phi = 45^{\circ}$

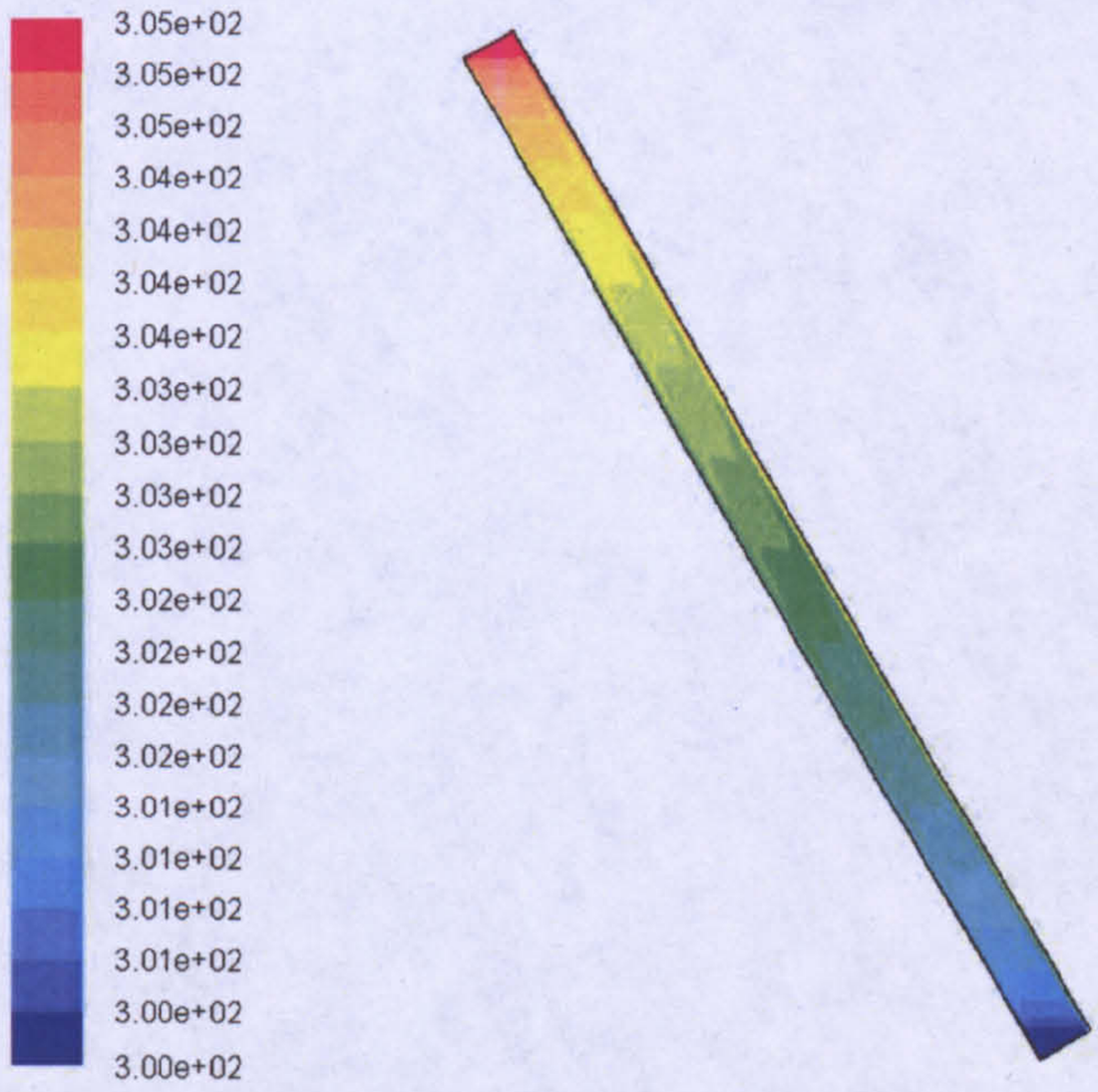

Figure 4.26.j: The contours of temperature at (K) $\phi = 60^{\circ}$

It can be noticed that at $\phi = 0^{\circ}$, there is no movement inside the fluid and hence velocity contours are not evident (fig 4.26.a). The fluid momentum, particularly the velocity magnitude can be noticed to be increasing with the increase in tilt angle (fig 4.26.b-4.26.e). The temperature profile varies but only slightly. This has been more clearly shown in fig 4.26.k.

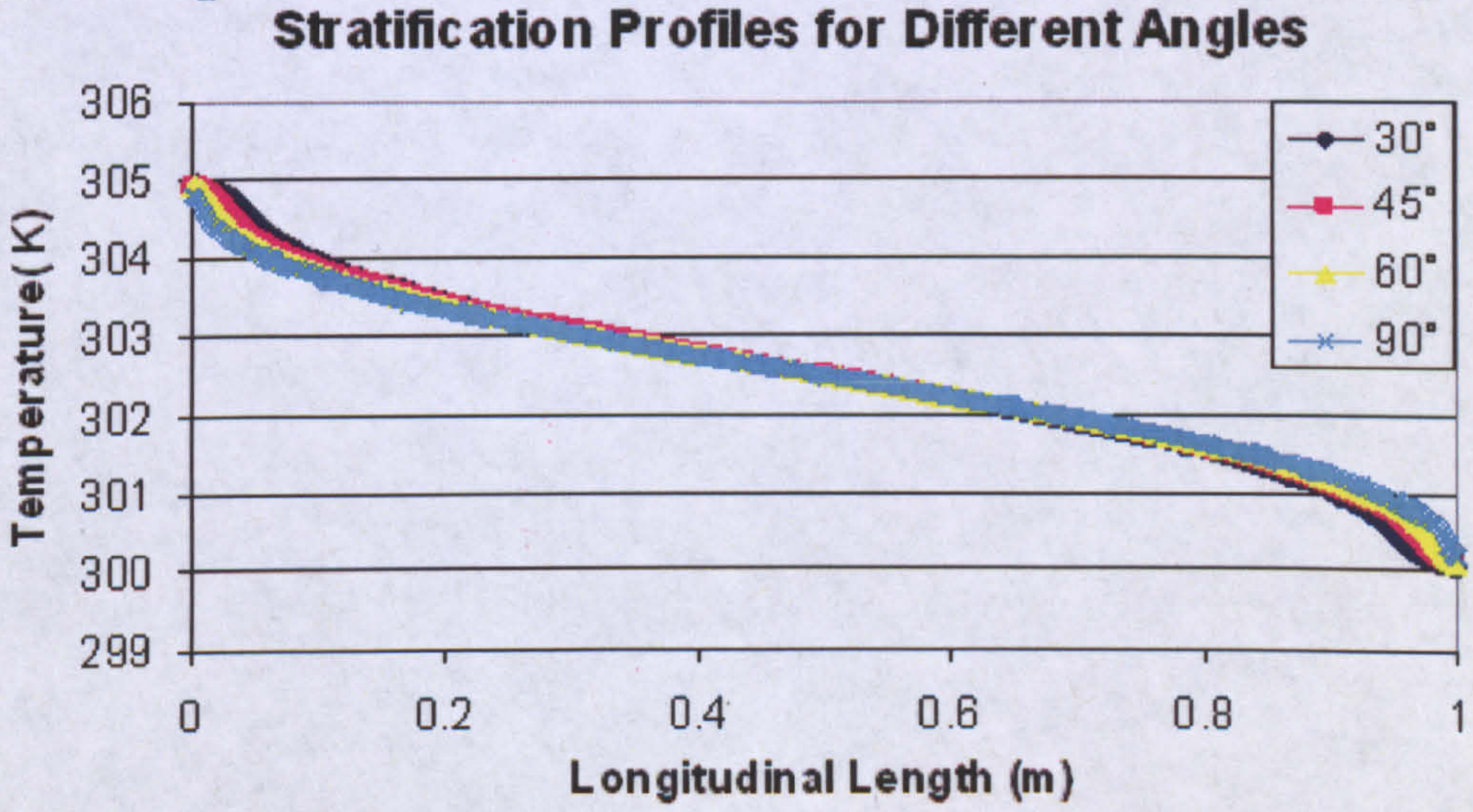

Figure 4.26.k: 2D CFD Stratification profiles for different angles

4.3.2.3 CFD Analysis of the Finned Cavity

CFD for the finned heater is essentially a 3D problem the analysis of which revealed the presence of additional of boundary layers (thermal and velocity) on the surface of the fins. It was also noticed that fins transport the heat to the bottom cooler parts of the heater. The fig 4.27.a shows the two planes on which the results were observed. The contours of velocity along the plane-A are shown in fig 4.27.b. It highlights the velocity to increase with the longitudinal length (along positive Y axis) and then decrease as it nears to top end of the water tank (maximum velocity of 7.91 mm/sec can be noticed). It should be noted that the following results are only for $\phi = 45°$.

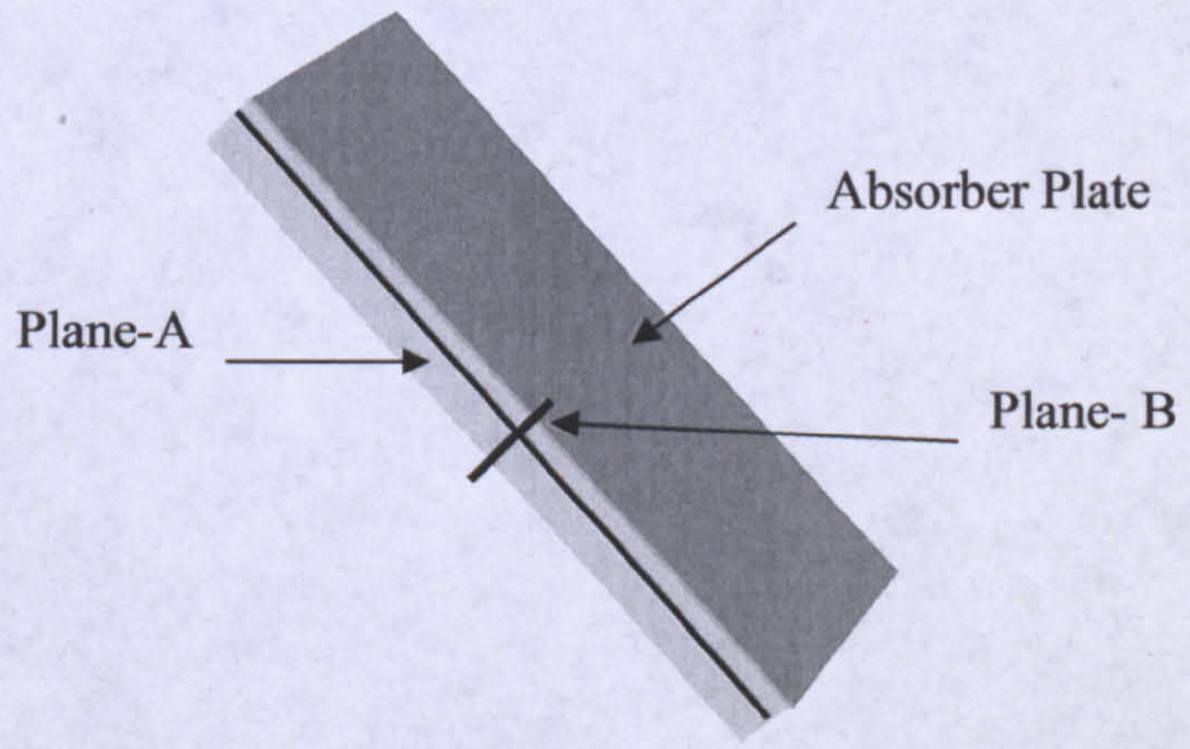

Figure 4.27.a: The planes inside the water tank for viewing CFD results ($\phi = 45°$)

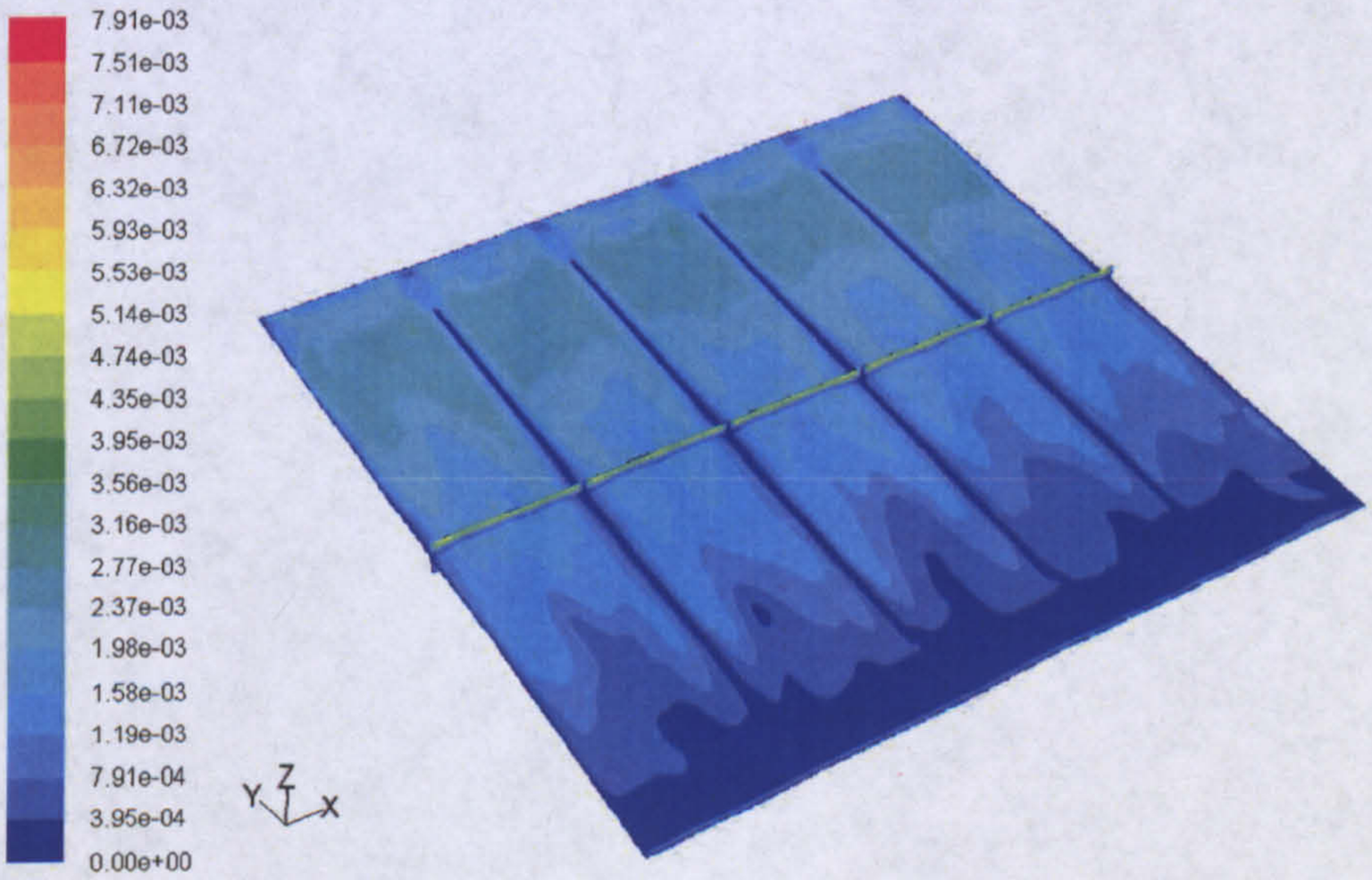

Figure 4.27.b: The contours of velocity on Plane-A at 300 sec

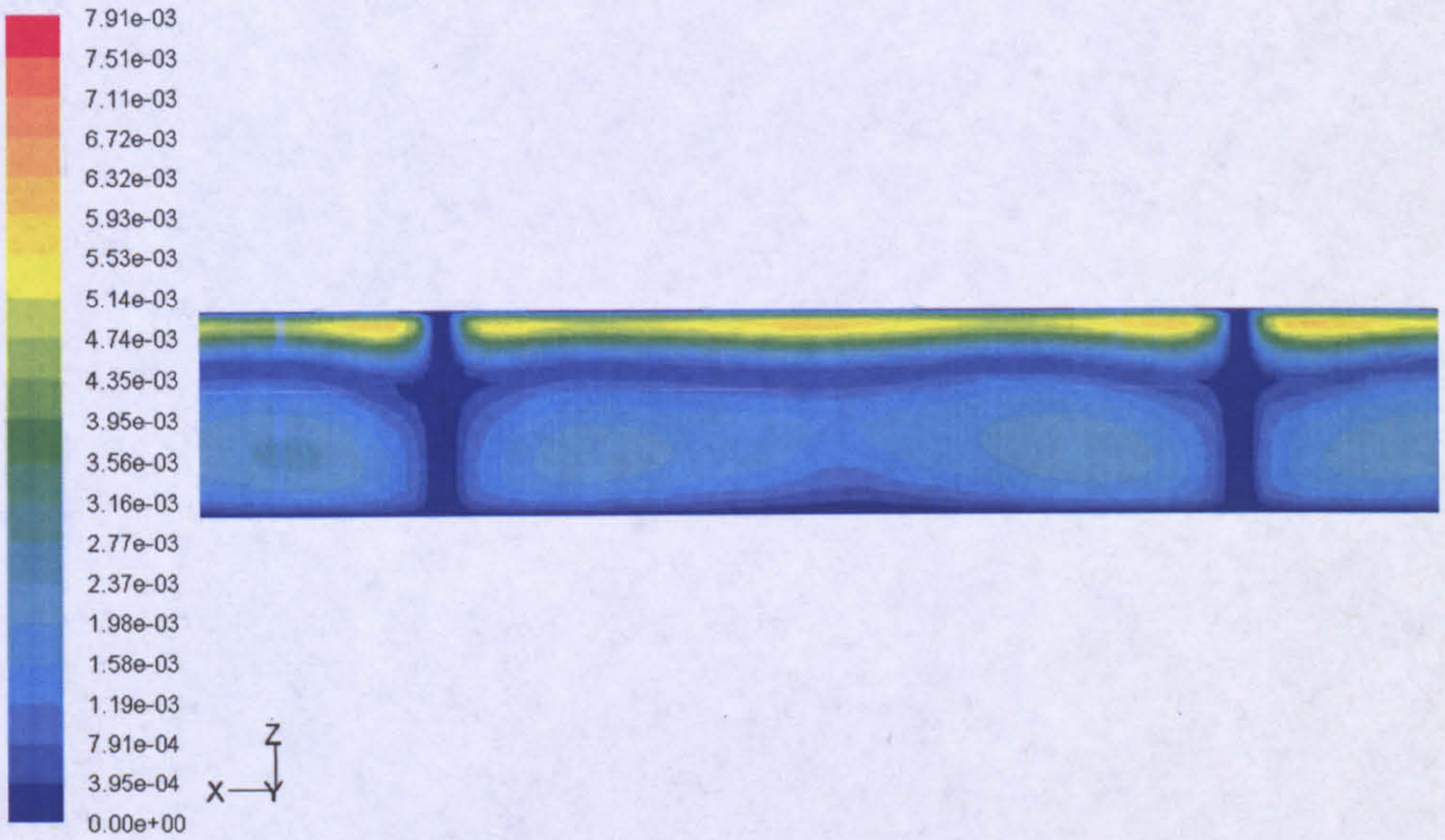

Figure 4.27.c: The contours of velocity in between two fins on Plane-B at 300 sec

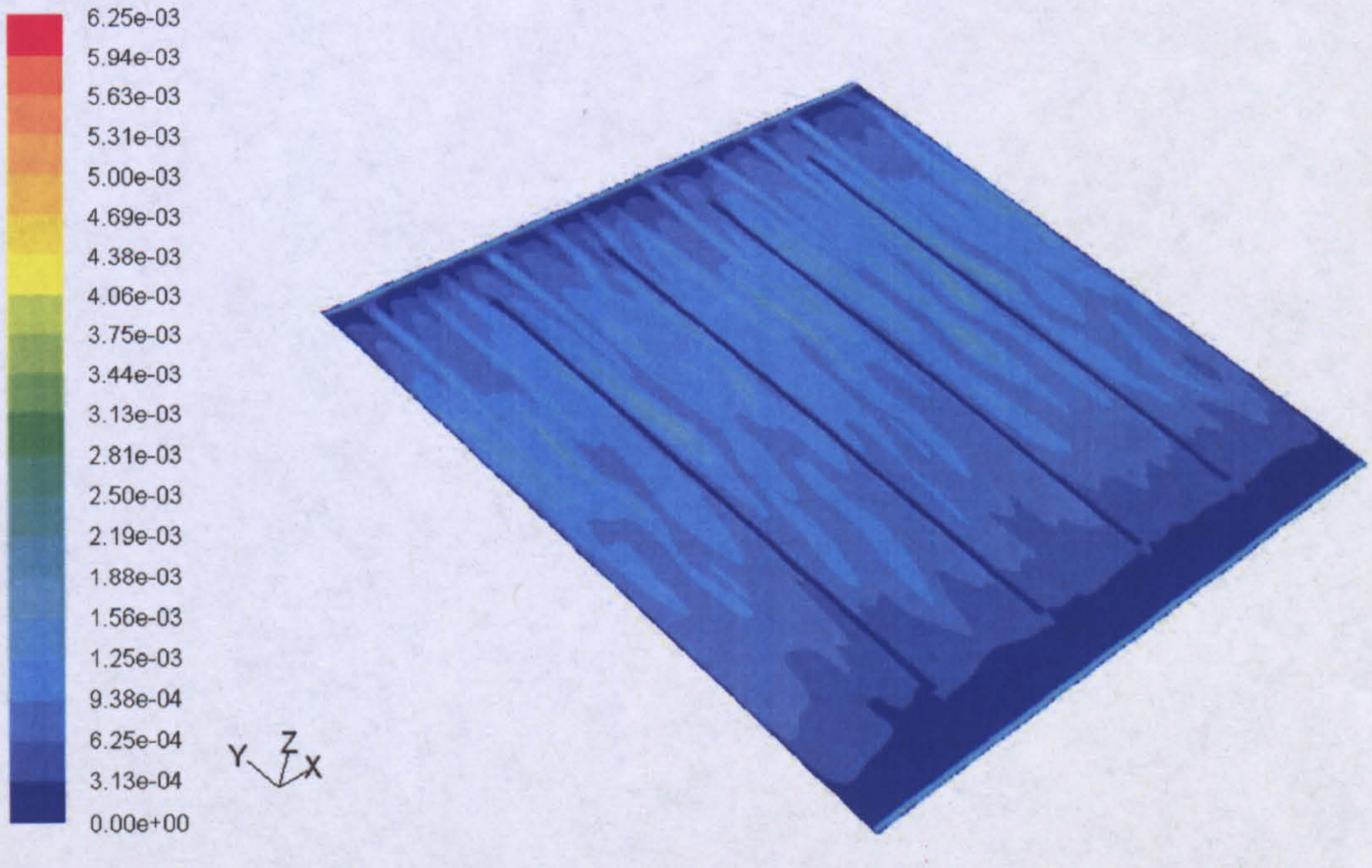

Figure 4.27.d: The contours of velocity on a Plane- A at 600 sec

Fig 4.27.d shows a drop in overall velocity magnitude for 10 minutes as compared to 5 minutes. Similarly the bulk fluid movement further drops with the passage of time as depicted in fig 4.27.e which shows a maximum velocity of 4.7 mm/sec at 20 minutes. For a time period of 60 minutes the velocity further drops (1.35 mm/sec) indicating diffusion taking over advection (see 4.27.f).

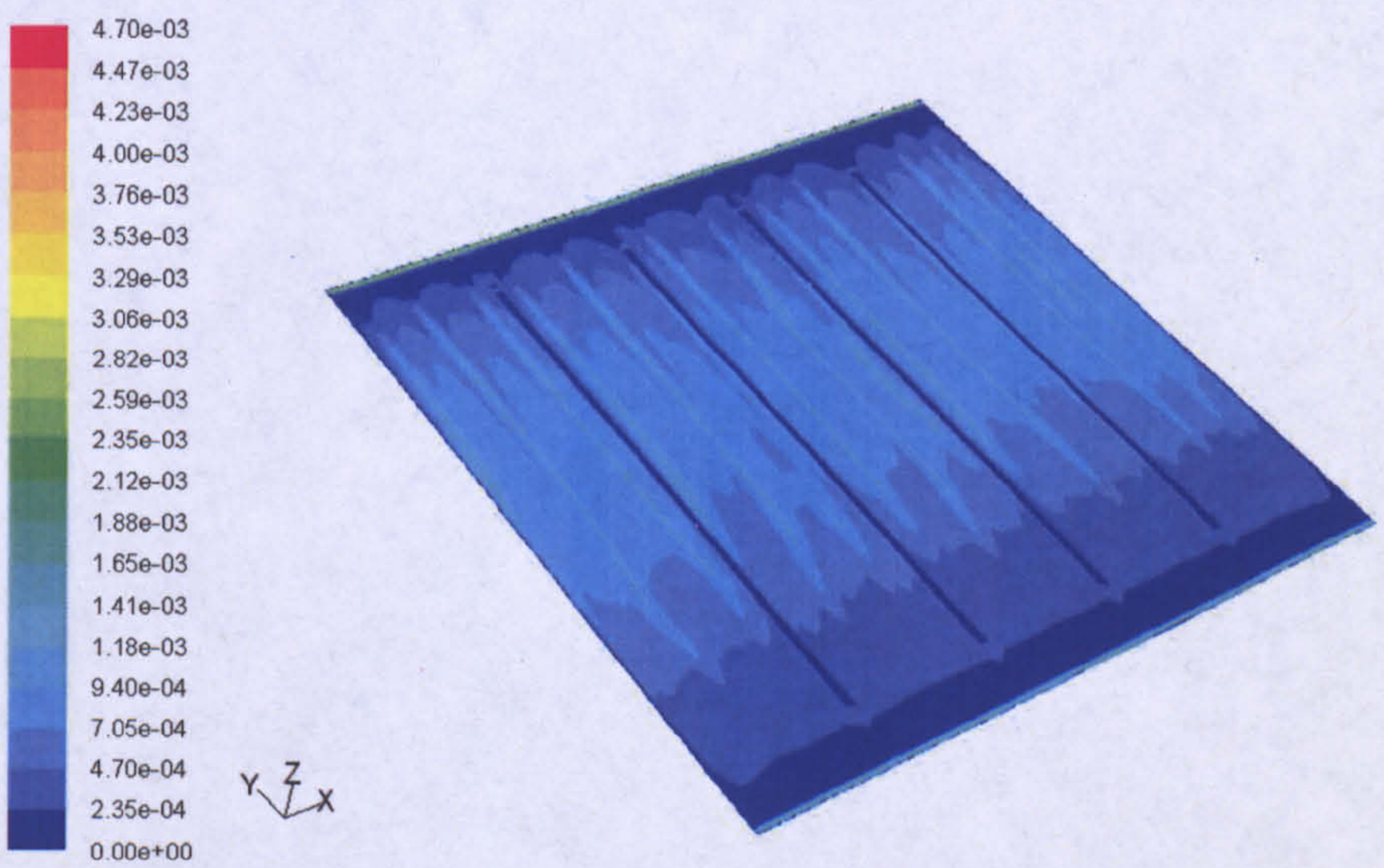

Figure 4.27.e: The contours of velocity on a Plane- A at 1200 sec

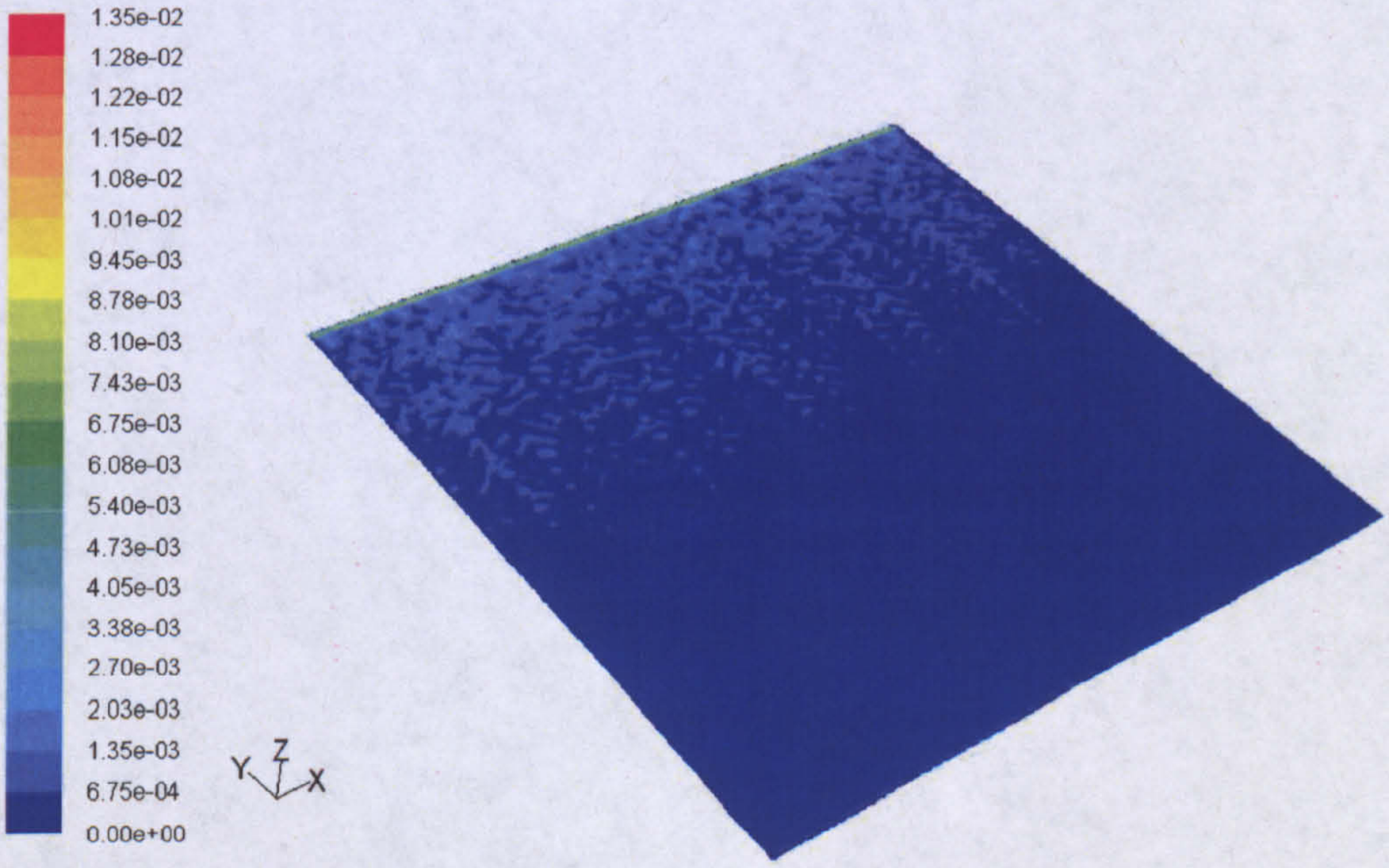

Figure 4.27.f: The contours of velocity on a Plane- A at 3600 sec

4.3.2.4 Conjugate CFD Analysis (Air-Cavity and Water Tank)

Conjugate CFD analysis of the air-cavity and water tank was carried out in 2D to inspect the heat transfer from the absorber plate. A five region mesh (fig 4.28.a) was employed for this purpose which included 2 solid regions modelling the absorber plate, the cover and three fluid regions modelling the water inside the tank, the air in the air cavity and the ambient air in contact with the cover. The collector was set to a tilt angle of 45°.

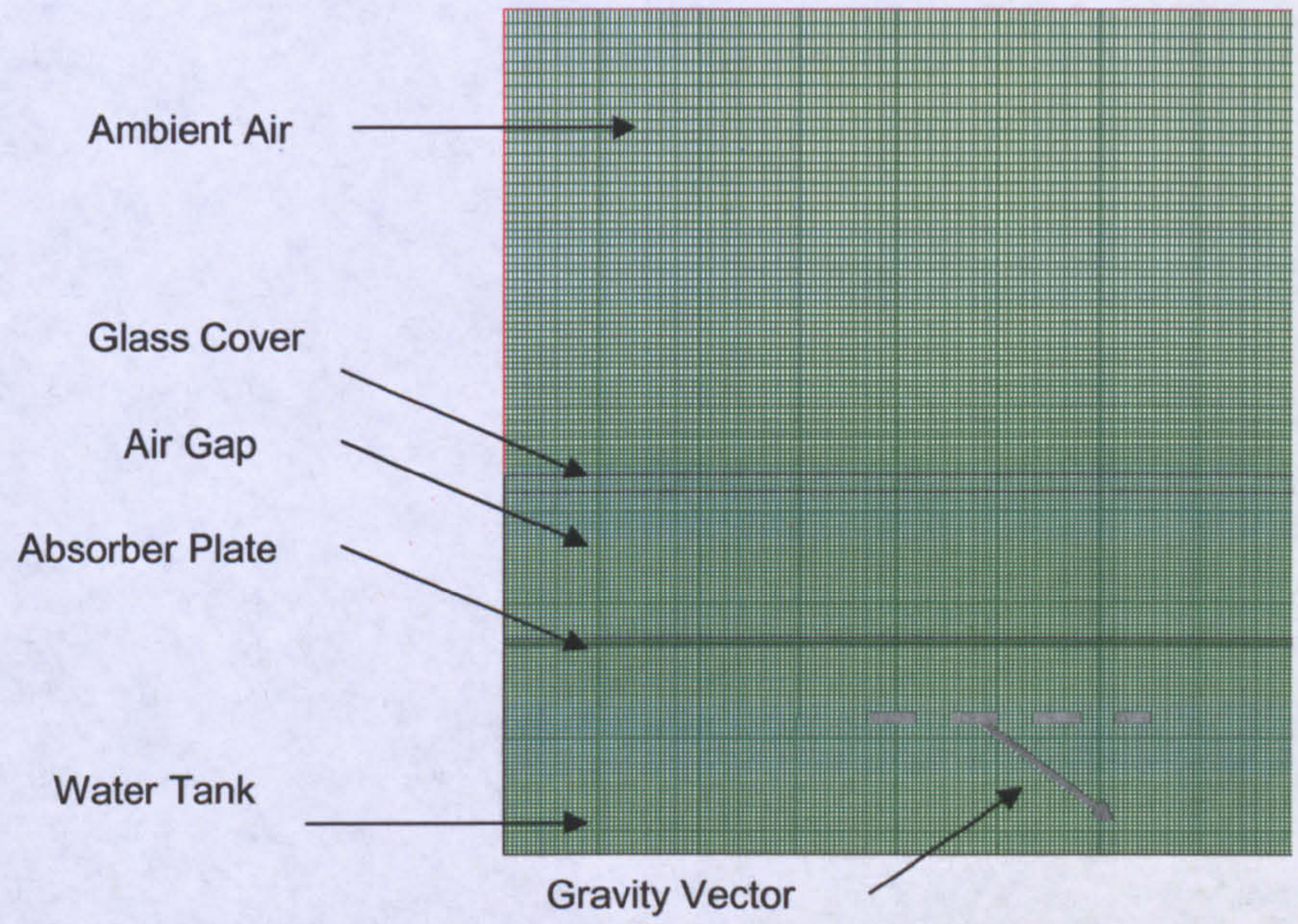

Figure 4.28.a: The 5 region mesh for conjugate analysis

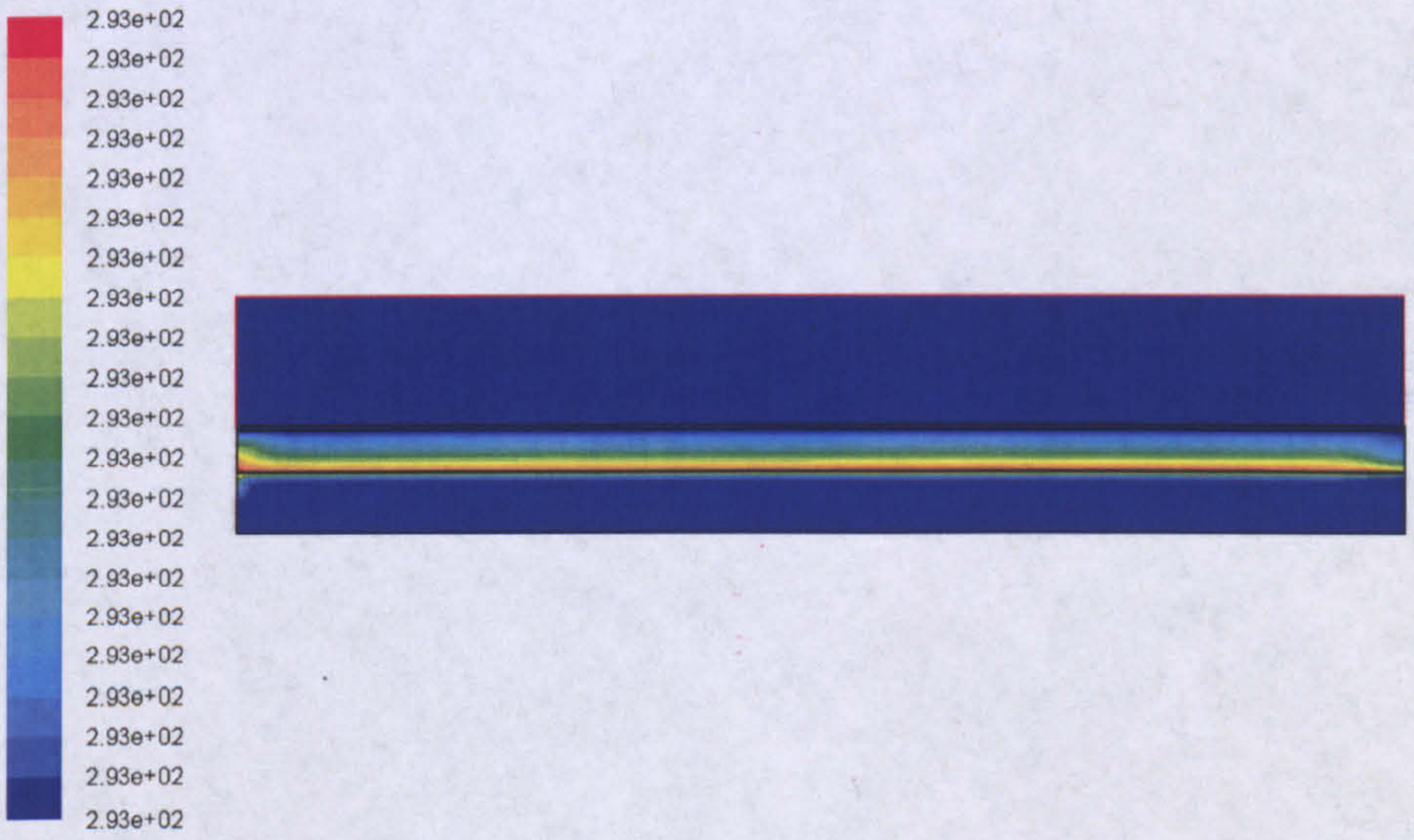

Figure 4.28.b: Contours of temperature (K) after 1 minute

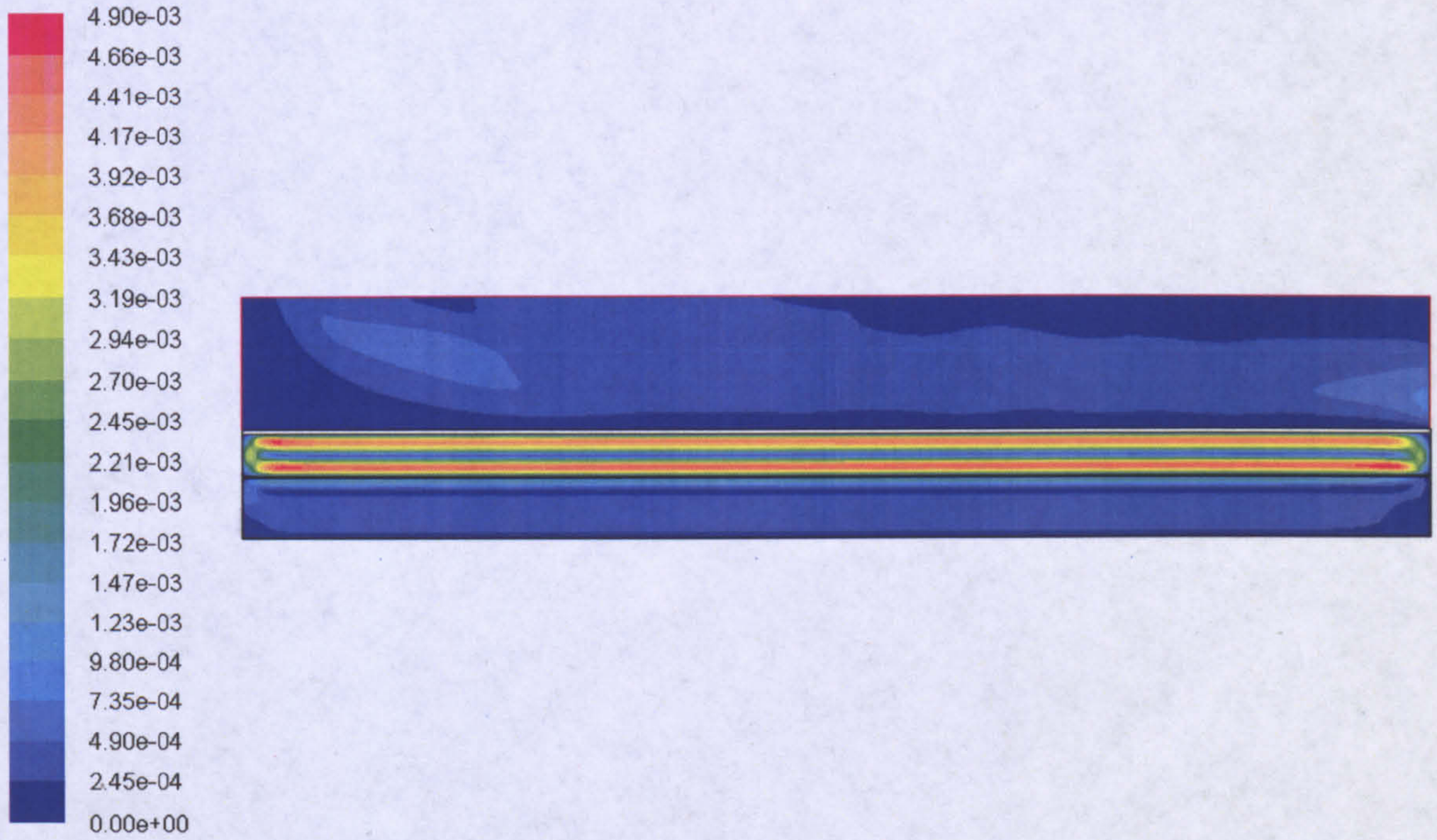

Figure 4.28.c: Contours of velocity (m/s) after 1 minute

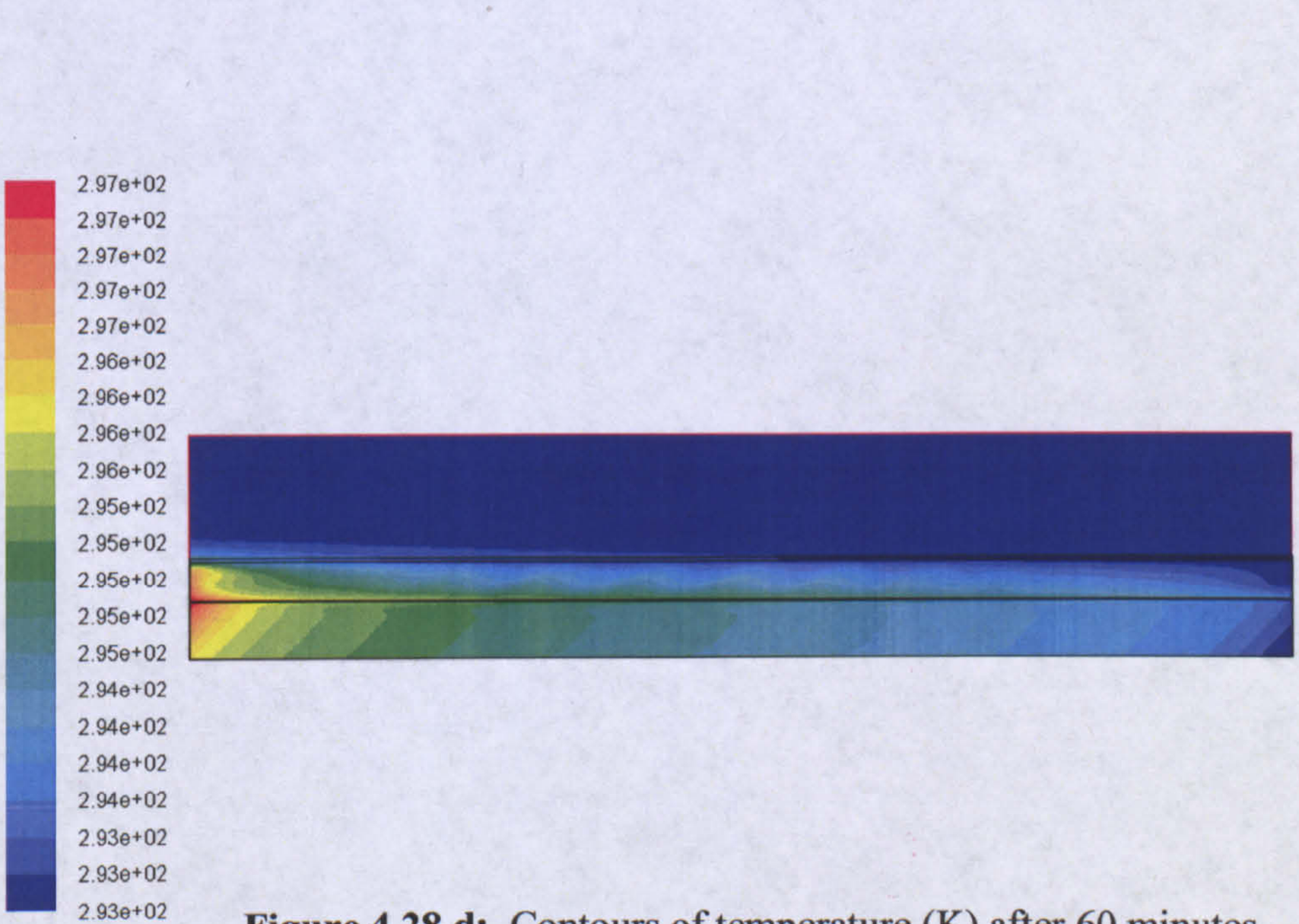

Figure 4.28.d: Contours of temperature (K) after 60 minutes

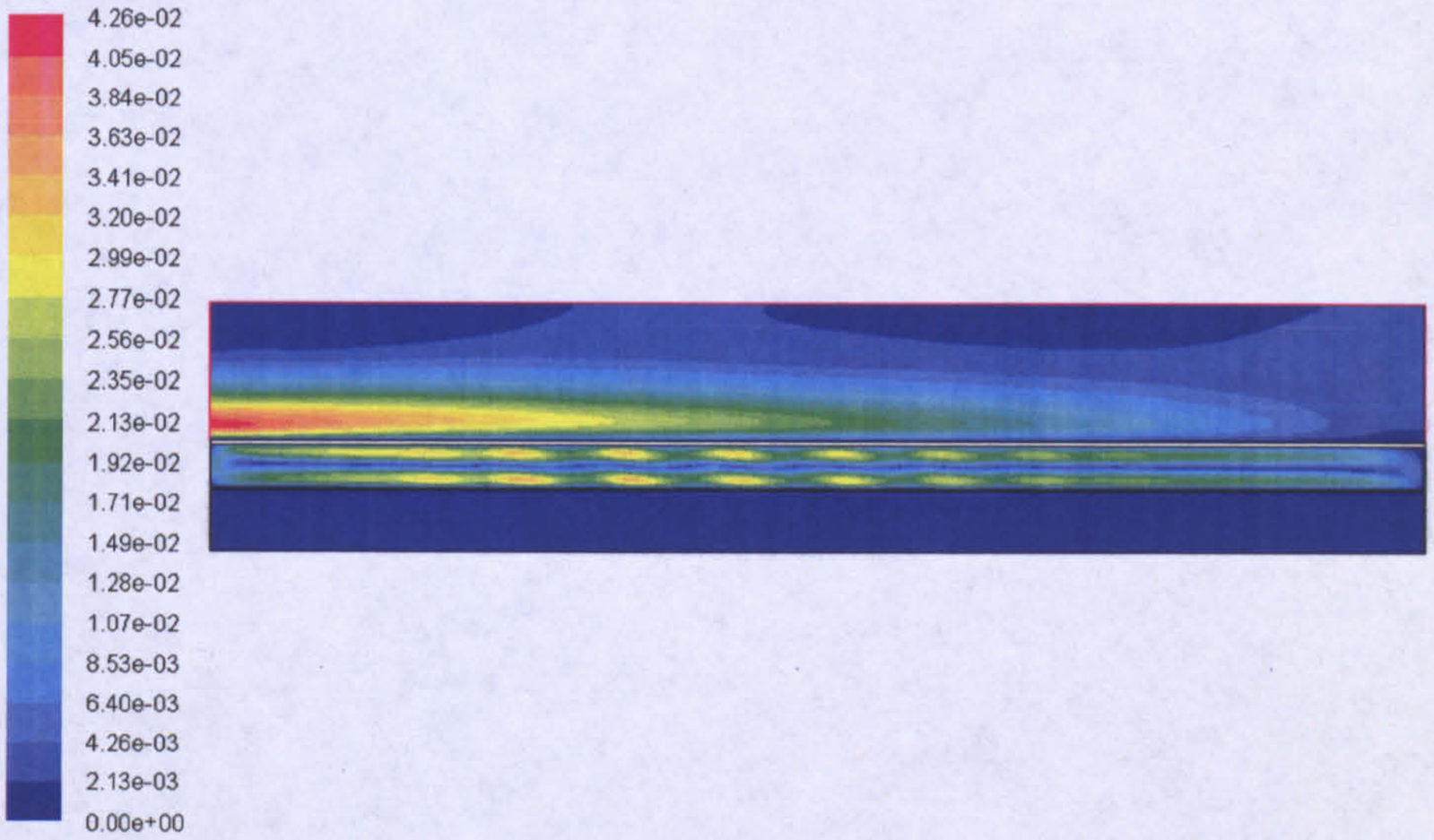

Figure 4.28.e: Contours of velocity (m/s) after 60 minutes

It was ascertained through CFD analysis that:

- The overall velocity inside the system increases (thus an increase Peclet number) with time till it reaches a peak value thereafter it decreases. This pattern in the velocity magnitude reflects in the efficiency curve which follows a similar trend. The efficiency curve and the graph for Peclet number (Pe) are compared (see fig. 4.29.a and fig 4.29.b).

- Fins are responsible for the increased advection inside the collector.

- The accumulation of hot water at the top of the tank reduces the velocity boundary layer and the overall Peclet number is decreased with time.

- After the initial capacitance effects are over, advection takes over diffusion as the major mode of bulk heat transfer. However, accumulation of hot water at the top results in the decline in advection, and diffusion again is the major mode.

- The top portion of the glass cover loses significantly more heat than the bottom.

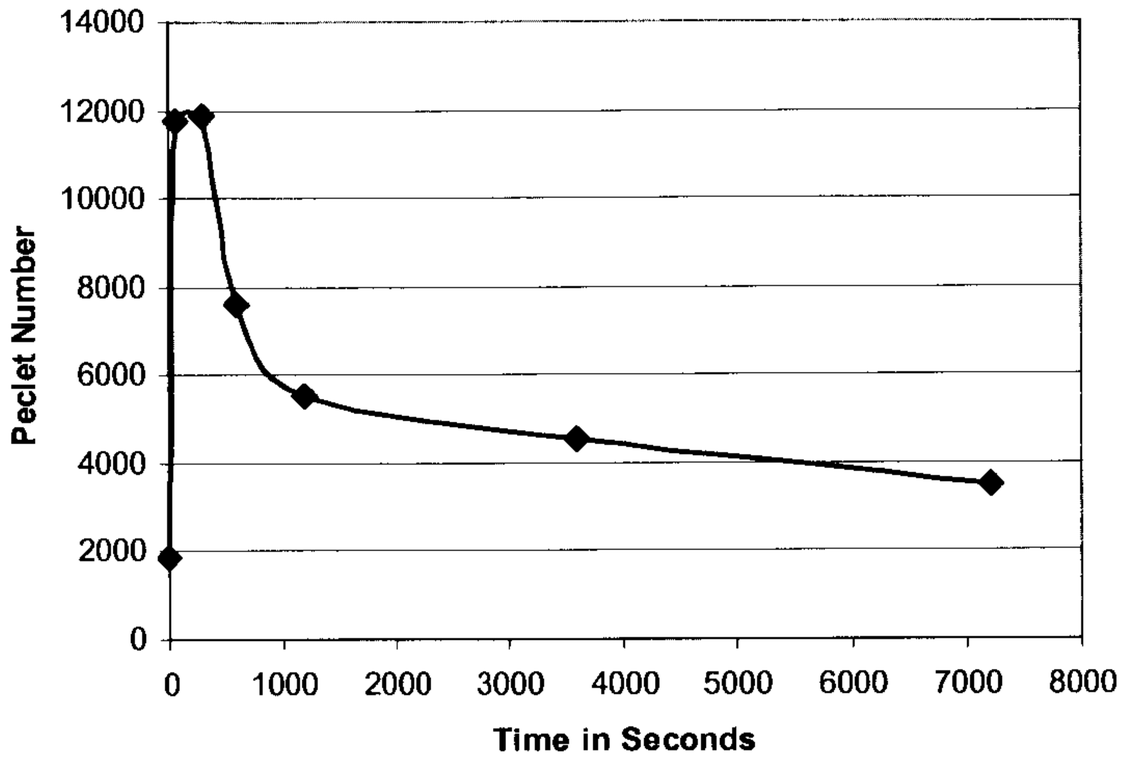

Figure 4.29.a: Peclet Number for 100 W with passage of time

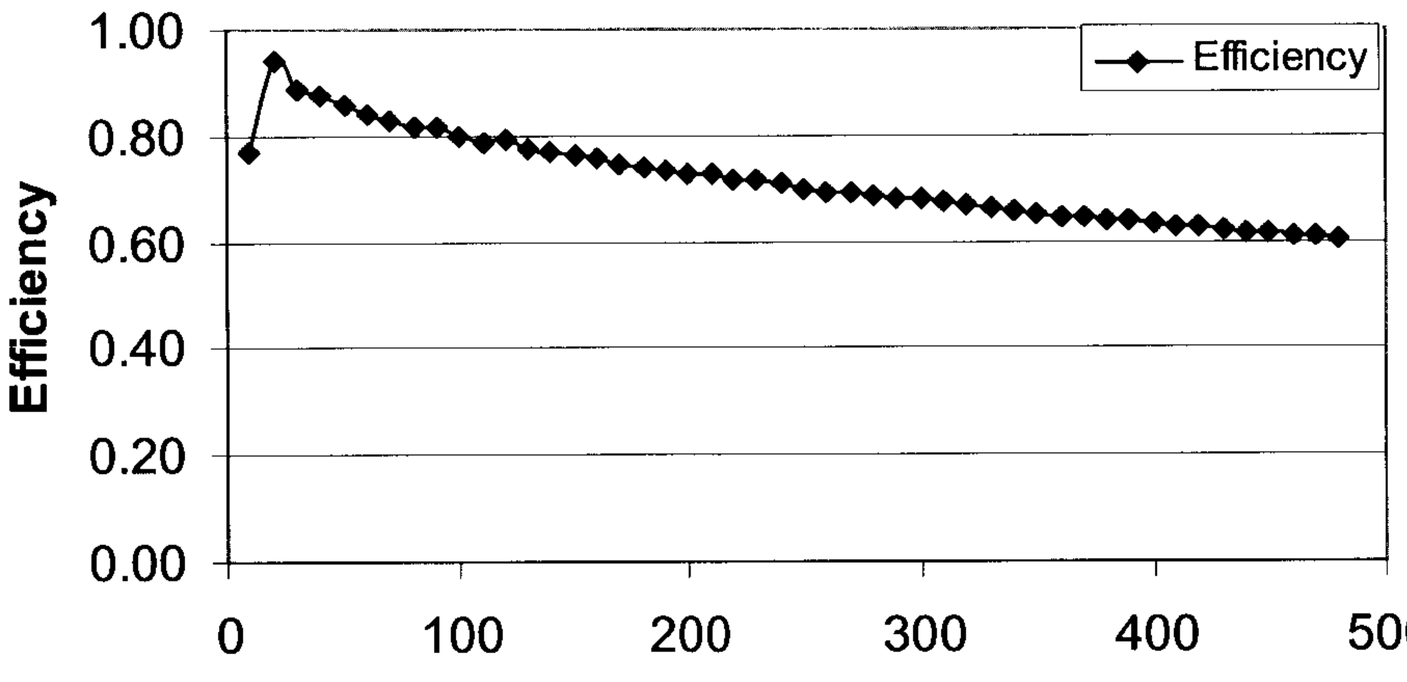

Figure 4.29.b: Typical Efficiency Curve (200W, $\phi = 45^{\circ}$)

4.3.3 Discussion on CFD

As discussed earlier in the text, CFD is prone to numerical errors. The improper domain setup, selection of discretization schemes and inappropriate boundary conditions can further lead to erroneous solution.

The second disadvantage is that although significantly higher details are gathered, a 3D mesh of about 1 million on a PC (1GB RAM, 2.8 MHz) takes about 1200 minutes to compute for 20 minute of chronological advancement in simulation. This figure indicates the heavy computational requirements. The more equations that are solved, the higher

will be the computational time. Nonetheless even with the possibility of these errors & computational requirements, CFD is the only method through which the behaviour of velocity and thermal boundary layers could be studied. Furthermore, once a problem is setup properly it can be used as a template for inspecting different scenarios by changing the BCs.

4.4 Discussion on "U" value

The estimation of U value (heat loss coefficient) brings forward an interesting paradox. It is crucial to assess this parameter for both the finned and the unfinned heaters. Would the U values be same for both the collectors? The heat loss from the collector is understandably not related to the fins inside the heater. It is dependent on the surface area, temperature of the absorber plate, heat content inside the water body and the insulation around the heater. The geometrical factors are identical for both the tested collectors. Therefore it is logical that the "U" value for both the collectors should be the same.

It is interesting here to probe into the question of how the collectors differ? Does the equality of "U" values herein imply the same level of performance if equal insolation is incident on both the heaters? A simple answer to this is "No". This is explained in the following passages.

The U value is generally considered as a constant (or linearly varying) for any collector for a certain range of operating temperatures. In practice however this is not the case and it follows an asymptotic curve when plotted against the plate temperature. However for the sake of explanation, if the U value is assumed to be a constant and "G_{in}" is the level of incident energy, the useful heat content of the heater is given by the following expression (useful heat is the energy absorbed by the collector).

$$Q_{useful} = G_{in} - U(T_w - T_a)\tau \qquad (4.21)$$

If "U" is the same for both the collectors then equation 4.21 would predict equal level of performance for both finned and unfinned collectors, which contradicts the experimental results. In order to better explain this complexity, three modes of collector operations are explained as follows.

Cooling mode: when there is no exposed irradiance (or heat flux in the case of laboratory experiments) on the collector and hence no addition of useful energy to the water. The collector is only losing energy at this point and the useful heat gain is zero.

Charging mode: When the collector is exposed to irradiance and the temperature change of water with time is high ($\frac{\Delta T}{\Delta \tau} > 0.0005$). More explicitly the differential change in the change in temperature $\frac{\partial \Delta T}{\partial \tau}$ is a non zero value.

Stagnation mode: The stagnation mode has already been defined in section 4.1.2.1, the term refers to the situation when the temperature rise in the collector is either very low or almost non -existent. i.e. the collector is exposed to insolation but almost all of it is being lost to the ambient.

Although the collectors (finned and non-finned) would perform the same when they are in the cooling mode i.e. they will lose heat at the same rate, when the collectors are charging, the finned heater would have a lower U value as compared to the unfinned heater. This is because a greater portion of insolation "G_{in}" absorbed would go to the water body inside the collector.

For the stagnation mode, the U values for both the heaters again will be the same.

The U value for the finned collector during the charging mode can be given as

$$U_{ch-f} = U_{ch-uf} - A_f \tag{4.22}$$

Where,

U_{ch-f} is the U value for the finned collector during the charging mode.

U_{ch-uf} is the U value of unfinned collector during the charging mode.

A_f is the fin advantage (W/K) i.e. it represents the extra amount of energy per degree temperature absorbed by the finned collector compared to unfinned collector.

In figs 4.30 the U value for the cooling mode ($U_{cooling}$) for the finned collector has been presented while $U_{ch\text{-}f}$,$U_{ch\text{-}uf}$ and A_f are elucidated later.

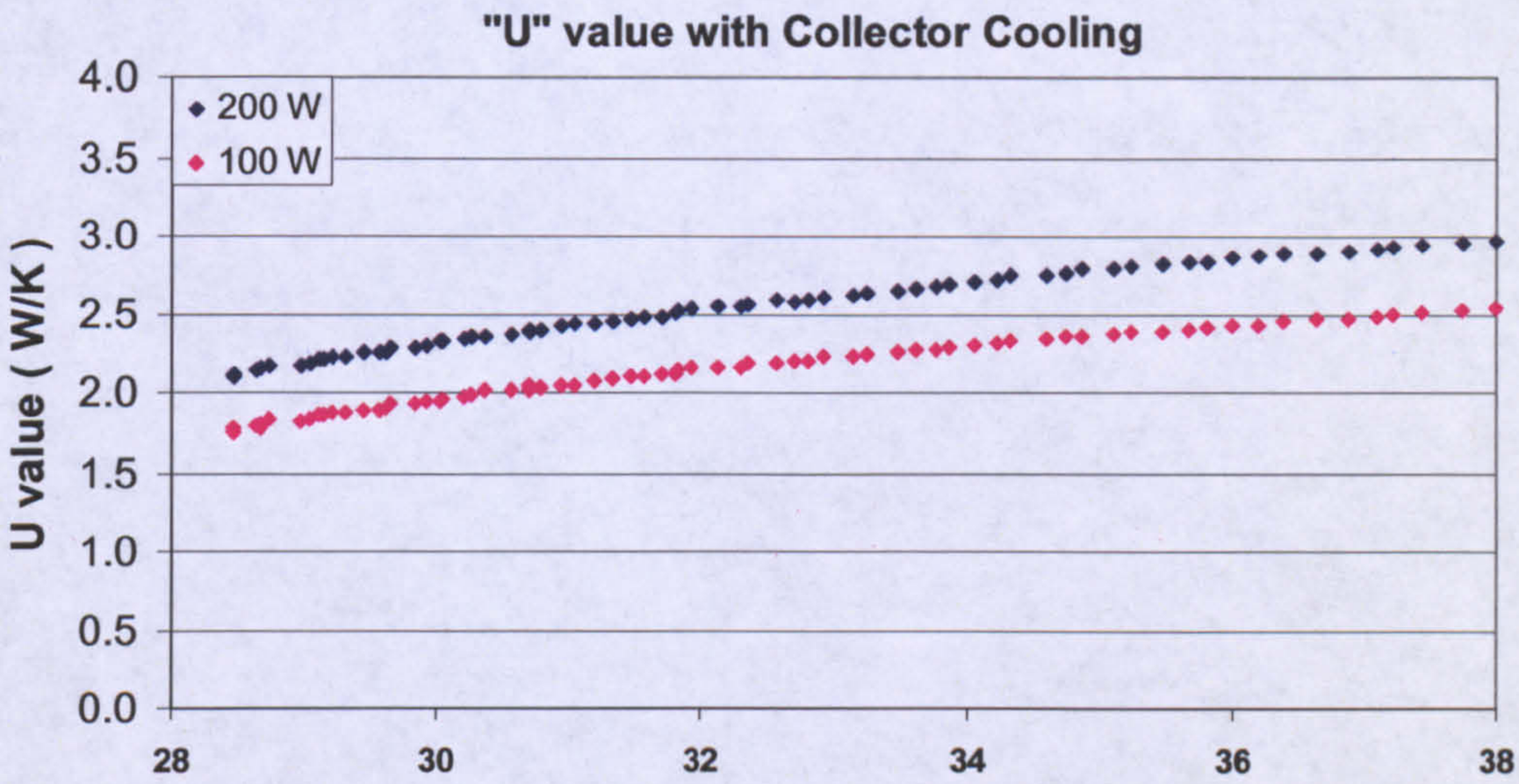

Figure 4.30: $U_{cooling}$ value plotted against the plate temperature for 100W & 200W

The U-value is plotted for the collector after removing the imposed heat flux of 100 W and 200 W in fig 4.30. It is apparent that the U value drops with time moreover, it can also be noticed that the "U" values are different for 100 W and 200 W owing to different energy content. This has been explained in more detail in the following passages.

For every collector, the U value is never a constant value and varies with the absorber plate temperature. Hence a more appropriate observation would be to check the variation of "U" with the absorber plate temperature. As a heating pad was used for heating up the absorber plate which in field test would not have been present, the resulting U values are an underestimate. Fig 4.31 shows the variation of "U" with the absorber plate temperature.

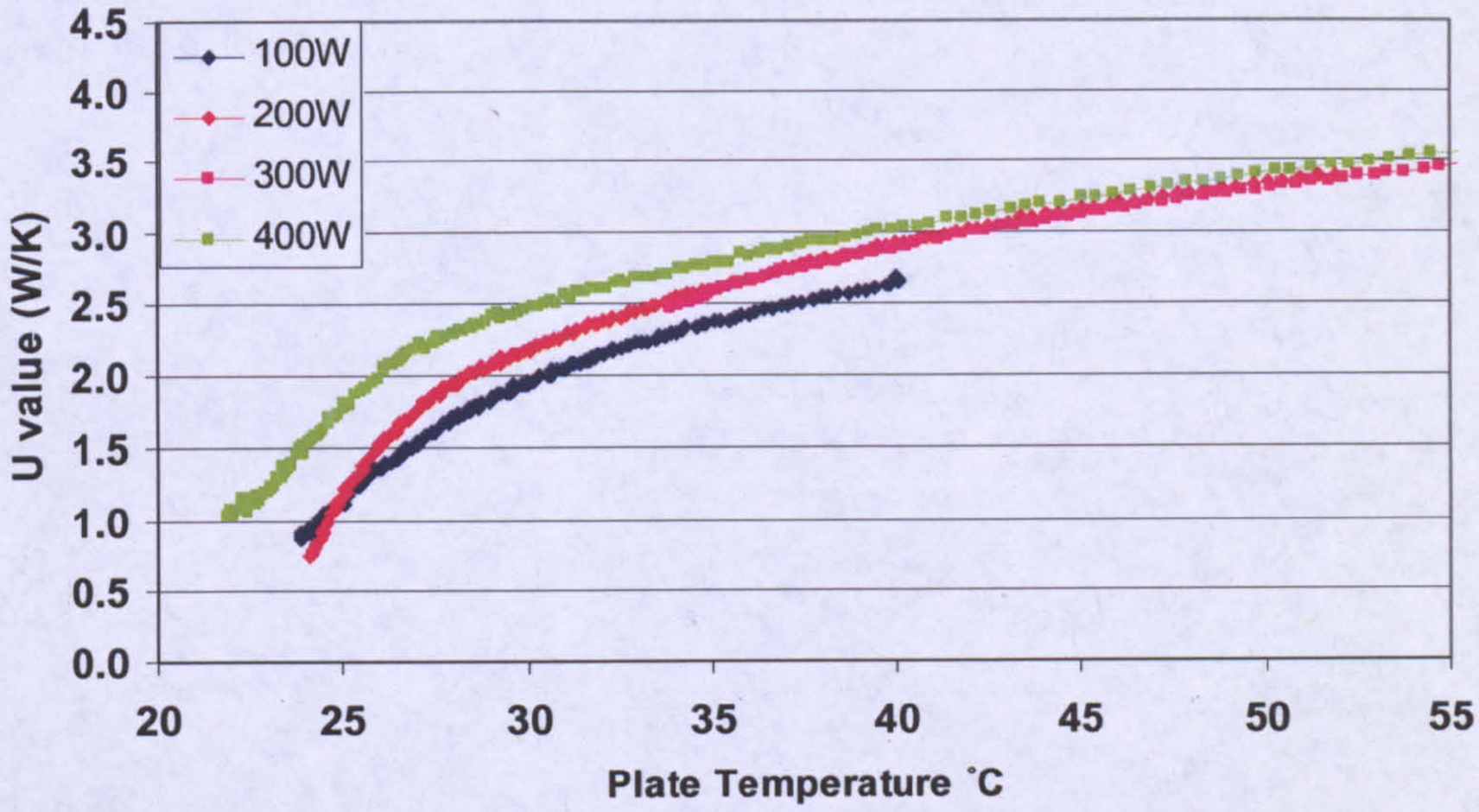

Figure 4.31: U value plotted against absorber plate temperature

As can be noticed from fig 4.31, apart from the variation of "U" between temperatures between 24°C to 28°C, there is a linear rise in "U" as expected, Where U was estimated by the following relationship.

$$U = \ln(T_p - T_a)$$

It is also appropriate to mention at this point that the heat flux (100 W, 200 W, 300 W and 400 W) shown in fig 4.31 are not the imposed level of heat flux. It is rather heat flux that was removed from the collector once it reached stagnation. Hence the depicted values are all $U_{cooling}$

There is a slight difference in the U values, as depicted by the various curves in fig 4.31. This difference can be explained by looking at the level of stratification inside the tank. Assuming 40°C to be the desired temperature, when the collector is imposed to a heat flux of 400W the top section will reach this temperature quicker as compared to 100W. On the other hand, the bottom section will remain at a lower temperature as compared to the collector imposed to 100W. The energy content in the collector is lesser as it is more stratified. On the other hand if the collector is imposed to a heat flux of 100W, the heating is more even which results in lesser temperature difference in top and bottom of

collector (lesser stratification). This is illustrated in fig 4.32. The cooling profile that was used for evaluating the value of "U" was different for each applied heat flux i.e. different sections of the collectors were at different temperatures and this resulted in slightly differing U values.

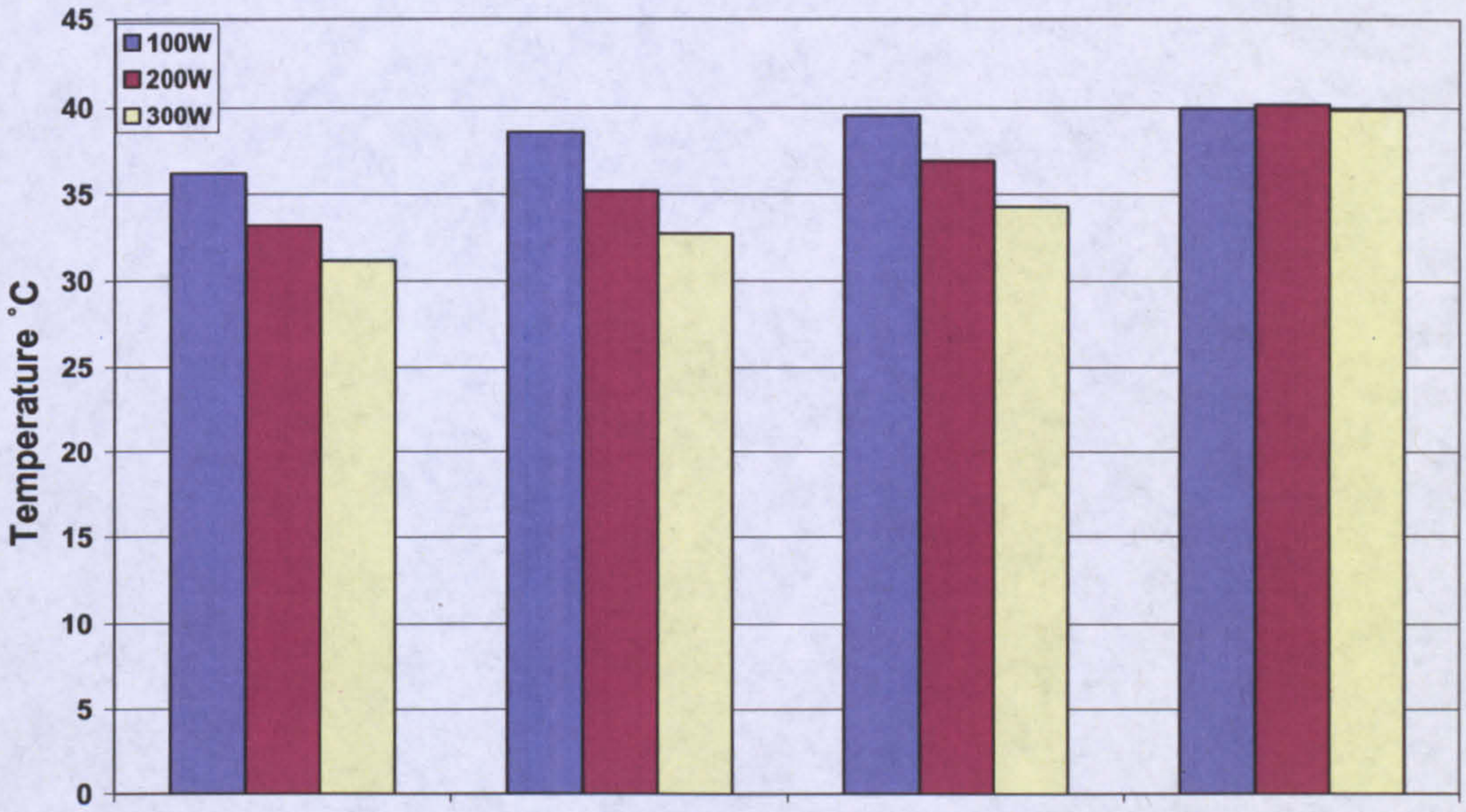

Figure 4.32: The temperatures at 4 sections of the collector for 100 W-300 W.

It is interesting at this point to look into the "U" values for the non-finned collector. In fig 4.33 the U values of the collector are shown. It can be noticed that the trend as well as the values, are very similar.

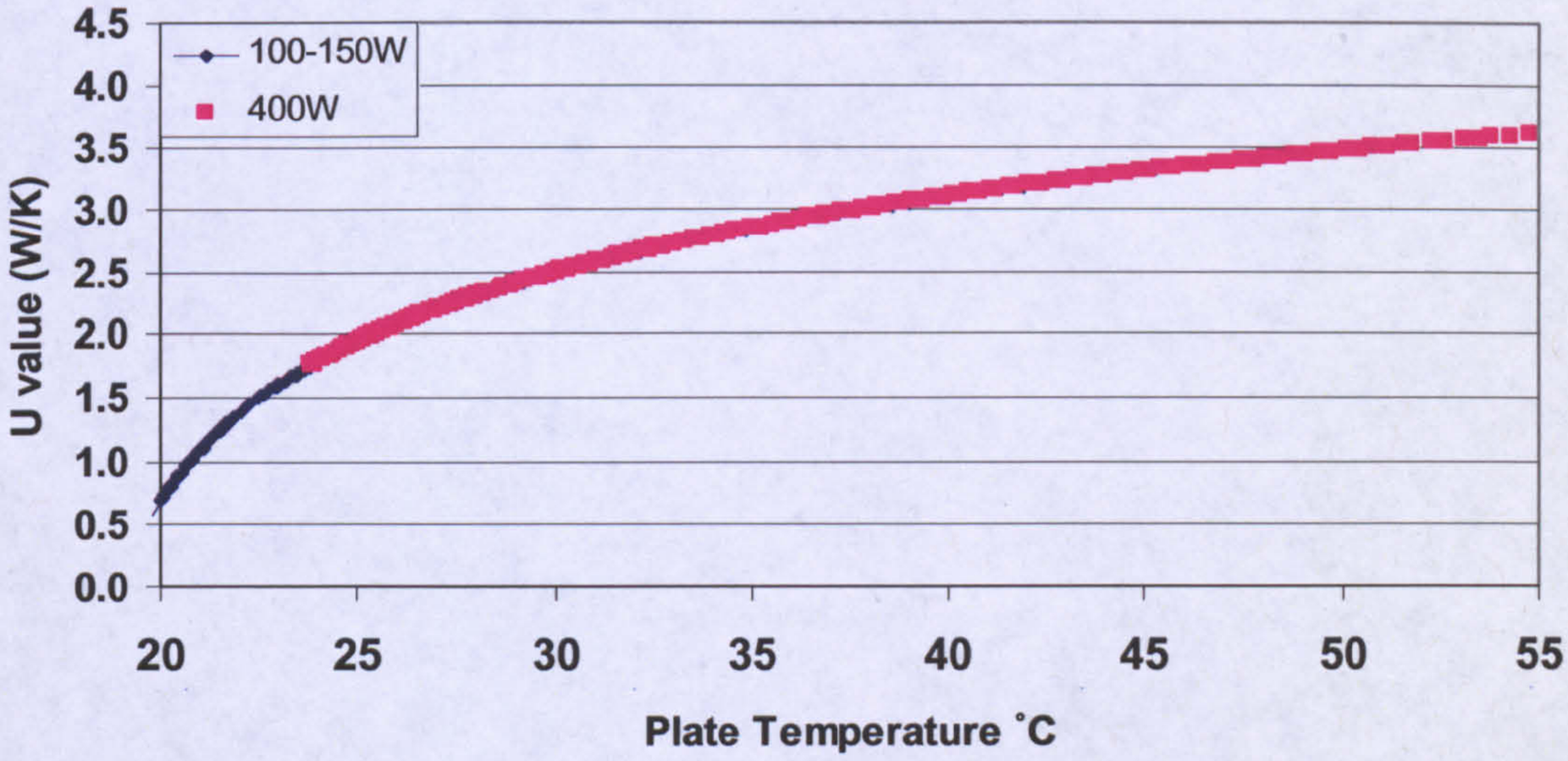

Figure 4.33: The drop in U value plotted against absorber plate temperature.

There is one thing to note though. The use of the rubber pad for heating lowers the value as it acts as an insulator, isolating the absorber plate from the air cavity. In actual the "U" values may reach up to 5 to 6 W/K with the heater operating under 40˚C and would be over 6-7 W/K for temperatures over 40˚C.

The $U_{cooling}$ and $U_{charging}$ for the finned and the unfinned heaters are compared in fig 4.34-35 for two different values of applied heat flux. It can be noticed that the U charging for the unfinned collector is higher than the corresponding value for the finned collector. This is line with the developed expression 4.22. The value for A_F is presented in fig 4.36. The decrease in the fin advantage is logarithmic with the increase in plate temperature.

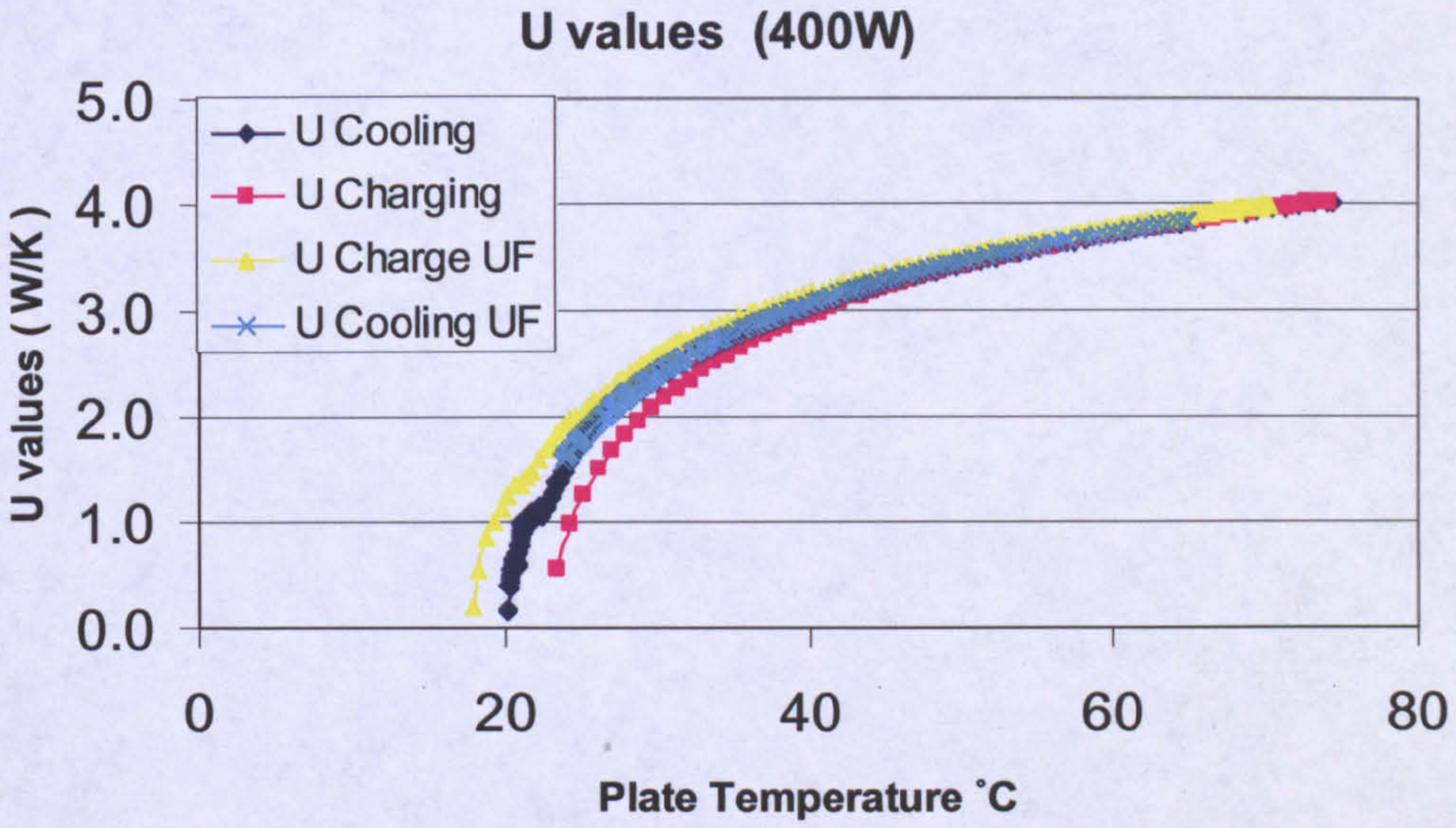

Figure 4.34: $U_{cooling}$ and $U_{charging}$ for 400 W of heat flux on finned and unfinned heater

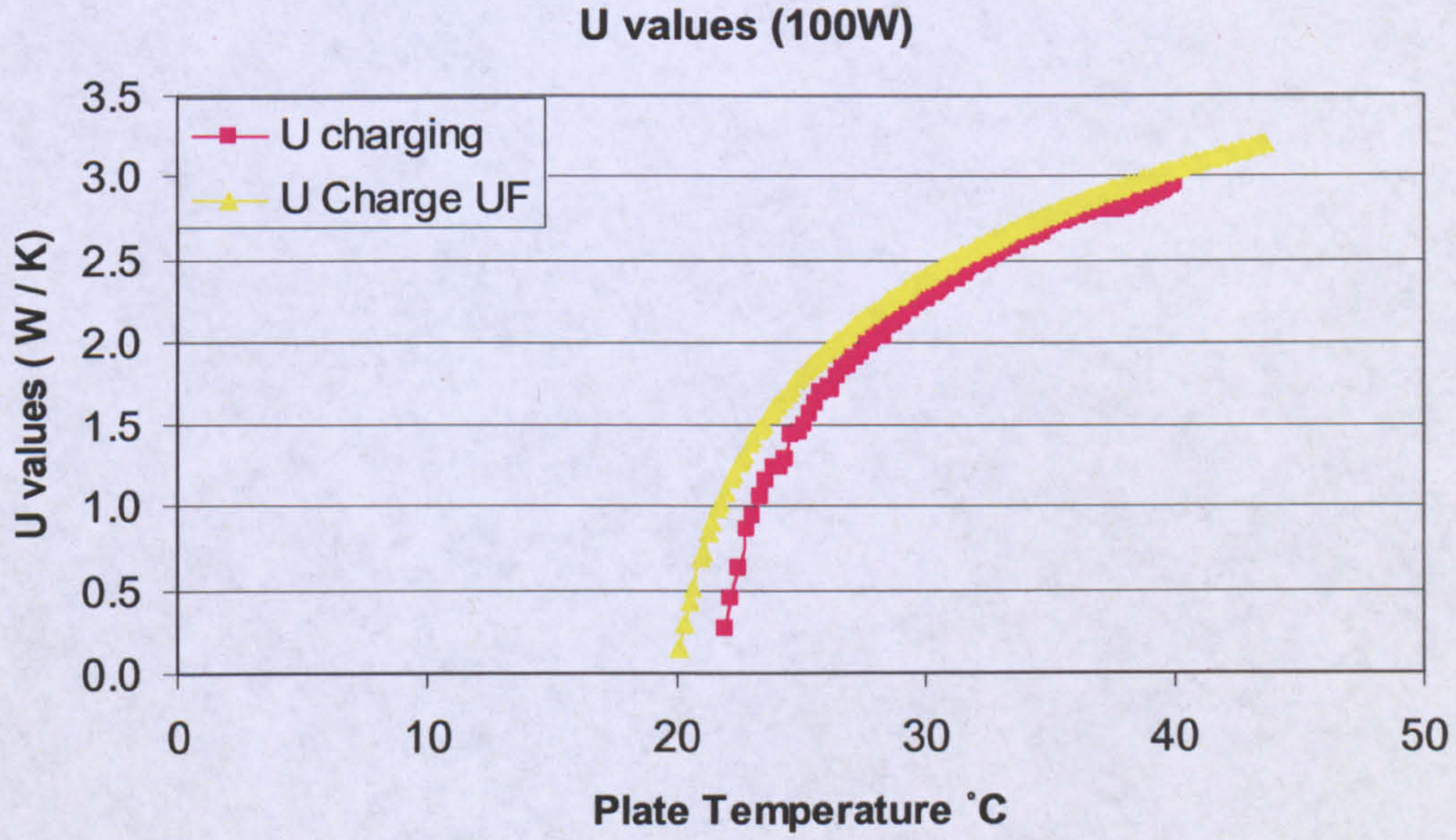

Figure 4.35: $U_{cooling}$ and $U_{charging}$ for 100 W of heat flux on finned and unfinned heater

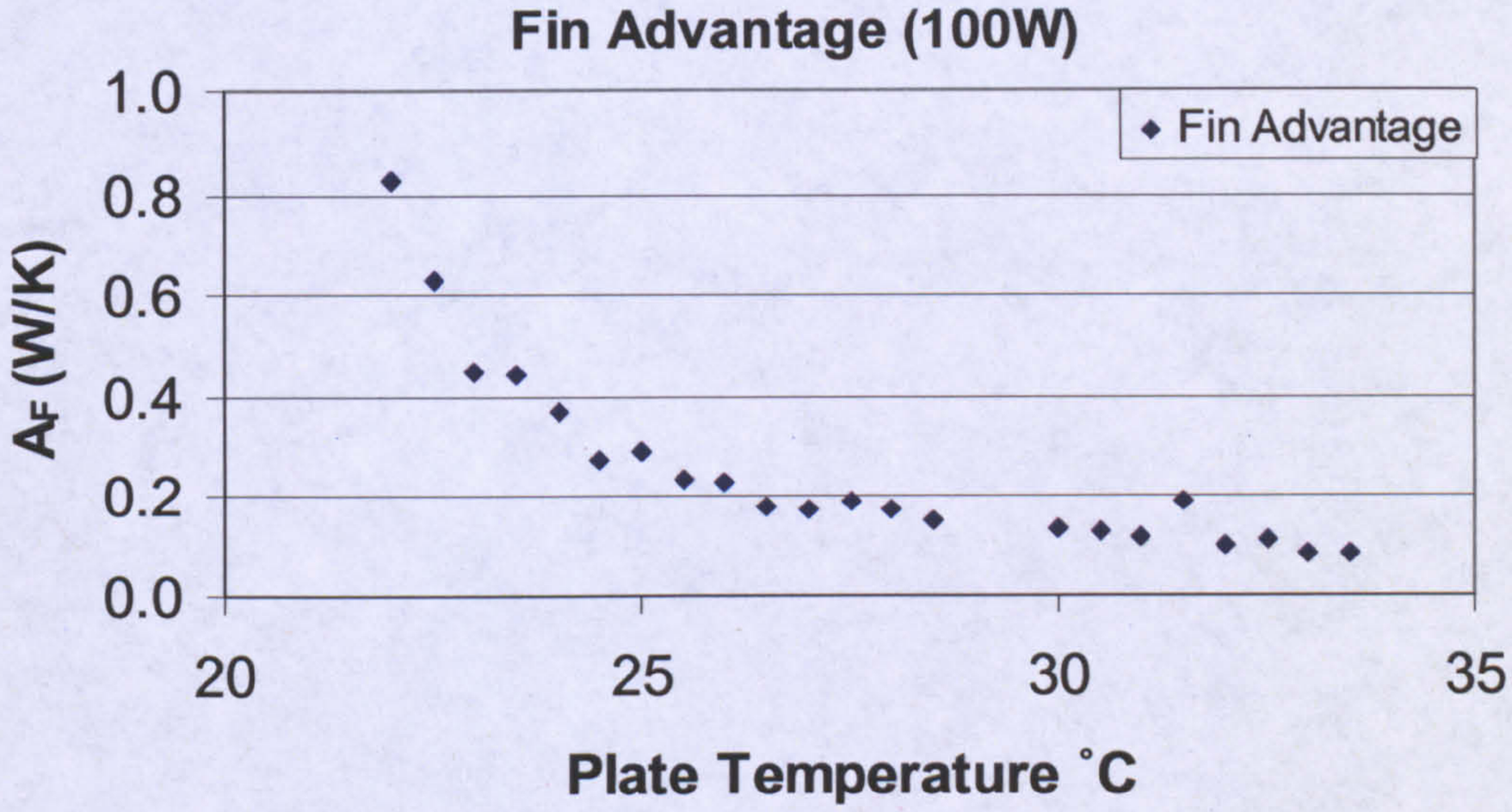

Figure 4.36: A_F for 100W of heat flux

The performance of the finned and unfinned collector is plotted hypothetically in fig 4.37. The collector is charged and then allowed to cool.

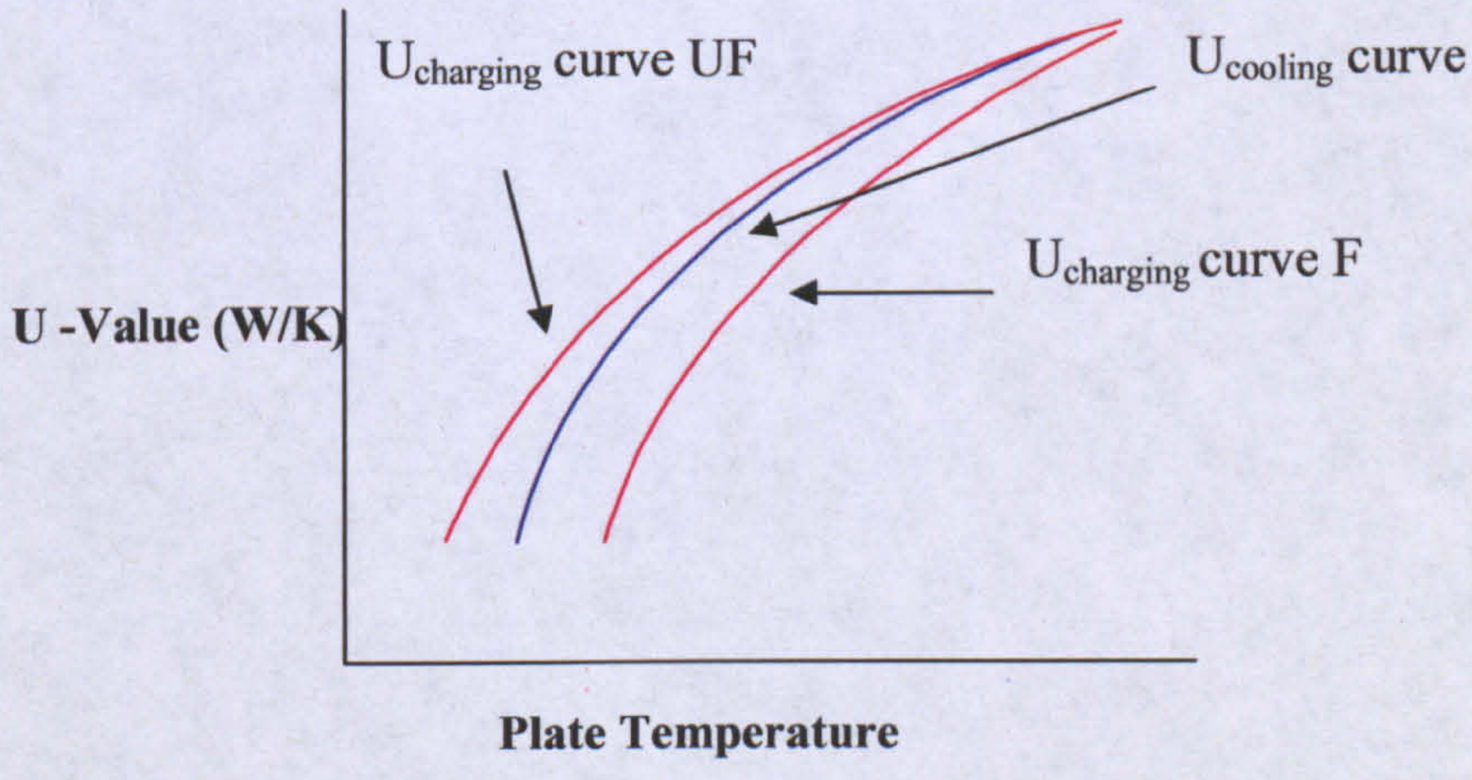

Figure 4.37: Hypothetical description of the $U_{charging}$ and $U_{cooling}$ for finned and unfinned collectors

4.5 Summary

ATA, CFD and Experimental testing were used to evaluate the collector's response to imposed heat flux. The merits and demerits of each method were discussed individually. The efficiency for the finned and the unfinned collectors were noted. The cooling profile and the heating profiles of the collector were analyzed. This leads to the computation of the "U" value that is a key parameter for characterizing the collector behaviour.

It was noted that the increase in temperature for both the finned and the unfinned heater was asymptotic. The rate of increase of the finned heater was higher than the unfinned heater. The reason for this increase, as put forward by CFD, was the formation of a thermal boundary layer and consequently velocity boundary layer on the surface of the fins. The fins also act as a medium to transport heat to the bottom, cooler layers of the heater.

For each value of heat flux, a certain stagnation temperature exists depending upon the ambient temperature e.g. for 100W a stagnation temperature of 40°C was found for unfinned heater and a value of 45°C was found for the finned heater. It was also noted that stagnation was achieved after a period of about 1440 min that corresponds to a period of one day. Practically the exposure of heat flux for such durations is meaningless but in order to evaluate the stagnation temperatures, and gather results that were later to be compared by simulation results, the exercise was imperative.

The use of TIM resulted in more energy retention by the collector.

Stratification inside the water tank increases with the time and the heat flux. The angle of inclination also has a bearing on the stagnation, with increasing angle resulting in an increase of stratification strength.

Good conformance between the results from ATA and experimental measurements was found. This suggests that the mathematical relationships used for the simulation hold. It

also gave an idea of the nature of losses that included both convective and radiative heat losses.

The results from CFD provided a clue to the efficiency behaviour that rises at the start till it reaches a peak value and thereafter decreases gradually. This coincided with the total advection inside the collector that followed a similar pattern.

The results from this chapter have been utilized in chapter 6 for optimizing the collector design.

TEXTBOX 3

U value:

U-Value is the measure of the rate of heat loss through a material, in the current case through the collector. The calculation of U-values can be rather complex - it is measured as the amount of heat lost through a one square meter of the material for every degree difference in temperature between the mean water temperature and the ambient temperature. It is indicated in units of Watts per Meter Squared per Degree Kelvin or W/m^2K. As the absorber plate area for the prototype collectors was 1 m^2, the U-value in this thesis has been presented as W/K.

Optical Efficiency:

The term optical efficiency refers to the ratio of energy received on the collector aperture to the total energy absorbed by the collector. The product of absorptance of the plate and the transmittance of glass ($\tau\alpha$) is a factor that used for calculating optical efficiency. The optical efficiency thus can take lower values if the number of covers is increased, selective is not employed and the incidence angle of insolation is not close to normal to the plane of collector.

Bénard Cells:

Bénard cells are convection cells that appear spontaneously in a liquid layer when heat is applied from below. They can be obtained using a simple experiment first conducted by Henri Bénard, a French physicist, in 1900. Each roll has opposite sense of direction compared to the adjacent cell. The strength of the cells depends upon the Rayleigh number. At very high Rayleigh numbers however, the movement becomes more chaotic indicating turbulence.

References

1. Duffie, J.A. and W.A. Beckman, *Solar Engineering of Thermal Processes*. 2nd Edition ed. October 1991: John Wiley & Sons Canada, Ltd.
2. J.M.S.Cruz, G.P.H.a.A.R., *Buoyancy-Drive Convective Heat Exchange In a Trapezoidal-Shaped Solar Collector/Thermal Store.* Proceedings of the 5th ASME/JSME Joint Thermal Engineering Conf, San Diego, CA, ASME, New York 1999 9pp, 1999: p. 9.
3. Zhai, Z. and Q. Chen, *Numerical determination and treatment of convective heat transfer coefficient in the coupled building energy and CFD simulation.* Building and Environment, 2004. **39**(8): p. 1001-1009.
4. Inc., F., *Fluent 6.2 Documentation,User's Guide 2005*. 2005.
5. Yin, S.H., T.Y.Wung and K. Chen,, *Natural Convection in Air Layer Enclosed within Rectangular Cavities,*. Int. J Heat and Mass Transfer,, 1978. **21**: p. 307 - 315.
6. Fluent Europe Ltd, *Fluent 6.2 Documentation Help*. Fluent User's Guide. 2004.
7. Gill, A.E., *Numerical Boundary Layer Regime for Convection in a Rectangular Cavity*. J. Fluid Mechanics, 1966. **26**: p. 515 -536.
8. Yang, Y., *Laminar natural convective flow in inclined rectangular glazing cavities.* CEERE, University of Massachusetts, Department of Mechanical Engineering and Industrial Engineering, January 2002.

Chapter 5

Flow Considerations

Draw-off, Supply and Connecting Systems

The performance of the collector is dependent not only upon the level of insolation but also on the supply of hot water. An inadequate draw-off pattern could result in dismal collector performance. The various parameters associated with the supply of hot water such as the required quantity of water, flow rates, desired temperature and existing stratification level inside the tank all influence the collector performance and thus cannot be ignored.

In the previous chapters, the focus was kept on the thermal performance of the collector components, whereas this chapter envisions a broader level of functionality. The integration of the collector in the domestic hot water supply system has been investigated herein. It also takes into account the collector performance for various draw-off patterns in search of an optimal draw- off scheme for Scottish conditions. The possibilities of freezing and boiling have also been investigated.

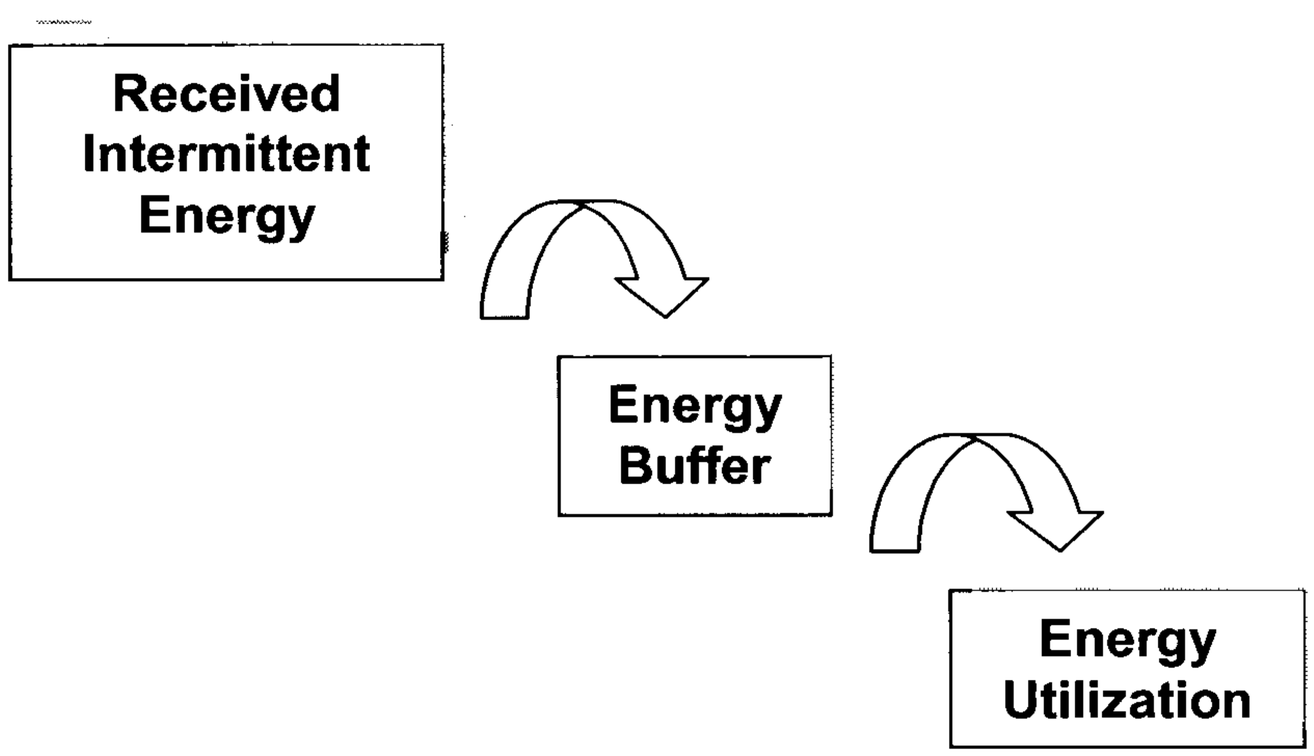

Chapter Map

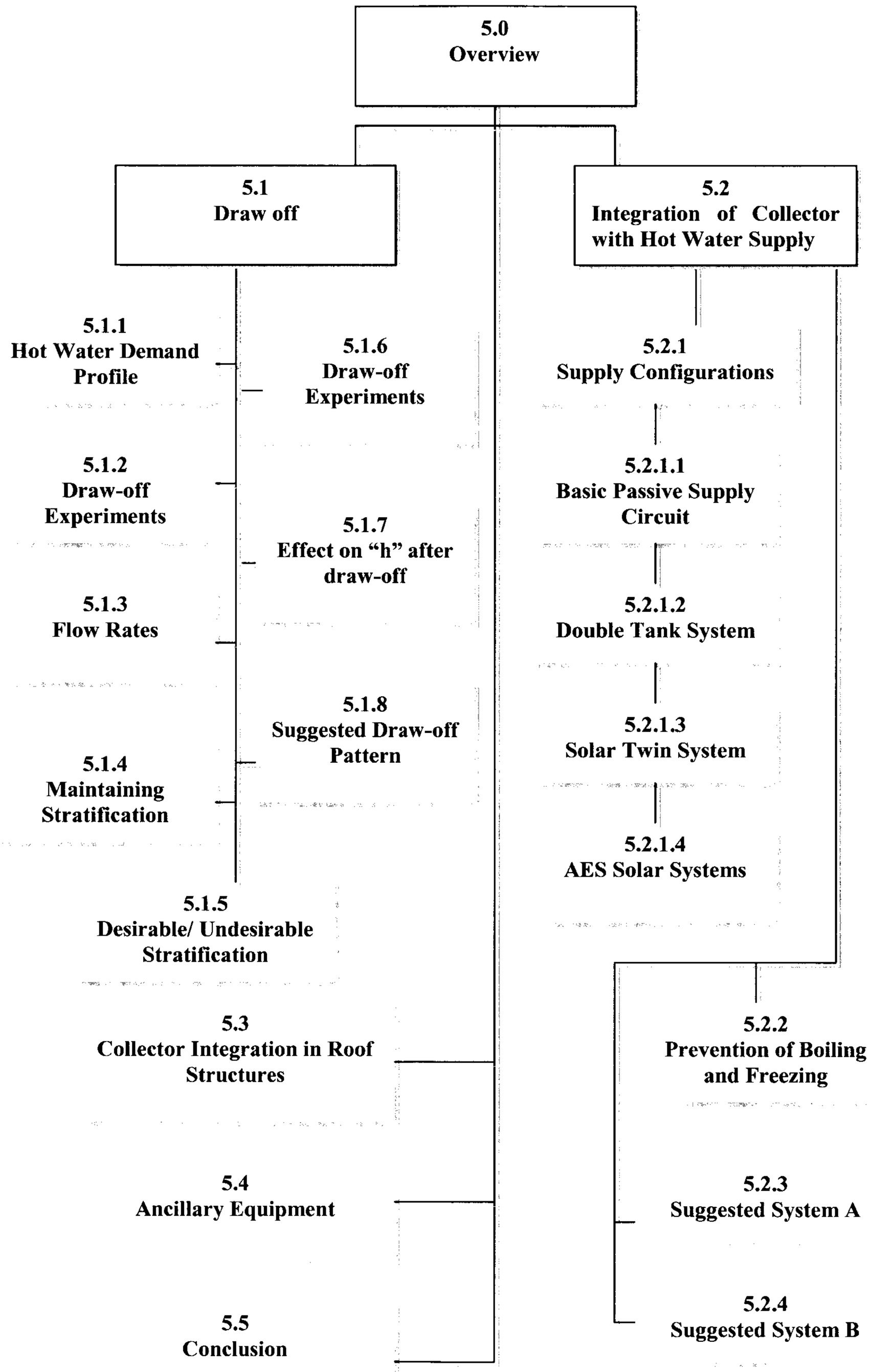
5.0
Overview
5.1
Draw off
5.1.1
Hot Water Demand Profile
5.1.2
Draw-off Experiments
5.1.3
Flow Rates
5.1.4
Maintaining Stratification
5.1.5
Desirable/ Undesirable Stratification
5.1.6
Draw-off Experiments
5.1.7
Effect on "h" after draw-off
5.1.8
Suggested Draw-off Pattern
5.2
Integration of Collector with Hot Water Supply
5.2.1
Supply Configurations
5.2.1.1
Basic Passive Supply Circuit
5.2.1.2
Double Tank System
5.2.1.3
Solar Twin System
5.2.1.4
AES Solar Systems
5.2.2
Prevention of Boiling and Freezing
5.2.3
Suggested System A
5.2.4
Suggested System B
5.3
Collector Integration in Roof Structures
5.4
Ancillary Equipment
5.5
Conclusion

5.0 Overview

The hot water draw-off from a collector particularly from an ICSSWH, is of paramount importance for effective output from the collector. Ideally, a collector should be able to furnish hot water at desired temperatures in the quantity required. However, the output of the collector is dependent on a number of factors; including:

- Inlet water temperature[1]
- Level of insolation
- Ambient temperature
- Stratification inside the tank
- Inlet/Outlet flow rates
- Quantity of water drawn

The variance of even one, if not all of these factors effects the thermal output. Some of these factors are uncontrollable, such as the inlet water temperature which is dependent on the mains supply and varies seasonally. Similarly, the level of insolation and the ambient temperature are also uncontrollable. The remaining three factors to an extent can be managed if not fully controlled. What this implies is that the hot water temperature from the collector will be irregular unless some additional means of energy confinement is introduced. This confinement or energy buffer takes the form of a storage tank. Hence in order to establish a reliable supply system, a storage tank is vital.

Apart from the control and reliability it is also important to maximize the yield of the collector, which in turn is influenced heavily by the "draw-off". The following sections explore in more detail the various factors that affect the output of the collector when integrated in the supply system.

---

[1] A note on the variation of inlet water temperature from the mains is given in textbox 4 (Pg 158. Some details on mains temperature were given in chapter 2.

5.1 The Draw-off

The term "Draw-off" herein implies the tapping/collection of hot water from the collector. The draw-off pattern from the solar hot water system is important to study to evaluate the practical performance of collector. It encompasses the following entities:

- Volume of the water drawn
- Time of the day it is drawn
- The number of times water is drawn
- And the flow rate of water drawn

To estimate the consumption of water, it is therefore important to explore previous studies that have examined the water consumption through a typical day for Scottish households. All these factors basically point towards a single parameter i.e. the amount of energy withdrawn from the collector. Therefore to deal with the factors mentioned above, a new variable, heat removal factor, is introduced in this section. It will be also important to review the hot water demand in order to determine the best possible draw-off profile. As mentioned in chapter 2 it is important to maintain high level of stratification as well as using low flow rates to deliver energy, these factors are explored herein and their optimal values are evaluated.

5.1.1 Hot Water Demand Profile

Hot water requirements vary from household to household, depending mainly upon the occupants (number & age) in any dwelling. It also depends upon the type of dwelling and day of the week. Data from UK-ISES typical demand profile is presented in table 5.1. A more local and thus relevant study is that of McLennan et al [1], who carried out a survey for the demand of hot water for 32 different households in Edinburgh. The hot water demand data by McLennan has been presented in table 5.2. The details of the survey are noted in the Appendix-F.

Table 5.1: Average hot water consumption for UK –ISES demand profile

Hours	Litres
7	0
8	17
9	45
10	18
11	5
12	5
13	15
14	15
15	5
16	5
17	10
18	15
19	45
20	45
21	15
22	10
23	20
24	10
Total	300

Table 5.2: Average Hot water demand profile by McLennan

Hours	Litres
5	1
6	1
7	4
8	22
9	10
10	5
11	5
12	4
13	4
14	2
15	2
16	1
17	2
18	4
19	16
20	13
21	7
22	9
23	5
24	1
Total	118

Comparing tables 5.1 and 5.2, it is evident that the peak demand hours are 8:00, 9:00, 19:00, 20:00 respectively. In light of these profiles, a hot water draw-off profile can be evaluated that would maximize the hot water produced.

5.1.2 Heat Removal Factor F_R

The heat removal factor (F_R) is the ratio of the actual thermal energy removed from the collector by the working fluid to the thermal energy that would have been removed if the entire absorber were at the fluid inlet temperature. As it is a ratio, it can take values from "0" to "1" with 1 representing the condition when the temperature where all the energy has been removed. The heat removal factor for the draw-off experiments are calculated and presented in table 5.4.

5.1.3 Flow Rates

The draw-off flow rates are also equally important, as is the improvement of heat gain, to improve the yield of the system. Improper draw-off can lead to a significant decrease in the collector performance, hence reducing the hot water output. For draw-off from a hot water tank connected to flat plate collector, several studies have been carried out. It has been shown by Hollands et al that low flow-rates from the storage tank, roughly $1/7^{th}$ the normal flow rates can improve the system performance. This is because the low flow rates increase the heat removal factor significantly. As described by Duffie and Beckman [2], until about the 1980's, flow rates were commonly around 0.015 kg/m^{2}s. More recently even lower rates are being used e.g. in Sweden rates of 0.002 to 0.006 kg/m^{2}s are used, where the flow rates are given in per m^2 of collector area. All these studies also give a clue to the draw-off practices adopted for ICSSWH.

5.1.4 Maintaining Stratification

The work on stratification by various researchers and their findings were noted in section 2.4. Stratification serves the dual purpose of adding more value to the output as well as retaining heat when the collector is shaded or during night time. The benefit of stratification can be better explained by considering two tanks of equal size with the same energy content. Consider one tank to be fully mixed (tank-A) while the other being stratified (tank-B). Let's assume that at a given time, only 5 lt is required from the tanks of capacity 50 lt. Let the temperature of the tank-A be "T_a" while the tank-B has a variable temperature with the water temperature of the top 5 lt at "T_b". As the tank-A is fully mixed; T_a would be the average temperature inside the tank. Whereas

in tank-B, in some sections the temperature would be less and in other would be greater than, T_a. Thus it can be logically inferred that $T_b > T_a$.

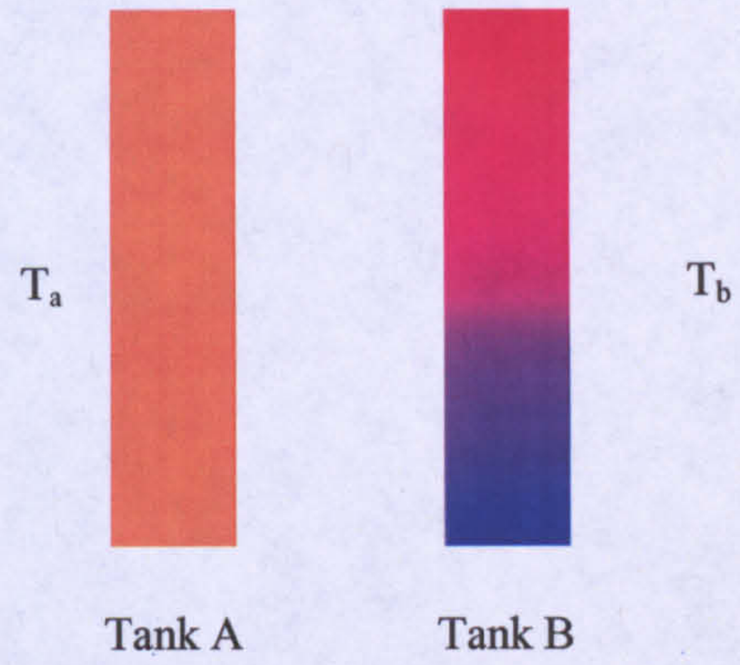

Figure 5.1: Schematic diagram showing stratification inside the vertical storage tanks

5.1.5 Desirable and Undesirable Stratification

As has been explained in the previous section, stratification inside the collector is desirable as it produces a better yield. However, from a heat transfer perspective, it can be undesirable as well. To better explain this, the schematic diagram of the collector is shown in figure 5.2. Because of the shape of the tank and tilt angle, a diagonal stratification (as seen from Y-Z plane) is expected along the length of the tank.

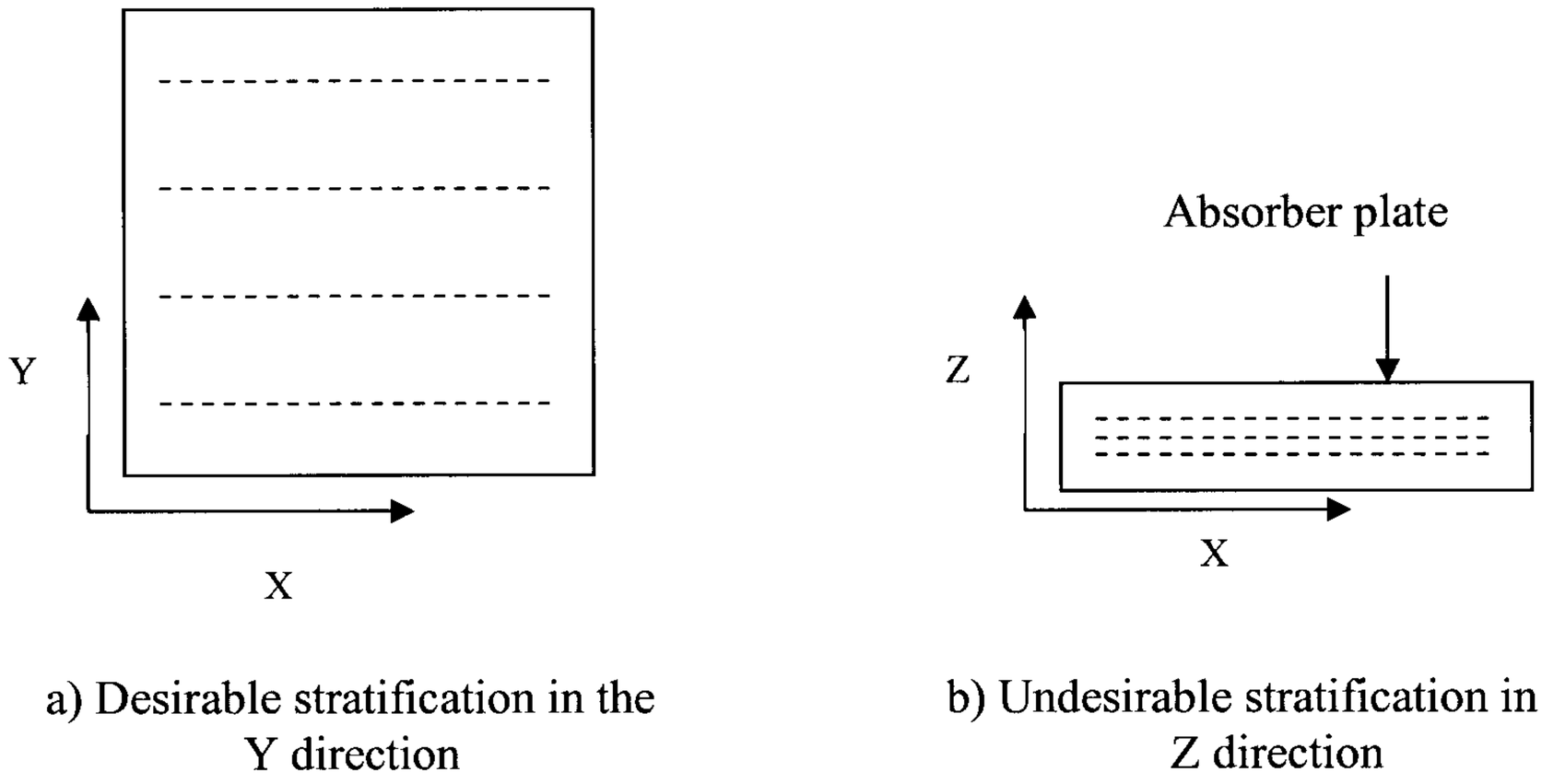

a) Desirable stratification in the Y direction

b) Undesirable stratification in the Z direction

Figure 5.2: Desirable and undesirable stratification

The stratification in the Y- direction (fig 5.2 a) is desirable as hotter water gets accumulated at the top for any draw-off. The stratification in the Z- direction is undesirable as the hot water accumulation at the top decreases the temperature between the absorber plates. This decreases the heat transfer from the absorber plate to the colder fluid.

5.1.6 Draw-off Experiments

Various experiments were carried out for draw-off with different conditions on the collector (finned), the details of which have been presented in table 5.3. The collector was set at the equilibrium temperature for various heat flux inputs. The draw-off flow rate varied between 1.6 lpm (litres per min) to 0.8 lpm. For the initiation, a constant value of 25 litres was set as the draw-off volume (half the capacity of the tank) from the finned heater. The draw-off tests were performed only for the finned heater.

Table 5.3: Details of the draw-off experiments

Test	Draw-off (litres)	Max Temp	Min Temp	Inlet Water Temp	Time (s)	Flow Rate (lpm)	Watts
1	25	56.4	48.9	19.8	1701	0.9	200
2	25	72.5	56.4	20.2	1714	0.9	300
3	25	81.4	62.6	21.4	916	1.6	200
4	25	93.2	72.3	21.8	1896	0.8	400
5	25	83.0	61.9	20.0	980	1.5	300
6	25	40.9	34.8	20.0	990	1.5	100
7	25	30.7	26.0	20.6	985	1.5	100

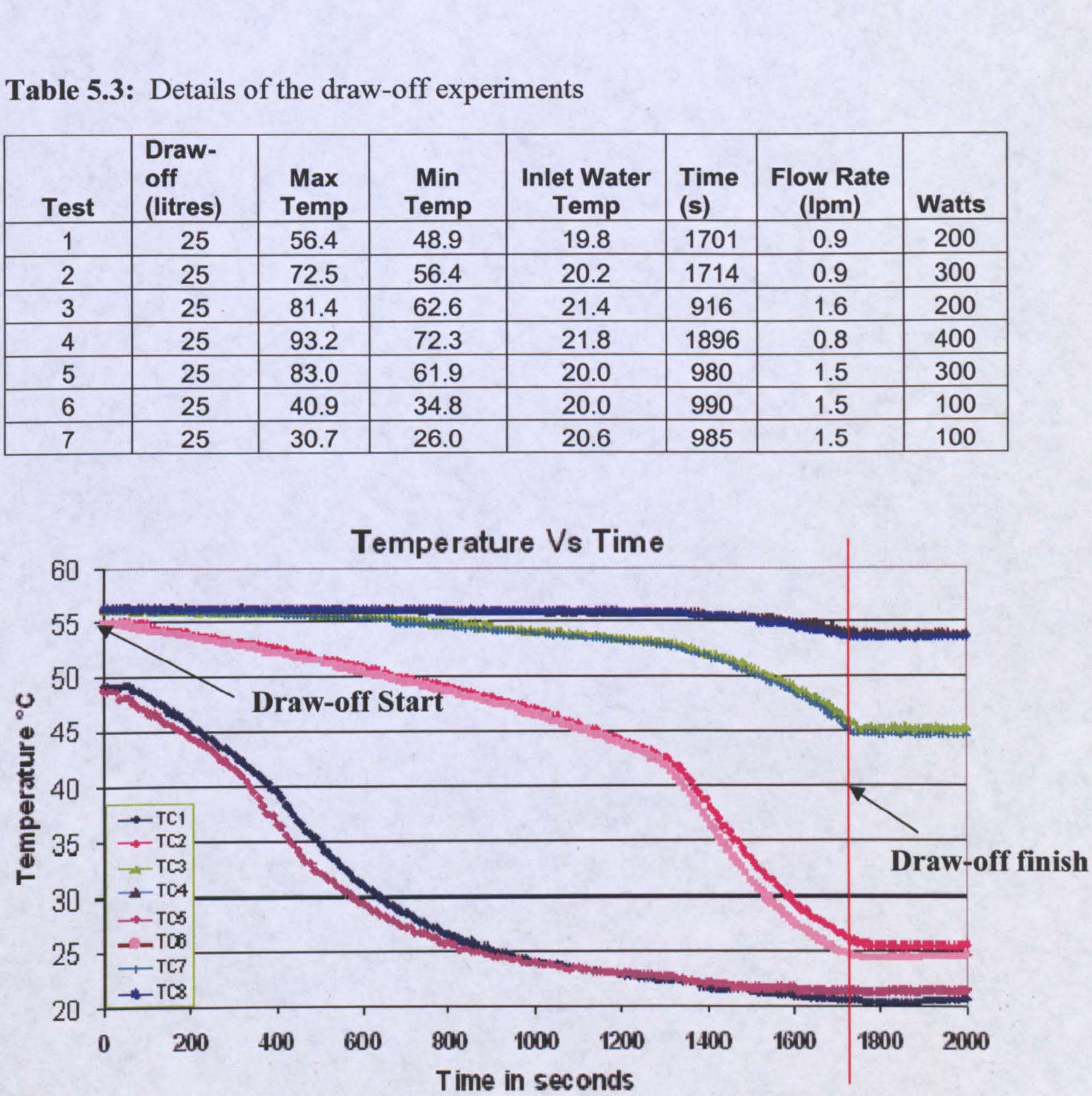

Figure 5.3: Temperature profile before, during and after draw off for Test 1

Fig 5.3 encompasses an interesting set of results. The measurements were taken at 10 sec intervals with the thermocouples at the same position as shown in fig. 3.3.3. A sudden drop in temperature for the thermocouples at the bottom of the tank is evident which later propagates to thermocouples on the upper portion i.e. the draw-off increases the overall stratification.

The water flushed out of the collector was collected in a vessel. A total of four thermocouples were employed to enable calculation of the average temperature of the drawn water. Fig 5.4 shows the schematic diagram of the vessel along with the position of thermocouples.

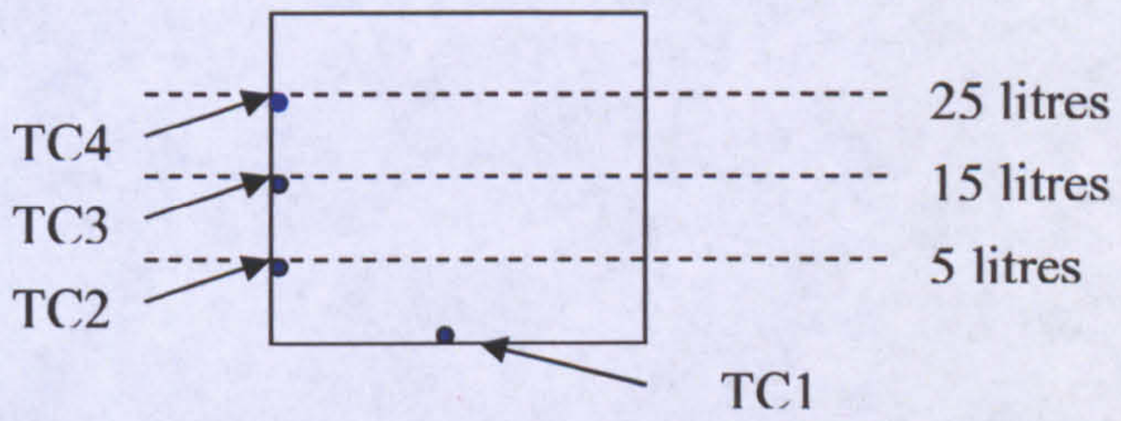

Figure 5.4: The position of the thermocouples in the collection vessel

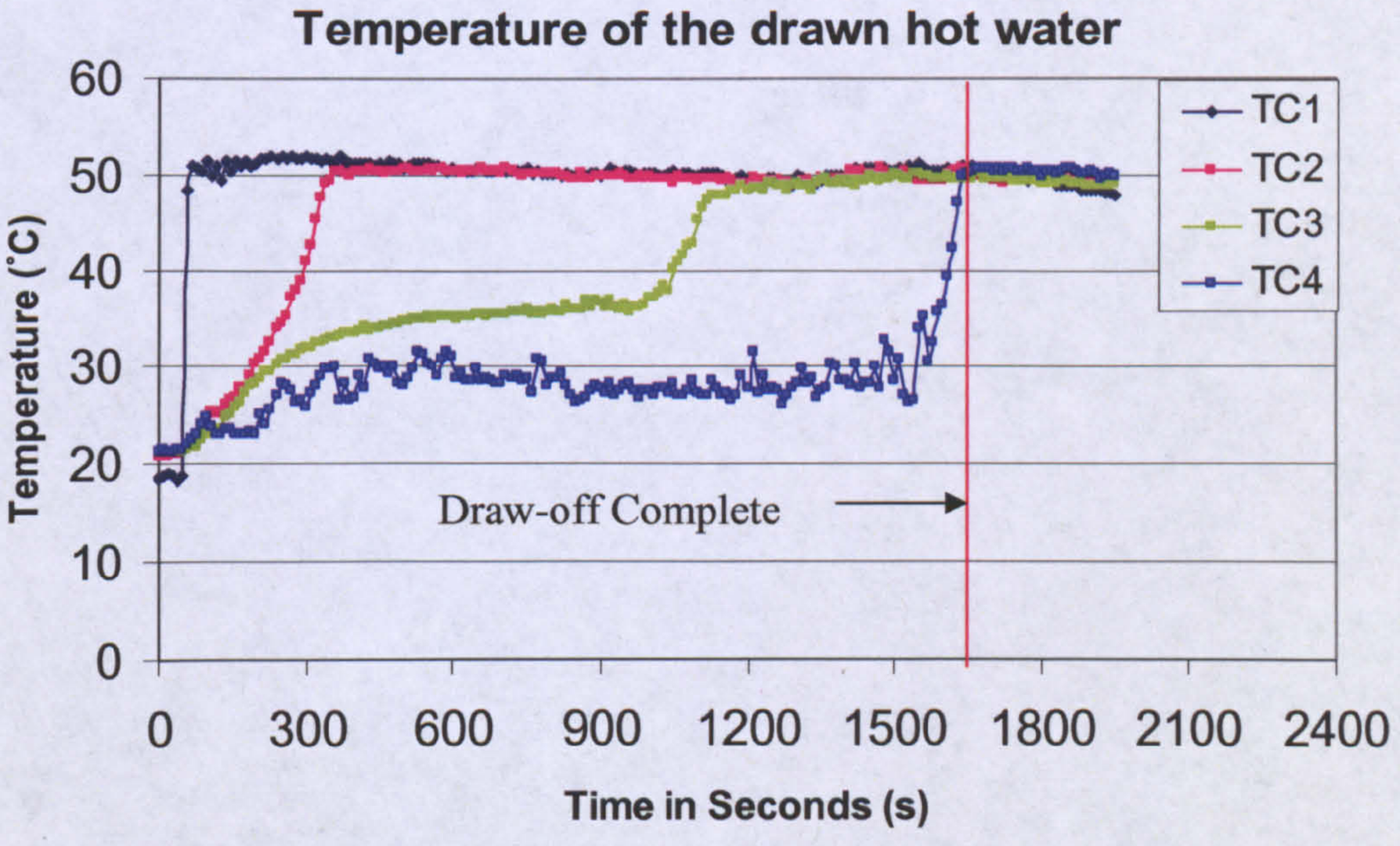

Figure 5.5: The temperature of water in the collection vessel for Test 1

In fig 5.5 the temperature profile of the drained water is shown as water is collected. It can be noticed that the temperatures go up sharply. This is when the water level reaches the thermocouples. What is more interesting to note is that the final output has a uniform temperature with no evidence of stratification whatsoever. This is because

the water gets mixed thoroughly when flowing into the collecting vessel. The results of the tests have been listed in table 5.4. It can be noticed that for readings 5, 6 and 7 the water collected up to 15 litres was above the mean temperature. This is purely due to the stratification inside the tank. The advantage can also be noticed by looking at the F_R values. For test 3 a very low value of F_R can be noticed (0.33). Trapped air that entered the collector through the inlet water blocked the outlet and resulted in bulging of the tank. This resulted in a sudden gush of water with the release of air from the outlet pipe and the drawn water in this case was found thoroughly mixed and therefore the benefit of stratification was wasted.

In order to better explain the draw-off test results, it would be appropriate at this point to look at the stratification profiles for each test that were recorded before making the draw-off. The profiles are depicted in fig 5.6 and indicate that Test-1 was carried out when the collector had achieved equilibrium as its stratification profile is convex (See section 4.1.2.7). This also suggests that water should be tapped before the stratification profile becomes convex so as to gain maximum advantage.

Table 5.4: Results from the draw-off tests

Test	Flow Rate (lpm)	Water inlet Temp	Mean Water Temp	Mean Water Temp (5 *lt* drawn)	Mean Water Temp (15 *lt* drawn)	Mean Water Temp (25 lt drawn)	F_R
1	0.9	19.8	53.8	51.5	50.3	50.1	0.50
2	0.9	20.2	65.2	62.5	62.1	61.6	0.50
3	1.63	21.4	72.2	72.9	70.4	68.7	0.49
4	0.8	21.8	83.5	75.9	78.2	78.1	0.33
5	1.5	20	72.7	76.9	74.1	71.4	0.58
6	1.5	20.5	38.1	40.1	38.9	38.3	0.53
7	1.5	20.2	28.3	29.7	29.1	28.8	0.55

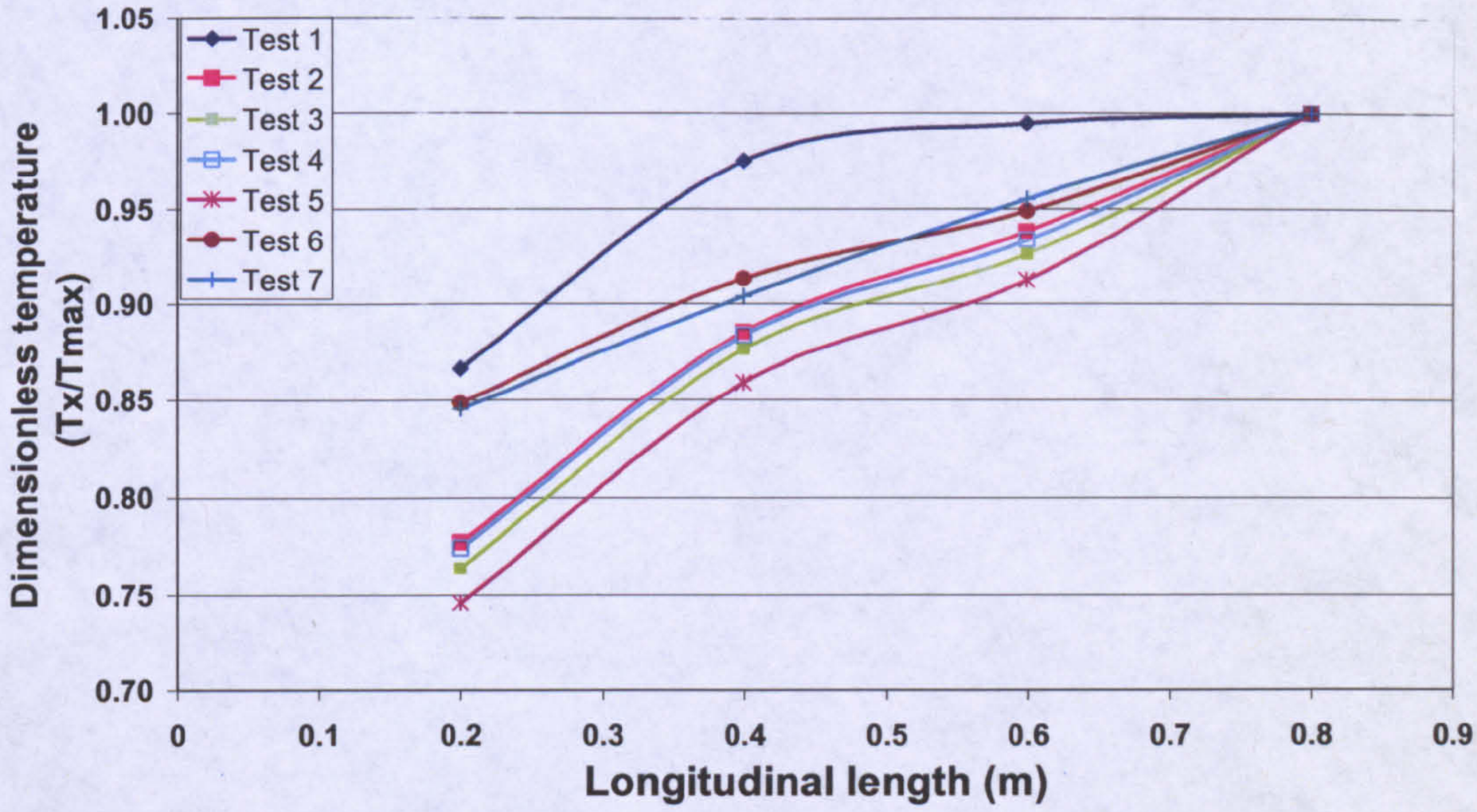

Figure 5.6: Stratification profile for the tests before the draw-off

It would be appropriate to mention at this point that a flow rate of 2.5 lpm was found as the limit for the prototype collector. Any further increase in the flow rate resulted in bulging of the collector. This bulging weakens the weld joints and hence draw-off flow rate should be maintained at values lower than 2.5 lpm.

5.1.7 Effect on "h" After Draw off

As soon as hot water is flushed and is replaced by cold inlet water, the system efficiency goes up because of the collector operating temperature going down (fig 5.3). It can also be noticed from the fig 5.6 that system maintains the temperature at the top end of the collector.

Because of the increase in stratification, the "h" value goes down. This was noted by calculating the energy absorbed by the collector for similar average water temperatures for pre and post draw-offs conditions and comparing the two as shown in table 5.5.

Table 5.5: Comparison of system performance for pre & post draw-offs for 400W.

Avg Water Temp ˚C	Energy Absorbed in 10 minutes Pre Draw-off (KJ)	Energy Absorbed in 10 minutes Post Draw-off (KJ)
50	135	64
55	123	63
60	85	55
65	72	46
70	65	27

The net effect is however the overall increase in the efficiency as the lowering of "h" is overcome by the increase in efficiency due to the drop in system temperature as can be noticed by the spike in the curve in fig. 5.7. To calculate the efficiency, the following procedure was performed. Firstly, the increase in temperature is noted by the thermocouples readings. This temperature was then used to calculate the average increase in temperature using the control volume approach. The change in total enthalpy of the system was calculated though the average temperature. This change enthalpy was then divided by the total energy imposed on the system.

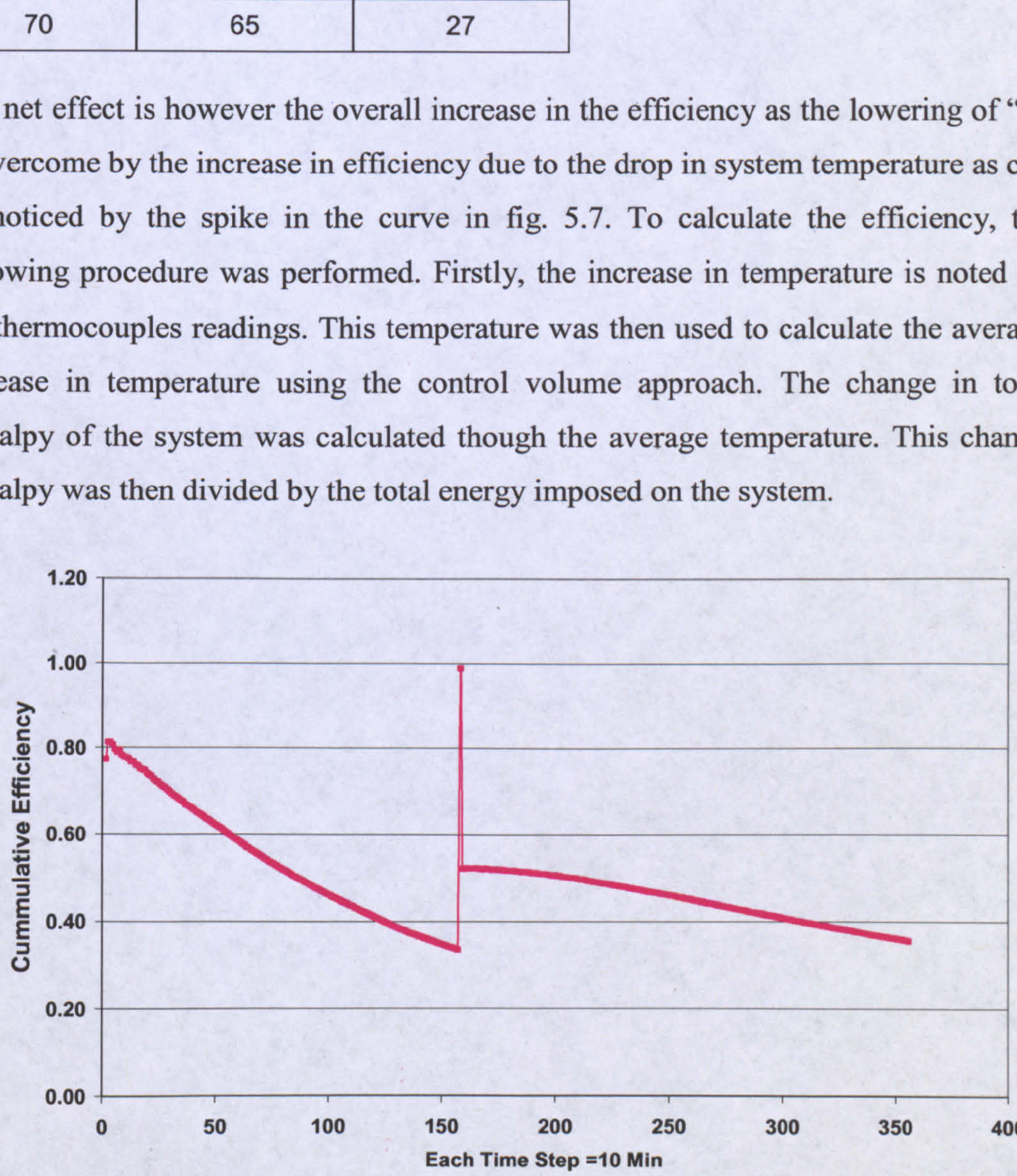

Figure 5.7: Collector efficiency behaviour after the induction of cold water

Fig 5.7 explains the behaviour of efficiency. The system was exposed to 400W till it nearly reached equilibrium temperatures as mention in section 4.1.2.1. 25 litres of

water was drawn-out of the system, the inlet water being at 22°C. The system draw-off rate was 1.1 *lpm* therefore it took about 21 minutes to draw-off the water.

This concludes that the draw-off overall has a positive effect on the system efficiency. Another positive outcome is that all of the 25 litres of the output water temperature that was collected at an average temperature of 80°C. Thus the stratification inside the collector prevents the mixing of water and higher temperatures of water are drawn from the output. It should also be noted here that the diagonal arrangement of the inlet and outlet ports additionally helps in preventing thermal mixing.

5.1.8 Suggested Draw-off Pattern

Through previous studies (Muneer et al [3]), it was noted that the best practice for a built-in collector is to draw all the water when it reaches a particular temperature. For tests done in Benghazi, Libya, 95% thermal efficiency was recorded for a draw-off pattern that removed water as soon as a temperature of 35°C was reached. This practice however might be better only for sunnier climates. For less sunny climates such as that in Scotland, where it takes longer to achieve this temperature it would be worthwhile to explore alternate draw-off patterns that resonate with domestic water consumption pattern. Four tests were devised and an ATA simulation was run. Table 5.6 carries the details of simulation:

For the sake of simplifying the problem, the draw-off schemes were checked with an assumed heat flux of 200W (constant 07:00 hrs- 17:00hrs). Similarly the ambient temperature and the inlet water temperatures were also assumed to be constant (15°C and 20 °C). The tests were done in accordance with the hot water demand studied earlier in section 5.11.

Table 5.6: Details of the draw-off simulation tests

Scheme	1st Draw-off Volume/ Time		2nd Draw-off Volume/ Time		3rd Draw-off Volume/ Time		4th Draw-off Volume /Time	
A	25 litres	09:00	25 litres	10:00	25 litres	13:00	25 litres	17:00
B	25 litres	08:00	25 litres	09:00	25 litres	12:00	25 litres	17:00
C	50 litres	10:00	50 litres	17:00				
D	50 litres	12:00	50 litres	17:00				

The results using the simulation are as follows:

Table 5.7: Results for Draw-off "A"

Draw-off Time (hrs)	Energy in Water (kJ)	Water Draw Temp (˚C)
09:00	216.56	22.58
10:00	44.19	20.53
13:00	458.77	25.46
17:00	647.41	27.71
Total Energy Extracted	1366.92	

Table 5.8: Results for Draw-off "B"

Draw-off Time (hrs)	Energy in Water (kJ)	Water Draw Temp (˚C)
08:00	44.00	20.52
09:00	44.04	20.52
12:00	458.77	25.46
17:00	823.84	29.81
Total Energy Extracted	1370.64	

Table 5.9: Results for Draw-off "C"

Draw-off Time (hrs)	Energy in Water (kJ)	Water Draw Temp (˚C)
10:00	54.88	20.65
17:00	657.94	27.83
Total Energy Extracted	712.82	

Table 5.10: Results for Draw-off "D"

Draw-off Time (hrs)	Energy in Water (kJ)	Water Draw Temp (˚C)
12:00	419.94	22.58
17:00	629.02	27.49
Total Energy Extracted	1048.96	

It can be noticed from tables 5.7-5.10 that scheme B is the best in terms of total energy extraction. The highest gain of energy came in the last draw-off which has a difference of 4 hours from the previous draw-off. Comparing schemes A and B with C and D, it is evident that 4 draw-offs are better than 2. Furthermore scheme D was found to be notably better than C. This is because of the allowance of heating up of the collector before drawing off water. The temperature behaviour of the collector is depicted in fig 5.8 (hour 1 on the x-axis represents 0800 hrs), the sudden dip in temperature is due to the fresh water entering resulting in the decrease in overall system temperature.

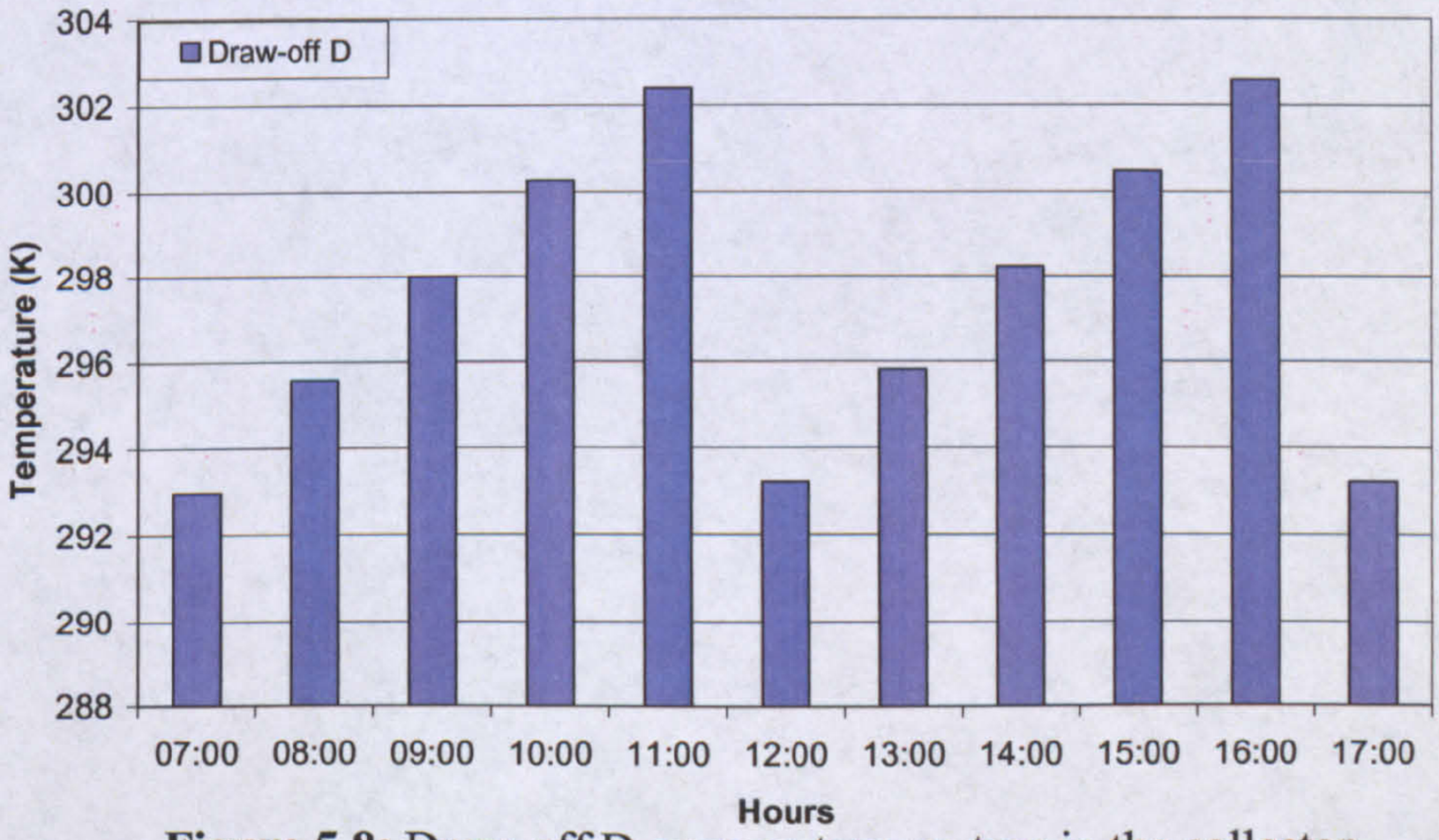

Figure 5.8: Draw-off D average temperature in the collector

5.2 Integration of Collector with the Hot Water Supply System

The integration of the SWH in the domestic hot water supply system is examined in this section. A good supply configuration needs to adapt to the existing hot water supply system. It should efficiently furnish hot water at the rates required ideally without the need of auxiliary pumping and should be able to withstand all weather effects (freezing and boiling). Depending upon the types of the existing hot water supply system (vented or un-vented) the following considerations need to be taken in account:

a) The prototype collector cannot withstand the high pressure in the mains (which has a pressure approx 1 bar and over).

b) In case of the collector operating on natural circulation, the high mains pressure or even the header tank pressure would overcome any thermosyphonic effects and would result in backflow.

c) The output of the collector is variable and is mainly dependent upon the incident radiation, the inlet water as well as the ambient temperature. Therefore, a source of auxiliary heating is required for a regulated output.

d) Heating of water results in expansion and thus the boiling off" of the trapped gases.

The hot water in a domestic hot water system is supplied either through an open vented system (un-pressurized) or an un-vented system (pressurized). The details of these systems are presented in Textbox 5. Un-vented systems are normally found in flats whereas open vented systems are mostly employed in detached houses. Therefore two different collector supply configurations should be targeted to cater for these systems. Figure 5.9 elucidates an open vented supply system.

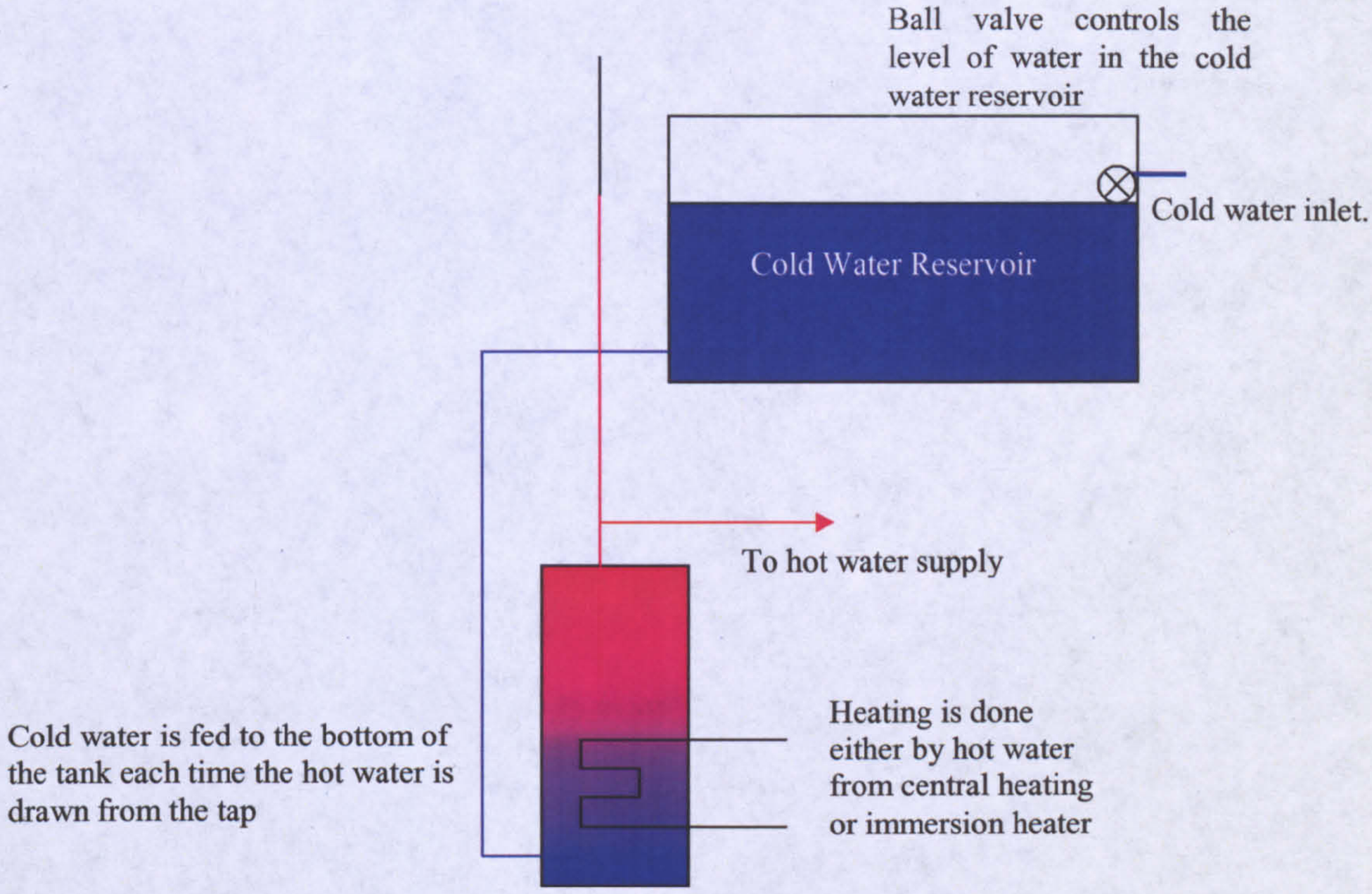

Figure 5.9: Plumbing details of an open vented hot water system without solar collector

5.2.1 Solar Collector Supply Configurations

Supply configurations can be categorized into two, namely active and passive systems. *Active systems* incorporate the use of pumping devices for charging/discharging the hot water to/from the collector. On the other hand "*Passive systems"* make use of thermosyphon effect circulating water to the hot water tank. For passive systems the stratification inside the hot water tank is critical for the supply. In most cases the use of pump is unavoidable particularly if the system is attached to domestic hot water system.

The selection or design of the supply configuration also depends upon the climate. For sunnier climates (higher insolation levels) a single storage tank is adequate. For colder climates a twin tank system is deemed more appropriate. The weather being maritime (moderate) or extreme also has its own bearing. Systems that have a single supply loop, i.e. they feed hot water directly from the collectors, can be used in warmer climates where the possibility of freezing is remote. Such systems are herein referred as *Direct systems*. The *Indirect systems* on the other hand utilize an anti-freeze solution as the working fluid for the collector. Two distinct advantages of this

approach are weather proofing of the system (freeze/boil protection). The other is that the collector is isolated from pressure of the hot water system and can operate on separate pressure level set by the feed pump. The disadvantage is the drop in overall efficiency owing to an increase in the heat transfer resistance due to the additional heat exchanger. An adequate supply configuration should ensure the following.

a) It is drawing maximum benefit from the collector in terms of energy removal.
b) It is designed to withstand the weather conditions.
c) It uses minimum plumbing devices to ensure less pressure and heat losses.

5.2.1.1 Basic Passive Supply Circuit

Fig 5.10 shows the simplest of the collector circuits is herein referred to as the basic supply circuit and was referenced from the work of Courtney et al [4]

The plumbing circuit shown in fig 5.10 operates on a thermosyphon effect. It has been suggested by Courtney et al [4] that the vertical distance between the collector and the hot water tank should be at least 300mm above the collector so as to avoid the back flow to the collector during night time when the collector cools down. This system is only suitable for locations where freezing is not a problem.

The advantage of this system is that it does not require auxiliary energy to remove hot water from the collector. The disadvantage is that the solar fraction F_R can be very low at times particularly during cloudy days. Furthermore since the collector is itself a roof mounted device therefore it is inconvenient to arrange to a cylindrical storage tank at least foot (0.3m) above it. Roofs normally converge, leaving lesser room at the top. It is therefore more usual to arrange a small pumping device which enables the storage tank to be placed in any convenient location [4].

This configuration can be directly applied to open vented systems. However with a slight modification it can also be used for a pressurized system as well. A heat exchanger can be used inside the storage tank that preheats the cold water before taking it to the boiler. In this case the advantage of direct heating of water is lost. This modification is shown in fig 5.10 (b)

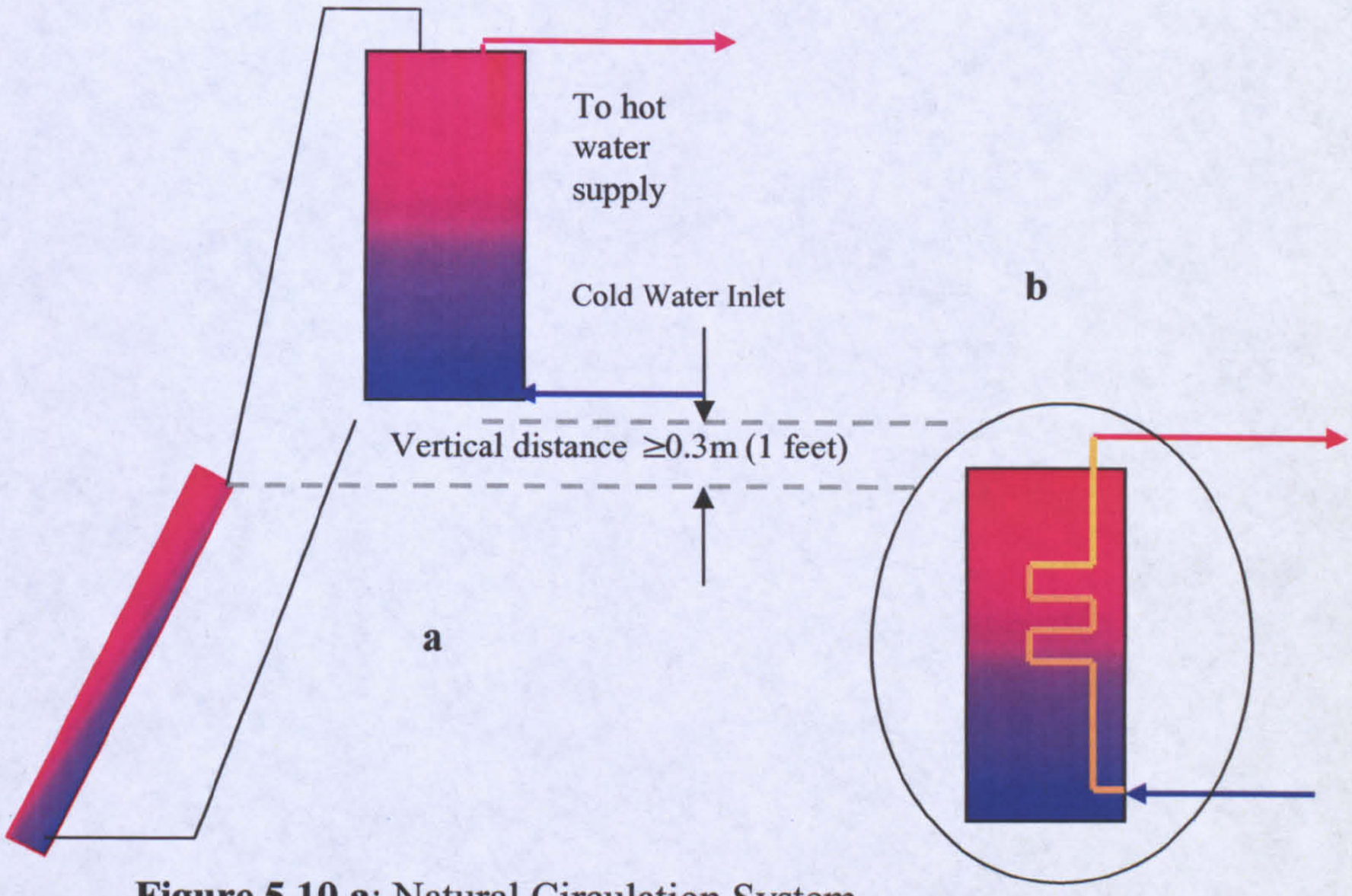

Figure 5.10 a: Natural Circulation System

5.2.1.2 Double Tank System

A twin tank system is a widely used system and has also been cited by Courtney et al [4] (see fig 5.11). It incorporates the use of auxiliary heating (immersion heater or indirect coil) in one of the tanks while heat exchanger in the other. This concept enables the maximum use of the collected solar energy.

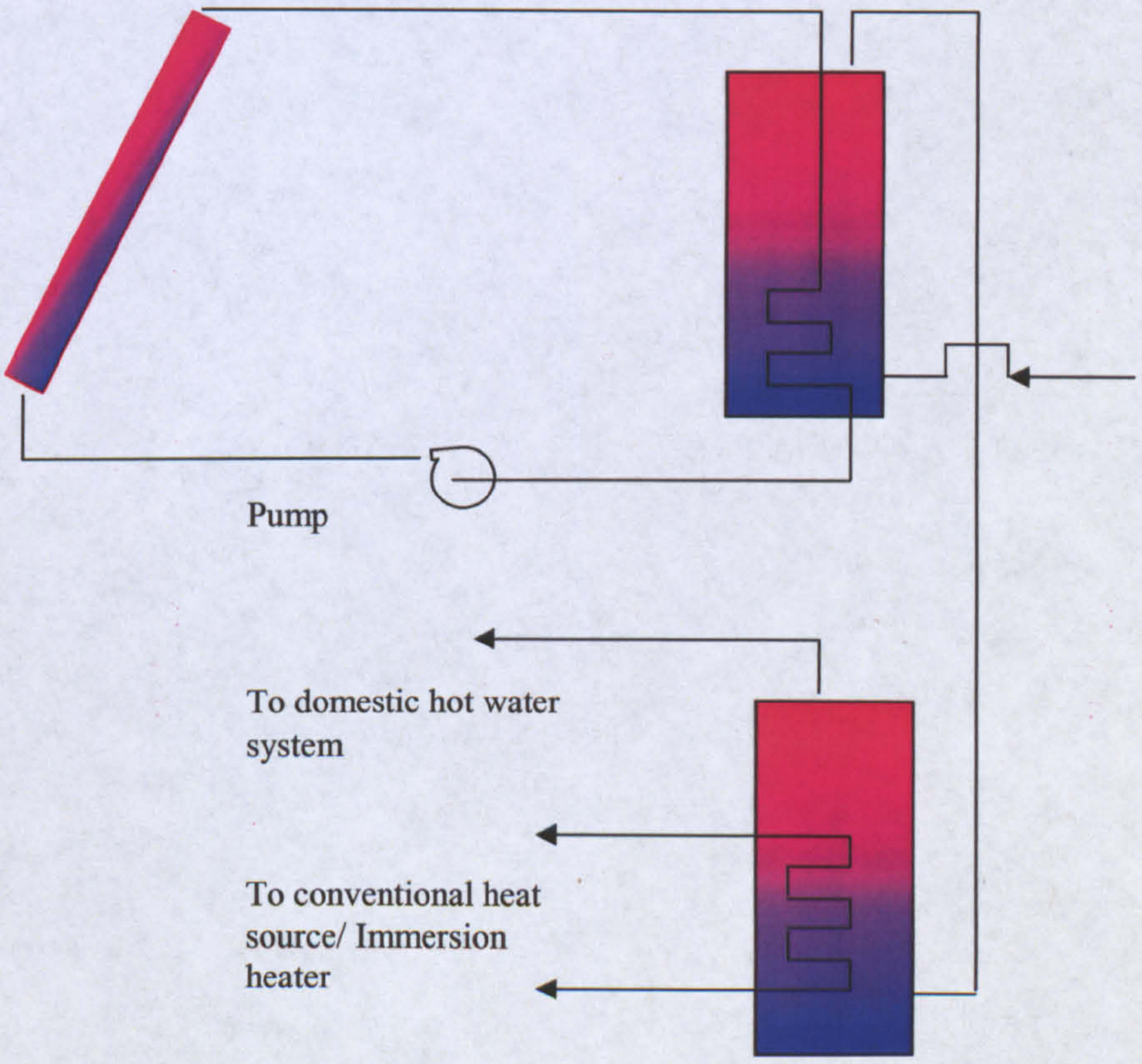

Figure 5.11: Double tank closed circuit configuration

As mentioned earlier, since it operates on an internal loop with the collector, the use of an anti-freeze can be incorporated and the collector is isolated from any external pressure of the supply system. Since it utilizes a feed pump, the reliability and the expected solar fraction can be appreciably high. Although the system requires auxiliary power (pump) to circulate the antifreeze however, the additional power supplied is offset by the increased F_R of the system.

5.2.1.3 Solar Twin System

A more innovative concept is that of the plumbing system by Solartwin [5]. It reduces unnecessary plumbing and utilizes effectively the vented hot water supply systems.

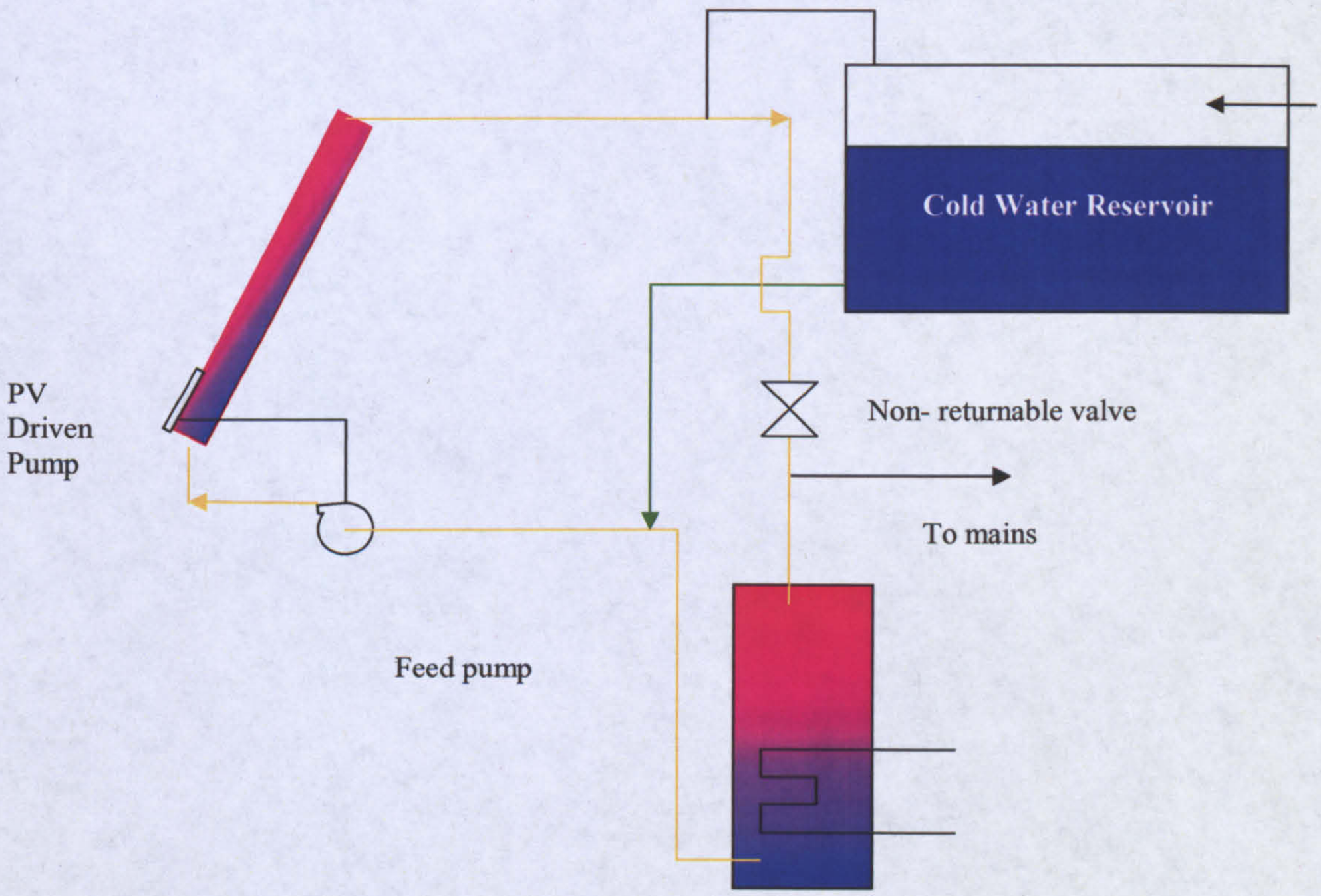

Figure 5.12: Plumbing Circuit System Solar Twin System

This system can be used for the integrated collector storage type. The use of anti freeze can also be incorporated. This system operates on two loops (see fig 5.12). Firstly when no water is being drawn off, the water is supplied by the bottom of the tank to the collector. On the other hand when the water is sufficiently heated, it is fed back to the storage tank. This circulation of water is indicated by the yellow lines in the figure. When the hot water is drawn from the storage tank, water from the cold

water reservoir is fed to the collector directly instead of the bottom of storage tank (green line becomes active). The reservoir water also pushes the water at the bottom of the tank, this flushes out the hot water from the top of the storage tank.

5.2.1.4 Supply Configuration by AES Solar Systems

The supply system employed by AES solar systems is given in fig 5.13 [6]. This system requires the use of two storage tanks. It requires a high amount of plumbing apparatus that results in an increased cost of the overall SWH system. The advantage of this system is that it can also heat the pressurized hot water and thus contribute to both solar and space heating. The drawback of having a high amount of plumbing does not only reflect in the installation cost but also results in increased heat and pumping losses during the operation of the heater.

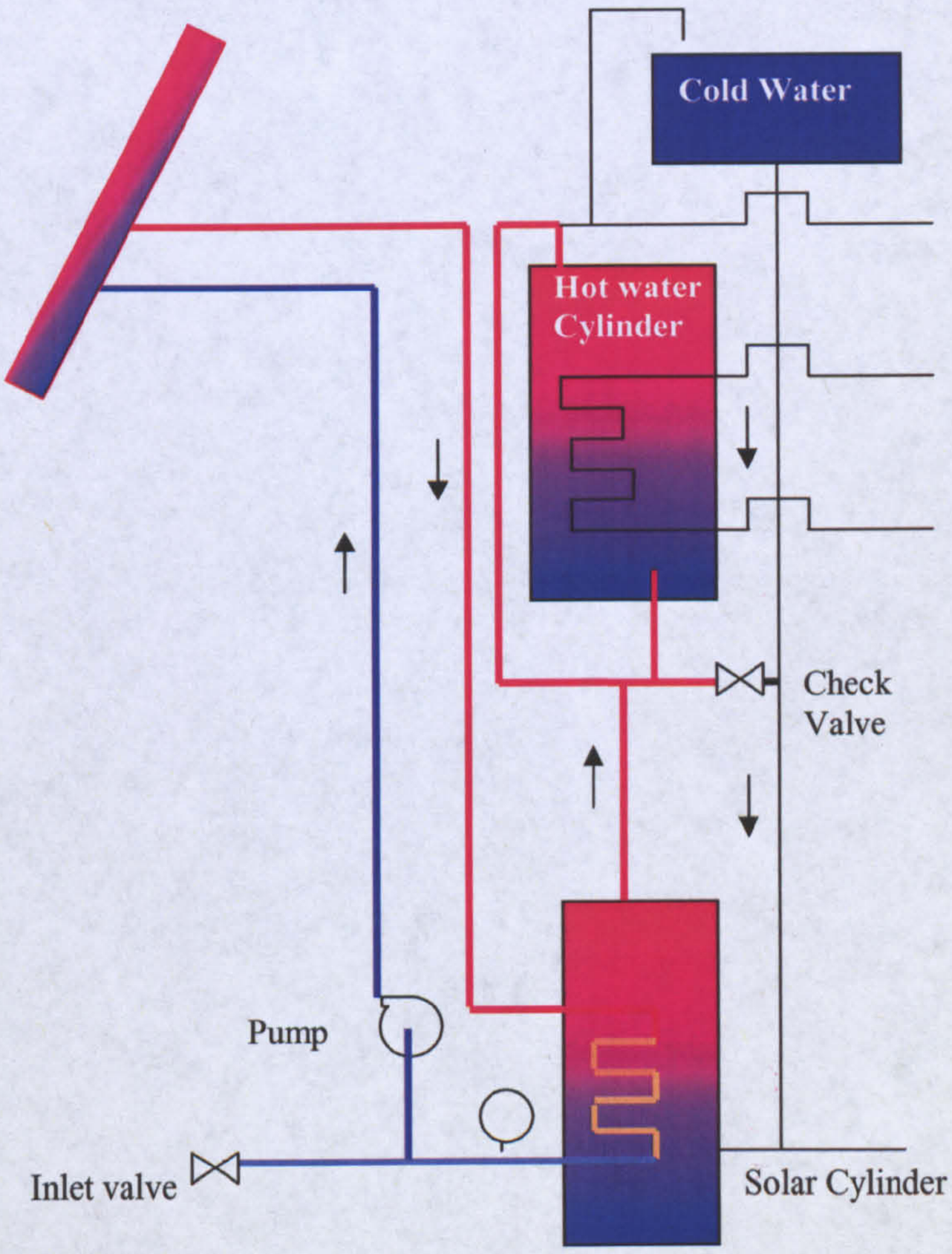

Figure 5.13: Plumbing circuit diagram by AES solar systems

5.2.2 Prevention of Boiling and Freezing

Boiling and freezing are possible problems that can occur in a collector in extreme weather conditions. Preventive measures thus should be taken for their alleviation. Boiling for Scottish conditions is not as big a problem as freezing. However, using the insolation data, it can be estimated through ATA simulation that boiling might occur. The possibility of boiling occurs in the case of nil or low amount draw –off from the collector during the day when the heater is exposed to high levels of insolation. This is a possibility during the summer time when the occupants are away. A look at the radiation data for Edinburgh reveals only a total of 375 hours of radiation between 300W-400W /m^2. Through experiments it was revealed that a total of 12 hours at least were required to achieve boiling in the collector at 800W owing to the large thermal inertia of the system. Considering the fact that the U value under laboratory condition was sufficiently low, it is safe to claim that under normal circumstances boiling is a remote possibility. However the use of an expansion vessel could be used to mitigate the possibilities in high insolation conditions, as it takes care of the boiling-off of the trapped gases inside the water, if any.

Freezing can induce serious damage on the collector body. For freeze prevention, Duffie and Beckman [2] have provided a range of solutions. These include the use of anti-freeze (Ethylene glycol-water or Propylene glycol water). As an antifreeze solution, such as ethylene glycol water solution is toxic, additional plumbing measures have to be taken into account. Some plumbing regulations permit the use of an anti-freeze with potable water only if they are separated by two metal interfaces. Using air as a heating medium has also been suggested as its leakage is not a problem and is non-toxic however, the thermal penalty associated with air as a working fluid is discouraging. Warm water can also be circulated through the heater, or a heating element inside the collector can keep the water warm, however this can lead to significant losses. The drain-back and the drain-out systems have also been described by Duffie and Beckman [2]. These systems involve the draining of water when they are not operating. In the drain-back system water drains back into the tank or a sump that is not exposed to freezing temperatures. In the drain-out systems water is drained out of the system to waste. Drain back collectors of various sizes are commercially available.

A more native work regarding freeze prevention is that of Grassie [7]. In his thesis, Grassie has suggested the use of flexible pipe made of EPDM rubber instead of copper tubes. This system allows the tube to expand at the time of freezing thus annulling the damage done by the expansion. It is also concluded that the FLEXSOL collector is not likely to suffer the detrimental effects of lime scaling. The idea can be taken forward for ICS by using the EPDM rubber pipes at the inlet and outlet pipes.

The use of collector plate and piping material that could withstand occasional freezing is another option. Designs have been proposed using butyl rubber risers and headers that can expand if water freezes in them.

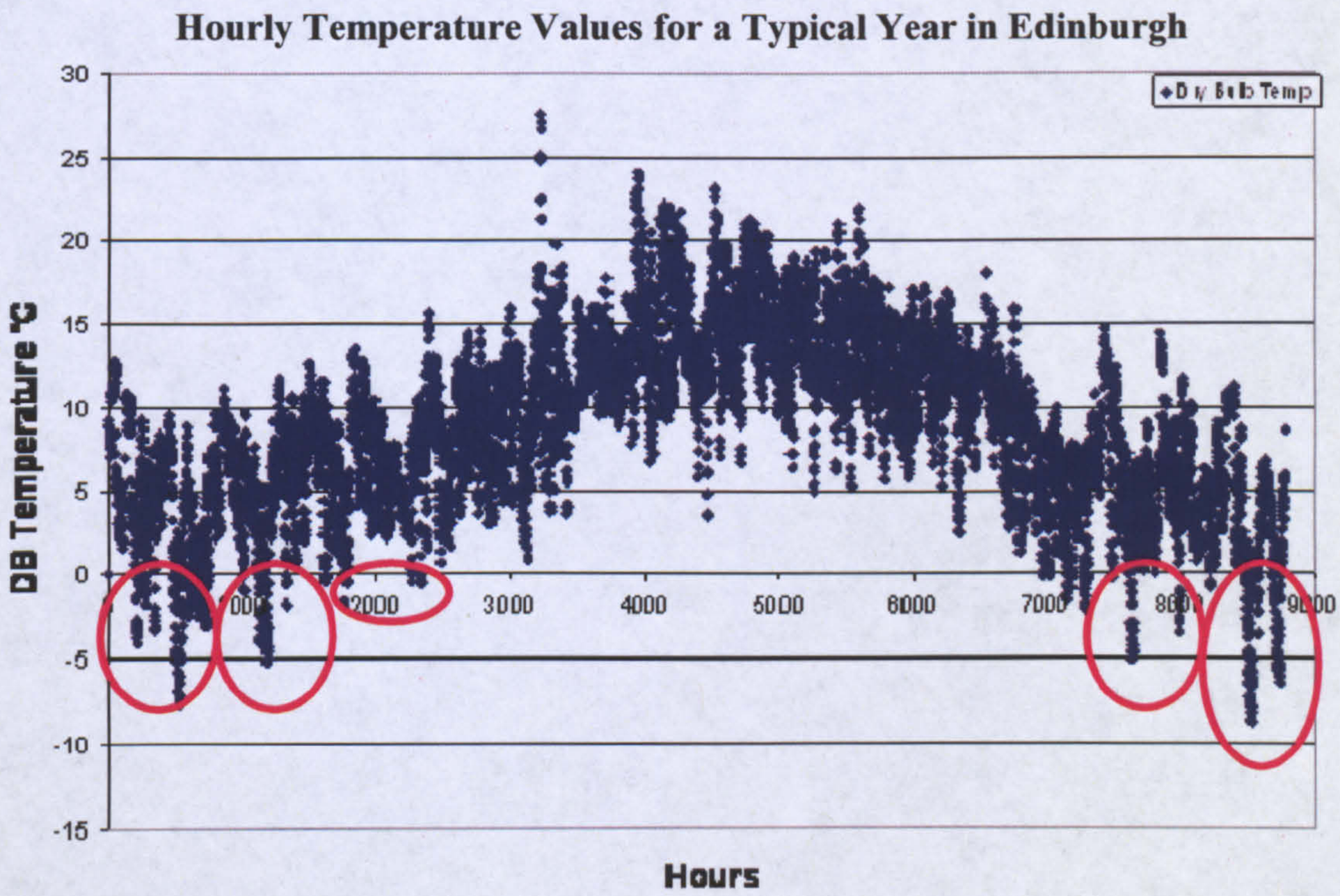

Figure 5.14: The hourly temperature values for a typical year (1992) in Edinburgh have been plotted

In fig 5.14, the hourly dry bulb temperature values for Edinburgh are shown. The areas of concern are circled in red, indicate subzero temperatures. Very low temperatures can be seen in January and December (where 0 hour indicates 12:00 am on the 1st of January). Occasional spells of cold are also noticeable in March and

October. A minimum temperature of -8.7°C was observed in late December. A total of 404 hrs of subzero temperatures (including 0°C) were recorded in the whole year (8760 hr), which amounts to 4.6% of time. Another 1387 hrs were recorded having temperatures between 4-0°C which amounts to a significant 15.83%. The figure is important, as below 4°C water behaves in an anomalous manner and expands rather than contracts on reducing temperature. This indicates that measures have to be taken to avoid freezing of the tank. The maximum temperature of 27.6°C was observed in early summer. After running the ATA simulation using the weather data, it was noted that even if the system is left unused, boiling is a rare possibility as peak temperatures of only 65°C were reached. This is because of the high thermal inertia of the system.

5.2.3 Suggested System Type- A

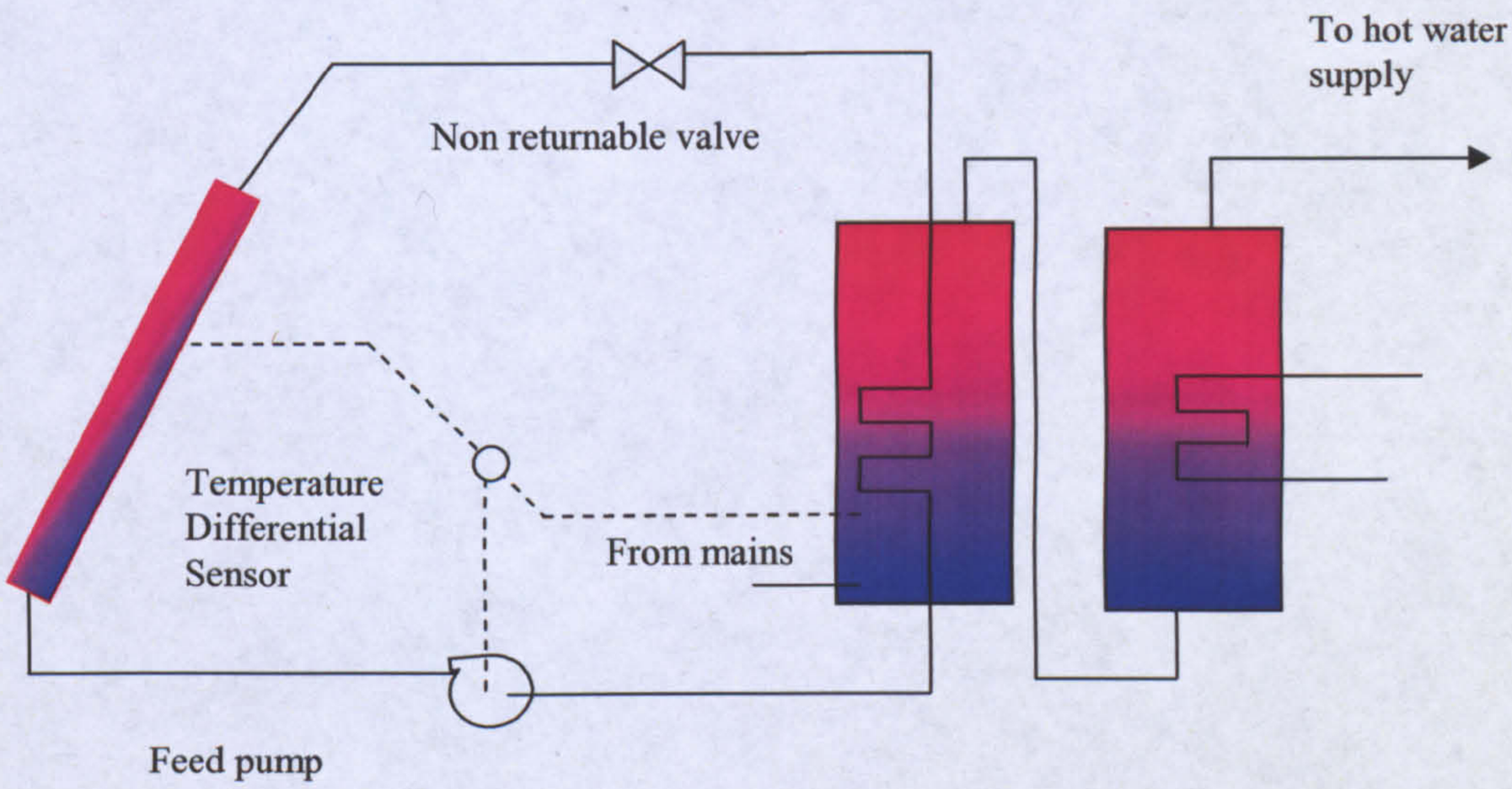

Figure 5.15: Suggested system (a) for the prototype ICS collector

On the basis of the various supply systems studied, the first proposed system (Type-A) is presented in figure 5.15. This system is proposed for houses with un-vented hot water systems and is based on two flow loops. The internal loop is used for circulation of anti-freeze solution. Water and glycol mixture is a common anti-freeze that can be used as it is low cost and relatively non-toxic as compared to others. As mentioned earlier, the use of secondary loop enables the collector to operate on pressures settled by the pump. Despite the advantages there are two notable drawbacks in the proposed system. It would require an additional tank, heat exchanger as well as extra piping. This increases the system costs markedly particularly for dwelling with no storage

tank in the previous systems (systems with combi boiler). The other disadvantage is the thermal penalty associated with an extra heat exchanger. This system is freeze tolerant and reliable. The pump circulation can be regulated connecting it with a temperature differential controller.

5.2.4 Suggested System Type-B

The second suggested system is depicted in figure 5.16. This system does not require an anti-freeze but does require a water reservoir (header tank) that supplies the head for flow of hot water. Therefore this concept is applicable to the *Open vented* systems only. The use of an air vent that provides room for the expansion of water in case of freezing and so do the EPDM rubber pipes at the inlet and outlet ports.

As soon as the hot water is used, equal amount of cold water enter into the collector that displaces hot water from the top. This water can be fed directly to the load or can be stored in the storage tank. The hot water tank can be positioned at a lower level than the collector.

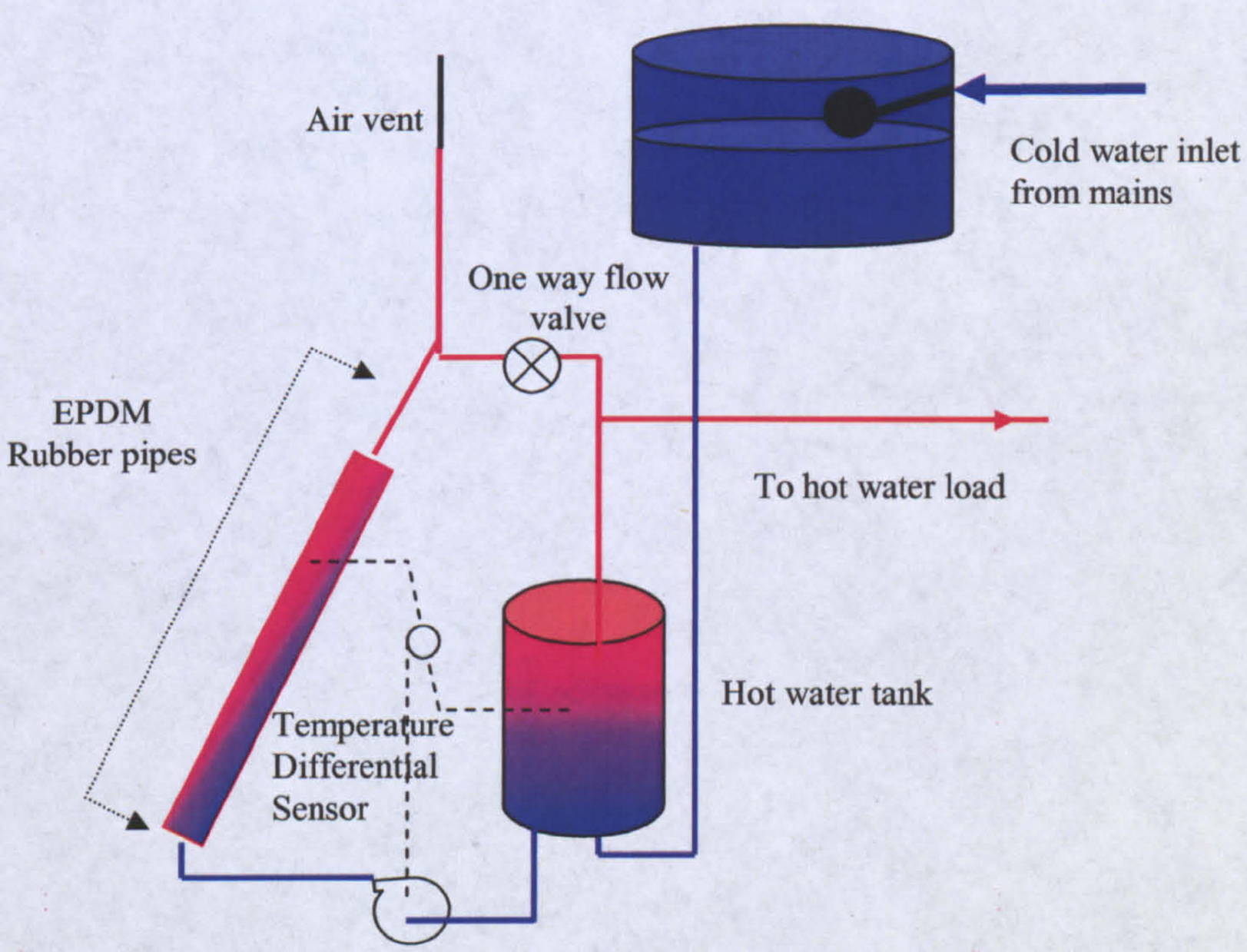

Figure 5.16: Suggested system (b) for the ICS prototype collector

The draw-off schemes that were studied earlier, can be employed in this system. For the suggested system-A, the draw-off schemes are unnecessary as it operates on different conditions that include heat exchanger and antifreeze.

5.3 Collector Integration in Roof Structures

The use of solar collectors has a direct impact upon a building that includes its performance and mainly its outlook. It is therefore important that the collector integrates into the roof top seamlessly such that it does not devalue the property outlook nor breach any housing codes and restriction which prevent use of protruding installations like television aerials, dish etc in conservation areas. On the other hand it is also equally important that the collector is placed at a non-shaded south facing roof. The roof angle also has a bearing on the collector performance as will be explored in chapter 6.

The roof material is taken into consideration by an architect when designing the roof structure of a house as is, the location of the house. In Britain, the further north the location, the greater the wind speed. This means that roofs with a slightly steeper pitch are needed in the north to minimize tile / slate uplift.

England is a bigger country than Scotland. When looking at tile / slate manufacturers guidance typically the advice given on roof pitch tends to be for milder weather than in Scotland receives.

Interlocking slates have a minimum pitch of 17.5 degrees. Dundee university conservation glossary lists slates as having a min pitch of 22° degrees. However, a general consensus brings out minimum 30° degrees for slates in Scotland.

5.4 Ancillary Equipments

A notable amount of research has been done on the ancillary components of SWH systems such as intake manifolds, valves, storage tanks etc. The use of these components helps increasing the efficiency or reliability. In many cases the components are used to prevent undesired behaviour of the system (back flow of water from the collector etc). These components are therefore discussed below in detail along with their advantages.

5.4.1 Storage Tanks

For storage tanks it has been suggested that the length to radius ratio should be as high as possible. This promotes stratification. The distance between the inlet and the outlet should be as long as possible. It has also been noticed in a recent study that obstacles improve the stratification inside the tank[8]. Cylinder capacity of 30 to 60 litres per square metre of collector area is recommended.

5.4.2 Inlet Manifold

The main idea of an inlet manifold is that water from the collector should ideally enter at the level where there is a corresponding the temperature in the stratified tank. Intake manifolds have taken different forms. Flexible pipe is one method, where the pipe flexes because of the density of water inside the pipe to the corresponding level temperature. The other type involves the perforations at various levels on the pipe surface (see fig 5.17).

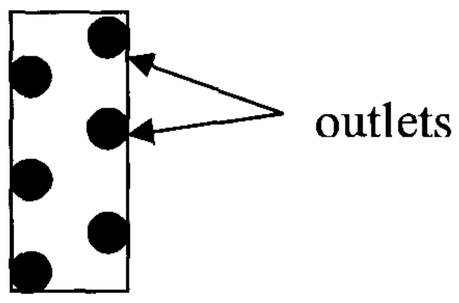

Figure 5.17: Inlet Manifold

More recently fabric design inlet stratifiers have been suggested by Anderson and Furbo [9]. The fabric is permeable and allows water or antifreeze solution to seep through at numerous levels. As the fabric manifolds are even less costly than their metallic or polymer counterpart they can be used in the optimized system.

5.4.3 Valves

Various flow valves for regulating the water supply are employed. These include the one-way valves that allow flow in one direction only. Such valves can be placed in between the collector and the tank if the collector is at a lower level than the tank. It will prevent the back flow of water and thus prevent night time-losses. Similarly temperature differential (solenoid) valves can also be used for systems that involve pumping. The use of valves increases system reliability.

5.4.4 Low Flow Rate Pumps

Low flow rate pumps are available but increase the cost of the system. The pumps required for the collector should ideally furnish low flow rate at high head values with capability of continuous supply. The pump should be wear resistant and hence should not have any components that wear out as it is going to be utilized for continuous periods ideally over the collector's life. Car windscreen pumps were studied for their low cost but they cannot be used for continuous operation or longer runs. The pumps should have no brushes that will wear out with time. Positive displacement pumps such as piston types are ideal for this purpose.

A general rule of thumb for Scotland is that the collector flow rate should be 0.5 lpm for each square meter of absorber plate area. Similarly AES solar systems recommend 1 lpm/m^2. These thumb rules are based on flat plate type collectors which have a much lower thermal inertia than ICS collectors. The ICS collector should have even lower flow rates for higher yield. If variable speeds pumps are used, they can be integrated with PV modules and result in significant advantage by finishing the need for additional power. Since PV delivers DC voltage such pumps should be able to operate on DC input. The other advantage of this system is that it will produce a higher flow rate at the time of higher irradiance and similarly for cloudy conditions the pump will either produce lower flow rates or stop. If the PV supplied variable speed pump is used it can result in system increase cost roughly by £100 [2]

[2] The ball park figures for the pump cost

5.5 Summary

It was determined from the draw-off experiments carried out that the flow rate has a notable effect on the output of the heater. Due to stratification, a reasonably higher yield can be drawn from the collector, particularly with the collector at lower temperatures, if the draw-off occurs more frequently.

Four types of draw-off schemes were analyzed. It was noted that more useful energy can be extracted from the collector with four draw-offs during the sunshine hours as compared to 2.

The efficiency of the collector increases each time a draw-off is made and results as a spike in the efficiency curve. The "h_w" value of the heater also drops significantly after the draw-off this is because of the increased level of stratification inside the tank. However, the overall affect an increase in efficiency of the collector. It was also noticed that the output from the collector is uniformly mixed/ un-stratified. The water can be collected at higher than the average temperature inside the collector if the collector is discharged to half (25 litres) or even lesser volumes.

In light of the study of various the hot water supply configurations for collector, two configurations were proposed one for open vented and the other for un-vented systems. The advantages and disadvantages of each of the proposed configuration were discussed. The advantages of a few of the ancillary components that have been produced particularly for SWH systems were also noted.

Textbox 4

A Note on Mains Water Temperature in UK

Mains water temperature in UK also varies with seasons. During the coldest times of the year, the temperature takes values of 10˚C. While during summer time water temperature can go up to 23˚C (As measured in the laboratory). The ideal, maximum safe temperature for home or hotel water is 40˚C. At 60˚C it takes only 6 seconds to sustain a first-degree burn [4]. Table 6.5 provides the details of burns, from the burn safety.

For cleaning and shower purposes water below 40˚C is required for washing and heating the temperature can be equal or over 60˚C. Campbell has carried out survey that takes 55˚C as the desired hot water temperature.

A Note on Mains Water Pressure in UK

Water pressure, in the mains network is not constant. Throughout the year, and from hour to hour throughout the day, water pressure changes in response to the demand for water being placed on the system. There may be times when the target cannot be met. Most commonly, this may be due to high water demand during hot summer months. Under those circumstances, it is unavoidable that pressure could fall below the target of 1 bar. Sometimes, routine maintenance and improvements to our mains network, or burst mains, can also reduce pressure [2].

Textbox 5

Open Vented System

This type of system uses two water tanks, both located in the loft, and a hot water storage cylinder. One tank draws water from the mains supply and feeds the storage cylinder which, when heated by the boiler, can release hot water to taps all over the house.

The second tank, commonly known as F&E (feed and expansion) tank, is usually smaller and maintains the correct level of water in the heating system. It also allows for expansion of the water in either tank when it gets hot.

Showers, taps and running baths can be drawn in any room at the same time, but care should be exercised that if the cylinder should run cold it will take a little time to reheat.

Unvented System

This type of system is very popular because it offers versatile output while saving space. All you need to accommodate is your choice of boiler, connected to an unvented hot water storage cylinder.

This type of system guarantees a consistent flow of hot water through a range of outlets simultaneously all delivered at mains pressure.

References

1. Campbell McLennan, *Solar Water Heating*, in *School of Engineering*. 2006, Napier University.
2. Duffie, J.A. and W.A. Beckman, *Solar Engineering of Thermal Processes*. 2nd Edition ed. October 1991: John Wiley & Sons Canada, Ltd.
3. T. Muneer, *Effect of design parameters on performance of built-in storage solar water heater.* Energy conservation and Management 1985. **25**(3): p. 277-281.
4. Courtney, R.G., *An Appraisal of Solar Water Heating in the UK.* 1975.
5. Solar Twin, *www.solartwin.com*. 2007, 9 Abbey Square, Chester, CH1 2HU
6. AES Solar Systems, *Plumbing Circuit Diagram*, in *http://www.aessolar.co.uk*. 2007.
7. Thomas Blanchflower Grassie, *Optimization of Fluid Flow in a Flat Plate Solar Water Heater*, in *School of Engineering*. 2001, Napier University: Edinburgh.
8. Altuntop, N., et al., *Effect of obstacles on thermal stratification in hot water storage tanks.* Applied Thermal Engineering, 2005. **25**(14-15): p. 2285-2298.
9. E. Andersen and S. Furbo. *Fabric inlet stratifiers for solar tanks with different volume flow rates*. in *Proceedings of EuroSun 2006*. 2006. Glasgow, Scotland.

CHAPTER 6

Optimization

Effective, Efficient Apparatus and System

Having examined the finned collector and confirming its superior performance over the non-finned design, extrapolations on the basis of existing results can now be carried out. These include undertaking the challenge to further increase the levels of performance. The study of limits and constrains of design aimed at expanding the performance envelope will pave the way for an optimal system.

Optimisation of any system is the ultimate goal. A state which when achieved leads to the requirements being met to the best of possibilities. It could be difficult to achieve, as several parameters that influence performance may not necessarily compliment each other and therefore a balance has to be struck and compromises have to be made. This chapter aims to unearth all possible design improvements for the fabricated prototype collector as well asses the best possible installation strategies.

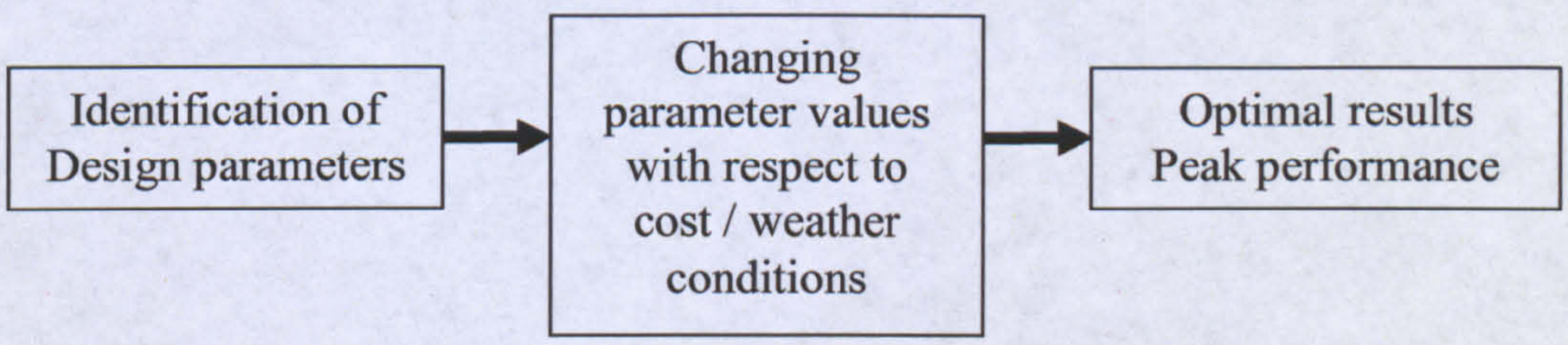

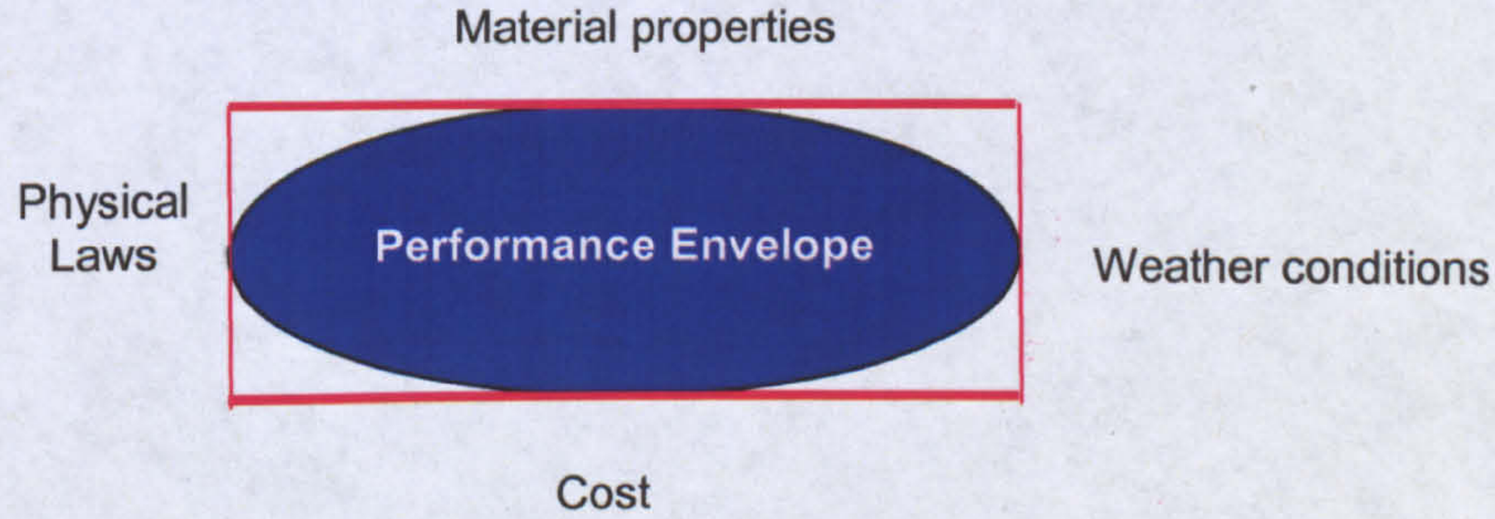

Chapter Map

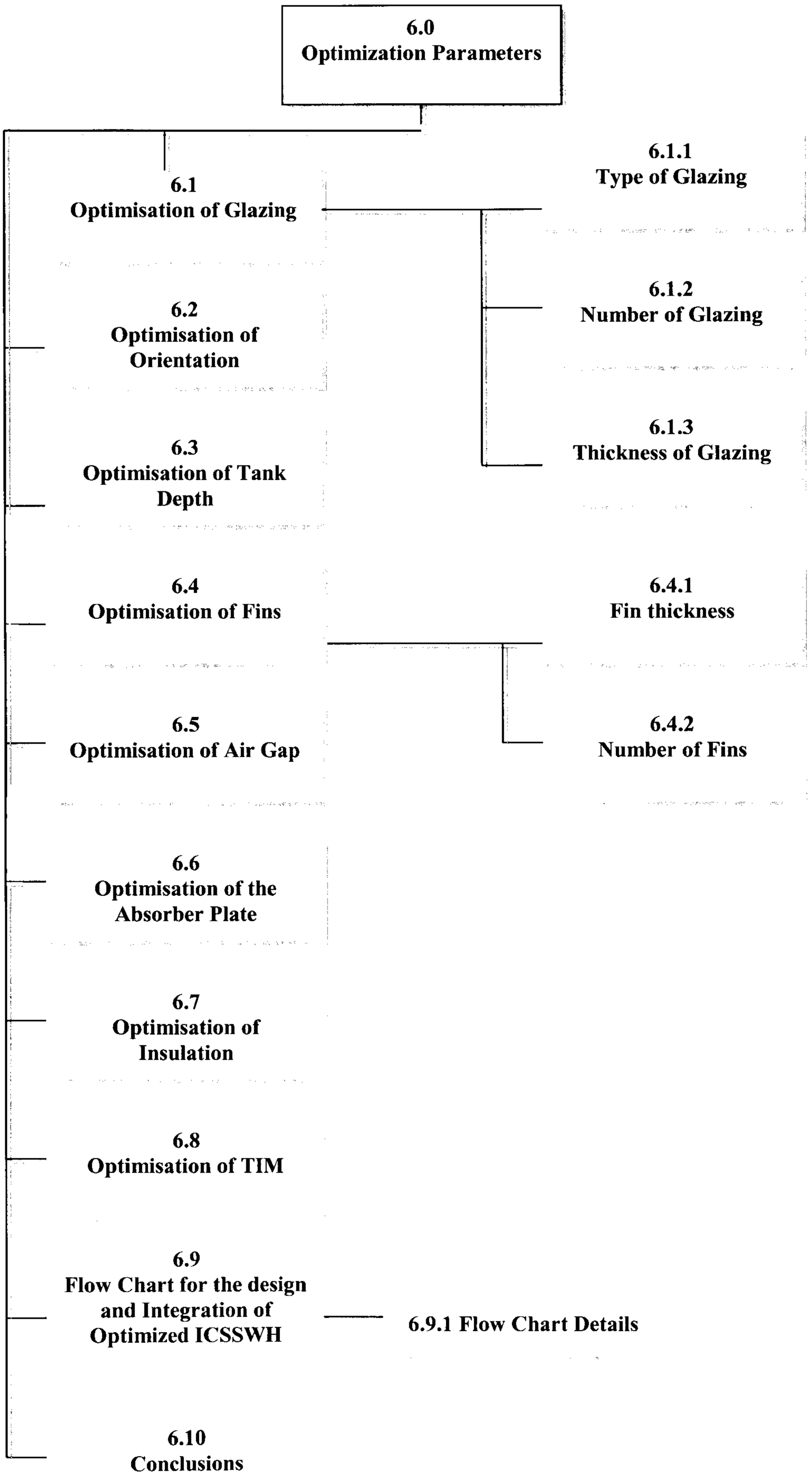
6.0
Optimization Parameters
6.1
Optimisation of Glazing
6.1.1
Type of Glazing
6.1.2
Number of Glazing
6.1.3
Thickness of Glazing
6.2
Optimisation of Orientation
6.3
Optimisation of Tank Depth
6.4
Optimisation of Fins
6.4.1
Fin thickness
6.4.2
Number of Fins
6.5
Optimisation of Air Gap
6.6
Optimisation of the Absorber Plate
6.7
Optimisation of Insulation
6.8
Optimisation of TIM
6.9
Flow Chart for the design and Integration of Optimized ICSSWH
6.9.1 Flow Chart Details
6.10
Conclusions

6.0 Optimisation Parameters

The results from experiments, ATA and CFD analysis, have provided an insight into the mechanics of heat transfer and the flow behaviour inside the collector. This has opened up new avenues for examining several "what –if" scenarios. The answers to these scenarios would lead to the best possible collector design that is effective both in terms of performance and costs.

The performance of the collector depends upon various factors. Few of these factors, that can be controlled are herein referred as the "design parameters". Some of these have been investigated in the previous chapters such as the air-gap, depth of the tank and the draw-off flow rates. The other design parameters, that include effect of fins, effect of glazing, effect of insulation, and the effect of the tilt angle, are further explored in this chapter. The sequence in which these parameters have been examined in this chapter is as follows.

a) Glazing
b) Orientation
c) Fins
d) Depth of tank
e) Insulation material

A prevailing concept surmises that increasing the performance of a system would increase the system cost (fig 6.1). This is a misleading statement as is revealed later in this chapter. Cost has been considered a boundary with its limit for the optimal collector to be £1000. Optimization carried out herein is not purely mathematical, where techniques such as linear programming are useful. Similarly, the cumulative effect of all the factors involved has not been considered. Only a step by step approach is adopted where each variable is assumed to have no influence over the other, to simply the solution.

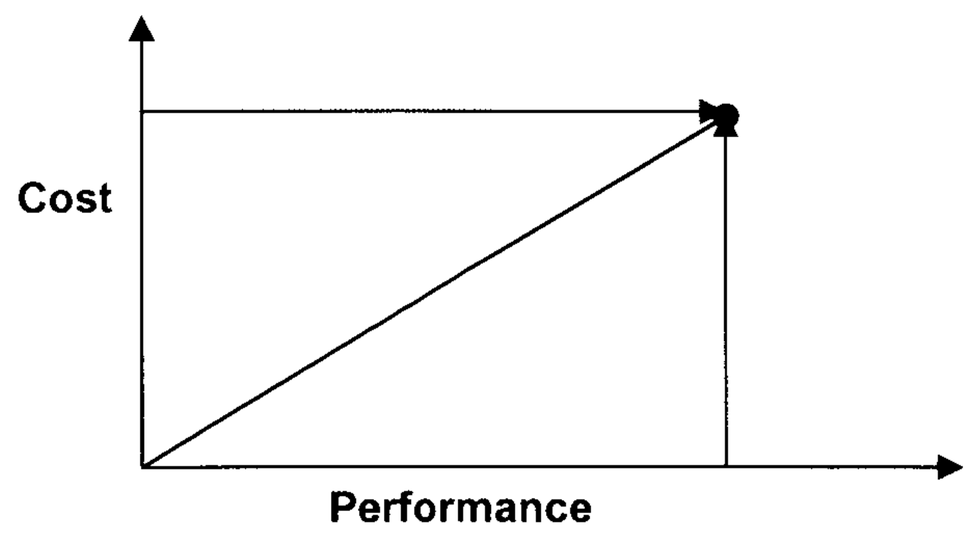

Figure 6.1: Hypothetical examination of Cost vs Performance

6.1 Optimisation of Glazing

The objective of glazing is mainly to prevent heat loss by acting as a barrier between the hot absorber plate and its surroundings. To estimate the number of glazing, glazing thickness and the distance between successive layers of glazing; a useful step at the outset is an overview of the composition of radiative and convective losses. This helps to assess if substantial convection loss exist, as the selection of glazing is more oriented towards reducing convective losses whereas coatings (for selective surfaces) reduce radiative losses. For this purpose the simulation (ATA) that was presented in chapter 4 has been revisited. The composition of the total losses achieved from the simulation is depicted in table 6.1 after a 24 hour cycle.

Table 6.1: The Convective and Radiative losses at $\phi = 45^{\circ}$

$Q_{Imposed}$ (Watts)	$Q_{Radiation}$ (Watts)	$Q_{Convection}$ (Watts)	Radiation/ Convection loss ratio
100	28	36	0.77
200	57	73	0.78
300	91	110	0.82
400	127	149	0.85
500	166	188	0.88

It can be seen from Table 6.1 that with the increasing heat flux, the ratio of radiative losses to convective losses increases. Nonetheless, it can be said with certitude that convection makes up over half of the total losses. These losses are significant and go well over 50% after the equilibrium state is achieved. The fact that the tests were carried out in laboratory suggests that in field conditions, severe winds in Scotland would further increase the convective losses.

6.1.1 Type of Glazing

As discussed earlier, various types of clear polymer sheets can be used as the top cover. These include Polymethyl methacrylate, Polyvinyl fluoride, Polyflourinated ethylene propylene (PTFE), Polytetrafluoro ethylene (PVF) and Polycarbonate.

The most common clear polymer cover is Polymethyl methacrylate (PMMA) which is normally sold under the trade names of **Plexiglas** or **Perspex**, and is more commonly

called **acrylic glass** or simply **acrylic**. Although PMMA has superior transmittance qualities compared to glass it is however softer and can easily get scratched. The other common material is polycarbonate; that too has high transmittance compared with ordinary flint glass. Table 6.2 shows the cost for various types of covers. It can be noticed that Plexiglas has the lowest cost however it has two disadvantages the first that it can be easily scratched thus blurring the surface and making it opaque. this can happen in case of hailstorm.. The second drawback is that the upper working temperature is very low i.e. 50°C -90 °C. If these temperatures are achieved- which is very much a possibility during summer- rapid degradation of the polymer would occur. This deterioration will outgas the polymer sheet, depositing a haze of condensed oily liquid on the inside surface of the glazing. Such haze will seriously reduce the collector efficiency. The use of plastics may also result in limitations or restrictions of collector use in high fire-risk residential zones by local building and safety departments. The thermal conductivity of all these materials are less than 1 W/mK and thus conductivity is insignificant in determining the choice for cover.

The superior transmittance of the polymers is countered by special high transmittance glass such as *Optiwhite Monolithic* glass by Pilkington. This glass has a transmittance of 0.91. Similarly, *Innosolar Energy* [2] a Chinese manufacturer also reports transmittance values of 0.91 for a 4mm thick glass.

An encouraging prospect is that the price of high transmittance glass is similar to ordinary flint glass. Therefore, in light of these features, it is clear that glass is the optimal choice. Nonetheless, polymer covers can be reconsidered if the weight of the collector is an issue.

Table 6.2: Cost matrix for different cover materials

Type	Thickness (mm)	Sheet Dimensions (mm)	Cost (£)	k W/(m·K)	Upper Working Temp (°C)	τ
Plexiglas	2	3050 x 1525	46.93	0.17-0.19	50 - 90	0.92
	3	3050 x 1525	70.42			
Poly -carbonate	2	3050 x 1525	106.29	0.19-0.22	115-130	0.90
	3	3050 x 1525	155.44			
Low Iron Glass[1]	6	1000 x 1000	57.75	0.78	>>500	0.89
Clear flint Glass	4	1000 x 1000	57.60	0.78	>>500	0.80
Toughened Flint Glass	4	1000 x 1000	104.60	0.80	>>500	0.70

Losses due to reflection are of the order of 7-8%. Pattern press on the glass decreases the reflectivity and so does an anti-reflective coating; thus total transmittance of up to 97% can be achieved through glass cover. It was noted in literature review, that low tempered plate glass of low-iron content possesses the highest transmission and lowest reflection. As the cost premium for low-iron glass is smaller than the increase in efficiency, so it is best suited for the final design. It is also important that absorptance of the cover should also be very low.

Some commercial concerns, for instance Solar Harvester, employ the use of Perspex (3mm acrylic geothermal cover with 89% transmission) for glazing purposes [3].

6.1.2 Number of Glazing

It has been underlined in several studies that increasing the number of glazing results in the reduction of heat losses. A study of windows by Muneer et al [1] for instance, reveals an interesting picture -as shown in figure 6.2 -which indicates various types of windows along with their heat loss coefficients. It can be noticed that the "U" value for triple and double glazed windows is substantially lower than single glazed windows. Similarly, performance of up to six glazing by Bishop [4] was inspected for extreme weather conditions of Denver, USA and encouraging results were reported.

---

[1] Pilkington Optiwhite

There are however a couple of setbacks associated with increasing the glazing layers; it not only raises the cost but also increases the transmission and reflection losses. Any loss in transmission results in direct reduction in collection efficiency.

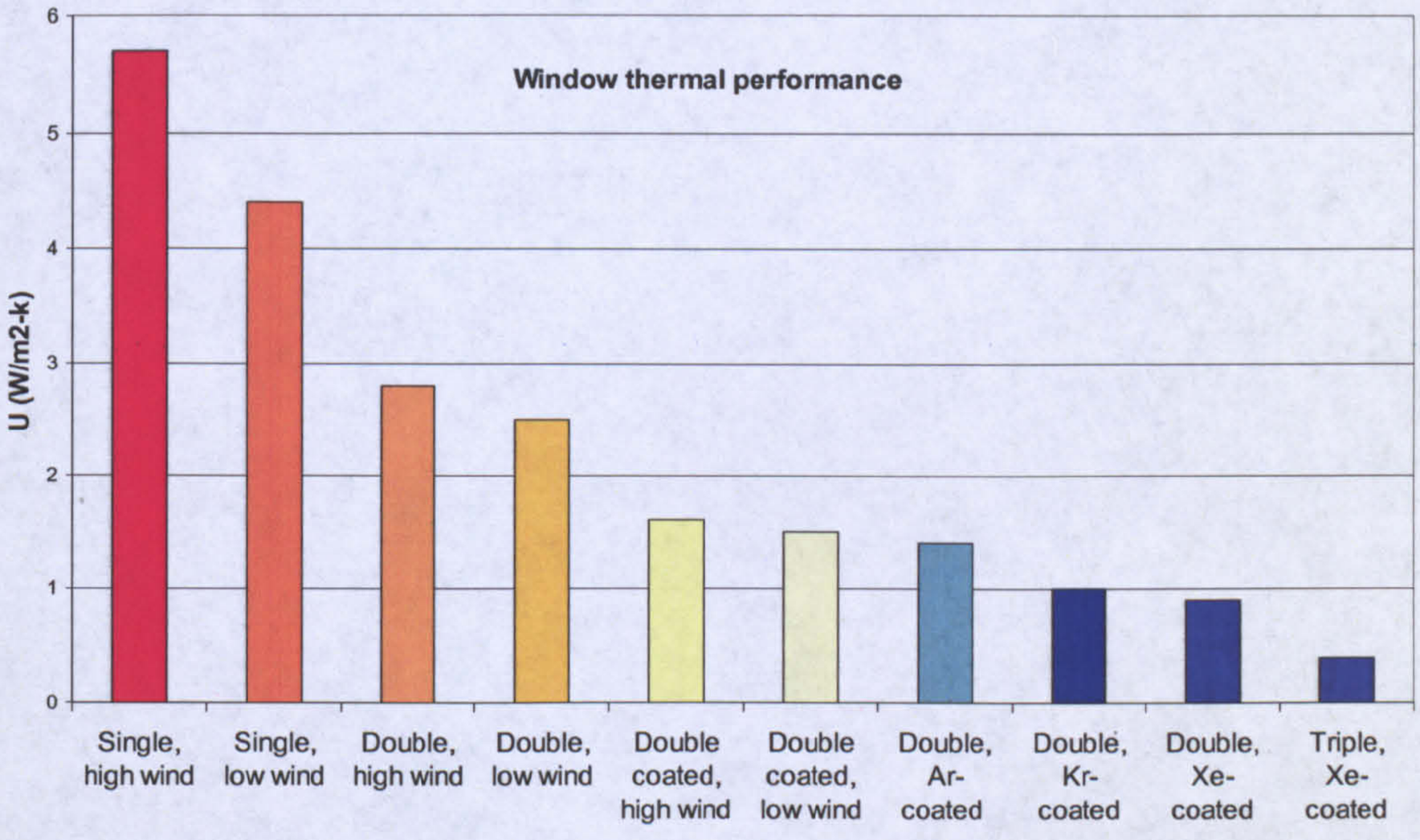

Figure 6.2: The U values for various types of windows[1]

Table 6.3: Window types and their U values

Window Type	U (W/m2-k)
Single, high wind	5.7
Single, low wind	4.4
Double, high wind	2.8
Double, low wind	2.5
Double coated, high w	1.6
Double coated, low wir	1.5
Double, Ar- coated	1.4
Double, Kr- coated	1
Double, Xe- coated	0.9
Triple, Xe- coated	0.4

The transmittance for single, double and triple glazed collectors has been inspected by Duffie and Beckman [5]. In figure 6.3 the transmittance of glass covers (refractive index 1.526) with the angle of incidence is shown. This figure is a reconstruction of the original figure for the measured transmittance performace reported by Duffie and Beckman.

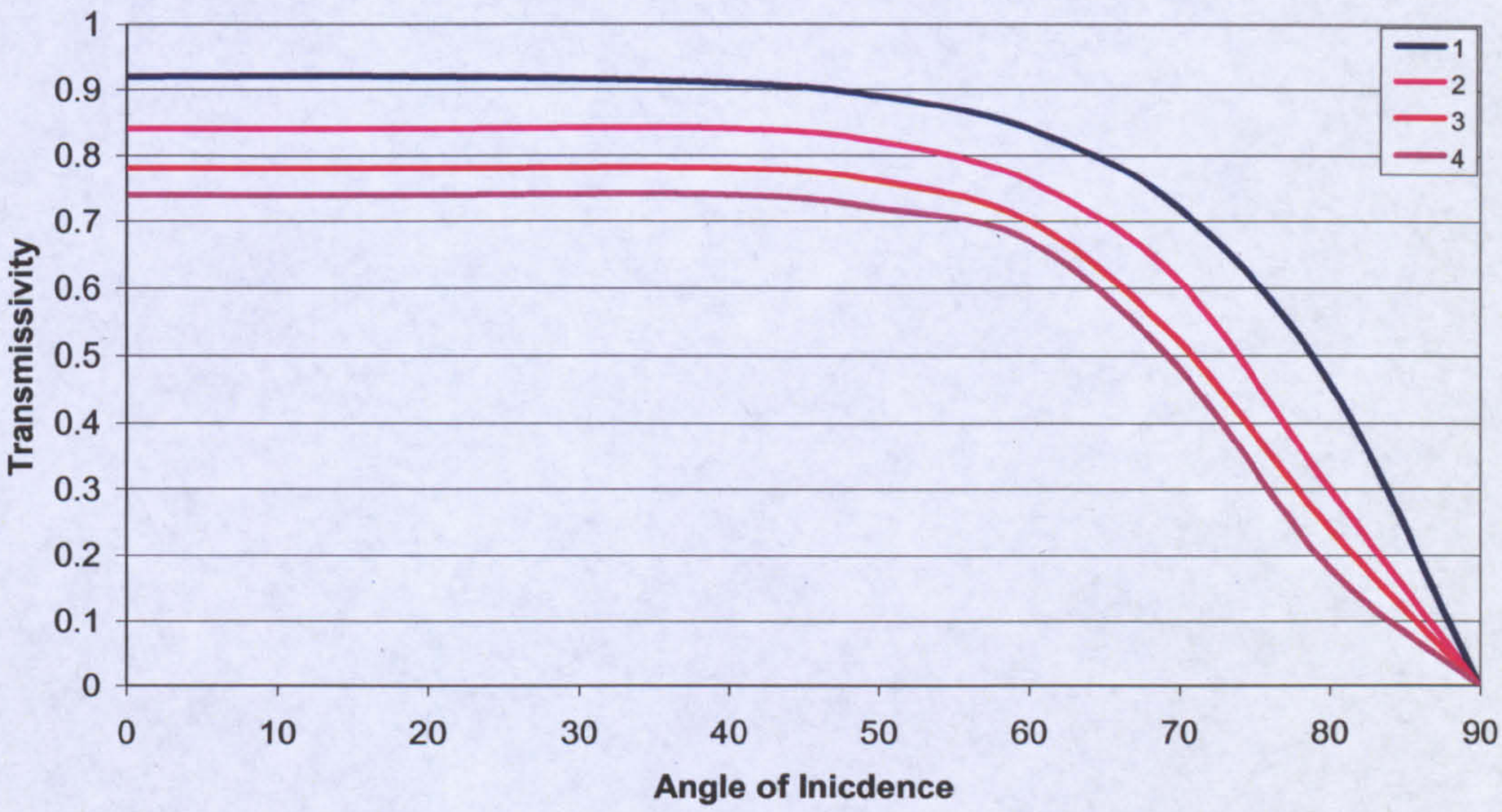

Figure 6.3: The transmissivity for 1, 2, 3 and 4 covers for non-absorbing glass covers

Fig 6.3 confirms that the choice of single, double or triple glazed non absorbing glass is an option as there is not a substantial decrease in transmissivity particularly between single and double glazing. This leaves the cost as the deciding factor for the glazing layers. Commercial solar hot water system providers such as *Solar Twin* systems employ double glazed covers for their collectors.

6.1.3 Thickness of the Glazing

Glass is available in various thicknesses based on the applications and standards. The glass thickness for a collector is decided mainly considering the wind load. The usual glazing thickness in buildings is from 3mm to 5mm while they are available in thickness of 2.5 -12mm. In the prototype collector, 4mm thick flint glass was used.

Increase of glass thickness results in the increase of transmission losses. On the positive side, it also results in increasing the conductive resistance. This poses a contradicting situation and therefore it is interesting to notice how these two parameters compare against one another. Table 6.4 illustrates the drop in transmissivity for Pilkington *Optiwhite Monolithic* glass. It can be seen that the

thermal conductive resistance value for the glass is very low and increase in thickness does not result in an appreciable increase in the conductive resistance. It can also be noticed that the transmittance goes down with increasing thickness however this drop too is insignificant. Therefore a better way forward, with the aim of minimizing losses, is not to increase the glass thickness but to increase the number of the glazing.

Table: 6.4: Conductance and transmittance of Optiwhite Monolithic Glass

Glass Thickness	Conductive Resistance	Transmissivity
mm	x/k	τ
3	0.00384	0.9
6	0.00769	0.89
10	0.01282	0.87
12	0.01538	0.86

The increase in the glazing not only increases the conductive resistance but also adds convective resistances between the absorber and 1st layer as well as between successive layers.

6.2 Optimisation of Collector Orientation

A general rule of thumb for collector orientation is that of a south facing roof with an angle 0.9 times the latitude of installation to be the optimal for maximum interception of insolation[5]. For extreme latitudes angles can be changed to $\phi \pm 20$ degrees (decreasing angle during summer, increasing it during winter) to further enhance solar gain. Although this rule is followed universally it is however intriguing to gauge its accuracy on the basis of its unspecific nature.

Using 27 year data for Edinburgh, the best possible orientation was evaluated. The results of insolation interception by a titled plane are plotted in fig 6.4.

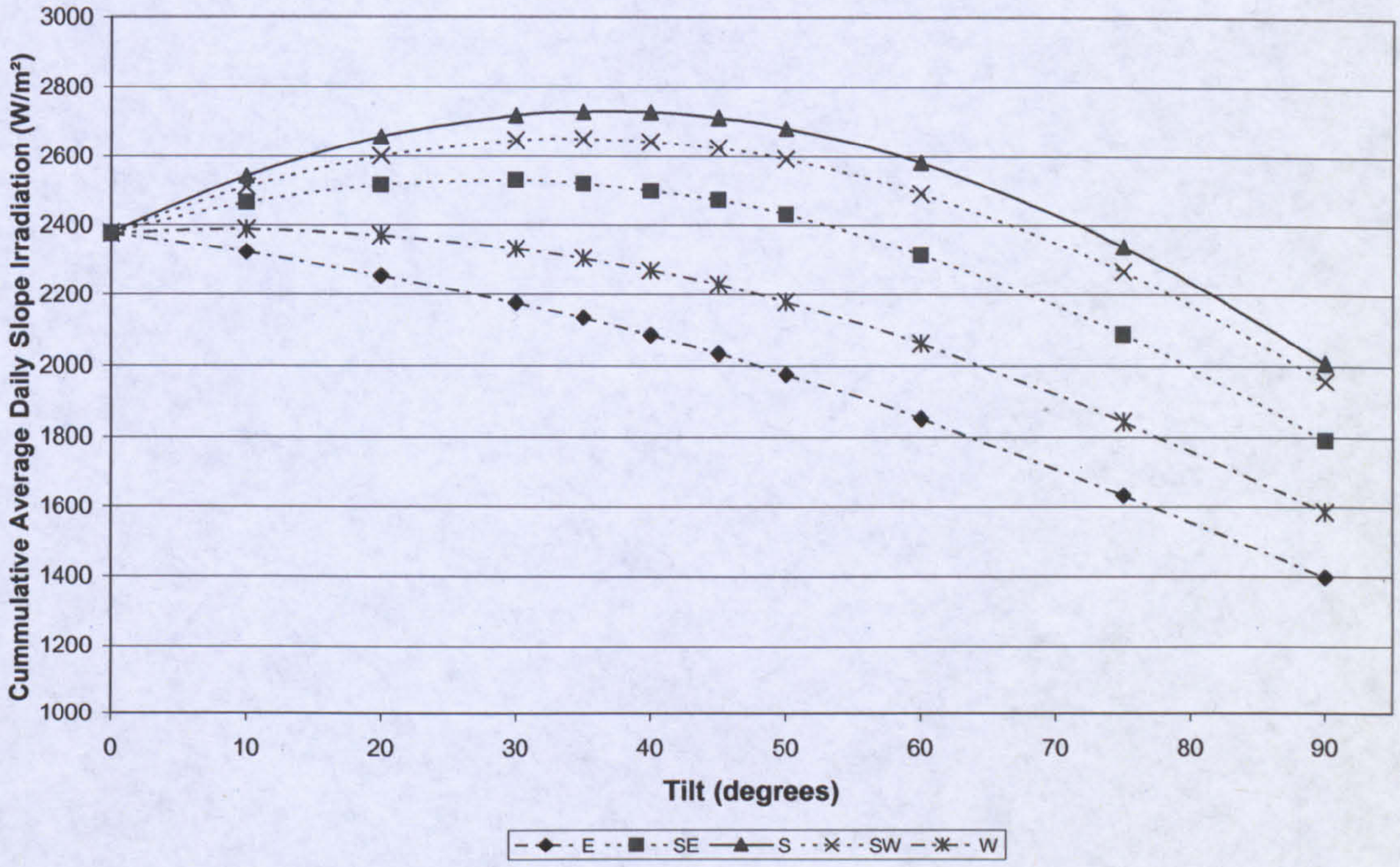

Figure 6.4: The slope irradiance with the tilt angle for Edinburgh.

From fig 6.4 it comes out that the optimal angle is 35˚as opposed to 49.5˚ suggested by the rule of thumb (55˚ being latitude for Edinburgh). It confirms that a south facing roof is the best direction. This result is encouraging as most roof slates in Scotland are angled between 33˚ and 36˚ for optimum performance. Roofs with steeper or shallow angles also exist where aesthetics overcome passive heating consideration.

In a published article co written by the author [6], it was calculated that the performance of the collector increases if ϕ is increased. This is because of the dual effect i.e. the losses through the air gap reduce with increasing angles whereas the heat gain is promoted with increasing angle. The "h" values are in the figure are both for the water tank and the air cavity.

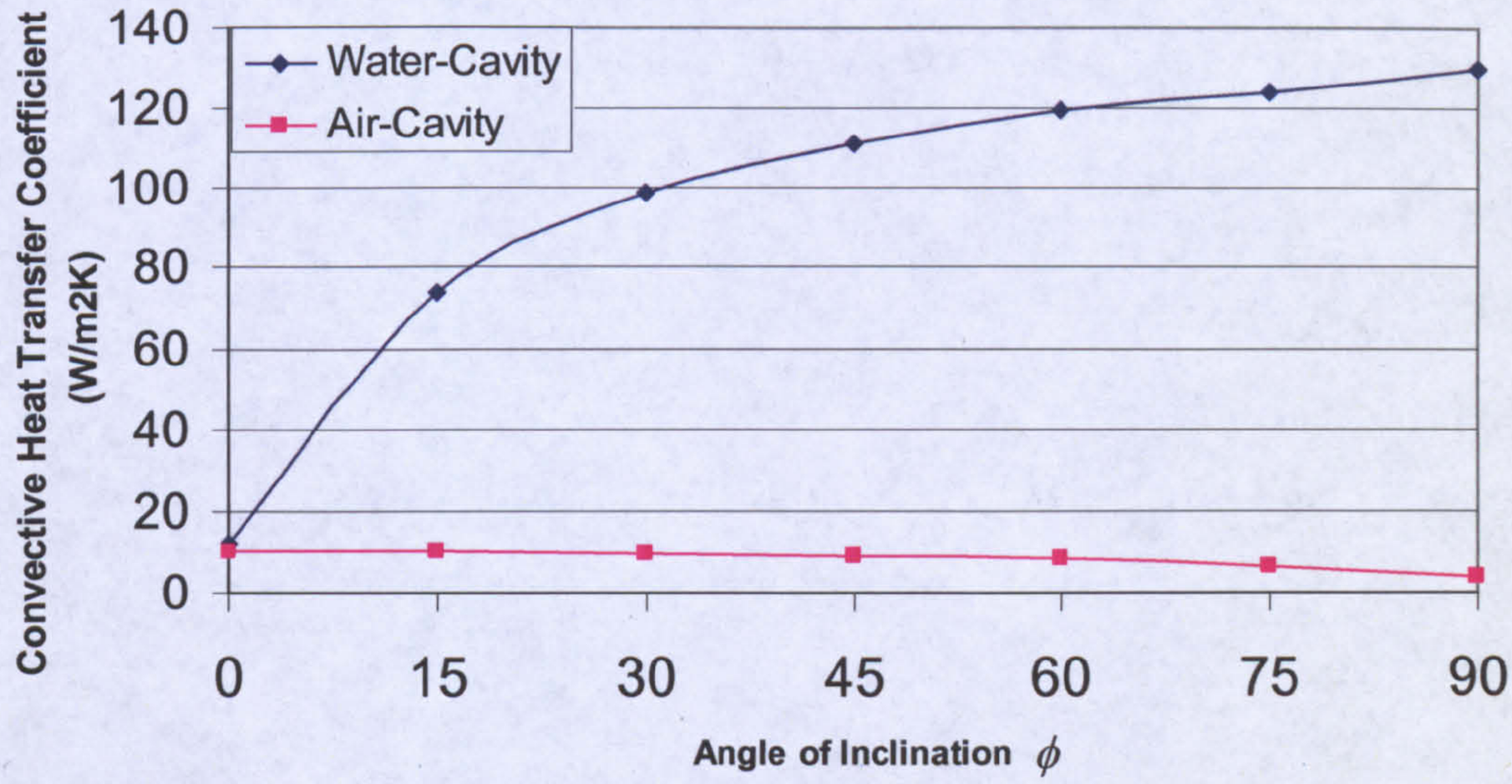

Figure 6.5: The heat transfer coefficient for air and water cavity

In fig 6.5, the heat transfer coefficient of the air-cavity and water tank are depicted. It can be for the air-cavity the heat transfer coefficient decreases with the increase in tilt angle whereas, the trend for water cavity is vice versa and is more pronounced. Combining the results depicted in fig 6.4 and 6.5 it is can be deduced that a slight comprise in insolation can lead to an overall improved performance. The slope irradiance for 35° and 50° facing south shows a difference of only 1.6 % (irradiance values of 2727 W/m^2 and 2681 W/m^2 respectively). The Nusselt number value of water-tank at 50° (Nu = 9.48) however is greater than the value for 35° (Nu = 8.56), a difference of 10.7%. It can also be noticed that the decline in irradiance is steeper after the ϕ=50°. Thus the ICS water heaters inclined at 50° will thermally perform better compared to a heater mounted at 35°. The other advantages are that higher inclination would give the heater a seasonal bias during the winter months when the requirement of hot water is greater.

6.3 Optimisation of the Tank Depth

For an ICS heater, the depth of the water tank is a parameter of paramount importance. The depth of the tank is basically tied to the following:

a) The level of insolation at the site of collector installation
b) The desired water temperature.
c) Consumption of hot water

Absorber plate area to collector volume ratio is also important (see section 3.1.5). It has been noticed in previous studies –concurring with thermodynamics- that at lower operating temperatures of a collector, the losses are minimal. On the other hand, high grade energy (high temperature water) cannot be obtained if the collector is designed to operate on low temperatures although it may have a higher efficiency. Hence the efficiency improvement is not the ultimate goal. A performance criterion has to be established first before moving further. Ideally, hot water should be furnished at the desired temperatures. As in the current research, only the hot water usage for washing and cooking purposes is being considered, a temperature of 40°C can be taken as the required output temperature (see table 6.5). J.M.Z Cruz et al [7] in his article has also taken 40°C as the outlet temperature to estimate the annual savings by SWH. For the prototype finned collector, the time period for reaching a specific temperature at different levels of insolation is presented in table 6.6.

Table 6.5: Time for inflicting a burn [8]

Temperature of water	Time to cause a bad burn
66°C	2 seconds
60°C	6 seconds
52°C	2 minutes
49°C	10 minutes

Table 6.6: Times for temperature rise

Heat Flux Watts	**Initial water temp ˚C**	**Time taken to reach 40˚C**	**Ideal time with starting temperature of 20˚C**
100	20	not achieved	696 min
200	20	500 min	349 min
300	20	260 min	234 min
400	20	250 min	174 min

* The average temperature of water, simulation does not take into account the stratification

The column for "ideal time" depicts the time period for 100% absorption of imposed energy by the collector (zero heat losses). The former column depicts the time period taken to reach the specified temperature (40˚C) with the inclusion of losses. Thus even with a constant heat flux of above 400 W, it would take more than 4 hours for the whole body of water to reach an average temperature of 50 ˚C. The insolation levels should be even higher to account for the optical efficiency. In this respect it would be of value to probe into insolation levels in Scotland. The sunshine hours for the insolation bands of 0-100 W, 100-200 W, 200-300W and 300-400W should be evaluated through weather data.

A break up of hourly solar insolation is presented in fig 6.6 and 6.7. It can be noticed that spells of insolation for the band 100 -200 W are more frequent as compared to spells of radiation over 200, 300 and 400 W. This gives a clue to water tank depth by highlighting that the design should be such that it is more effective at lower insolation levels.

Increasing the depth more than 50 mm would mean longer time periods required for achieving 40˚C. Furthermore the weight of the SWH will also increase. On the other hand decreasing the tank depth results in lesser capacity and lower thermal inertia. Thermal inertia is important in case of extreme weather conditions as it provides a degree of protection for freezing and boiling. On this basis it can be said with reasonable degree of confidence that 50 mm thickness is suitable for collectors in Scotland if water temperature at 40˚C is required.

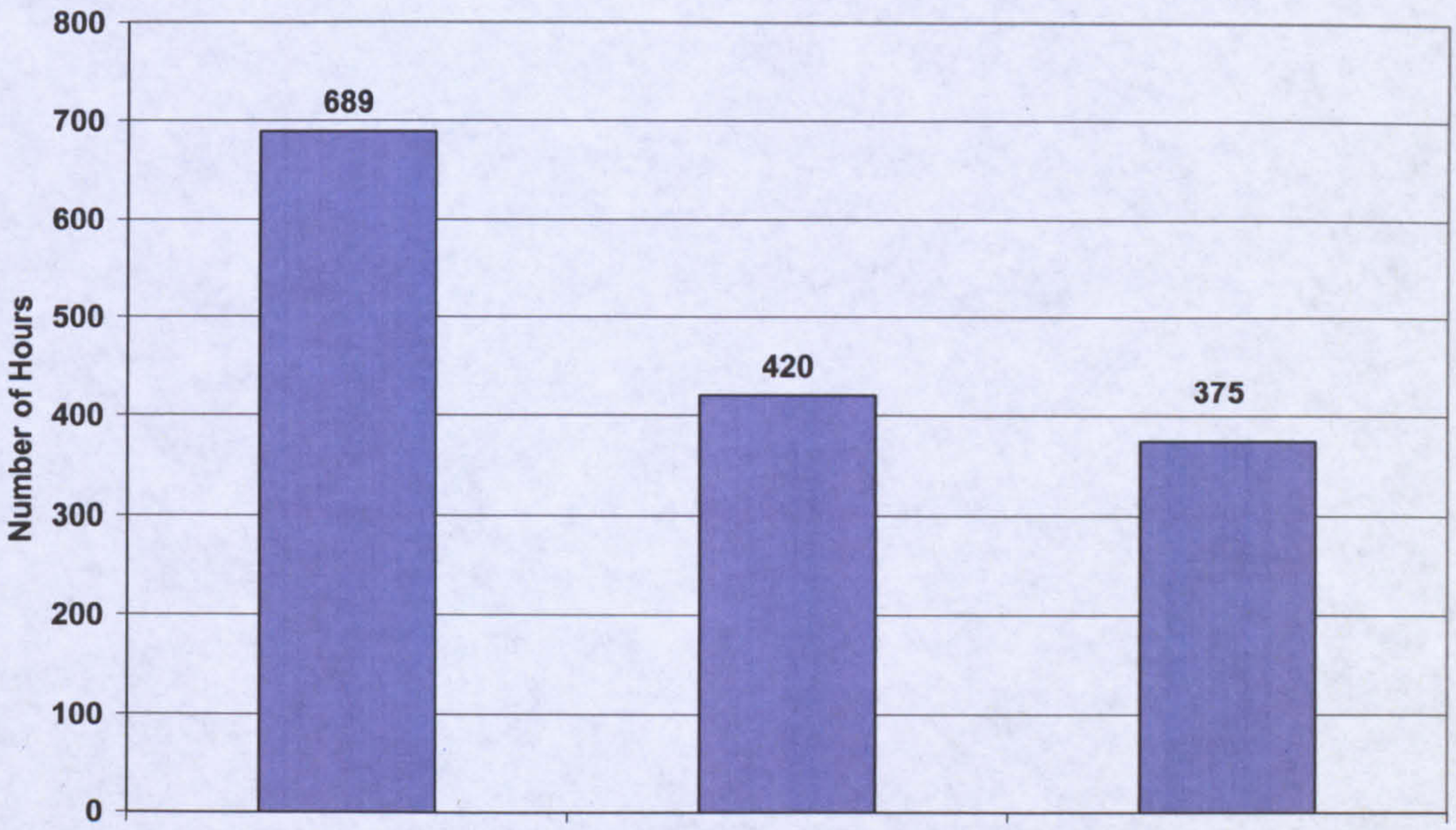

Figure 6.6: Number of hours in a year for the insolation bands

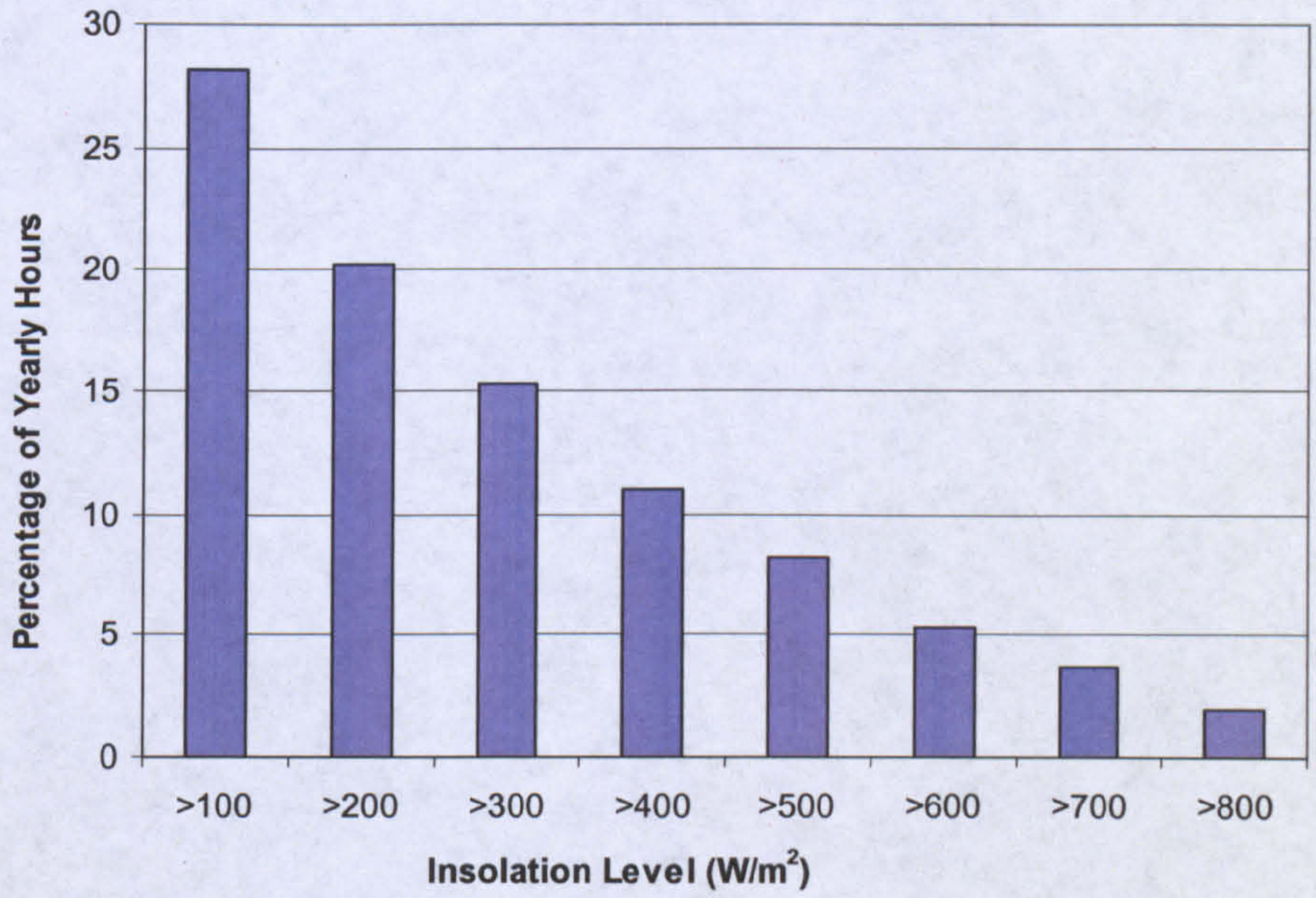

Figure 6.7: Number of hours in a year for different insolation bands

6.4 Optimisation of Fins

The optimisation of fins is a broad topic in itself and is only briefly touched herein. It was noted in the previous chapters that fins improve heat transfer. The apparent explanation for this was that fins transfer the heat to the bottom cooler, sections of the fluid and the additional thermal and consequent development of a velocity boundary layer enhances advection and hence heat absorption. A total of 4 fins were placed at

distance of 200mm from each other. To calculate the optimal number of fins, a deeper understanding of fin mechanics is required. Similarly the issues regarding the cost –benefit comparison of fins can be answered with more certainty.

The fin performance is influenced by the following:

a) Depth of the water tank
b) The angle of the water tank
c) Thickness of the fins
d) The dimension of the cross-section of the tank
e) Stratification inside the tank

6.4.1 Fin Thickness

Fins were made out of the same sheet as the collector tank. Therefore the cross-sectional thickness of the fins was 1.5 mm. Detailed diagram of the fins is presented in chapter 3. It is recommended to keep thin fins as compared to thicker fins. The reason for this being that heat goes to a greater depth in a thin fin for the same heat content as compared to thicker fins. As the objective of the fin is to transport the heat to the bottom cooler layers, thin fins would be more effective than thick fins. A slightly more detailed work in fin thickness can be found in the earlier work of Muneer et al [9] that quantitatively shows the drop in fin efficiency with the fin length and thickness.

6.4.2 The Number of Fins

Another interesting area of investigation is the number of fins. In the prototype collector, 4 fins were inserted with a spacing of 200 mm between them. The question of whether this being the best arrangement needs to be answered to estimate the optimal design. Because of the tilt of the heater a velocity boundary layer develops on the surface of the fins. A hypothetical representation of the velocity and thermal boundary layer is shown in fig 6.8.a

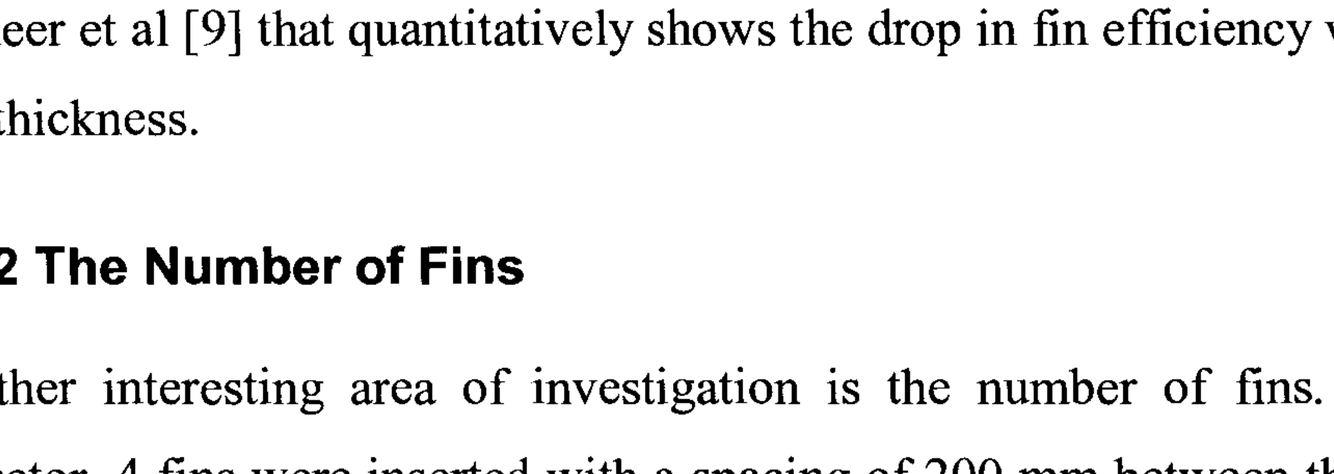

Figure 6.8.a: Hypothetical depiction of thermal and velocity BL

To resolve the fins, a 2D CFD analysis was carried out assuming outer face of the absorber plate (fig 6.8.b) at a constant temperature. The 2D cross section of two collectors with 4 and 6 fins were modelled in Fluent with the tilt angle assumed to be zero (cross-sections shown in fig 6.8.b). The heat absorbed by both the collectors was then calculated. A constant temperature of 313 K was set on the absorber plate with the fluid temperature being 293K. The 6- finned collector performs better at the start by supplying more energy to the water body. With the passage of time, the heat transfer rate decreases and eventually is surpassed by the 4-finned collector as the hot water starts accumulating at the top (see table 6.7). The accumulated hot water acts as a barrier between the cold fluid and absorber plate and has been defined earlier in detail in section 5.1.5. Form table 6.7 it can be noticed that the average temperature of the collector with 6 fins is higher, even though the heat transfer rates for 4 finned collector are superior after 40 minutes. From a practical point of view, it is advantageous to have rapid heating as solar radiation is intermittent and is unlikely to be available in long spells particularly in Scotland.

Table 6.7: The results for 6 and 4 finned collector

	20min	**30min**	**40min**	**60min**	**Average T (K)**
4 Fins	1324 J	969 J	725 J	415 J	310.2
6 Fins	1447 J	987 J	682 J	331 J	311.2

Thus 6-fins can be employed as they only marginally add to the collector cost. The behaviour of fins is inspected more deeply in fig 6.9 and 6.10 in which the results from 2D analysis have been shown. In the middle of cell of the water tank (the portion between the two fins in the water tank) the temperature profile can be seen decreasing logarithmically with the depth of the tank. It can also be noticed (fig 6.9) that due to accumulation of hot water beside the absorber plate (z- direction stratification), the fin temperature is lesser near the top end (next to absorber plate) of the tank. This indicates that fins are not transferring heat to the water accumulated at the top the vice versa however is true. This fact is also confirmed by fig 6.10 in which the heat transfer coefficient on the surface of the fin has been plotted. The negative heat transfer indicates the heat transfer from the water to the fin at the top portion rather than the other way around. Towards the bottom of the collector it can be seen that the fin contributes to adding heat to the cooler water. A bulge in the heat transfer

coefficient confirms this behaviour. Thus once the water gets heated and accumulates at the top, the fins are responsible for transporting heat from the hot water at the top the cold at the bottom. Fig 6.11 and 6.12 show the velocity and the temperature contours respectively of the area between the two fins.

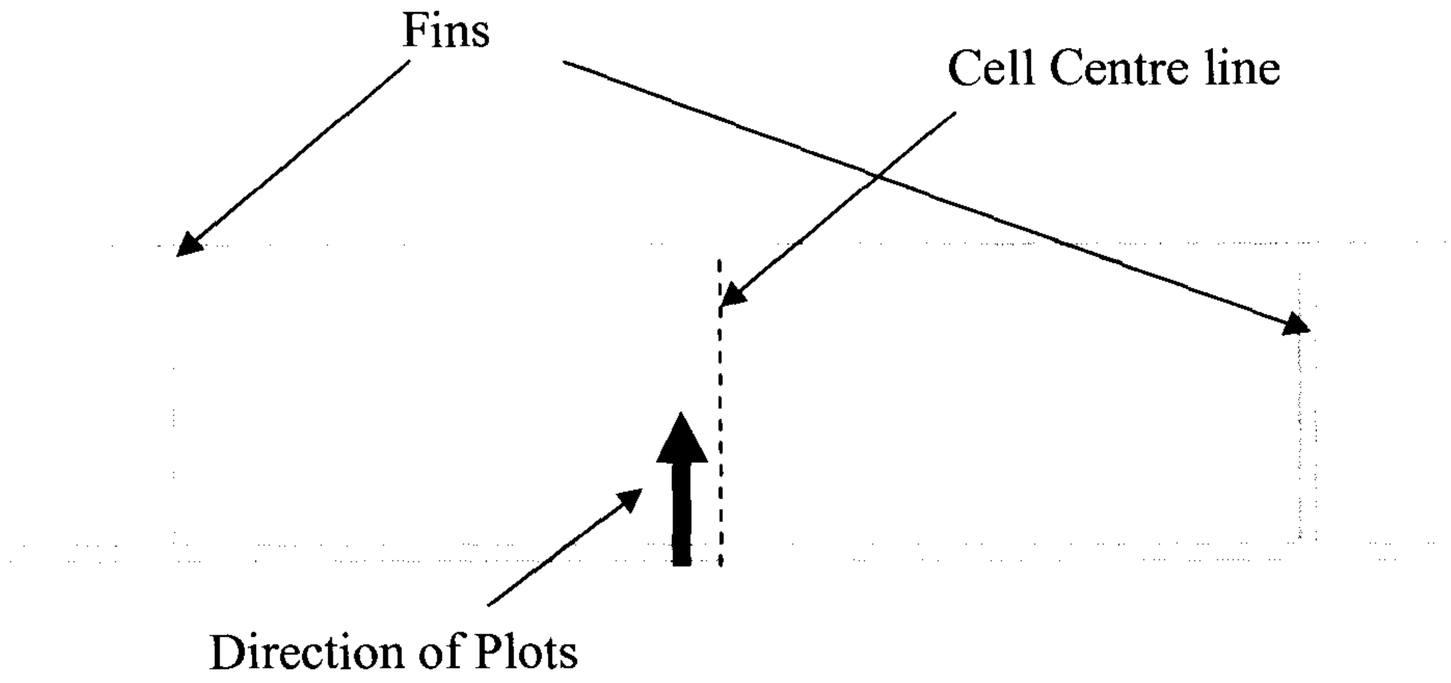

Figure 6.8.b: Geometry definition for CFD plots

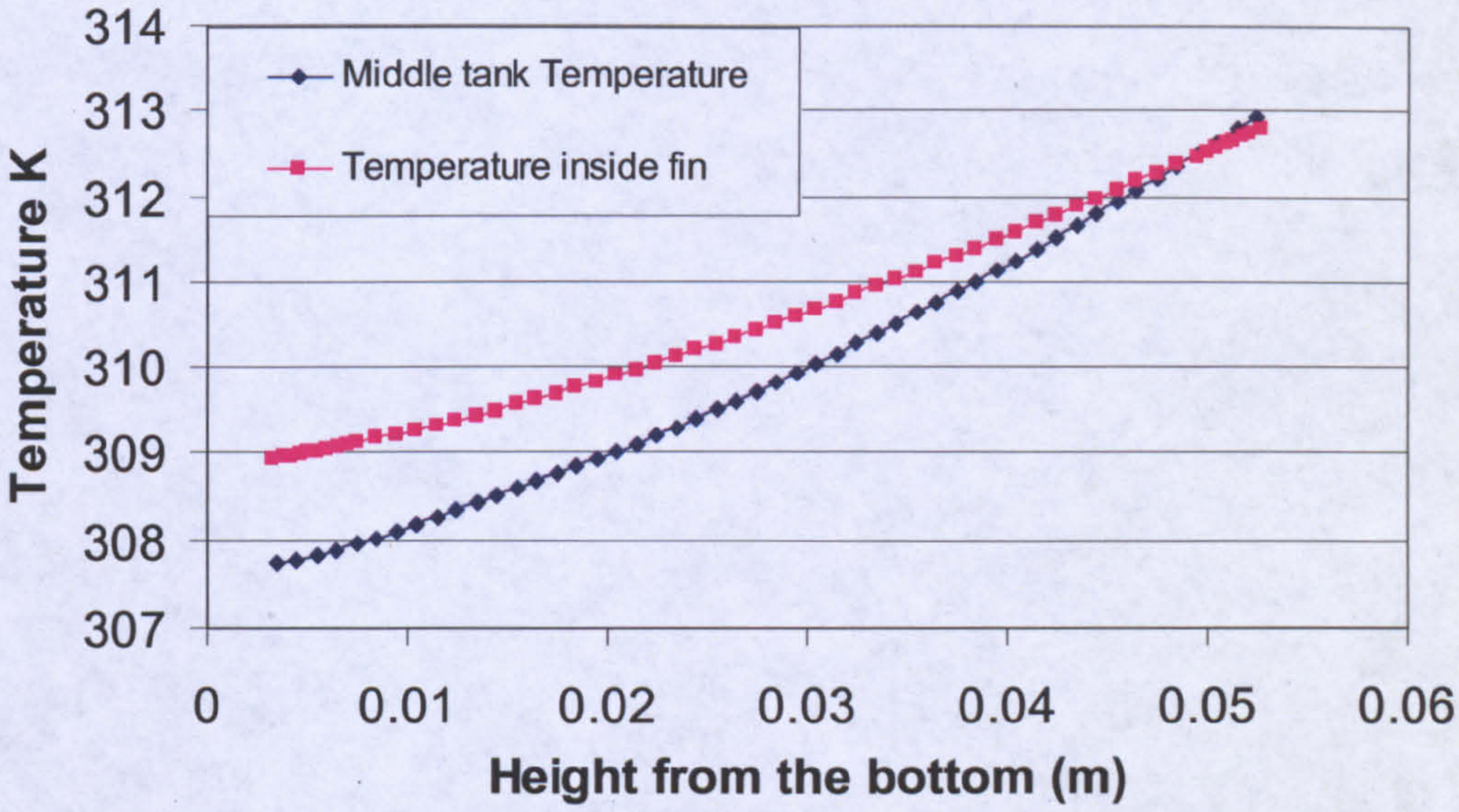

Figure 6.9: Temperatures inside the fin & the cell centre after 60 minutes

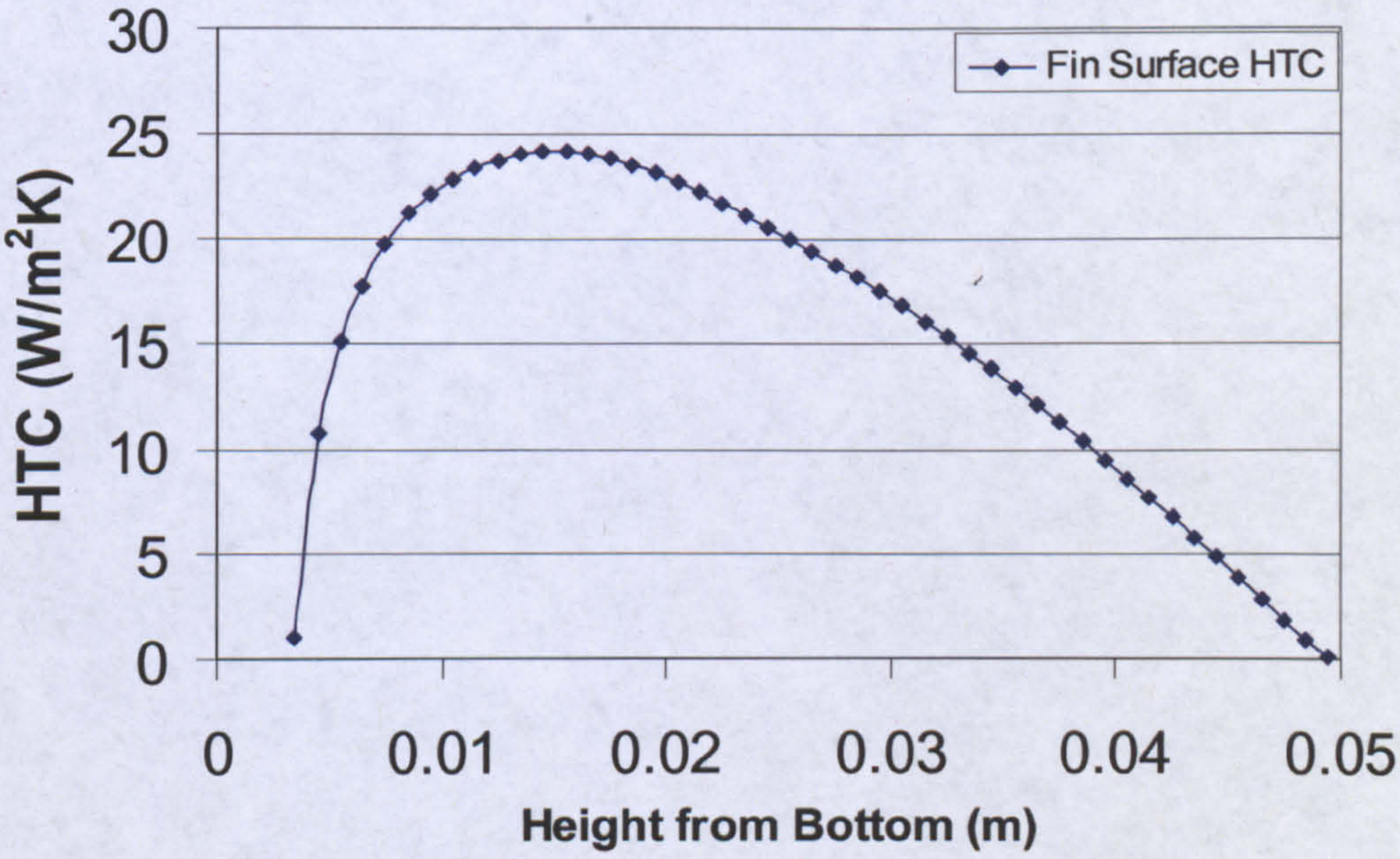

Figure 6.10: HTC on the fin surface after 60 minutes

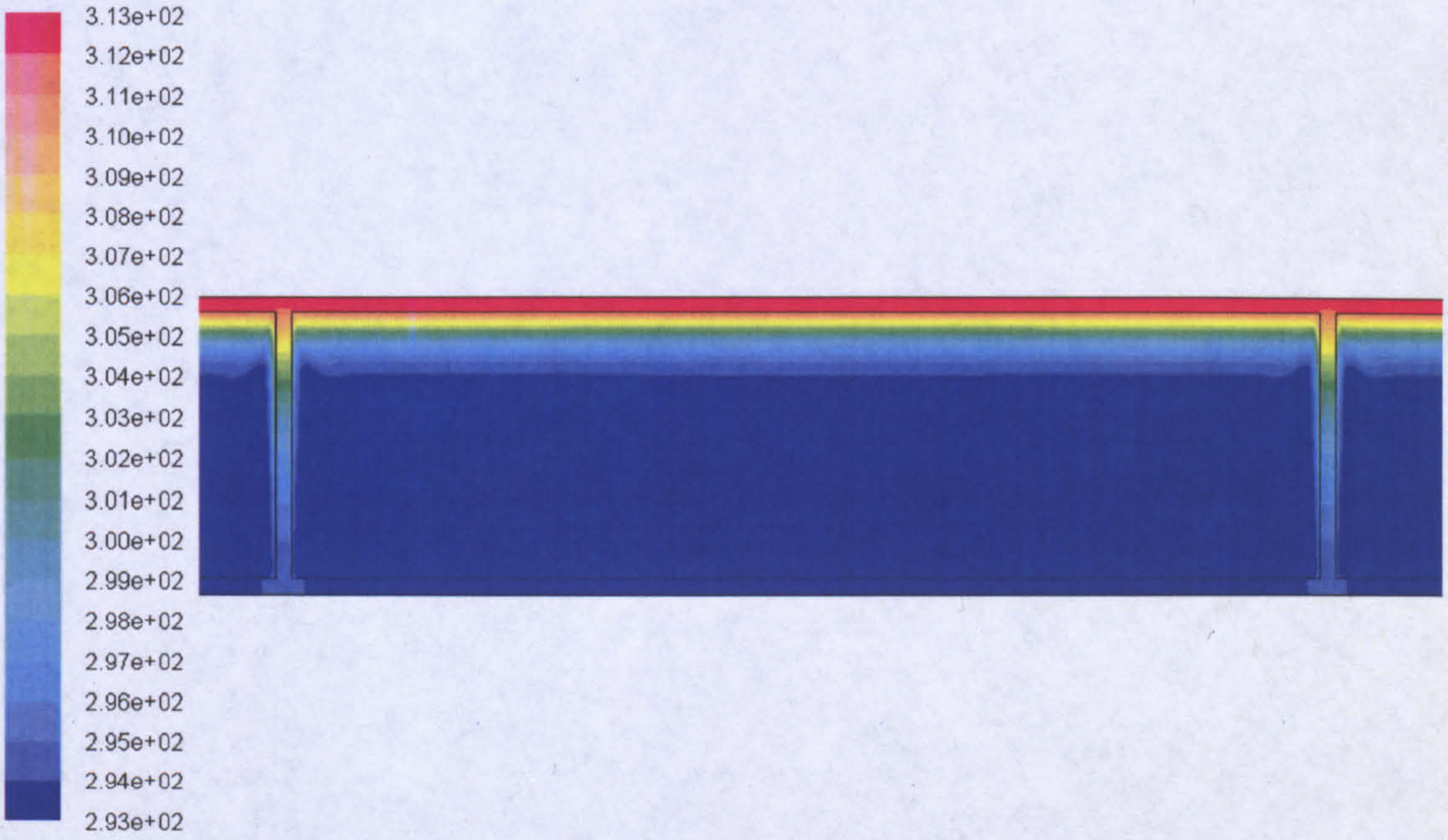

Figure 6.11.a: Temperature distribution after 60 sec

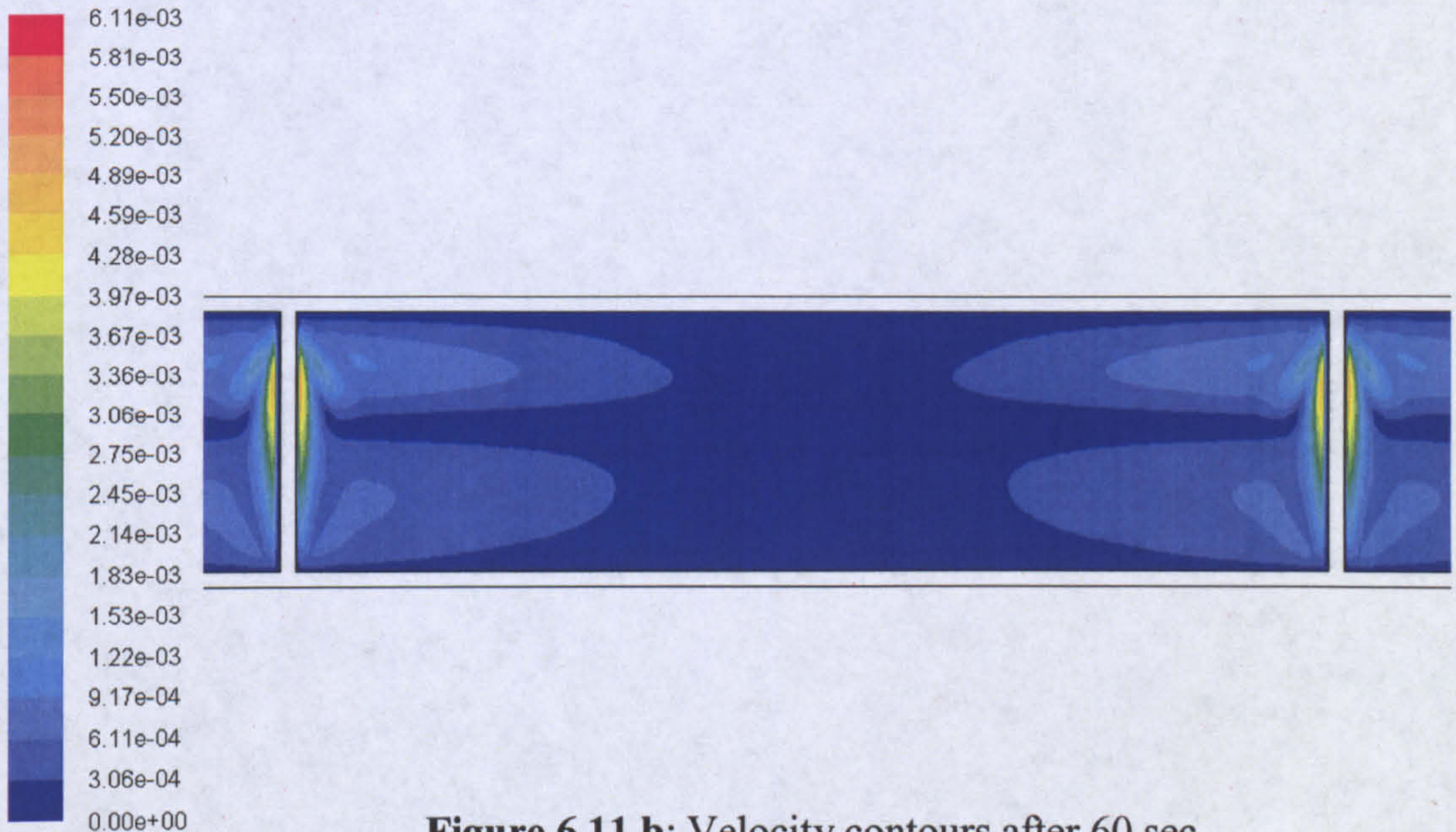

Figure 6.11.b: Velocity contours after 60 sec

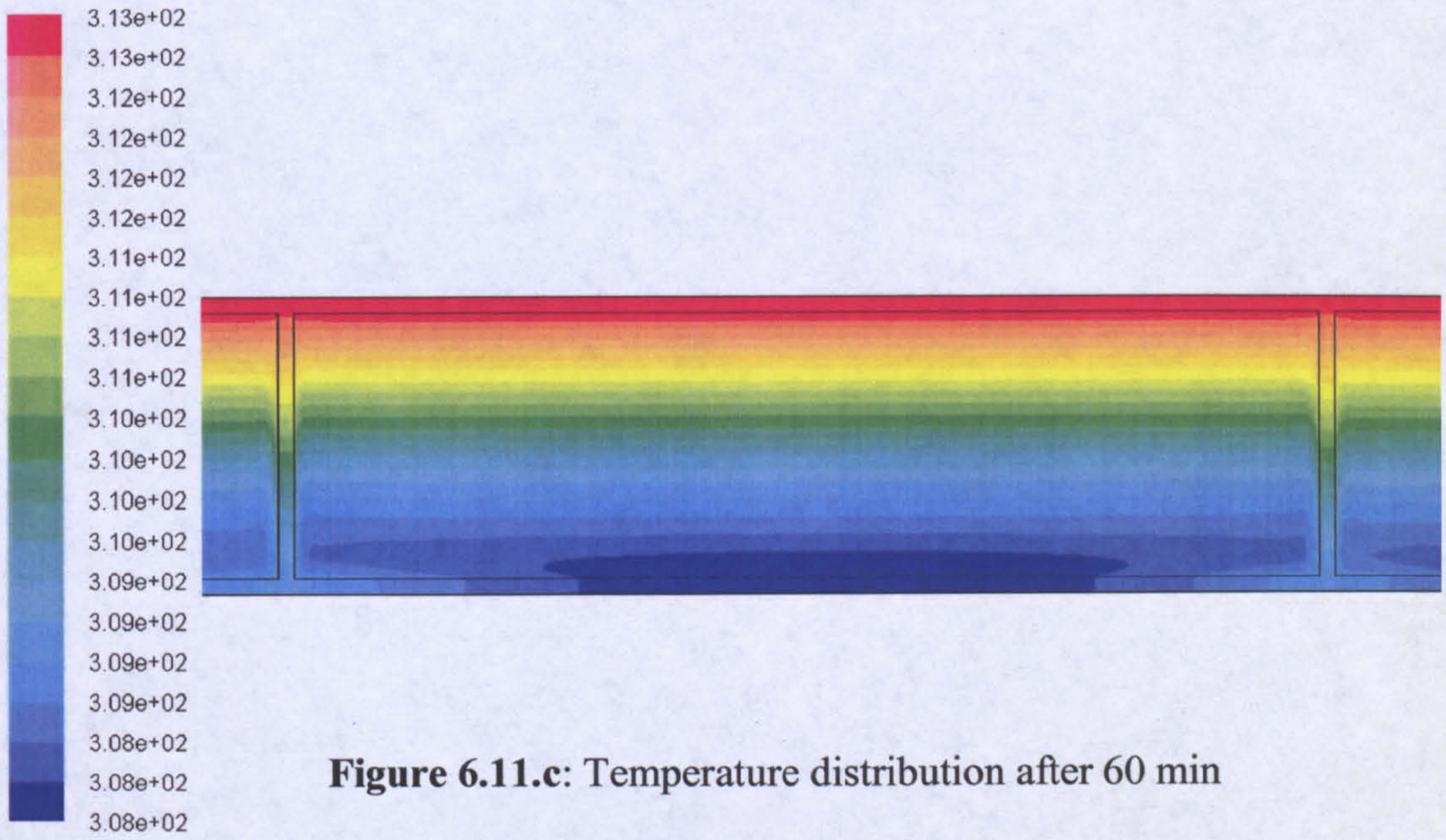

Figure 6.11.c: Temperature distribution after 60 min

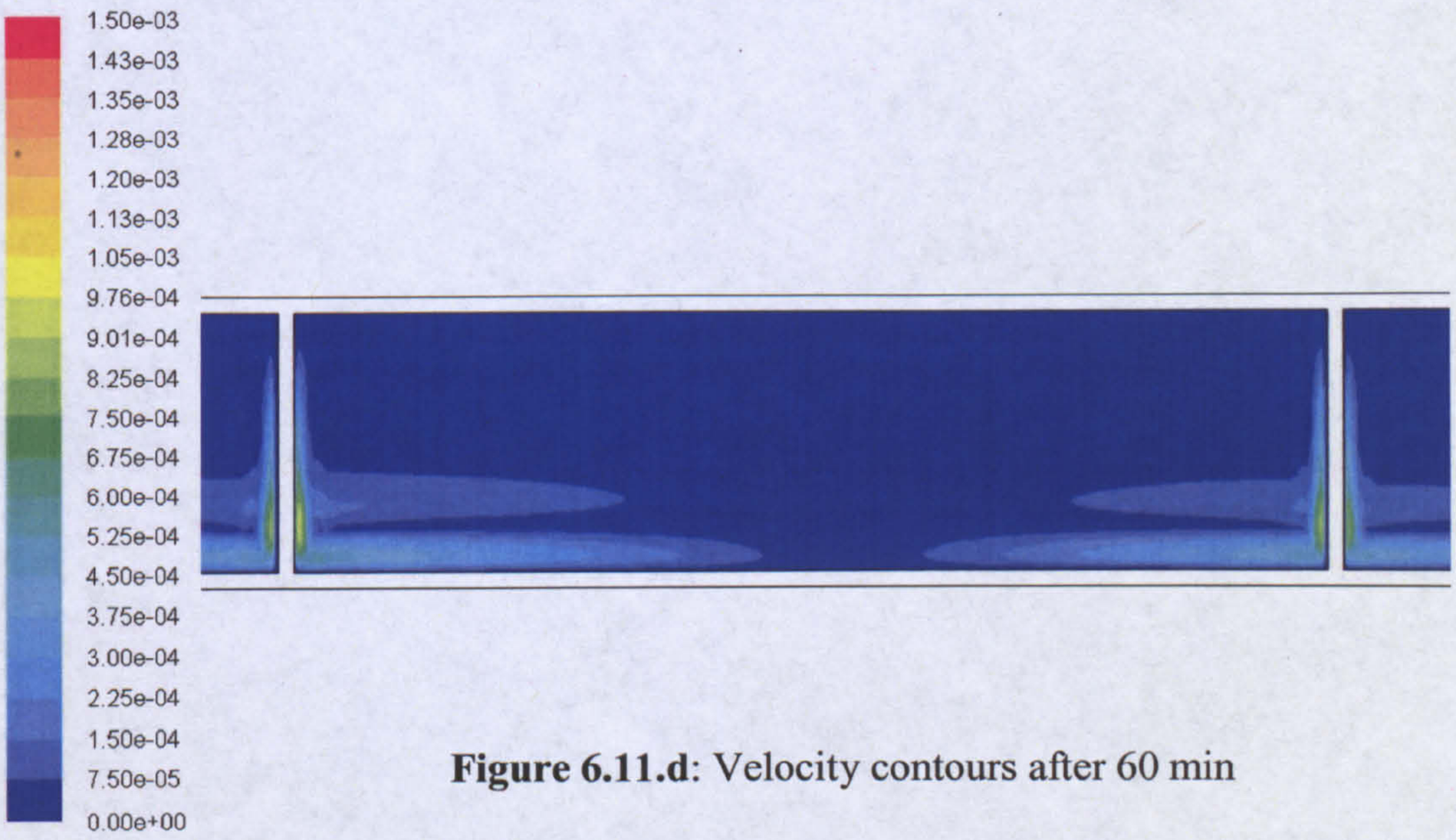

Figure 6.11.d: Velocity contours after 60 min

The spread of temperature increase with time can be seen in figures 6.11.a and 6.11.c. More importantly, the velocity magnitude can also be seen to drop as more and more body of water gets warmer. The fluid movement at the top (near the absorber plate) ceases as can be seen in figure 6.11.d. This is inline with the 3D analysis that was reported earlier in section 4.3.2.3. The stagnant body of water, in the middle of the fins is also evident in both 6.11.b and 6.11.d which initially lead to the idea of adding more fins so increase advection.

6.5 Optimisation of the Air Gap

The air-gap has been thoroughly reviewed in the previous chapters. From the earlier studies it can be gathered that there is no single depth of air-gap that would perform well at all locations. Changes have to be made as per the angle of inclination of the collector which is dependent upon the latitude of location. Similarly it is also vital to estimate the temperatures at which the collector is operating before settling the air-gap.

A larger air-gap proves better in the case of lower collector temperatures (mainly the water temperature in ICS). This is explained by considering pure conduction as the only mode of heat transfer (no convective rolls). In this case, the larger the air-gap the greater the conductive resistance and consequently, the lesser the heat loss.

At higher collector temperatures, the larger width of the air-gap results in aiding convection as it provides more room for air to move. In the prototype collector an air gap of 35mm was maintained. In fig 6.12- 6.17 the relationship between the Nusselt number, Rayleigh number and the width of the air-gap has been examined closely. The plotted were generated using Hollands' regression (eqn 3.8). The heat transfer coefficient (HTC) has also been plotted.

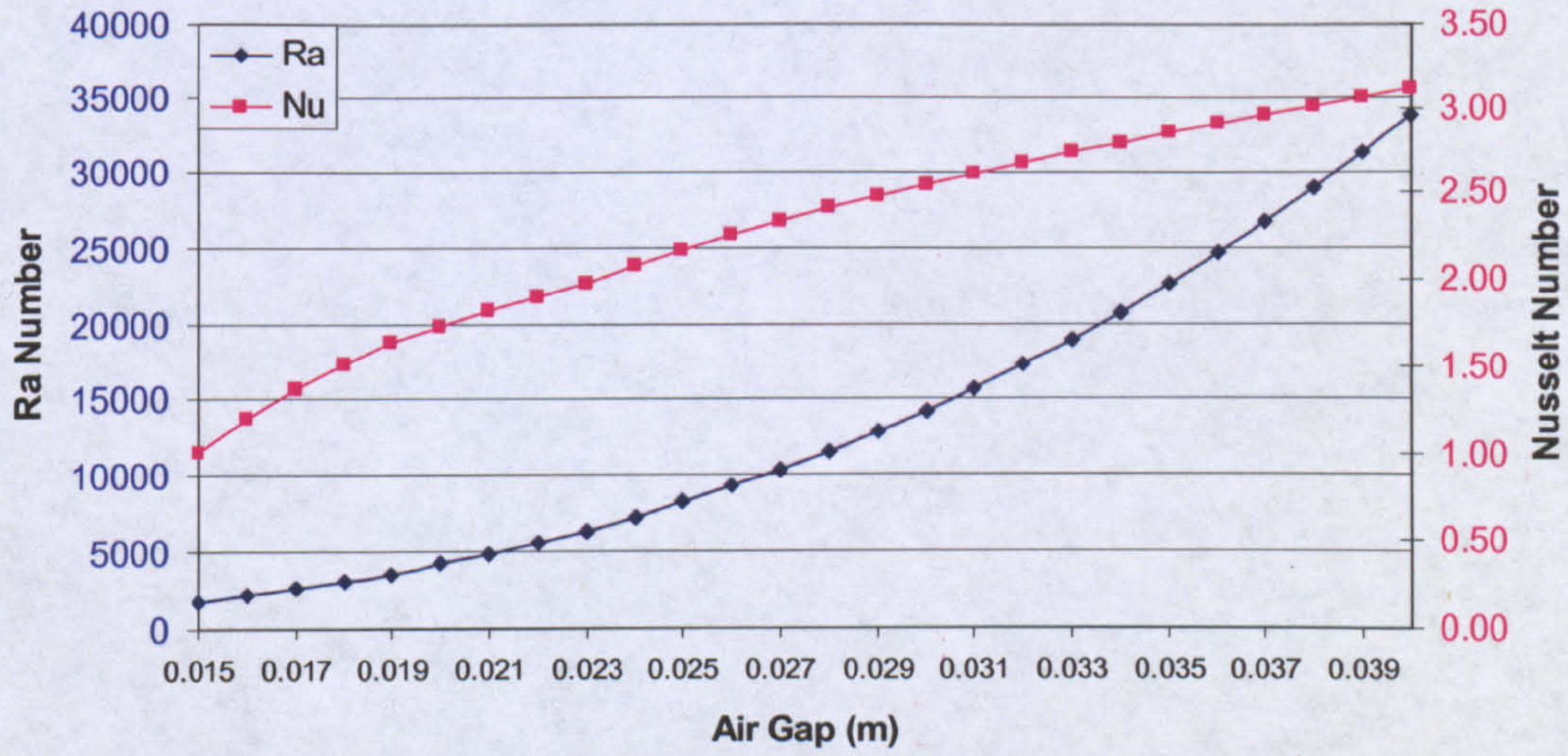

Figure 6.12: The relationship of Ra and Nu at absorber plate temperature of 20 °C

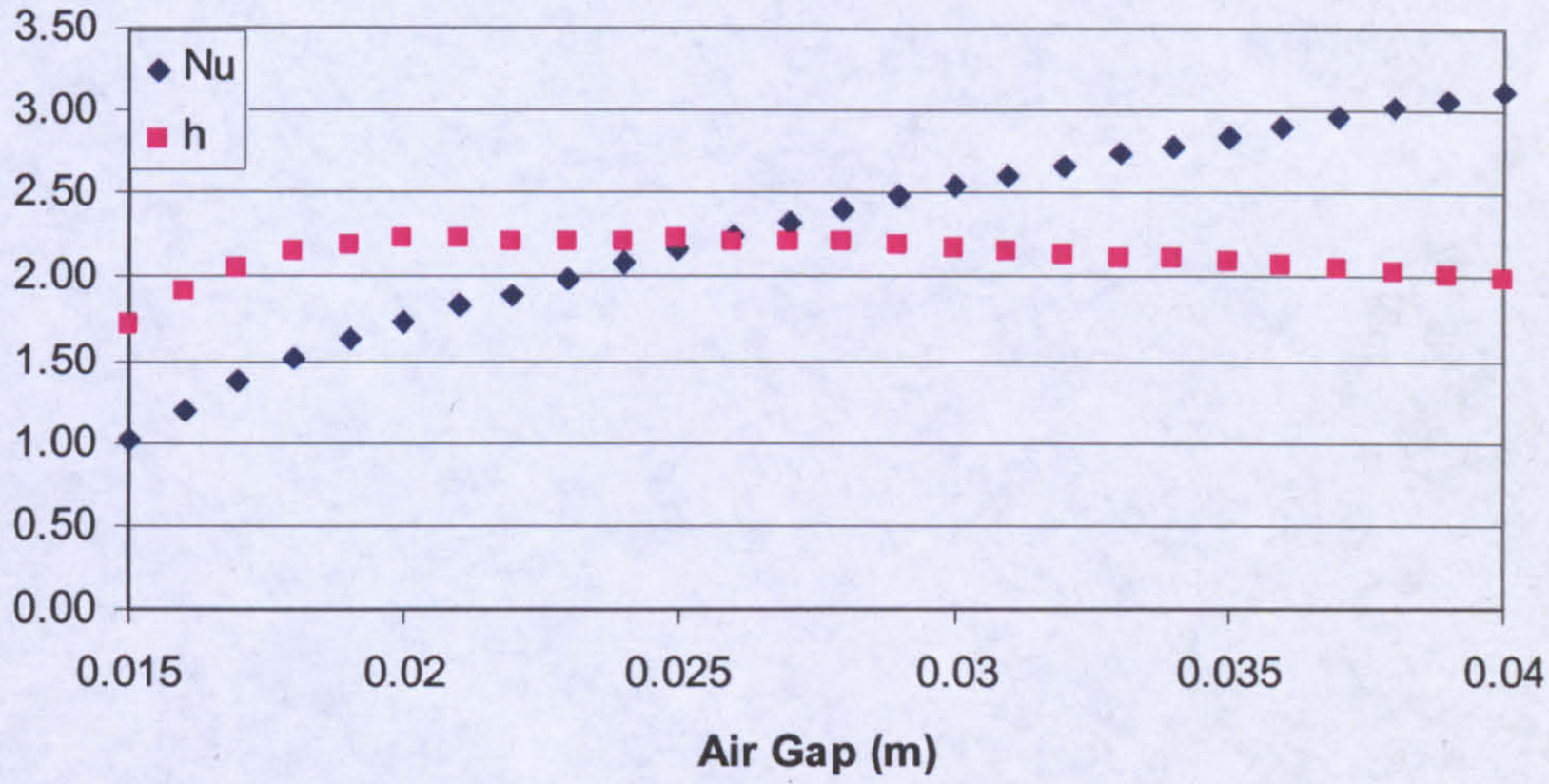

Figure 6.13: The relationship of Nu and h at absorber plate temperature of 20 °C

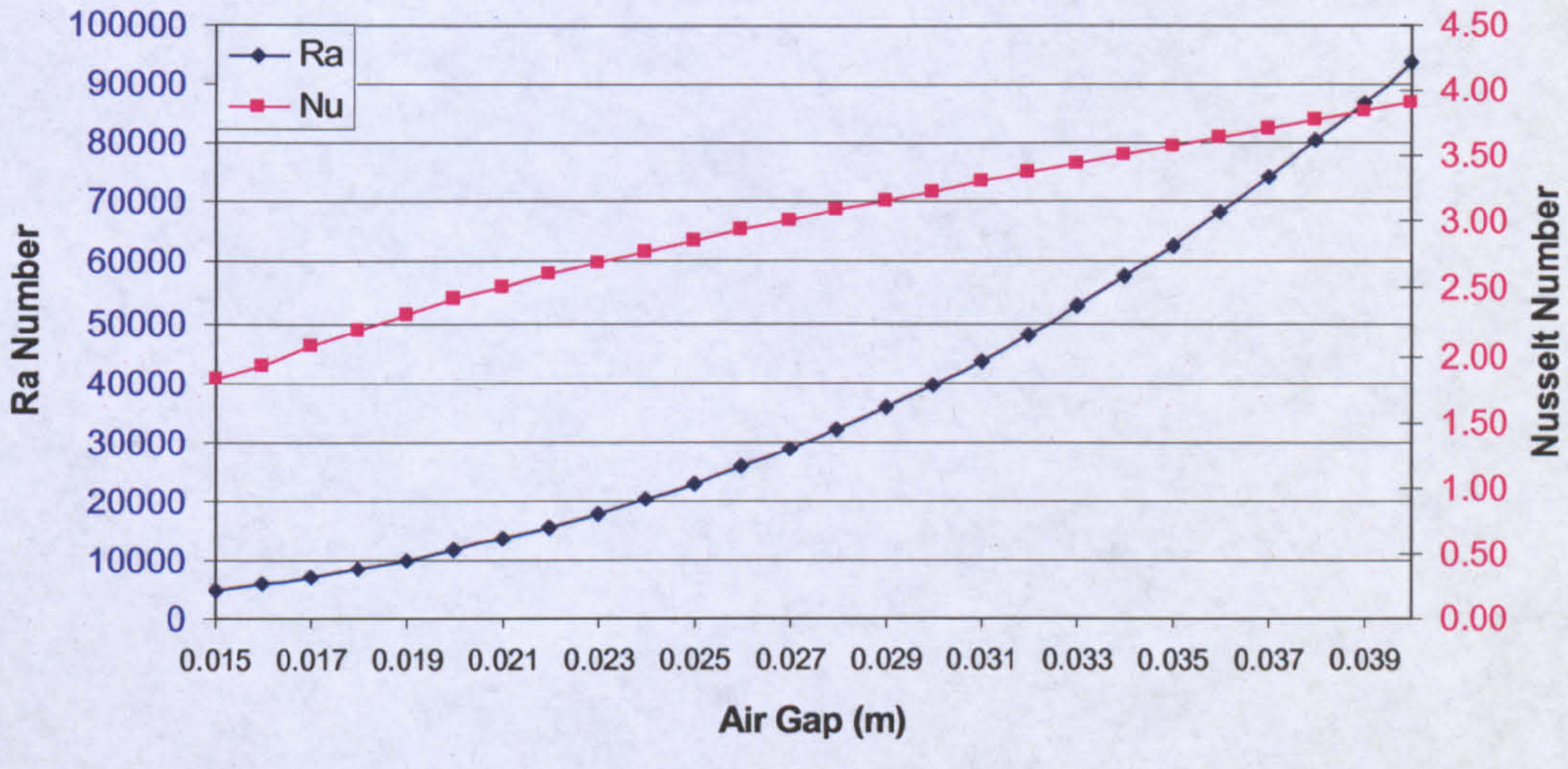

Figure 6.14: The relationship of Ra and Nu at absorber plate temperature of 30 °C

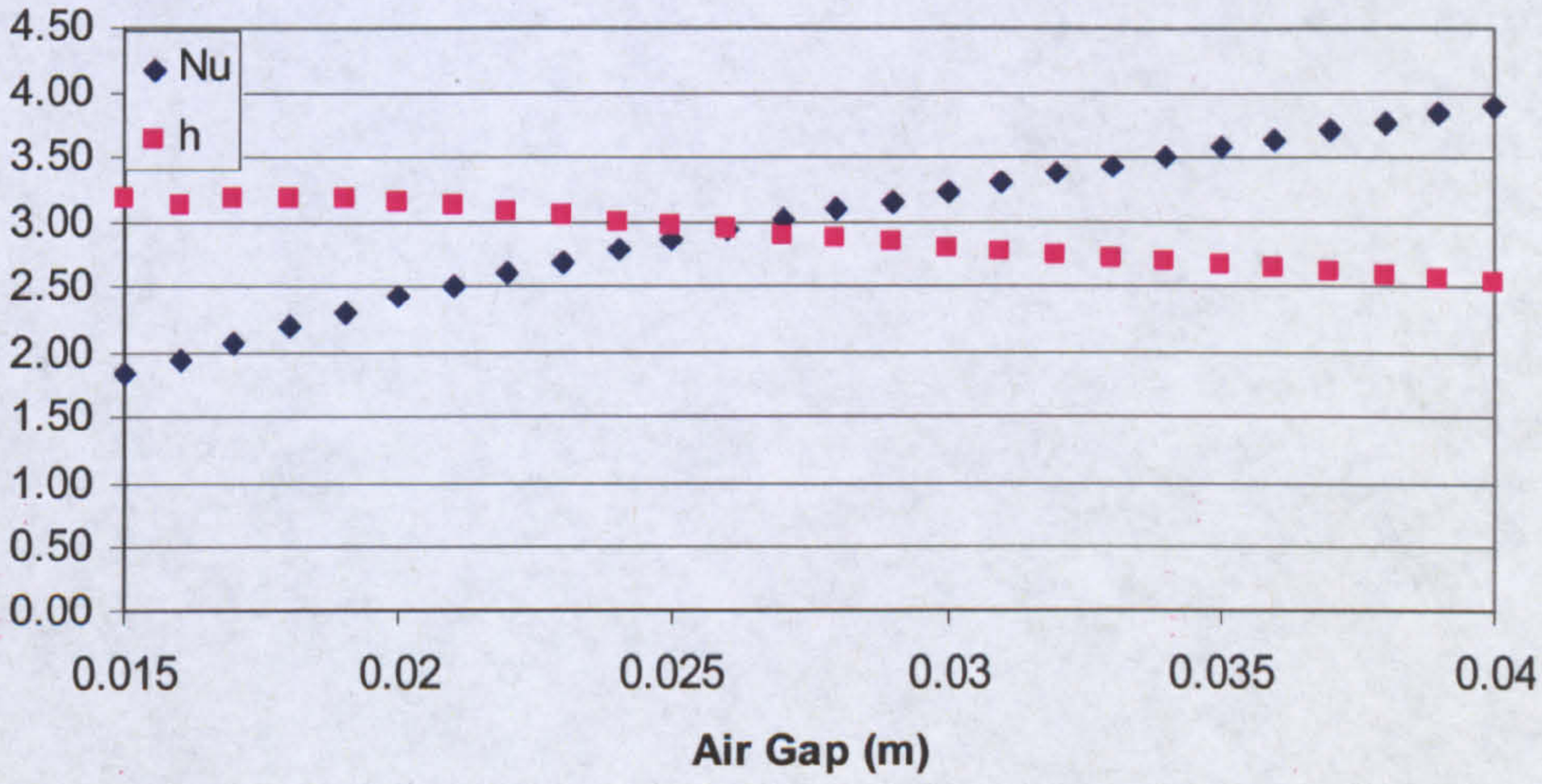

Figure 6.15: The relationship of Nu and h at absorber plate temperature of 30 °C

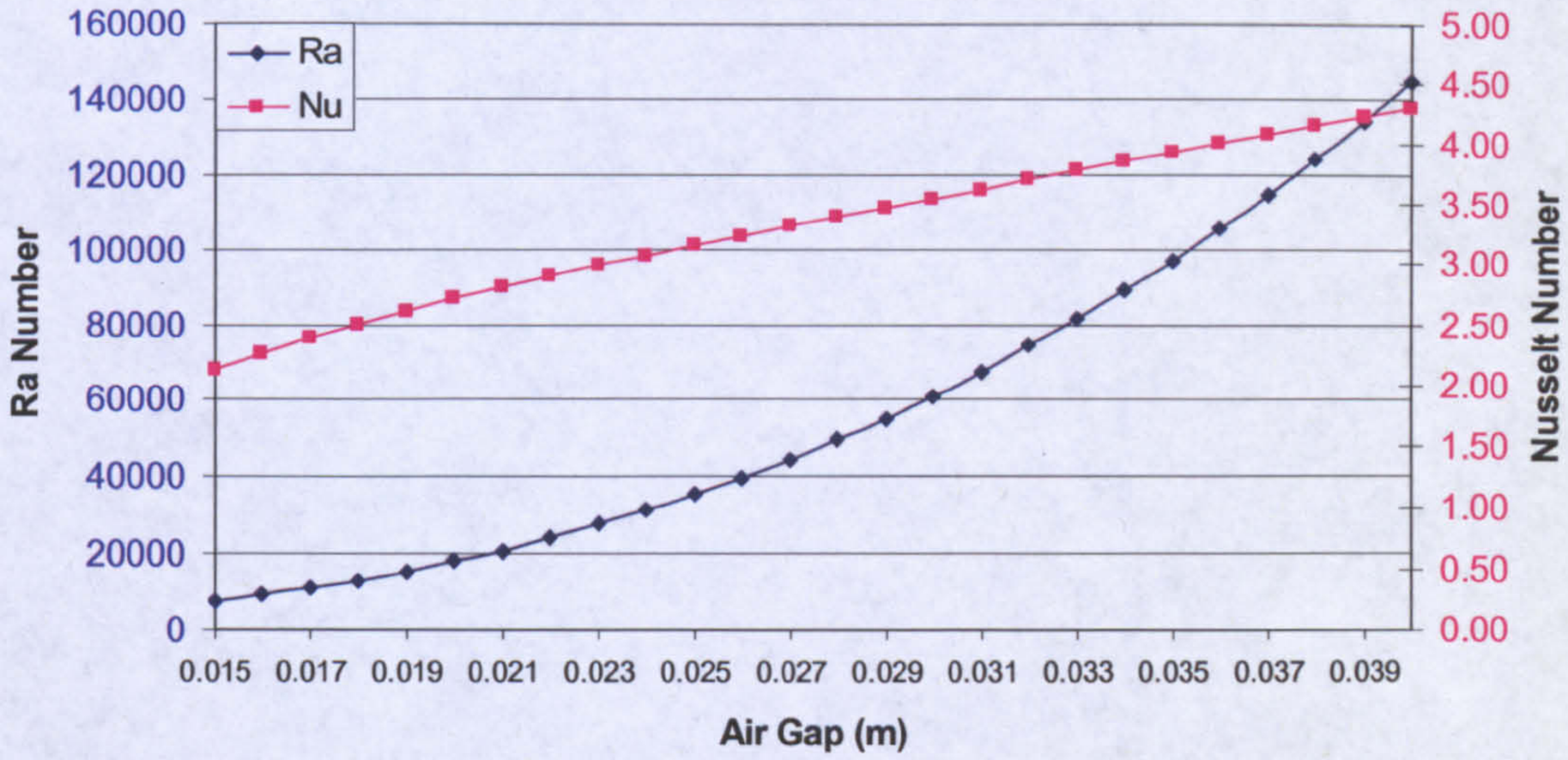

Figure 6.16: The relationship of Ra and Nu at absorber plate temperature of 40 ˚C

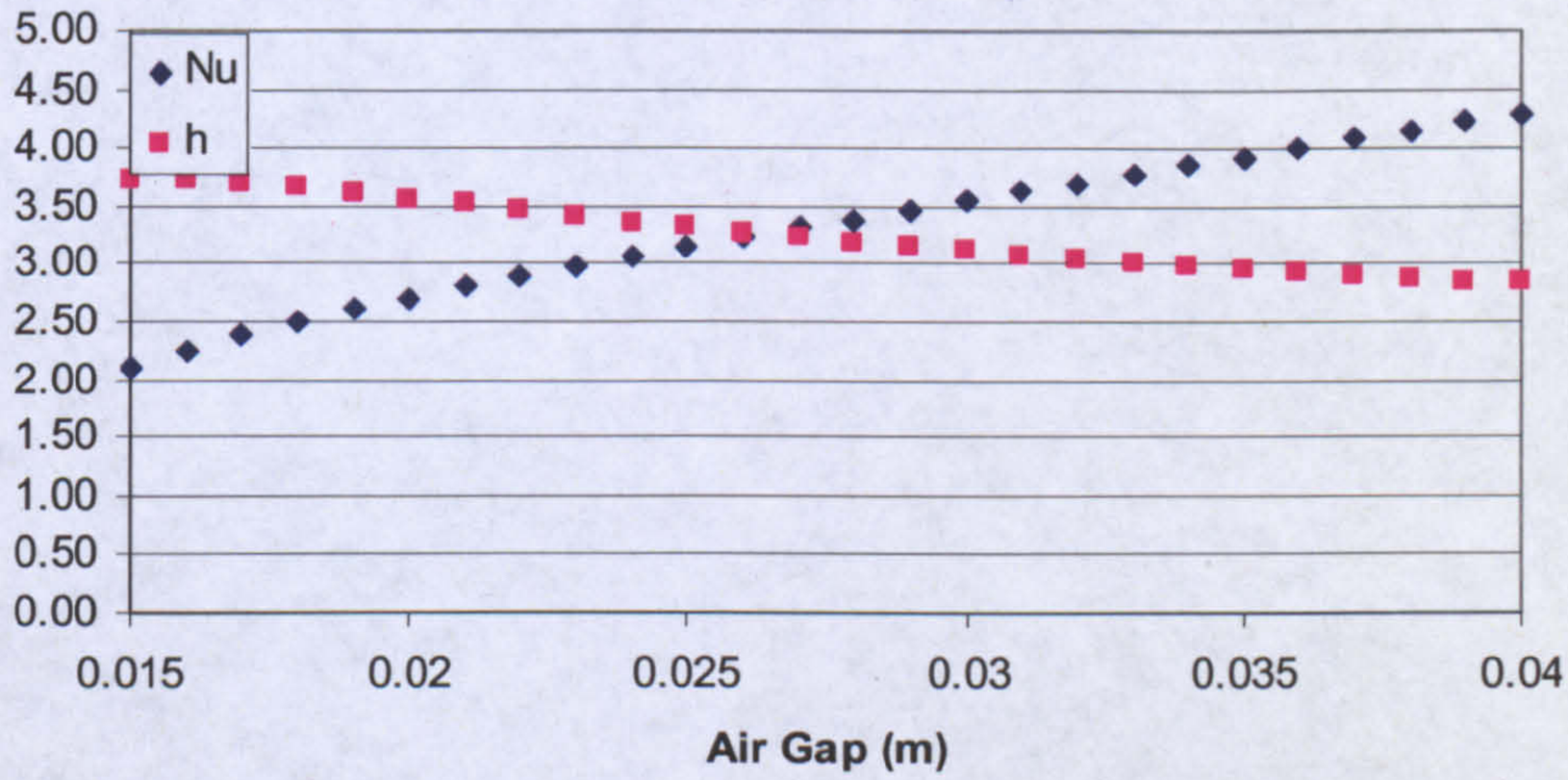

Figure 6.17: The relationship of Nu and h at absorber plate temperature of 40 ˚C

It can be noticed that for 3 different values of average absorber plate temperatures, different values of optimal air-gap (lowest heat transfer coefficient) thickness were noted. The cumulative outcome for Scottish condition where the prototype collector is estimated to operate at temperatures range of 20- 40˚C, 35 mm seems the appropriate value for the air gap.

6.6 Optimisation of the Absorber Plate

As has been discussed earlier the absorber plate is the driving force of the collector. Therefore it should be made sure that the absorptance of the plate is high. By applying

selective coating high absorptance can be achieved. It has been mentioned by Courtney et al as discussed in Chapter 3, that in Australia selective coatings are less costly as compared to the UK. Roughing the water side of the absorber plate is also estimated to increase the heat transfer, as roughness induces turbulence which improve mixing and hence heat transfer. Matt black paint on the other hand is less costly and easily available. Selective coating although would add to the cost of the collector, nonetheless it would pay-off in the long run by enhancing the performance of the collector. This has been experimentally proven by Duff and Hodgson[10]. Therefore selective coating outweighs the matt black paint in terms of advantage thus is recommended for the optimal design.

6.7 Optimisation of the Insulation

100 mm of glass wool insulation was applied all around the collector. From previous studies it was found that Muneer et al has applied 50 mm thickness of insulation for the collectors tested in Pakistan [11] and 100 mm for Benghazi. Garg and Rani [12] similarly have mentioned using 50mm of insulation thickness around the collector that has a very similar construction. It has to be d that the thickness of the outer wooden frame also adds to the thermal resistance.

As the insulation is inexpensive, it can be used in large quantities without the fear of over-design. One should be careful though of the overall size of the collector. The greater the thickness of insulation around the collector, the bigger will be the outer wooden frame. This will not only result in an increase cost but also increased weight of the collector. The insulation again depends upon the operating temperature of the collector and weather conditions. If the collector reaches high temperatures when cool ambient conditions exist, the insulation requirement in such case would be the highest. 100 mm glass wool insulation would mean a conductive resistance of x / k = 0.714 Km^2/W. This implies that the collector is well insulated even for the harshest of weather conditions.

6.8 Optimisation of the TIM

Transparent insulation material such as multiwalled Polycarbonate sheets can be placed in the air-gap to prevent losses particularly during the night. These sheets are

available with high level of transparency (clarity) thus having a minimal impact on the optical efficiency of the collector. It was noticed earlier through conjugate CFD analysis that more than 80% of the heat lost occurs through the top 20% of the glass cover in case of single glazed collector. For the 16 mm multiwalled sheet used (as in the experiments) the light transmission provided in the specification sheet was 78% (τ =0.78). This means a reduction in the optical efficiency by 4.4% if it's applied only at the top for a length of 200 mm (see 4.8a).

CFD analysis for the collector with TIM was carried out, the results are shown in fig 6.18. It was noticed in an earlier analysis that the heat losses from the top portion of the collector were high owing to a higher local heat transfer coefficient. In fig 6.18, the convective heat transfer coefficients for collector with TIM and without TIM are compared and it can be noticed that by the application of TIM, a notable reduction in the heat transfer coefficient occurs. However the experiments for the same did not indicate notable energy retention. There are two reasons for this behaviour, firstly the air leakage from the air-cavity that might have occurred and secondly due to the gap that was not completely filled by TIM material (16 mm thickness sheet was used hence a gap of 19mm still remained).

For the optimal design, the usage of TIM is recommended (filling the air gap completely) as it marginally adds to the cost (£ 26 /m^2)[2], reduces slightly the optical efficiency but is valuable in preventing the nocturnal losses.

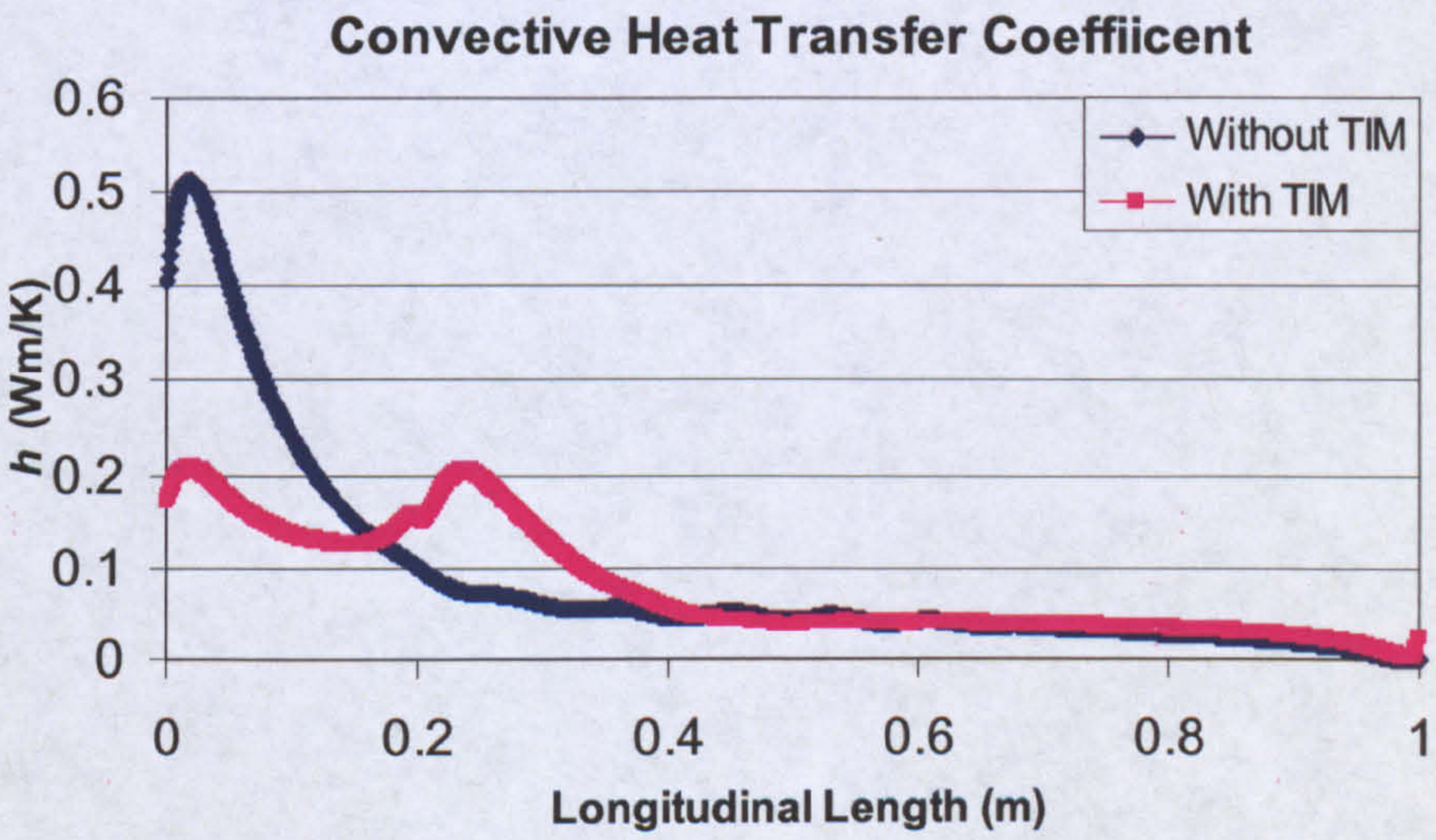

Figure 6.18: Surface heat transfer coefficient for the glass cover to the ambient air

[2] http://www.cloudtops.com/polycarbonate_verolite_pricing.htm

6.9 Flow Chart for Design & Integration of Optimized ICSSWH

A flow chart is presented for the interest of the reader that summarizes the steps to the selection and manufacturing of solar water heater. Details on each of the steps are presented on the following page.

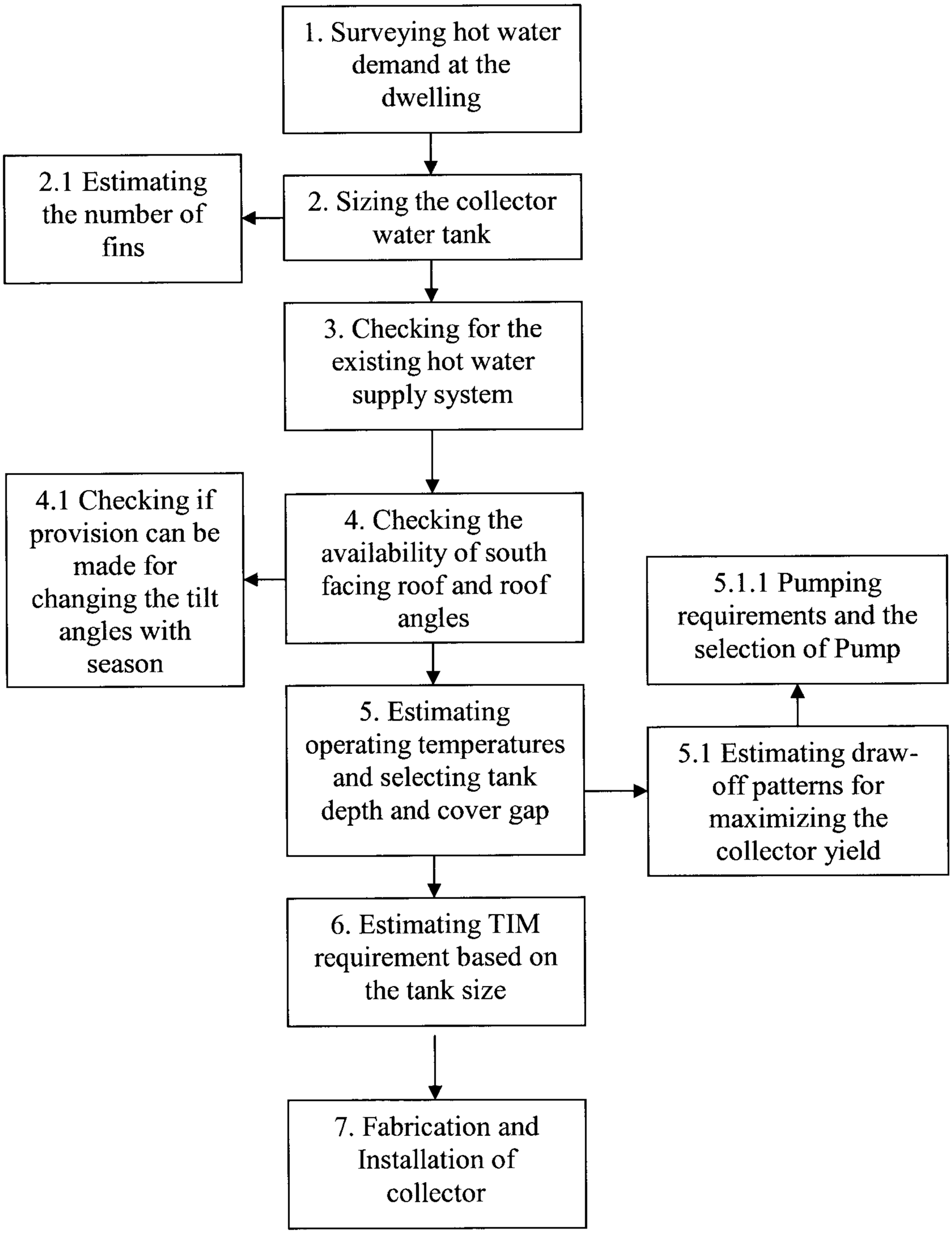

Figure 6.19: Flow chart for the design and integration of optimized prototype collector

6.9.1 Flow Chart Details

The details for each of the steps in the flow chart (fig 6.19) are mentioned below with corresponding numbers.

1. Hot water demand can be evaluated by either measuring the consumption pattern for a week or using the average consumption profile for the UK or Scotland as shown in table 5.1 -5.2

2. The collector has to be sized with each meter square of absorber plate area for every 50 litres of water

2.1 Depending upon the lateral width of the collector, the number of fins has to be estimated. The optimal distance between the fins for a tank depth of 50mm was found out to be 160mm.

3. If the existing hot water system is un-vented, then "Suggested Supply System –A" (section 5.2.3) will be used. The collector is this case would be made in thicknesses of less than 50mm (e.g. 30mm or 20mm). In the case of vented system, "Suggested Supply System-B", would be used.

4. Roof angle influences the stratification which affects the draw-off pattern. It has to be noted, that higher angles promote thermal performance as well as stratification. For flat roof, a stand for the collector would have to be additionally designed to tilt the collector at the desired angle.

4.1 By using hinge joints at the bottom of the collector and flexible pipes at the inlet and outlet ports along with a load distributing plank, the collector angle can be changed (increased) during the winter time when the solar inclination angle is low. This will increase the collector yield outside the summer season.

5. The operating temperatures of the collector can be estimated using the simulation, once the water tank and consumption pattern is known. 40 mm gap if maintained between the absorber plate and cover would reduce the heat losses. If the gap of

40mm is not maintained than it should be kept at a number which corresponds to TIM layer thickness available in the market. The distance between subsequent covers can be kept between 20-40 mm.

5.1 The draw-off pattern should be analyzed for the collector using the simulation in accordance with the consumption pattern.

5.1.1 A high head, low flow rate pump should be incorporated and programmed to operate on specific times with respect to both the collector temperature and the consumption pattern.

6. The selection of TIM size will be done based on the tank depth and the distance between cover and the absorber plate. For tanks with smaller depths and thus low thermal inertia, such as for in un-vented system it is more suitable to cover the entire absorber plate with TIM rather than a portion of it.

6.9 Conclusion

The design of the prototype collector was examined with an aim to increase its effectiveness and extract greater output from the collector. In order to optimize the system, it is vital that the weather conditions are taken into account as they govern the collector operating temperatures. The band of temperature in which the collector operates for most part of the year, or in the time of the year where its yield is maximum, is therefore an important parameter. Or in other words the operating temperature is the fundamental parameter around which the other parameters were settled. It was also deduced that tank depth was the consequent parameter that was to be set before other parameters. Once that was done, it was noticed that an air gap of 35 mm was suitable for Scottish conditions with the collector estimated to operate in the temperature range of 20 ˚C -40˚C.

For the cover, it was assessed that double glazed collector would out perform the single glazed one particularly in Scotland where windy conditions prevail for most part of the year. Increasing the covers would results in transmission losses.

Addition of fins reduces the amount of stagnant body of water and it was analysed that 6 fins are better than 4 fins as they induce more rapid heating on the onset of insolation.

It was noted earlier that triangular and trapezoidal shaped collectors perform better than the rectangular shaped collector, however due to aesthetic reasons and roof integration rectangular tank remained the choice for the optimal design. The tank dimensions can be 1m x 1m x 0.05 m or 2m x 1m x 0.05 depending upon the hot water demand. In either case the collector performance remains the same as the vertical aspect ratios do not change. It was also found that that collector depth of 50 mm is appropriate owing to the capacity and thermal inertia needed for Scottish conditions. Selective coating should be applied on the absorber plate and the inner surface should be roughened to induce turbulence that will lead to increased heat transfer. 100 mm of glass wool insulation for Scottish conditions are adequate as the collector is deemed to operate on relatively lower temperatures compared to flat plate collectors.

The application of TIM is important in the optimal design as it would retain heat during night time although reducing the optical efficiency during the charging mode. 200 mm of clear multiwalled polycarbonate sheet at the top end of the collector is recommended with a thickness the size of air-gap.

References

1. Muneer T; Abodahab N, W.G., Kubie J, *Windows in Buildings, Thermal, Acoustic, Visual and Solar Performance.* . 2000: Oxford: Architectural Press.
2. Innosolar Energy Co, L., *Low Iron Glass Properties*. 2007, www.innosolar.cn: Guangdong, China.
3. Harvester, S., *Solar Harvester Information Sheet*, in *http://www.sun-harvester.co.uk/case.htm#SUN%20HARVESTER%20INFORMATION%20SHEET;*. 2007.
4. Bishop, R., *Superinsulated Batch Heaters for Freezing Climates.* Proceedings of the eighth National Passive Solar Conference,Sante Fe,New Mexico, USA, 1983: p. 807–10.
5. Duffie, J.A. and W.A. Beckman, *Solar Engineering of Thermal Processes*. 2nd Edition ed. October 1991: John Wiley & Sons Canada, Ltd.
6. Henderson, D., et al., *Experimental and CFD investigation of an ICSSWH at various inclinations.* Renewable and Sustainable Energy Reviews, 2007. **11**(6): p. 1087-1116.
7. Jose´ M.S. Cruz, Geoffrey P. Hammond, and Albino J.P.S. Reis, *Thermal performance of a trapezoidal-shaped Solar collector / energy store.* Applied Energy, 2002. **73**: p. 195-212.
8. University of Michigan Health System, *Burn Safety* C.S.Childrens Hospital, Editor. 2007, http://www.med.umich.edu/1libr/pa/pa_hotwatr_hhg.htm: Michigan.
9. Muneer, T., S. Maubleu, and M. Asif, *Prospects of solar water heating for textile industry in Pakistan.* Renewable and Sustainable Energy Reviews, 2006. **10**(1): p. 1-23.
10. William S. Duff and D. Hodgson, *Testing of a Flat Plate Collector with Selective and Non selective Absorbers that are otherwise Identical* in *Colorado State University, Fort Collins CO 80523, USA*, Colorado State University, Fort Collins CO 80523, USA
11. Muneer, T. and M. Asif, *Prospects for secure and sustainable electricity supply for Pakistan.* Renewable and Sustainable Energy Reviews, 2007. **11**(4): p. 654-671.
12. H.P. Garg and Usha Rani, *Theoretical and experimental studies on collector / Storage type solar water heater.* Solar Energy, 1982. **29** (6).

Chapter 7

New Avenues

Extension, Extrapolation and New Horizons

Almost imperatively, every research leads to junctures and passages with unknown ends, progress towards all of these cannot be made as the scope and time frame of the exercise limits the investigation. These include many potential areas, which can be explored in great detail and can yield fruitful results

This chapter not only explores the new avenues that have potential of growing into full research areas in their own right but also how the existing research can be improved and taken forward.

7.0 Overview

It is impossible to label any research as closed and the current work is no exception. It is more likely than not for a study to branch into many new areas of exploration. To undertake the exploration of these new areas is a matter of judgement that is gauged by the knowledge profitability in that direction. Nonetheless the areas that can advance and improve the current research have been highlighted herein.

Experiments were carried out in the laboratory; analysis was done using the meteorological data, and more insightful CFD studies were conducted. Even in the presence of the results from the mentioned, it would be in-appropriate to drop the idea of further tests of the collector as well as inspecting its true performance by installing it in a domestic hot water system. This and other such ideas have been presented in detail in the following sections.

7.1 Field Tests

The author feels that there is a strong need for conducting field tests for the fabricated collector, particularly during the summer time. Although the collector was tested in the laboratory with calibrated instruments, the actual performance of the heater in true weather conditions would yield important results. The field testing would bring into play several factors that were ignored (such as the effect of direction and velocity of wind). It would also help to benchmark the simulation results that have the provision of accepting the weather data as an input to predict the collector performance. Similarly laboratory tests can be carried out for wind speed for a more quantitative analysis of its influence on collector. Like wise the impact of wind direction of the collector can also be lab tested.

7.2 Testing of the Optimized Collector

As noted in the previous chapter that the prototype design could be improved for superior performance by changing several design parameters. A few of these recommendations were the use of additional glazing, employing selective surface, roughening the fins on the absorber side and inclusion of transparent insulation

material (TIM). Similarly, that the addition of a baffle plate reduces the heat loss during the night time as ascertained by Garg and Rani [1] is additionally recommended along with recently designed fabric manifolds for the storage tank by Anderson and Furbo [2] that maintains stratification in the event of a draw-off. The fabrication, laboratory tests as well as the field tests of the optimized collector would lead to a progress that is important for the commercial acceptance of the product.

7.3 Analyzing System Performance

Relatively less data is available for the performance of any solar collector when it is integrated in a domestic hot water system. The performance of the complete system could bring out many factors that would influence the heater design. The system performance therefore is an area that could be explored in detail.

7.4 Tests with Antifreeze and FPV (Freeze Protection Valves)

As was noticed in chapter 5, due to the drop in the ambient temperatures, particularly during the winter times, the collector becomes increasingly susceptible to freezing. Although the thermal inertia of the water body does restrict the possibility to some extent, the use of anti-freeze is the infallible option. In chapter 5, two supply configurations were proposed with one of the systems using anti-freeze. The current research was carried out for water as the working fluid. Although the results can be extrapolated to antifreeze such as water-glycol mixture, it would be worthwhile to conduct physical experiments for the same.

7.5 Collector Fabrication/ Market Survey/ Feasibility Report

The collector cost can see a substantial decrease if manufactured in countries like China, India, Pakistan or Taiwan. It was noticed through price lists (on the internet) and requested quotations that a difference of up to 10 times existed in the cost for the glazing. Similarly the cost of manufacturing the collector is higher in Scotland as labour is relatively expensive. The overall cost of the collector can go down significantly if it is manufactured in the developing countries.

Research can also be carried out on price reduction in the case of mass production of the collectors. Setting up of jigs and fixtures as well as the estimation of required labour and batch production of the collector would bring down the cost of the collector substantially. A market survey can be similarly carried out to find out the demand of the collector. This area can be explored in-depth to determine the feasibility of the product.

7.6 Monitoring Environmental Impacts

The life cycle assessment as well as the environmental payback for the collector has not been dealt with in this research. The annual carbon dioxide savings by the collector have not been estimated. Once unfamiliar, these terms today are becoming increasingly popular as the general public is getting more and more aware of the detrimental effects of greenhouse gases. Likewise the media and the government are also embedding a conscience among people for reducing their impact on the environment. Campaigns and drives are now getting stronger and so are government policies on environment. Carbon taxing and fixed Carbon quotas for instance are being discussed by the office holders and policies are being laid down. In light of this upshot in awareness, it would be fruitful to study the environmental impact of the collector.

7.7 Safety, Health and Environmental Issues

The popularity of any device installed on a dwelling is not merely associated with costs. Building regulations and planning permission also come into play. Therefore it would be equally important to improve the product aesthetics that would retain if not increase value of the property.

From the safety and health prospective, another aspect that could be examined is Legionella factor. Legionella is a gram negative bacterium, including species that cause legionellosis or Legionnaires' disease, most notably L. pneumophilia. Common sources include cooling towers, domestic hot-water systems, fountains, and similar disseminators that tap into a public water supply[3]. The possibility of legionalla and its eradication is a possible avenue of study. Fire proofing of the collector is another possible area of studied.

An encouraging prospect in Scotland is that of the energy certificates that will rate a house on its energy efficiency. The rating will have ten levels A-G, where A represents the most efficient. These energy certificates will reflect on the value of the property. The properties with renewable energy devices would have better ratings, a lesser carbon foot print and hence an increased value. It is worthwhile to probe into the building regulations that are associated with the collector installation.

7.8 Pumping Devices

Although in chapter 5, flow circuits for the prototype collector were developed, it would be interesting to investigate the pumps that are available in the market. Low flow rate pumps that can deliver water or antifreeze at high heads can be surveyed. PV driven pumping systems can also be examined. It has been worked out that PV driven pumps can significantly improve the yield of the collector without the need of auxiliary energy to the system [4].

References

1. H.P. Garg and Usha Rani, *Theoretical and experimental studies on collector / Storage type solar water heater.* Solar Energy, 1982. **29** (6).
2. E. Andersen and S. Furbo. *Fabric inlet stratifiers for solar tanks with different volume flow rates*. in *Proceedings of EuroSun 2006*. 2006. Glasgow, Scotland.
3. Wikipedia, *Legionella*. 2007, http://en.wikipedia.org/wiki/Legionella.
4. T.D. Short; J.D. Burton, *The benefits of induced flow solar powered water pumps.* Solar Energy, 2003. **74**: p. 77-84.

Chapter 8

Conclusions

Hindsight, Foresight and Wisdom

Contribution to the sphere of knowledge is the goal of all research. The collection of information culminates into knowledge and the use of that knowledge for benefit is wisdom. This chapter aims to answer what contribution to knowledge was made and what wisdom was accumulated.

The summary of the findings of this project have been laid out in this chapter in a manner that is sequential and built around the objective of the project. The practical implications of the research have also been addressed in this chapter.

8.0 Conclusions

It is often the case with scientific investigations that more questions than answers are produced. Some questions are answered with more substance and certainty while others remain with a degree of inconclusiveness. Nonetheless, all of them have their own significance as they steer the research to its ultimate course.

After a review of both the concurrent and earlier investigations, it was deduced that despite their drawbacks, ICS type collectors present a low cost solution with a great potential for improvement in design suitable for Scottish conditions. [Section 1.4, 1.6]

The ICS collector was chosen as the prototype design and thus two collectors were fabricated for experimentation purposes. These collectors had identical design apart from the fins which were installed in one of them. The fins were placed along the longitudinal length of the collector such that they connected the absorber plate and the back plate. Sheet metal bar bent into C-channel shape were welded to the absorber and the back plate to create the fins.

Apart from their use to improve heat transfer, they also provide structural strength to the collector against the hydrostatic pressure that forces the collector to bulge. The fin type collectors have been reported to give a higher yield –up to 10% -for field tests carried out in Pakistan by previous investigators from this university. The mechanism of heat transfer through fins had not been analysed in detail and therefore presented room for investigation. It was envisaged that a comparison of fins with unfinned collector would yield important results that would help in carving out an optimized collector design for Scotland.[Section 2.2.1]

The prototype collectors were tested side-by-side with identical experimentation schemes. It was found that the finned heater out-performed the unfinned heater. The percentage difference between the efficiency of finned and non-finned heaters depended upon the amount of imposed heat flux as well as the total time of exposure. The difference in general in the performance was around 10% [Section 4.1.2.3].

It was also found that the collector tilt angle is important for stratification as well as the thermal performance of the collector. An increase in inclination angle improved the thermal performance as indicated by both experimental results and analytical studies [Section 3.2 ,4.1]

Several important results were gathered during the course of experiments, Abbreviated Thermal Analyses (ATA) and CFD. Therefore it is appropriate to enlist them as bullet points for a conclusive summary.

Results gathered from the experiments are as follows:

- For a constant amount of heat flux, the rise in temperature is asymptotic in both the collectors. The rate of increase of temperature is specific for each level of applied heat flux.
- For each value of each flux, there is a specific equilibrium temperature which when achieved results in all of the input heat flux going into losses.
- The rise in the glass cover temperature initially is higher than predicted by both CFD and ATA owing to relatively lesser capacitance effects.
- A high degree of stratification (difference in temperature between top and bottom section up to 12˚C) inside the water tank was noted which increased with the increasing heat flux. Similarly draw-off also induced a high degree of stratification (over 40˚C).
- The increase in stratification leads to the decrease in water side heat transfer coefficient.

- After the heat flux was removed, the cooling profile is a logarithmic decrement, inline with Newton's law of cooling.

The following findings were obtained through abbreviated thermal analysis:

- The radiation losses are of the same order as the convective losses for a single glazed collector and surpass convective losses for double and triple glazed covers.

- The losses from the air- cavity are in line with the behaviour encompassed by Hollands' regressions.
- The U value from the abbreviated thermal analysis matches the experimentally evaluated U value.

The estimation of the "U" values of the collector required an in-depth examination. The "U" values for both type of collectors i.e. finned and unfinned are the same when the collectors are shaded because of the identical external geometry. On the other hand, the "U" values are different when the collector is exposed to insolation. This lead to formulate three different types of "U" values namely $U_{cooling}$ and $U_{charging}$ and $U_{stagnation}$. It was later noted that $U_{cooling}$ and $U_{stagnation}$ are the same for both collectors and the only difference lay in $U_{charging}$. The following relationship was found to accurately describe the U value:

$$U_{ch-f} = U_{ch-uf} - A_f$$

Where $U_{ch\text{-}f}$ is the coefficient when the finned collector is charging while $U_{ch\text{-}uf}$ is the same coefficient for unfinned collector. The A_f is the fin advantage that was found to decrease with rise in average collector temperature. Through experiments a maximum U value was found to be 4.1 W/m^2K, however this was calculated in the presence of a heating pad that resulted in the reduction the actual U value. [Section 4.4]

The stratification inside the collector was important to study for two different reasons. It increased the yield of the collector as well as influenced the waterside heat transfer coefficient. In the event of a draw-off, it was noticed that the stratification inside the collector increased significantly (up to 59.1°C). The behaviour of the heat transfer coefficient on the waterside was important to monitor after the drawing-off water. Increased stratification hampered the "h" value while freshly induced cold water lowered the overall system temperature. After a careful analysis, it was observed that "draw-off" results in the overall increase in thermal efficiency as the lowering of system temperature has a greater impact compared to reduction in h value. [Section 5.1.7]

The top portion of the collector was found to lose more heat than the bottom. This again was inline with the heat loss through air-cavity as revealed by earlier studies. Transparent Insulation Material (TIM) was applied to the top 20% length (0.2m) of the collector. It was found that TIM did not decrease the heat transfer coefficient substantially; however it is still recommended for the optimal design for its prevention of nocturnal losses. [Section 4.3.2.5]

The collector draw-off readings were carried out and confirmed that low flow rates of hot water removal result in higher yield. It was also noted that the collector tends to bulge when subjected to higher pressures induced by a higher flow rate of supply water. Thus a flow rate of 2.5 lpm was determined as a limit for the prototype collector. Various types of collector supply circuits were studied. These included natural circulation, forced circulation, directly supply and with anti-freeze circulation loops. A couple of supply systems employed by commercial concerns were also studied; these included the Solar-*Twin* system that allows the expansion of pipes and joints in the event of freezing. In light of these designs a new supply system was introduced the costs of which were in line with the previously developed systems. The proposed system worked on an anti-freeze (glycol+ water) loop. The collector plumping circuit utilized extra pipes with a small pump (low head) for maintaining low flow rate. It is important to note that the prototype collector cannot operate on mains pressure. [Section 5.1- 5.2]

The optimization of the collector was carried out starting from individual components. The glazing was analyzed first for its material, number of covers and properties. Although polymer covers are findings increasing application in solar collectors, glass still remains the prime choice for collectors on account of its durability and high transmittance. It was calculated that double glazed collectors will have a superior performance as compared to single glazed collectors particularly in Scotland where the hourly average of wind speeds is over 7.5m/s (at height of 50m, no figure for wind speed at lower altitude exists as landscape has appreciable effect on the velocity) thus resulting in high heat lost. The conclusion was reached albeit the drawbacks of the increase in glazing covers - that include alleviated costs as well as transmission loss. It was earlier noticed that low iron content glass has high transmittance. Pilkington Opti-white was chosen as a best choice for its transmittance of over 89%.

The selective coating on the absorber plate was opted for instead of matt black paint. The difference between the costs of the two was negligible; the difference in performance of however was notable. On similar grounds it was also proposed that 6 fins should be added instead of 4 to enhance the performance [Section 6.1-6.6]

Noting that the draw-off has a significant influence on the collector performance, four different draw-off schemes for the collectors were devised and tested. These schemes were developed inline with the daily hot water consumption pattern in Scotland. It was noted that a better practice in terms of energy extraction is to empty half the collector's water i.e. 25 litres at four intervals in a day rather than emptying the full collector (50 lt) twice a day. It was also noted that at low temperatures, due to the stratification inside the collector, water can be tapped at above average temperatures of collector if it is partially emptied. [Section 5.1]

Having gone through the different supply configurations in domestic hot water systems, two different supply circuits were proposed for vented and unvented hot water systems. In each of the proposed supply circuits, measures for freeze proofing were incorporated.

Selection of the tank depth was compounded by the involvement of several parameters affecting the performance such as the collector efficiency, the capacity of the tank, weight of the tank the available levels of insolation and the hot water demand. To reduce this complexity, 40°C was set as the desired outlet temperature. The selection of a depth of the tank of 50 mm for the prototype collector was kept not based on calculations but rather in light of earlier studies done on similar collectors for Pakistan and Libya where the depths were greater. The simulation results indicated that 50 mm thickness was better compared to higher depth values as Edinburgh had more sunshine hours in the band of 100W to 200W than any other radiation bands. Smaller tank depths (40mm) would reduce the capacity but can be employed if consumption is small. On the other hand, in cases when antifreeze is used inside the collector, the use of shallower tank depths (40mm-30mm) is recommended as high grade energy is required due to the presence of a heat exchanger in the supply circuit.

It was concluded that an air-gap of 35 mm was appropriate for Scottish conditions with $\phi = 50^{\circ}$ as the collector angle. It was also proposed that units of cross-sectional areas 2 x 1 m could provide more capacity (100 litres) and yet maintain the same performance of the 1 x 1 m collector units.

The optimized collector was not fabricated and tested but it presents an opportunity to spur into a separate research in its own right. Based on the evidence from existing tests it can be stated with confidence that the optimized collector is deemed to work better than existing the prototype. Some of the possible areas of extending the research were field tests of the optimized heater, assessing environmental impact of the collector and the cost reduction in the case of mass production.

8.1 Contribution to Knowledge

This research involved a systematic study of the finned type ICS collector for Scottish conditions by means of experimentation, thermal modelling and CFD analysis. The following points highlight the contribution to knowledge by this research.

Two Integrated collector storage solar water heaters were fabricated at Napier University (one with- fins and one without). The exercise yielded foresight to better manufacturing (productive and low cost) practices for the collector fabrication, such as the use of seam welding. The collector can thus now be fabricated under £700 as compared to commercially available collectors priced over £2500.

Data was obtained through experiments on both the collectors for monitoring behaviour at different conditions. This data provided a detailed account on the collector behaviour mainly thermal efficiency and stratification levels for different angles and heat flux with the passage of time.

A single node model of the collector accurately simulated the collector behaviour and showed close conformance with the experimental data. This quantified the useful energy storage, convective and radiative losses as well as the U value.

CFD modelling for the collector components separately as well as conjugate analysis revealed the air and water movement patterns inside the collector. The air patterns showed the presence of longitudinal loops that strengthened with the increase in tilt angle while the water patterns showed a decrease in the overall fluid movement with the passage of time.

Plumbing circuits were laid out for both vented and unvented systems based on the limitations of the flow rates and the low pressure levels the collector can bear. Emptying 25 litres four times a day, if set as the draw-off pattern was found to maximise the energy yield from the collector.

Improvements in design based on the performance of prototype collectors were suggested while keeping the costs to a minimum. This included addition of cover, TIM on the top portion, selective coating on the absorber plate, inclusion of two additional fins, incorporating the use of low-iron glass and setting the angle of inclination to ϕ=50 (for Edinburgh conditions).

Future work particularly the field test of the collector, monitoring of the environmental impacts, health and safety issues were identified to improve the current research.

Appendix- A

Yearly Weather Data for Edinburgh

The yearly data in the electronic form can be found in the attached CD-ROM, under the following path:

Appendix-A\Weather Data.xls

The variation of the received insolation on a plane with respect to different tilt angles can be referenced by the following:

Appendix-B\ insolation on a titled plane.xls

Appendix- B

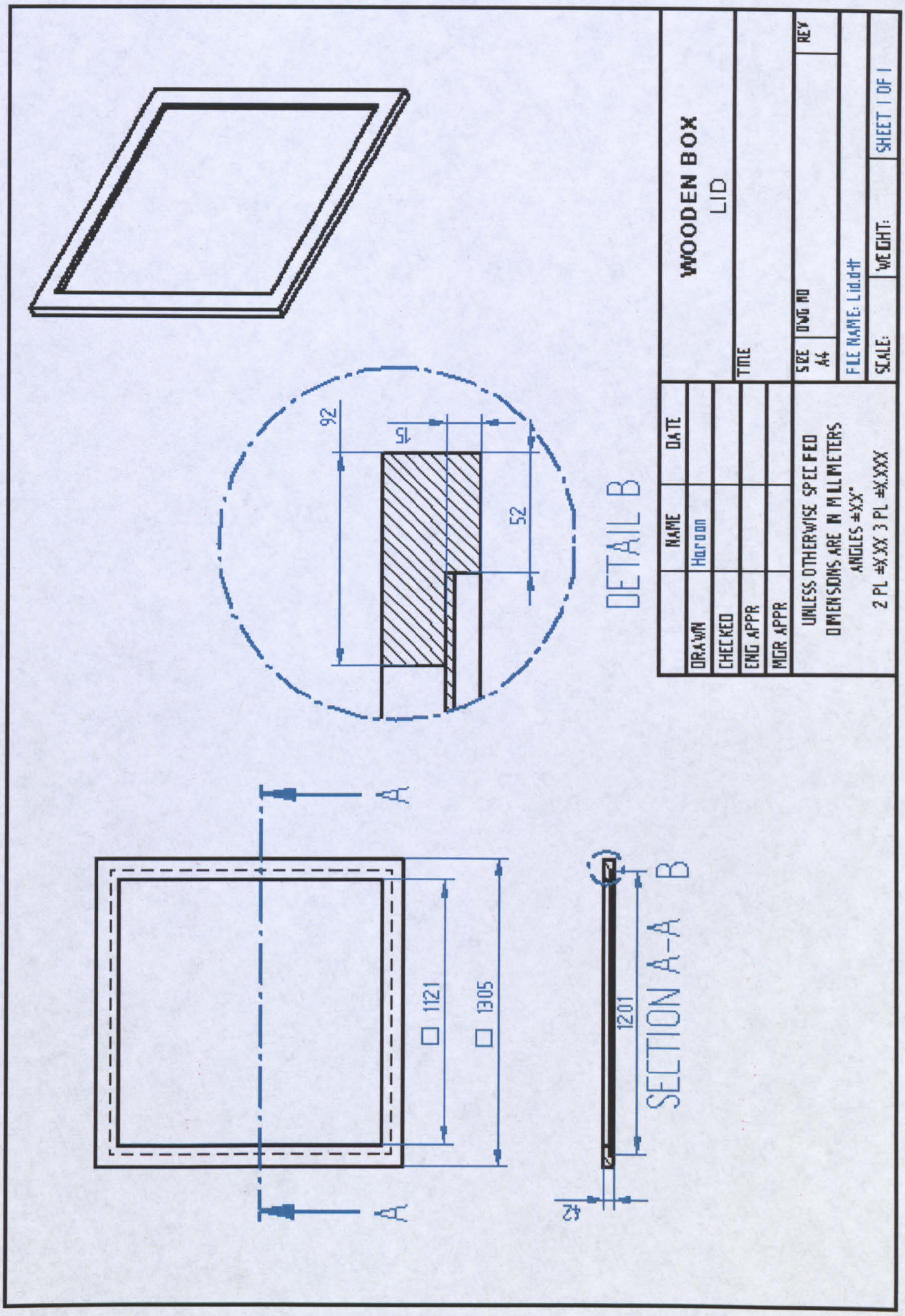
WOODEN BOX
LID
REV
SHEET 1 OF 1
NAME
DATE
DRAWN
Haroon
CHECKED
ENG APPR
MGR APPR
TME
SIZE A4
DWG NO
FILE NAME: Lid.dft
SCALE:
WEIGHT:
UNLESS OTHERWISE SPECIFIED
DIMENSIONS ARE IN MILLIMETERS
ANGLES ±X.X°
2 PL ±X.XX 3 PL ±X.XXX
DETAIL B
92
15
52
A
1121
1305
1201
SECTION A-A B
42

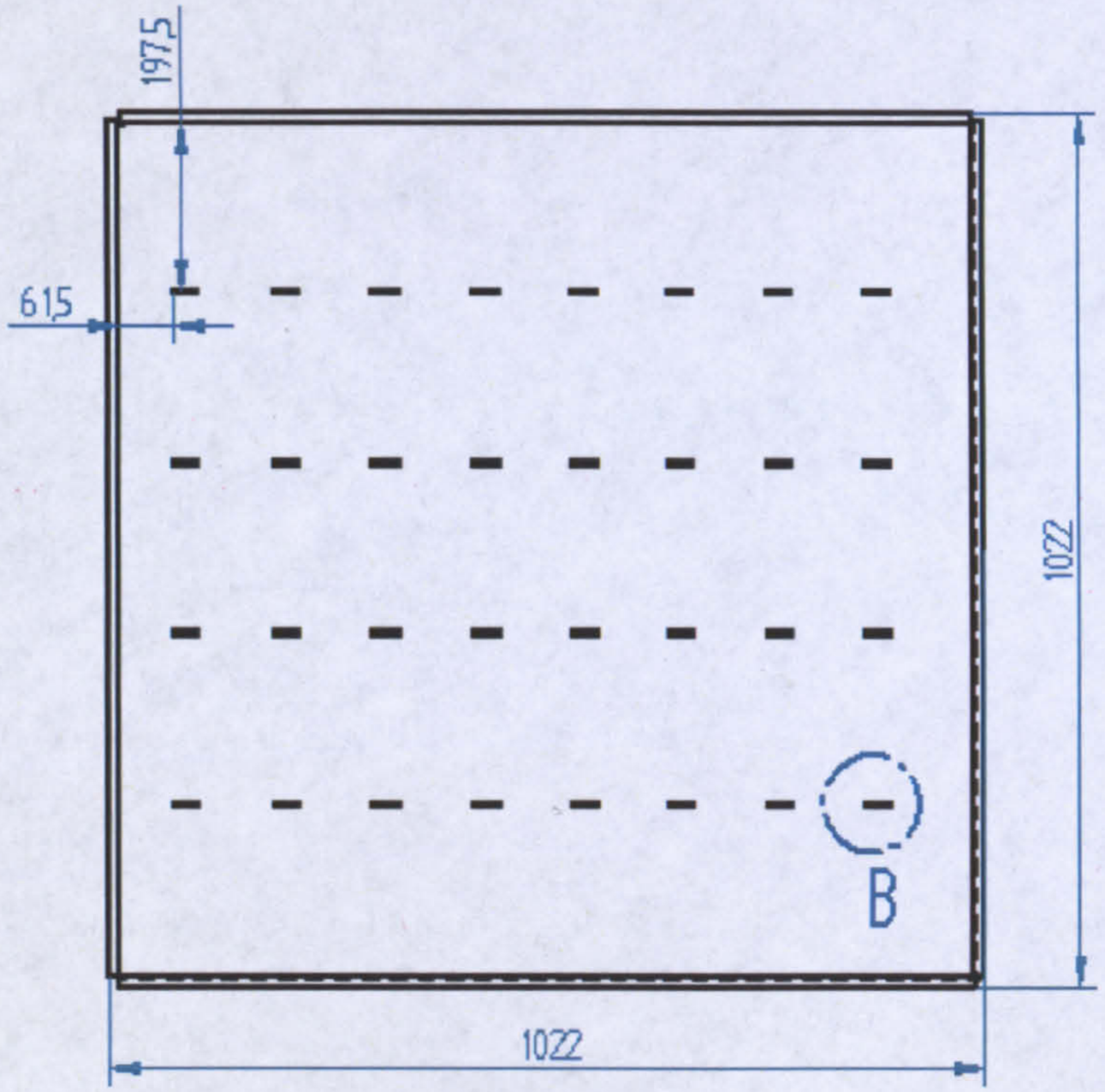

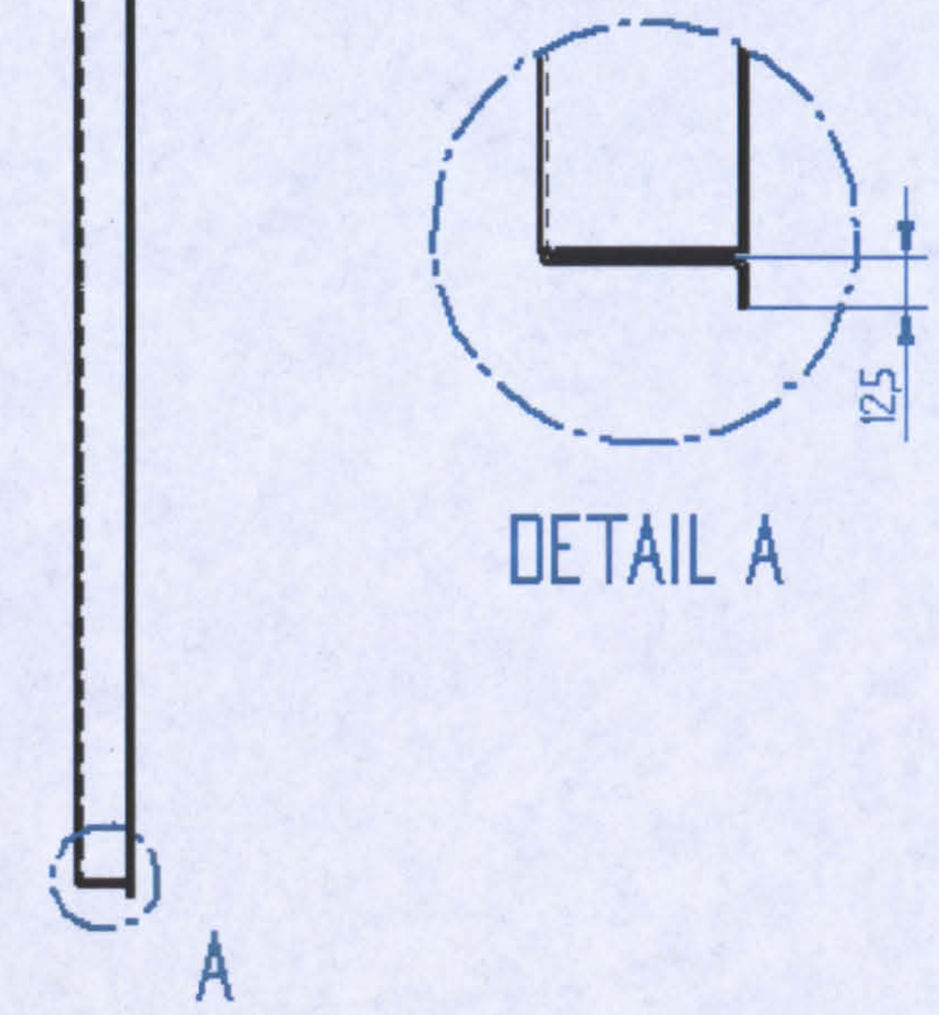

DETAIL A

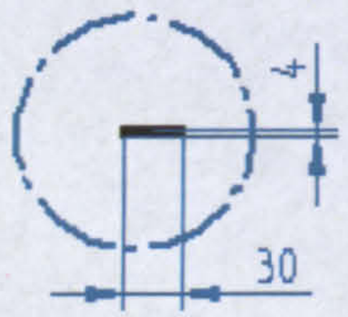

DETAIL B

REVISION HISTORY

REV	DESCRIPTION	DATE	APPROVED

	NAME	DATE
DRAWN	Haroon Junaidi	12-10-04
CHECKED		
ENG APPR		
MGR APPR		

UNLESS OTHERWISE SPECIFIED
DIMENSIONS ARE IN MILLIMETERS
ANGLES ±XX°
2 PL ±XXX 3 PL ±XXXX

Napier University
School of Engineering

TITLE: Solar Water Heater Modelling

SIZE	DWG NO	REV
A4		

FILE NAME: Solar Water Heater.dft

SCALE:	WEIGHT:	SHEET 1 OF 1

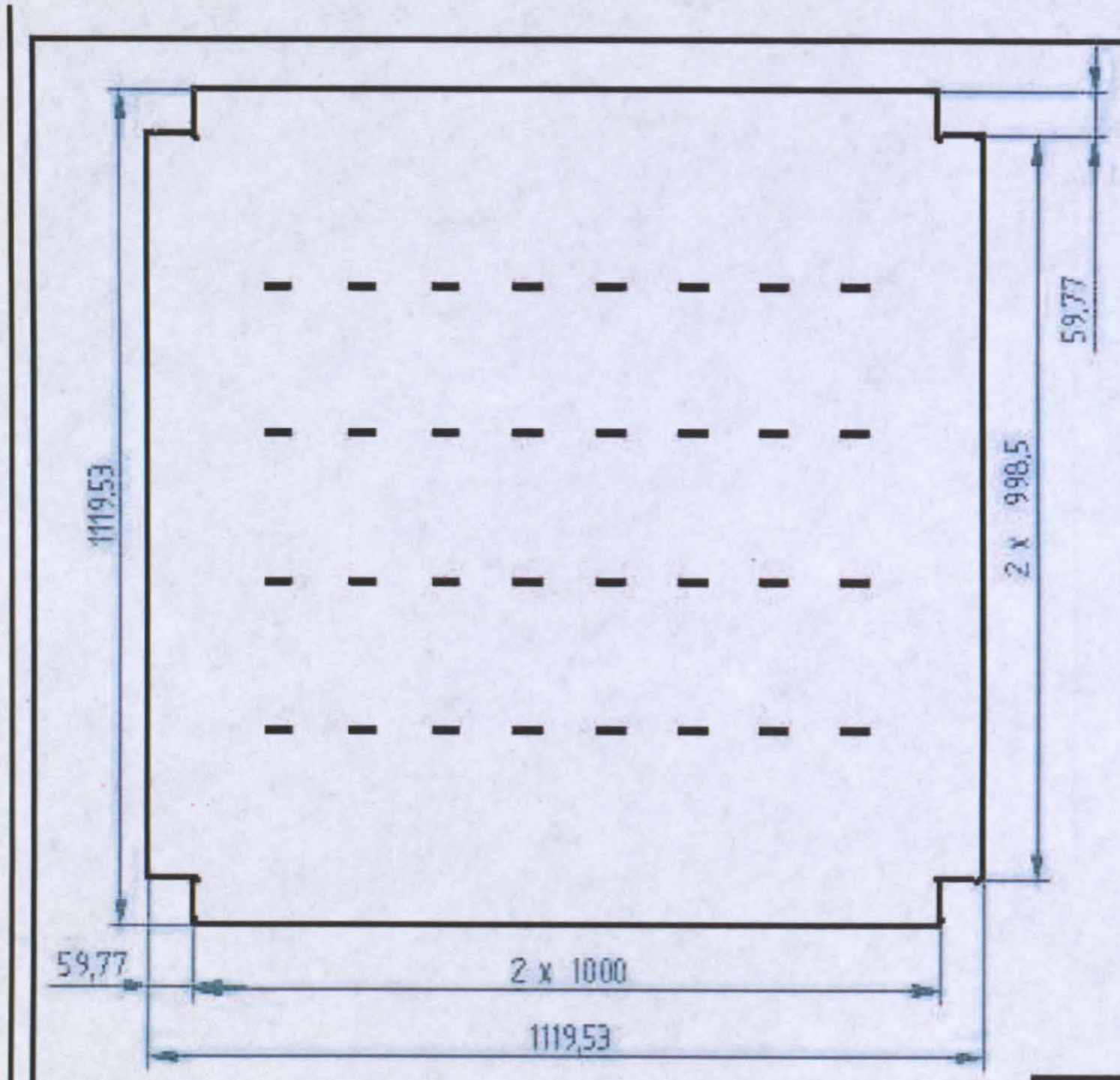

REVISION HISTORY			
REV	DESCRIPTION	DATE	APPROVED

	NAME	DATE
DRAWN	Horann Junaid	12-10-04
CHECKED		
ENG APPR		
MGR APPR		

UNLESS OTHERWISE SPECIFIED
DIMENSIONS ARE IN MILLIMETERS
ANGLES ±XX°
2 PL ±XXX 3 PL ±X.XXX

Napier University
School of Engineering

TITLE
Solar Water Heater Modelling

SIZE A4 | DWG NO | REV

FILE NAME: Solar Water Heater_blanksize.dft

SCALE: | WEIGHT: | SHEET 1 OF 1

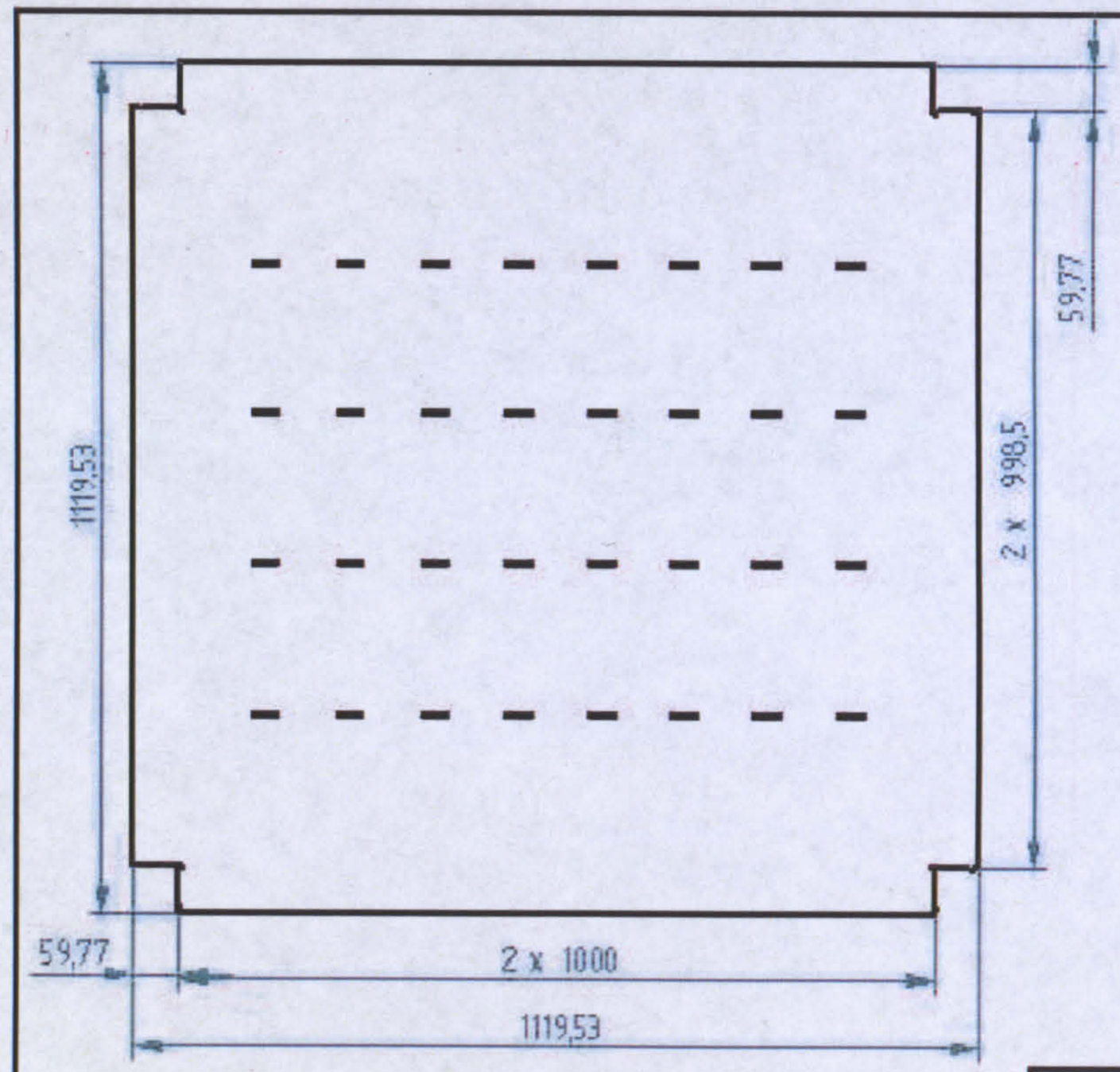

REVISION HISTORY			
REV	DESCRIPTION	DATE	APPROVED

	NAME	DATE
DRAWN	Hernann Jinnaid	12-10-04
CHECKED		
ENG APPR		
MGR APPR		

UNLESS OTHERWISE SPECIFIED
DIMENSIONS ARE IN MILLIMETERS
ANGLES ±XX°
2 PL ±XXX 3 PL ±X.XXX

Napier University
School of Engineering

TITLE: Solar Water Heater Modelling

SIZE A4 | DWG NO | REV

FILE NAME: Solar Water Heater_blanksize.dft

SCALE: | WEIGHT: | SHEET 1 OF 1

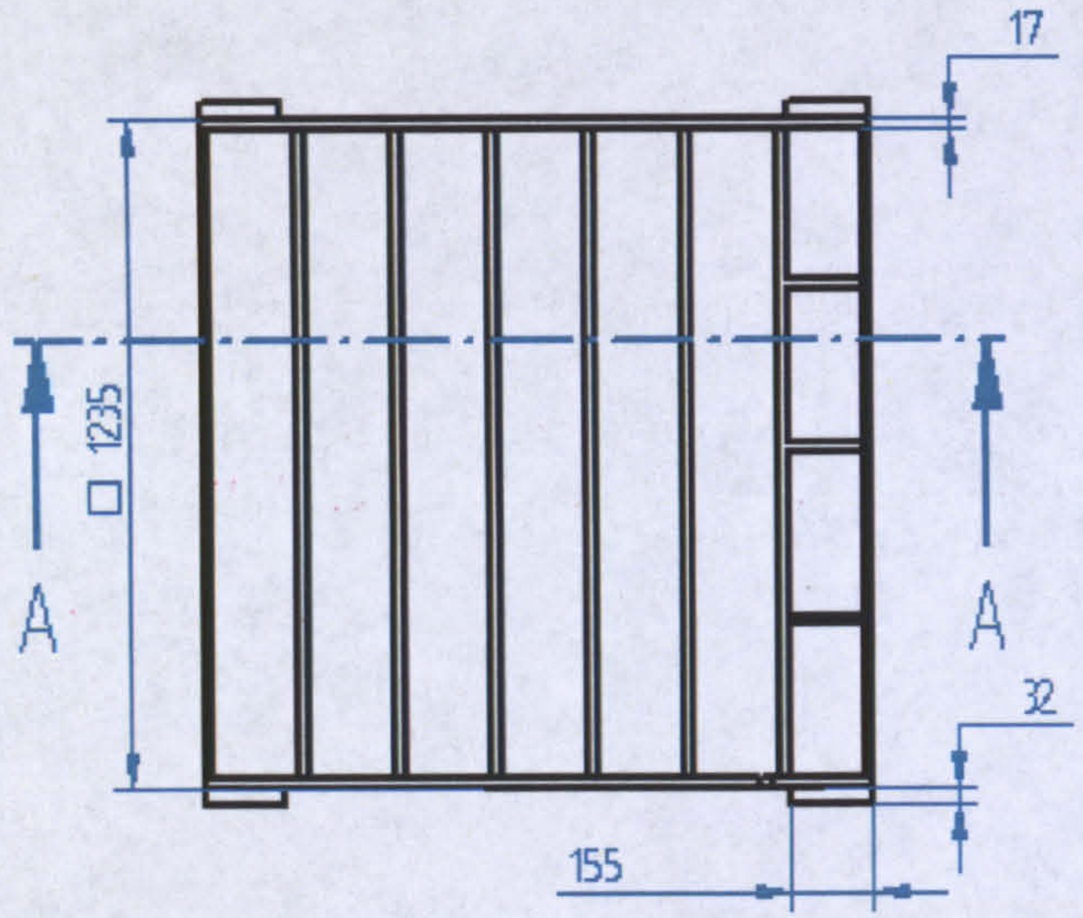

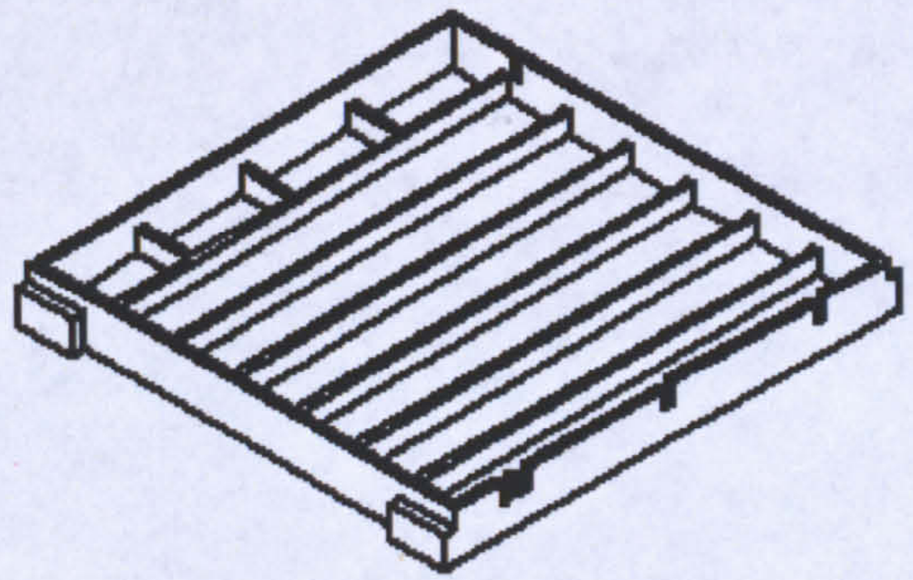

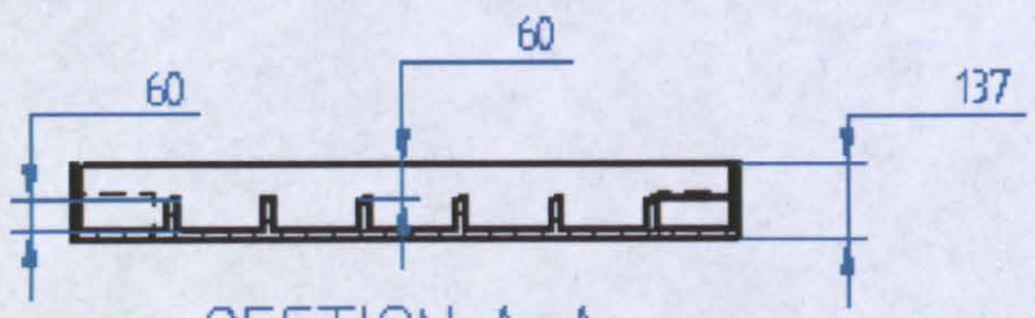

SECTION A-A

	NAME	DATE
DRAWN	Haroon	
CHECKED		
ENG APPR		
MGR APPR		

UNLESS OTHERWISE SPECIFIED
DIMENSIONS ARE IN MILLIMETERS
ANGLES ±X.X°
2 PL ±XXX 3 PL ±XXXX

WOODEN BOX
Bottom Half

TITLE

SIZE	DWG NO	REV
A4		

FILE NAME: wooden box.dft

SCALE:	WEIGHT:	SHEET 1 OF 1

Appendix -C

DATA SETS for Experimental Results

Table for file names in the CD

File Name	Heat Flux	Tilt Angle	Collector Type
Dataset 1	100 W	0	Unfinned
Dataset 2	200 W	0	Unfinned
Dataset 3	300 W	0	Unfinned
Dataset 4	400 W	0	Unfinned
Dataset 5	100 W	30	Unfinned
Dataset 6	200 W	30	Unfinned
Dataset 7	300 W	30	Unfinned
Dataset 8	400 W	30	Unfinned
Dataset 9	100 W	45	Unfinned
Dataset 10	200 W	45	Unfinned
Dataset 11	300 W	45	Unfinned
Dataset 12	400 W	45	Unfinned
Dataset 13	100 W	60	Unfinned
Dataset 14	200 W	60	Unfinned
Dataset 15	300 W	60	Unfinned
Dataset 16	400 W	60	Unfinned
Dataset 17	100 W	0	Finned
Dataset 18	200 W	0	Finned
Dataset 19	300 W	0	Finned
Dataset 20	400 W	0	Finned
Dataset 21	100 W	30	Finned
Dataset 22	200 W	30	Finned
Dataset 23	300 W	30	Finned
Dataset 24	400 W	30	Finned
Dataset 25	100 W	45	Finned
Dataset 26	200 W	45	Finned
Dataset 27	300 W	45	Finned
Dataset 28	400 W	45	Finned
Dataset 29	100 W	60	Finned
Dataset 30	200 W	60	Finned
Dataset 31	300 W	60	Finned
Dataset 32	400 W	60	Finned
Dataset 33	100 W	45	TIM
Dataset 34	200 W	45	TIM
Dataset 35	300 W	45	TIM
Dataset 36	400 W	45	TIM

Appendix- D

Visual Basic Application Code for ATA

(Comments are highlighted in green)

```
Sub compute01()
Tw = Sheets("Calc-steel").Cells(4, 21).Value 'Input
For x = 4 To 27
Tam = Sheets("Calc-steel").Cells(x, 22).Value
Vel = Sheets("Calc-steel").Cells(x, 23).Value
Ep = 0.8 'C  Emissivity of
Angle = Sheets("Input").Range("I5").Value
Gin = (12 / 13) * Sheets("Calc-Steel").Cells(x, 19).Value
mcsteel = 13.356 'kJ
mcwater = 208.323 'kJ
Ta = Tam + 273.15
Tsky = 0.0552 * Ta ^ 1.5
hwind = 2.8 + 3 * Vel
Eg = 0.8

Tp = Tw + 4
Tc = Tp - ((Tp - Ta) / 3)
deltime = 360

For iminute = 1 To 10

For i = 1 To 10
Ucar = (Eg * 0.0000000567 * (Tc ^ 4 - Tsky ^ 4)) / (Tc - Tsky)
Ucac = hwind
Uca = Ucac + Ucar

BEmm = (1 / Eg) + (1 / Ep) - 1
Upcr = (0.0000000567 * (Tp + Tc) * (Tp ^ 2 + Tc ^ 2)) / BEmm

Tfag = (Tp + Tc) / 2

Sheets("PropAir").Range("M15").Value = Tfag
visair = Sheets("PropAir").Range("Q15").Value
kfag = Sheets("PropAir").Range("R15").Value
visair = visair * 0.000001
Raag = (9.81 * (1 / Tfag) * (Tp - Tc) * 0.035 ^ 3) / (visair)

term1 = 1.44 * (1 - (1708 / Raag * Cos(Angle)))
term2 = 1 - ((1708 * Sin(1.8 * Angle) ^ 1.6) / (Raag * Cos(Angle)))
term3 = ((Raag * Cos(Angle) / 5830) ^ (1 / 3)) - 1
```

```
term4 = Application.Max(term1, 0)
term5 = Application.Max(0, term3)
Nuag = 1 + term2 * term4 + term5

'Calculation of total conductance from plate to glass cover
Upcc = Nuag * kfag * 0.001 / (0.035)
Upc = Upcc + Upcr

'Calculation of Rayleigh Number for Water
Sheets("WaterProps").Range("T25").Value = 0.5 * (Tw + Tp)
Betaw = Sheets("WaterProps").Range("AJ25").Value
Prw = Sheets("WaterProps").Range("AK25").Value
Visw = 0.000001 * Sheets("WaterProps").Range("AC25").Value
Denw = Sheets("WaterProps").Range("W25").Value
kw = 0.001 * Sheets("WaterProps").Range("ae25").Value
Raw = Prw * 9.81 * Betaw * 0.000001 * (1 ^ 3) * (Tp - Tw) / ((Visw / Denw) ^ 2)

'Calculation of Nusselt Number
Nuw = 0.56 * ((Raw * Cos(Angle)) ^ 0.25) * ((1 / 0.05) ^ (1 / 6))
hw = Nuw * kw / 1
Uw = hw

'Back losses
Ubloss = 0.72

'Iterations for Tp & Tc

Tp = (Gin + Upc * Tc + Uw * Tw) / (Upc + Uw)
Tc = (Upc * Tp + Uca * Ta + Ucs * Tsky) / (Upc + Uca + Ucs)
Next i

'Quseful = 0.001 * deltime * Uw * (Tp - 0.5 * (Tp + Tw))
Quseful = 0.001 * deltime * (Gin - Upc * (Tp - Tc) - Ubloss * (Tw - Ta))
Tw = Tw + Quseful / (mcwater + mcsteel)
Next iminute


Sheets("calc-steel").Cells(x, 24).Value = Tsky
Sheets("calc-steel").Cells(x, 25).Value = Uca
Sheets("calc-steel").Cells(x, 26).Value = Upc
Sheets("calc-steel").Cells(x, 27).Value = Uw
Sheets("calc-steel").Cells(x, 28).Value = Tp
Sheets("calc-steel").Cells(x, 29).Value = Tc
Sheets("calc-steel").Cells(x + 1, 21).Value = Tw
Sheets("Radiative losses").Cells(x, 1).Value = Ucar
Sheets("Radiative losses").Cells(x, 2).Value = Tc
Sheets("convective losses").Cells(x, 1).Value = Ucac
Sheets("convective losses").Cells(x, 2).Value = Tc
Next x
End Sub
```

Visual Basic Application Code for Draw-off Simulations

```
Sub compute01()

Tw = Sheets("Calc-steel").Cells(4, 21).Value 'input water temp.
Twi = Sheets("Calc-steel").Cells(4, 21).Value 'input water temp initial

For x = 4 To 27
Tam = Sheets("Calc-steel").Cells(x, 22).Value
Vel = Sheets("Calc-steel").Cells(x, 23).Value
Ep = 0.8 'Constant Emissivity of plate
Angle = Sheets("Input").Range("I5").Value
Gin = (12 / 13) * Sheets("Calc-Steel").Cells(x, 19).Value
mcsteel = 13.356 'kJ
mcwater = 208.323 'kJ
Ta = Tam + 273.15
Tsky = 0.0552 * Ta ^ 1.5
hwind = 2.8 + 3 * Vel
Eg = 0.8 'Constant emissivity for glass

' Initialisation of Tp & Tc
Tp = Tw + 4  '2 Degrees were added as an assumption
Tc = Tp - ((Tp - Ta) / 3)
deltime = 360

For iminute = 1 To 10

'Start iterative loop
For i = 1 To 10
Ucar = (Eg * 0.0000000567 * (Tc ^ 4 - Tsky ^ 4)) / (Tc - Tsky)
Ucac = hwind
Uca = Ucac + Ucar

BEmm = (1 / Eg) + (1 / Ep) - 1
Upcr = (0.0000000567 * (Tp + Tc) * (Tp ^ 2 + Tc ^ 2)) / BEmm

'Calculation of Rayliegh number for air cavity
Tfag = (Tp + Tc) / 2

Sheets("PropAir").Range("M15").Value = Tfag
visair = Sheets("PropAir").Range("Q15").Value
kfag = Sheets("PropAir").Range("R15").Value
visair = visair * 0.000001
Raag = (9.81 * (1 / Tfag) * (Tp - Tc) * 0.035 ^ 3) / (visair)

'Calculation of Nu for air cavity by Holland Regression
term1 = 1.44 * (1 - (1708 / Raag * Cos(Angle)))
term2 = 1 - ((1708 * Sin(1.8 * Angle) ^ 1.6) / (Raag * Cos(Angle)))
term3 = ((Raag * Cos(Angle) / 5830) ^ (1 / 3)) - 1
```

```
term4 = Application.Max(term1, 0)
term5 = Application.Max(0, term3)
Nuag = 1 + term2 * term4 + term5

'Calculation of total conductance form plate to glass cover
Upcc = Nuag * kfag * 0.001 / (0.035)
Upc = Upcc + Upcr

'Calculation of Rayleigh Number for Water
Sheets("WaterProps").Range("T25").Value = 0.5 * (Tw + Tp)
Betaw = Sheets("WaterProps").Range("AJ25").Value
Prw = Sheets("WaterProps").Range("AK25").Value
Visw = 0.000001 * Sheets("WaterProps").Range("AC25").Value
Denw = Sheets("WaterProps").Range("W25").Value
kw = 0.001 * Sheets("WaterProps").Range("ae25").Value
Raw = Prw * 9.81 * Betaw * 0.000001 * (1 ^ 3) * (Tp - Tw) / ((Visw / Denw) ^ 2)

'Calcuating water conductance
Nuw = 0.56 * ((Raw * Cos(Angle)) ^ 0.25) * ((1 / 0.05) ^ (1 / 6))
hw = Nuw * kw / 1
Uw = hw

'Back losses
Ubloss = 0.72

' Iterations for Tp & Tc
Tp = (Gin + Upc * Tc + Uw * Tw) / (Upc + Uw)
Tc = (Upc * Tp + Uca * Ta + Ucs * Tsky) / (Upc + Uca + Ucs)
Next i

If x = 8 Then
Tw = Twi
GoTo Mark4
End If

If x = 13 Then
Tw = Twi
GoTo Mark4
End If

Mark4:

'Quseful = 0.001 * deltime * Uw * (Tp - 0.5 * (Tp + Tw))
Quseful = 0.001 * deltime * (Gin - Upc * (Tp - Tc) - Ubloss * (Tw - Ta))
Tw = Tw + Quseful / (mcwater + mcsteel)
Next iminute
```

```
Sheets("calc-steel").Cells(x, 24).Value = Tsky
Sheets("calc-steel").Cells(x, 25).Value = Uca
Sheets("calc-steel").Cells(x, 26).Value = Upc
Sheets("calc-steel").Cells(x, 27).Value = Uw
Sheets("calc-steel").Cells(x, 28).Value = Tp
Sheets("calc-steel").Cells(x, 29).Value = Tc
Sheets("calc-steel").Cells(x, 30).Value = Quseful
Sheets("calc-steel").Cells(x + 1, 21).Value = Tw
Next x
End Sub
```

Appendix-E

The CFD case and mesh files are available in the CD in the following directory:

CFD files

Simulation files for ATA with the VBA code are available in the following directory

ATA Simulation files

Appendix F

Details of the survey for Hot water demand by Campbell McLennan.

1. Water consumption in various activities.

	l/min	time (sec)	litres	frequency/week	litres/week
Shower	6.08	300	22.8	12	273.6
Bath	19.56	210	68.46	2	136.92
Hand Basin	5.12	15	1.28	5	6.4
Kitchen Sink	6	75	7.5	7	52.5
Dishwasher	n/a	n/a	n/a	n/a	n/a
Washing Machine	-	-	65	3	195
				Total litres/week	664.42

2. Details of the survey:

Completed Surveys: 32

No. of occupants in property	1	2	3	4	5	6
No. of properties with daytime occupancy	1	6	4	2	1	2
No of properties daytime unoccupied	6	9	0	1	0	0
Total Properties	7	15	4	3	1	2

Number of Occupants Aged	under 5	5 to 17	18 to 60	Over 60	Total
With daytime occupancy	8	8	30	4	50
Daytime unoccupied	0	2	26	0	28
Total	8	10	56	4	78

List of Publications

- D. Henderson, H. Junaidi, T. Muneer, T. Grassie, J. Currie; "Experimental and CFD investigation of an ICSSWH at various inclinations" Renewable and Sustainable Energy Reviews Volume 11, Issue 6, August 2007, Pages 1087-1116;

- "Finite Volume CFD package (Fluent) for Convective Heat Transfer cases", Junaidi, H; Henderson, D; Grassie T; Currie, J; Muneer, T; International Journal of Mechanical Engineering Education (In print)

- Study of the Modified Built-in Storage (Integrated Collector Storage) Solar Water Heater for Scottish Weather Conditions, Grassie, T; Junaidi, H; Currie, J; Muneer, T; Henderson, D; EUROSUN 2006, Glasgow, UK ;27-30 June, 2006

- Study of Stratification in ICSSWH (Integrated Collector Storage Solar Water Heater); H. Junaidi; D. Henderson, T. Muneer, T. Grassie, J. Currie; 9th AIAA/ASME Joint Thermophysics and Heat Transfer Conference; San Francisco;5-8 June 2006